CHEMICAL REVIEWS

Review

Cite This: Chem. Rev. 2020, 120, 200−268

pubs.acs.org/CR

Photo- and Redox-Driven Artificial Molecular Motors

Massimo Baroncini,*[,†,‡] Serena Silvi,*[,†,§] and Alberto Credi*[,†,‡]

[†]CLAN-Center for Light Activated Nanostructures, Istituto ISOF-CNR, via Gobetti 101, 40129 Bologna, Italy

[‡]Dipartimento di Scienze e Tecnologie Agro-alimentari, Università di Bologna, viale Fanin 44, 40127 Bologna, Italy

[§]Dipartimento di Chimica "G. Ciamician", Università di Bologna, via Selmi 2, 40126 Bologna, Italy

ABSTRACT: Directed motion at the nanoscale is a central attribute of life, and chemically driven motor proteins are nature's choice to accomplish it. Motivated and inspired by such bionanodevices, in the past few decades chemists have developed artificial prototypes of molecular motors, namely, multicomponent synthetic species that exhibit directionally controlled, stimuli-induced movements of their parts. In this context, photonic and redox stimuli represent highly appealing modes of activation, particularly from a technological viewpoint. Here we describe the evolution of the field of photo- and redox-driven artificial molecular motors, and we provide a comprehensive review of the work published in the past 5 years. After an analysis of the general principles that govern controlled and directed movement at the molecular scale, we describe the fundamental photochemical and redox processes that can enable its realization. The main classes of light- and redox-driven molecular motors are illustrated, with a particular focus on recent designs, and a thorough description of the functions performed by these kinds of devices according to literature reports is presented. Limitations, challenges, and future perspectives of the field are critically discussed.

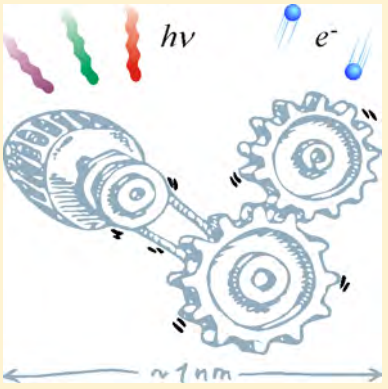

CONTENTS

Special Issue: Molecular Motors

Received: May 9, 2019
Published: August 15, 2019

DOI: 10.1021/acs.chemrev.9b00291
Chem. Rev. 2020, 120, 200−268

1. INTRODUCTION

Living organisms are equipped with a myriad of complex molecular assemblies, called motor proteins, that work inside cells for ordinary needs like machines in a manufacturing plant.[1−4] Scientific progress in the past decades has shown that these extremely small motors are in fact the most useful machines for humankind, because they are tasked with executing crucial processes for life. The most important and best known motor proteins are those of the myosin[5] and kinesin[6] families, ATP synthase,[7] and the bacterial flagellar motor.[8] Myosin and kinesin are linear motors powered by a chemical reaction—namely, the hydrolysis of adenosine triphosphate (ATP)—and are responsible for, among other functions, contraction and relaxation of muscles and transport of cargos around the cell, respectively. ATP synthase and the bacterial flagellum are rotary motors, both driven by transmembrane proton gradients, whose functions are manufacturing of ATP in all organisms and locomotion in some classes of bacteria, respectively. Another remarkable example is DNA polymerase, which moves along DNA while performing transcriptions.[9,10] Several other key biological processes, such as protein folding and unfolding,[11] are driven by molecular motors.[1−4] Surely, these biomolecular mechanical devices provide a compelling demonstration of the feasibility and utility of nanotechnology and constitute a sound scientific basis for attempting the construction of wholly artificial machines that operate at the molecular scale.

Although the latter idea was proposed for the first time by Richard Feynman in his landmark 1959 talk,[12] only in the past three decades has the progress in several areas of chemistry—primarily, the tremendous development of new synthetic, analytical, and computational tools to make and investigate complex molecular assemblies—enabled its practical realization. In the 1980s, research in supramolecular chemistry triggered the creativity of the chemical community, and the possibility that the concepts of macroscopic device and machine, typical of engineering, could be transferred to the molecular level started to arise.[13,14] Specifically, it was proposed that molecules could be used as building blocks to construct nanoscale devices and machines by a bottom-up approach.[15] In the following years, as a result of the rapid growth of supramolecular chemistry[16]—particularly in its broader meaning of the chemistry of multicomponent species—and mastering of the mechanical bond between molecules,[17,18] it became clear that the molecular bottom-up approach offers virtually unlimited possibilities for the realization of nanoscale machines. Single-molecule microscopies have provided direct observations of molecules as nanoscale objects endowed with size and shape that can move, interact, and react. Indeed, the visualization by fluorescence microscopy of the rotation of a single molecular filament driven by an F_1-ATP synthase motor[19] was not only a remarkable research achievement but also an exciting moment for nanoscientists. Finally, the physical concepts underlying the motion of very small objects[20,21] and the operating principles of biomolecular motors[22] started to be elucidated in the chemical community,[23] leading to an increased mechanistic understanding of artificial molecular machines and providing rational guidelines for their design and interpretation of their behavior.

Nevertheless, the construction and operation of systems with a level of structural and functional sophistication close to that of natural molecular motors is still a prohibitive task. What chemists have been doing is making simple prototypes consisting of a few molecular components that can move relative to one another in a controllable way and tackling the challenging problems posed by the interfacing of such devices with the macroscopic world in terms of energy supply, information exchange, and in more recent years, the task performed. The many remarkable achievements in this area have been evidenced in several reviews[24−41] (including some focused on redox-driven[42−46] and light-driven[47−54] systems), themed issues,[55−58] edited books,[59−61] and monographs.[62−65] The scientific value of molecular machines was highlighted by the award of the 2016 Nobel Prize in Chemistry to Jean-Pierre Sauvage,[66] Fraser Stoddart,[67] and Ben Feringa[68] well before these systems could impact significantly on people's lives.[69] Clearly, besides the relevance for fundamental science, the Nobel Committee recognized the huge potential of molecular machines for major progress in several areas of technology and medicine, with ground-breaking applications limited only by imagination.[70]

This review will cover the progress achieved in the past 5 years in the area of molecular motors operated by redox and/or photochemical processes. Molecular motors are a subcategory of molecular machines (see section 1.1 for definitions). In order to provide a complete and meaningful representation of this rapidly growing area, studies prior to 2014 that are particularly significant for historical, tutorial, or scientific reasons or are still the sole examples of a given type of device will also be included. We will focus on systems in which the motor function is inherent either to the individual molecule or, in the case of supramolecular complexes, to a minimal number of molecular components. Therefore, materials and devices whose motorlike behavior is determined by the collective action of molecular switches (which are not motors) and/or rectification features arising from the anisotropy of the material or its environment will not be considered here. Interested readers can refer to recent articles[71−82] and reviews[83−91] on redox- and photoinduced mechanical actuation and propulsion in nanostructured systems and materials.

1.1. Terms and Definitions

As discussed in the previous section, the macroscopic concepts of device and machine can be transferred to the molecular level. A molecular device is defined as an assembly of a discrete number of molecular components designed to execute a predetermined task.[15,16] While each part performs a single act, the multicomponent (supramolecular) assembly can achieve a more complex function that results from the cooperation of the molecular components and is therefore inaccessible to them individually. A machine is a device characterized by the use of mechanical power, i.e., controlled motion;[92] analogously, a molecular machine is a type of molecular device in which the components can be set in motion relative to one another in a controlled manner, resulting in the potential ability to carry out a function.[36,38,62,63]

The comparison between macroscopic and molecular machines based on the iconic juxtaposition of movements such as stretching, rotation, shuttling, braking, etc. has the advantage of providing a simple representation of molecular machines (e.g., by cartoons that clearly show the mechanical function) and has greatly contributed to the popularization of

DOI: 10.1021/acs.chemrev.9b00291
Chem. Rev. 2020, 120, 200−268

the topic and the growth of this new research area. As the field has evolved, however, it has became clear that such a comparison exposes one to the risk of overlooking the fundamental differences between the macroscopic and molecular realms. Indeed, nanoscale machines are not shrunk versions of the macroscopic ones, and their operating mechanisms cannot be devised on the basis of simple scaling rules.[93] For example, the effects of gravity and inertia, which are so important for macroscopic motion, are fully negligible at the molecular scale, where viscous forces resulting from intermolecular interactions—including those with solvent molecules—dominate. Another fundamental issue is the fact that molecules are constantly moving because of their kinetic energy and that of their surrounding molecules as determined by the temperature. Such random thermal fluctuations, or Brownian motion, seem to preclude the controlled precision typical of machinelike operation. Motor proteins, however, demonstrate that appropriately designed molecules can perform specific and directed movements when triggered by external stimuli.

A crucial point for the present discussion is the definition of "molecular motor" and its relation to "molecular machine" and "molecular switch". In line with recently proposed and generally accepted definitions[36,38,63,65] evolved from earlier descriptions,[24,25,62] a molecular motor can be considered as a type of molecular machine capable of performing work on its environment in a progressive fashion. This result is achieved by using an energy source to repeat directionally controlled movements, which is the key challenge behind the construction of molecular motors.

The peculiarity of a molecular motor can be better understood by comparison with the behavior of a molecular switch (Figure 1).[94,95] The latter is a multistate system whose properties (and the consequent changes caused in the surroundings) are a function of its state. The interconversion between two given states of a molecular switch can usually occur by the same pathway traveled in opposite directions (Figure 1a). In such a case, any mechanical effect produced on the environment is canceled out when the switch returns to its original state (unless the switch is coupled with another stimuli-controlled process that desymmetrizes the switching cycle, in which case a ratchet is obtained—see section 1.2). In particular switches, however, it can happen that the "forward" transition between two states follows a route different from that of the "backward" transition. A typical and simple example is that of a rotary device undergoing 360° unidirectional rotation through two directionally correlated half-rotations (Figure 1a). This kind of switch can influence a system as a function of the switching trajectory, and a task performed in a full cycle is not inherently nullified.

Hence, generally speaking, molecular motors are also switches whose states differ from one another for the relative positioning of some molecular components. To be a motor, however, a switch needs to possess the additional feature of cycle directionality described above. Only molecular motors can use an energy source to drive a molecular-scale system progressively and repetitively away from chemical equilibrium. The vast majority of artificial molecular machines reported to date do not possess such an ability and are therefore mechanical switches but not motors. As pointed out in the previous section, in this review we will deal exclusively with molecular motors.

1.2. Directional Motion in Molecular Systems

Molecular-scale objects are subjected to the ceaseless random motion caused by thermal energy. At ambient temperature, this

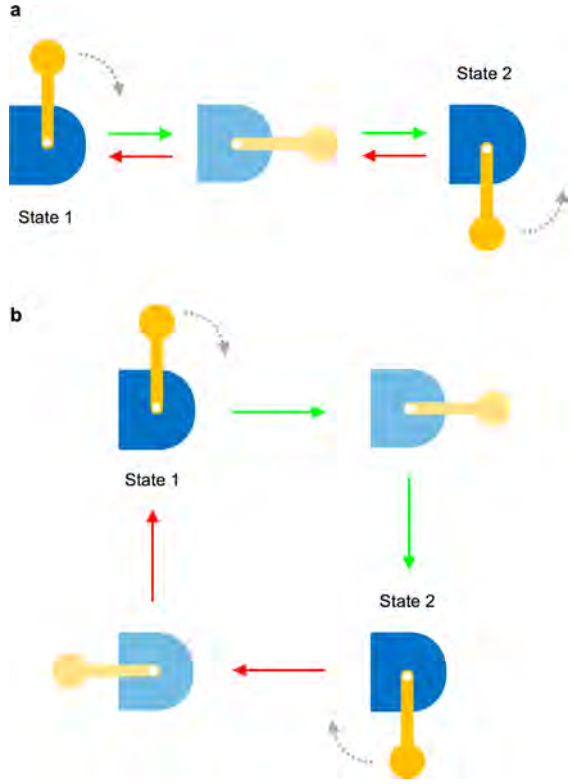

Figure 1. In a rotary switch (a), the interconversion between two states can take place by the same pathway traveled in opposite directions. The work done in the "forward" half-cycle (green arrows) is canceled in the "backward" one (red arrows). In a rotary motor (b), the forward and backward transitions between the two states follow different pathways, and net work can be performed. Transition states are represented with pale colors.

motion is disruptive: the thermal noise power experienced by a molecule ($\sim 10^{-8}$ W) is at least 8 orders of magnitude larger than the power typically provided to a motor protein by the fuel reaction.[21] Therefore, obtaining controlled and directed movement at the molecular scale is like walking in a hurricane or during an earthquake: as the latter cannot be stopped, the only way to move forward is to exploit its random shakes.[96] This is exactly what biomolecular motors do: they use an energy source to bias Brownian motion such that the moves in a given direction are more likely than those in other directions. This result is achieved by employing ratchet mechanisms, which operate by breaking spatial and time-reversal symmetries along the direction of motion with the application of a time-dependent potential with repeating asymmetric features.[97] Ratchets of interest in the present context can be divided in two categories: energy ratchets and information ratchets. Here we recall the basic aspects of these mechanisms with the help of examples showing their chemical implementation. For consistency with the scope of this review, we describe systems activated by redox and/or optical stimuli. A more thorough discussion and other representative examples of ratchet mechanisms applied to molecular machines can be found in refs 23, 31, 36, 38−40, and 98−102.

1.2.1. Energy Ratchet. In an energy ratchet, or flashing ratchet, the moving object is subjected to a potential energy profile that is modulated periodically by means of an external stimulus. The energy landscape consists minimally of two alternating maxima and minima that are repeated in space or

DOI: 10.1021/acs.chemrev.9b00291
Chem. Rev. 2020, 120, 200−268

time (Figure 2). A Brownian particle is initially located in the absolute minimum; raising such a minimum and/or lowering the adjacent minimum such that the wells are inverted in depth will generate a driving force for the particle to move to the new absolute minimum by thermal motion. To achieve directionality, also the relative heights of the two maxima need to be modulated in order to make the forward motion faster (i.e., more likely) than the backward one. The changes in the depth of the minima and the height of the maxima are produced by (an) external signal(s) and have to be repeated to afford progressive and directed transport of the Brownian object. Notably, the modulation of the energy profile occurs independently of the position of the particle.

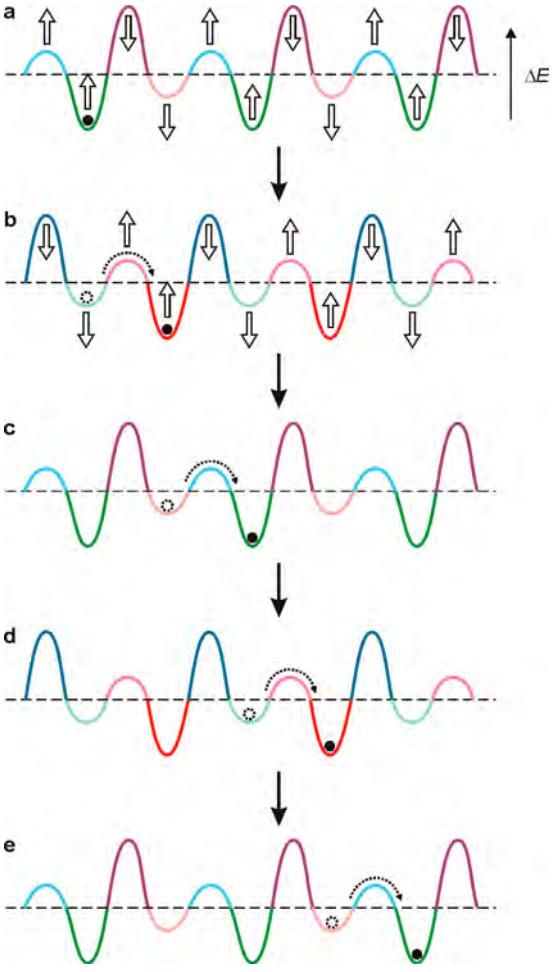

Figure 2. Operation of an energy ratchet (or flashing ratchet). Repeatedly changing the relative depths of the energy wells and the relative heights of the energy barriers, as shown by the open arrows in (a) and (b), causes a particle (black circle) to be moved directionally by exploitation of its Brownian motion.

The concept of an energy ratchet has been nicely put into practice with mechanically interlocked molecules (MIMs) such as rotaxanes[23,103] and catenanes.[103,104] An interesting example based on redox and optical stimulation is the [2]rotaxane (*E*)-$\mathbf{1}^{4+}$ (Figure 3).[105] Such a multicomponent species is based on a well-studied architecture[106] comprising a cyclobis(paraquat-*p*-phenylene) (CBPQT) tetracationic macrocycle[107] as a π-electron acceptor and an axle containing tetrathiafulvalene (TTF) and 1,5-dioxynaphthalene (DNP) units as π-electron donor ring recognition sites. In $\mathbf{1}^{4+}$, a photoactive 3,5,3′,5′-tetramethylazobenzene moiety (AB), which can be reversibly and efficiently switched between its *E* and *Z* configurations by light irradiation, is located between the TTF and DNP units. Since the TTF unit is more π-electron rich than the DNP one, the electron-poor CBPQT ring preferentially encircles the TTF unit rather than the DNP one in the starting co-conformation (Figure 4).

Upon chemical or electrochemical oxidation of the TTF site to its radical cation, the potential energy well determined by the donor−acceptor interaction with the CBPQT ring is canceled, and a driving force for the motion of the ring toward the DNP unit is created. If the AB unit is in its *E* configuration, such a ring shuttling occurs at a high rate (Figure 4). Reduction of the previously oxidized TTF unit produces a driving force for the return of the macrocycle to the original position. The results showed that on the experimental time scale, this process is immediate if the AB unit is in the *E* configuration but does not occur at all if the AB unit has been photochemically isomerized to the *Z* form prior to the TTF reduction (Figure 4). This behavior can be explained by considering that the $E \rightarrow Z$ isomerization of azobenzene affords a large geometrical change capable of substantially affecting the energy barrier for the shuttling of the macrocycle along the axle component. Indeed, the *Z*-AB unit poses a much larger steric hindrance to ring shuttling than does the *E* isomer, and the CBPQT ring is trapped in a nonequilibrium state (Figure 4b). At the end, a Brownian particle (the macrocycle) has been transported energetically uphill as a result of the redox-induced modulation of the energy wells and the photoinduced modulation of the energy barrier.

In this particular system, the correct sequence of changes in the minima and maxima necessary for the flashing ratchet is ensured by the orthogonality of the processes triggered by the redox and optical stimuli. An intrinsically synchronized modulation can be achieved by using a single stimulus that triggers simultaneous changes in the wells and barriers (see, e.g., sections 2.3 and 3.3). It is important to note that a rotaxane-based energy ratchet such as $\mathbf{1}^{4+}$ is able to produce a nonequilibrium distribution of rings between the two stations and that while such a distribution is being reached the system

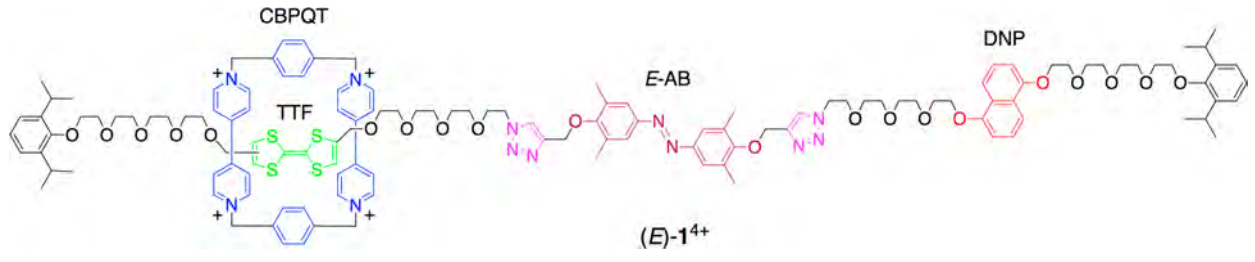

Figure 3. Structural formula of the photo- and redox-responsive rotaxane (*E*)-$\mathbf{1}^{4+}$.[105]

DOI: 10.1021/acs.chemrev.9b00291
Chem. Rev. 2020, 120, 200−268

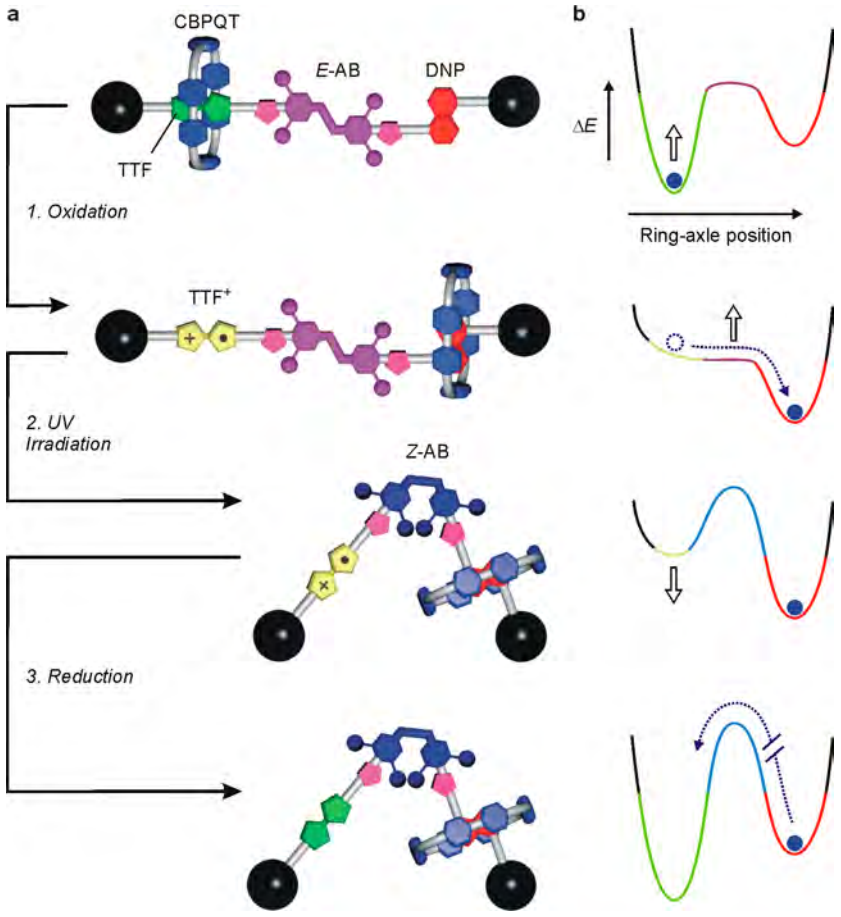

Figure 4. Schematic representation of the redox and photochemically triggered switching processes in rotaxane $\mathbf{1}^{4+}$.[105] (a) Initially the CBPQT ring encircles the TTF site on account of stronger π-electron donor−acceptor interactions than with the DNP site. Oxidation of the TTF site while the azobenzene unit (AB) is in the *E* configuration (process 1) is followed by the fast translation of the ring to the DNP site by Brownian motion. Irradiation of the oxidized rotaxane at 365 nm causes the isomerization of the azobenzene unit to the bulkier *Z* configuration (process 2) without affecting the position of the ring along the axle. Upon regeneration of the TTF primary station by reduction (process 3), a driving force for the return of CBPQT on the TTF site is created; however, because of the presence of the *Z*-AB stopper, the ring remains blocked in a nonequilibrium state. Therefore, as shown by the simplified potential energy curves (b), the macrocycle has been moved energetically uphill by an energy ratchet mechanism.

could in principle do work. When a steady state is obtained, however, no more rings are transported (i.e., no more work can be performed), and reset may occur only by a reciprocal path (in the case of $\mathbf{1}^{4+}$, this is enabled by thermal or photochemical $Z \rightarrow E$ isomerization). Hence, this kind of device cannot be considered a molecular motor. Despite this limitation, rotaxane-based ratchets have proved useful to gain a better understanding of rectification of Brownian motion and its realization with synthetic molecules. Furthermore, the "unproductive steady state" problem can be circumvented by (i) dethreading the ring from a different extremity of the axle with respect to that where it was threaded (see the pseudorotaxanes in sections 2.3 and 3.3) or (ii) linking together the two extremities of the axle, devoid of the stoppers, to obtain a [2]catenane (see section 3.5). The infinite periodicity of the potential energy profile that is necessary for the continuous directed motion of the Brownian particle is restored in space in the pseudorotaxane and in time in the catenane. In both cases, directed motion can continue even when the applied stimulus produces a stationary distribution of the components, and a molecular motor is obtained.

1.2.2. Information Ratchet. In an information ratchet, the energy profile is modified as a function of the position of the particle along its path. As in the previous case, the object moves by Brownian motion; directional control is achieved by selectively decreasing the barrier "in front" of the particle relative to the desired direction of motion (Figure 5) or selectively increasing the barrier "behind" the particle. It should be noted that the relative depths of the energy minima are unchanged. An information ratchet, as the name suggests, implies the transfer of information from the particle to the energy profile. This cannot happen for free, or the second law of thermodynamics would be violated: the information transfer process must be powered by an energy stimulus.

The first example of a molecular information ratchet is the rotaxane $\mathbf{2}^{2+}$ shown in Figure 6.[108] The system consists of a dibenzo[24]crown-8 (DB24C8)-based macrocycle surrounding an axle endowed with two recognition sites for the ring, namely, a dibenzylammonium (DBA) unit and a monobenzylammonium (MBA) unit. These sites bind the ring by hydrogen bonding with comparable affinities but are distinguishable for the purpose of monitoring the system. A methylstilbene unit (MS) asymmetrically divides the axle into two compartments, each containing an ammonium site. When the MS unit is in the *E* form, the ring can travel randomly along the full length of the axle; conversely, when the MS unit is in the *Z* form, the ring is trapped in one of the two compartments. Therefore, similar to the azobenzene moiety in the previous example, the stilbene unit

DOI: 10.1021/acs.chemrev.9b00291
Chem. Rev. 2020, 120, 200−268

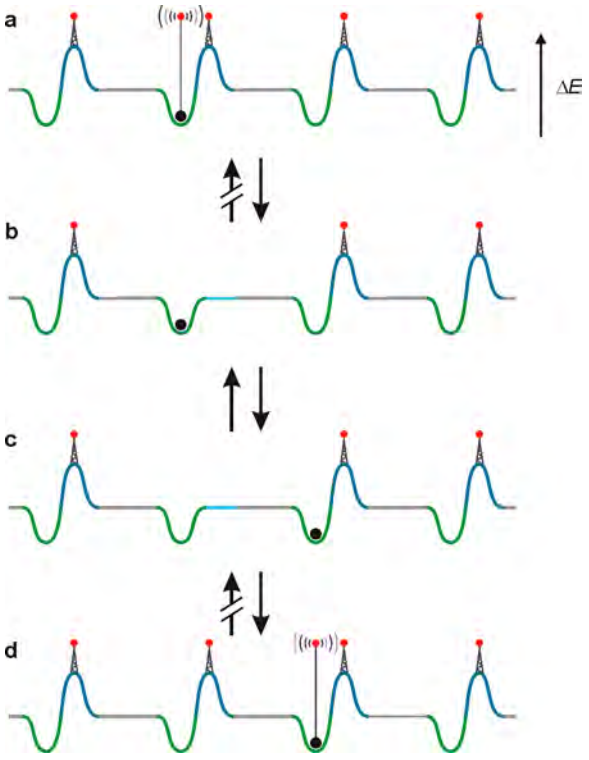

Figure 5. Operation of an information ratchet. A Brownian particle (black circle) can move directionally by selective lowering of the barrier in front of it along the direction of motion. This requires transfer of information from the particle to the landscape, which can be achieved, for example, if the particle signals its position by interacting with the landscape in a distance-dependent manner, as schematically depicted in (a) and (d).

plays the role of a photocontrolled gate for the motion of the macrocycle between the two recognition sites. With the stilbene unit in the *E* form—that is, with the gate open—the system is at thermal equilibrium, and the distribution of the ring between the two sites, namely, 65(DBA):35(MBA), reflects their relative affinities for the ring (Figure 6a). To drive the ring distribution away from equilibrium, the gate should be closed most of the time and opened preferentially when the macrocycle occupies a specific position (in this case the DBA station). The first requirement is obtained by adding to the solution a suitable photosensitizer (benzil), which leads to a photostationary state rich in the *Z* form of MS by *inter*molecular triplet sensitization. The second requirement is accomplished by appending to the ring another photosensitizer (benzophenone) that is capable of causing the *E*–*Z* photoisomerization of the stilbene gate by *intra*molecular triplet sensitization. Benzophenone was chosen because it leads to a photostationary state richer in the *E* isomer of MS compared with benzil. A key feature of the system is that the DBA station is very close to the stilbene gate, whereas the MBA station is far from it. Therefore, it can be expected that intramolecular (benzophenone) sensitization (i.e., gate opening) is more efficient when the macrocycle is in the DBA compartment, whereas the efficiency of intermolecular (benzil) sensitization should be independent of the position of the macrocycle. Conditions are chosen so that the benzophenone-sensitized isomerization dominates (gate open) when the ring is in the DBA compartment—that is, held near the gate (Figure 6b)—whereas the benzil-sensitized reaction dominates (gate closed) when the ring is in the MBA compartment—that is, held far from the gate (Figure 6c).

The system starts with the gate open (*E*-MS) and an equilibrium ring distribution of 65(DBA):35(MBA). Light irradiation in the presence of a suitable amount of benzil brings the system to a photostationary state in which the ring distribution becomes 45(DBA):55(MBA). In other words, about one-third of the macrocycles that occupied the more energetically favorable DBA site at equilibrium have been moved to the less favorable MBA compartment. Ultimately, the difference in the photoreactivities of the various interconverting isomers of $\mathbf{2}^{2+}$ (Figure 6) leads to a ring distribution between the two sites under light irradiation that is different from that observed at equilibrium in the dark.

It should be pointed out that in this system photons are not used to modify the binding energy between the ring and either station but rather to power an information transfer process, as schematically indicated in Figure 5. In fact, driving the ring distribution away from its equilibrium value is ensured only by the fact that the macrocycle "signals" its position to the gate, which opens (or closes) accordingly. The similarity of these processes with the hypothetical task performed without an energy input by Maxwell's demon in the famous thought experiment has been extensively discussed.[31,36,109] However, rotaxane $\mathbf{2}^{2+}$ and other similar molecular information ratchets[99,104] do not threaten the second law because of the required energy input. For the reasons discussed in the previous section, $\mathbf{2}^{2+}$ is not a molecular motor because directed transport steps cannot be repeated in a short rotaxane structure. A way to obtain an infinitely periodic energy profile with a small molecule is to resort to a catenane structure.[104]

1.3. Energy Supply and Autonomous Behavior

As pointed out earlier, movement is an intrinsic (and unavoidable) property of molecular systems. Because of the second law of thermodynamics, however, molecular machines cannot be driven by thermal energy at a constant temperature: to perform a task they have to be fueled by an energy source. This feature is shared with macroscopic machines. A common operation mode of the latter relies on temperature differences obtained by burning of a fuel, as happens in combustion engines. As pointed out by Feynman,[12] such a mechanism is impossible for molecular machines because of the very fast heat dissipation over nanometer distances. Nevertheless, the vast majority of biomolecular motors are powered by an exergonic chemical reaction—namely, ATP hydrolysis—that happens at constant temperature. In these systems, motion arises from a complex mechanochemical cycle that couples binding/unbinding events with the fuel reaction in such a way that the energy of ATP hydrolysis is eventually converted into mechanical work.[1−6]

The way in which energy is administered to an artificial molecular motor is a crucial issue that has to be carefully considered from the initial design stages to the experimental validation of the motor operation. Three fundamental approaches can be employed to supply energy to chemical systems and thus to power molecular machines and motors.

1.3.1. Chemical Stimulation. The most straightforward way to feed energy into a chemical system is by adding a reactant ("fuel") that undergoes an exoergonic reaction, as happens in biomolecular motors. Ideally, the fuel has to be delivered where and when needed. Its reaction will necessarily generate products ("waste") that, even in the favorable case where they do not interfere with the operation of the machine, will accumulate in

DOI: 10.1021/acs.chemrev.9b00291
Chem. Rev. 2020, 120, 200−268

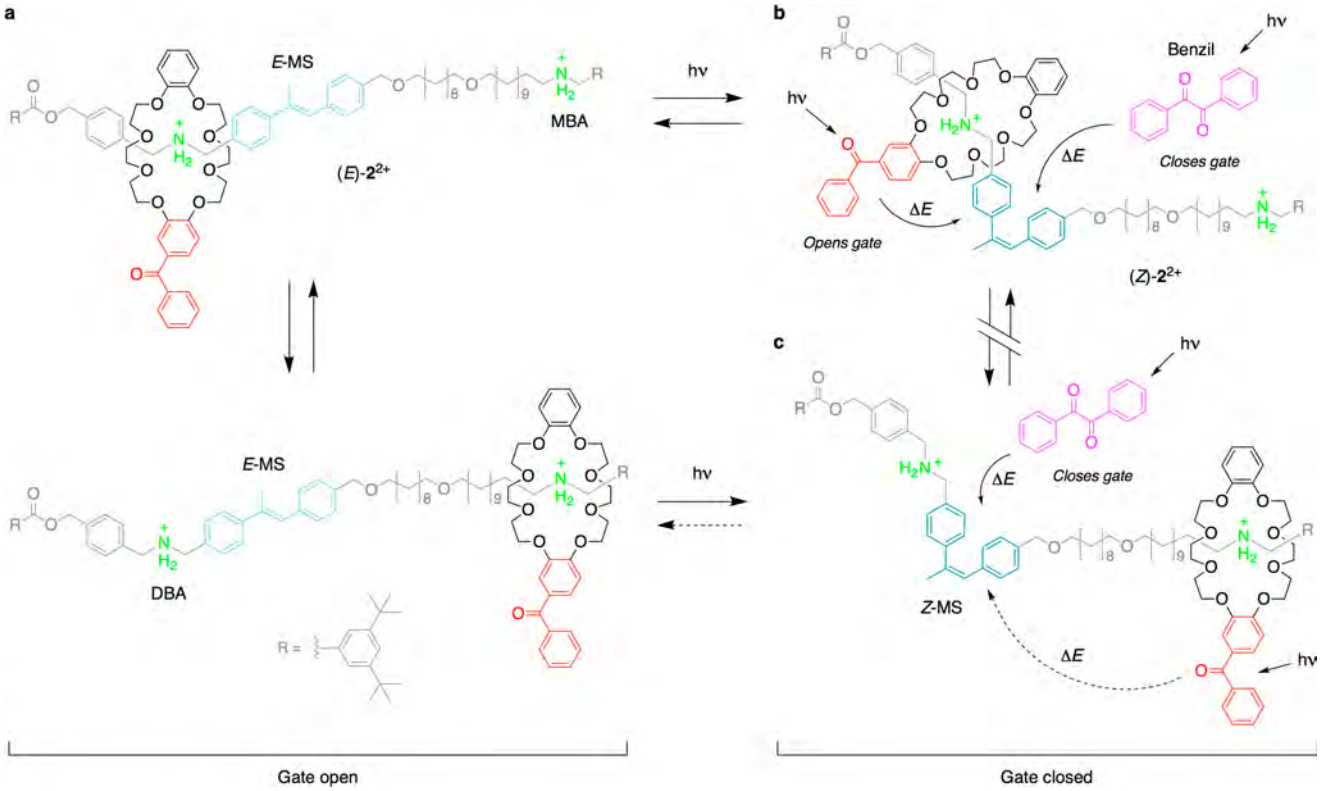

Figure 6. Molecular information ratchet based on the photoisomerizable bistable rotaxane $\mathbf{2}^{2+}$.[108] Dashed arrows indicate processes that are unlikely to occur.

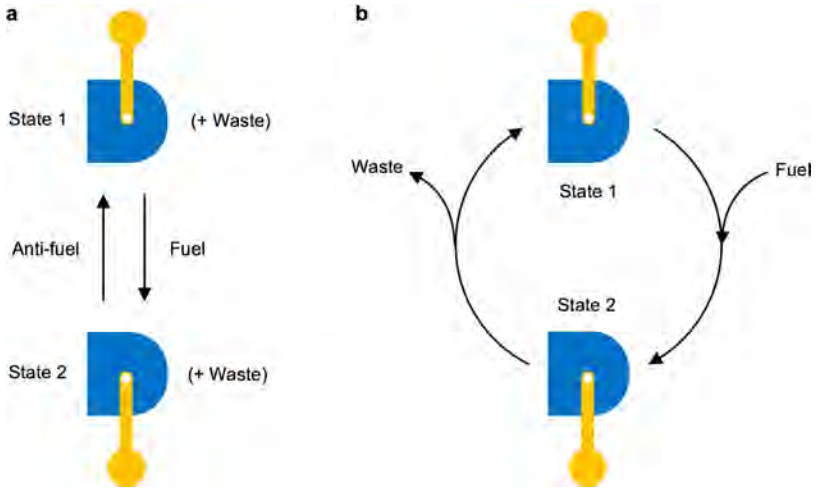

Figure 7. (a) Schematics of a molecular system that exploits two different reactants (a fuel and an antifuel) to switch between two structurally different equilibrium states. Repeated switching (cycling) requires the sequential addition of fuel and antifuel. (b) An autonomous chemically driven molecular machine that exploits the catalytic decomposition of a fuel to perform the transformation between two structurally different states. The process can continue indefinitely without the intervention of an operator as long as the fuel is available. In both cases, waste products are formed.

the reaction medium unless they are appropriately removed. It is worth noting that the waste of ATP-driven motor proteins—namely, ADP and inorganic phosphate—is not only removed but also recycled into new fuel by ATP synthase, providing a magnificent example of circular economy at the molecular scale.

An important quality of chemically driven molecular machines is the way in which they exploit the fuel. If the reaction of the fuel leads the system into a new equilibrium state, as happens in thermodynamically controlled molecular switches, another reactant (the "antifuel") must be added in sequence to reset the switching process and close the cycle (Figure 7a). Such behavior, which requires alternating additions of fuel and antifuel (simultaneous addition of the fuel and antifuel would normally lead to a fast reaction between them, thereby nullifying their function), results in an "operator-dependent" working cycle. In other words, the machine is not capable of using the chemical energy input in an *autonomous* fashion. This is the most common situation for artificial molecular machines and motors developed to date, in which the fuel/antifuel are typically oxidant/reductant or acid/base reactants.

DOI: 10.1021/acs.chemrev.9b00291
Chem. Rev. 2020, 120, 200−268

In contrast, biomolecular motors can autonomously repeat their operating cycle without external intervention as long as the fuel is available. This is the case because such systems exploit the fuel in a catalytic manner; that is, they act as catalysts for the decomposition of the fuel (Figure 7b). While performing the catalytic cycle during which the fuel is transformed, the molecular motor travels along different mechanical states, ultimately exhibiting controlled motion. As a matter of fact, myosin and kinesin are catalysts for the hydrolysis of ATP that are able to use the resulting energy to bias Brownian motion. Only one case of an autonomous fuel-driven synthetic molecular motor has been described to date,[104] and examples based on redox processes have not yet been reported.

A key feature of the catalytic operation mode is that the different mechanical states of the motor are not equilibrium states for the whole system (motor *and* fuel). The system operates away from thermodynamic equilibrium, which is eventually reached when the fuel is gone. It is worthwhile to recall, however, that out-of-equilibrium conditions can also be obtained with carefully designed molecular machines that consume a fuel and an antifuel in a nonautonomous fashion (see, e.g., section 2.3). Therefore, the ability to autonomously exploit an energy source is a desirable but not essential requirement for a molecular motor.

1.3.2. Electrical Stimulation. Macroscopic motors powered by electrical energy are widely used in all fields of technology. One may wonder whether it is possible to use electrical energy to power molecular motors too. If one considers molecular motors operating via chemical reactions, the answer is yes, because it is well-known that redox reactions promoted by the application of electrical potentials can cause structural changes in (supra)molecular systems.[42−46,110,111] If a reversible redox couple is utilized, after the forward reaction is triggered, the return to the starting species is made possible by changing the applied potential, and a switching process can be carried out without the formation of waste (although waste products may be formed at the counter electrode, they can be kept separated from the operating environment of the machine). Electrical potentials, unlike the addition of chemical oxidants and reductants, are readily turned on and off and can be applied locally with high resolution by means of ultramicroelectrodes and related probe microscopy techniques.[112] Electrochemistry offers powerful analytical tools (e.g., the various kinds of voltammetry) to characterize molecular-scale systems from both the thermodynamic and kinetic points of view as well as convenient ways to interface them with the macroscopic world through modification of the electrodes. In summary, by exploiting electrochemically induced processes, one can "write" (i.e., cause changes) and "read" (i.e., monitor) chemical systems with control in time and space.

Electrical energy can also be supplied to chemical systems without causing redox processes. For example, individual molecules deposited on a conducting surface could be electronically and/or vibrationally excited by the application of an appropriate voltage with a local probe, such as the tip of a scanning tunneling microscope (STM). In recent years, this approach was followed to accomplish directed motion of single molecules on surfaces,[113] leading to outstanding examples of rotary motors[114,115] and "nanocars"[116,117] that can be engaged in nanoscale races.[118,119] Another possibility is to use externally applied variable electric fields to drive the directional rotation of surface-mounted molecular rotors comprising dipolar subcomponents.[27,32,120] Systems of this kind are not only highly fascinating from a fundamental viewpoint but also potentially useful for nanofluidics and the development of ferroelectric materials. Although several molecular dynamics simulations studies are available, in only a few cases have the molecules been synthesized and investigated under the influence of an electric field.[121,122] These devices will not be described in detail here because redox processes are not at the basis of their functioning.

1.3.3. Optical Stimulation. Although sunlight is the sole energy input on which our planet can rely, the direct conversion of solar radiation—or, more generally, light energy—into mechanical movements is a rare event in nature. At the molecular level, a remarkable example of photoinduced motion to perform functions is provided by retinal, the chromophore involved in vision and in bacteriorhodopsin proton pumps.[123] In biological systems, light energy is converted through photosynthetic processes to produce chemical fuels for the very same reasons related to the exploitation of solar energy in technology: sunlight power is diffuse and intermittent, and it has to be converted to other forms to be accumulated or transported.[124,125] On the contrary, chemical fuels such as the ATP suitable for powering biomolecular motors can be stored and delivered on command.

Nevertheless, light energy can cause reactions that involve large structural changes in molecular systems, thus transforming optical stimuli into motion. Several classes of photochemical reactions of organic and inorganic species, such as isomerization, dimerization, addition, rearrangement and decomposition, may be considered for this purpose.[126−128] It is also well-known that electronically excited states generated by the absorption of light possess significantly different redox and acid−base properties with respect to the ground state, thus allowing photoinduced electron- and proton-transfer processes, which can also cause major displacements of the molecular parts in multicomponent systems. For a more detailed description of these phenomena, see section 3.2.

The use of optical stimuli to power artificial molecular machines has several advantages with respect to chemical fuels. First of all, by relying on clean and reversible photochemical reactions, it is possible to design machines powered solely by light that do not generate waste. Modulation of the wavelength and intensity of light in relation to the absorption spectrum of the targeted species enables careful control of the amount of energy supplied to the system. Such energy can be transferred to the molecule without any physical connection, or "wiring", to the source; the only requirement for remote excitation is the transparency of the matrix at the irradiation wavelength. Light may also be delivered to particular places (e.g., inside an instrument or in the human body) with the aid of optical fibers. Modern light sources such as lasers and light-emitting diodes enable investigations in very small spaces and extremely short time domains, and excitation with nanometer resolution is possible with near-field techniques. Conversely, parallel addressing of a very large number of individual molecular machines can be achieved upon irradiation of large areas and volumes. Another significant difference between chemically driven and light-driven molecular machines[129] is that photoinduced processes can directly result in motion and generation of force, thus deterministically relating the energy input with the "power stroke" of the machine. Last but not least, as already pointed out in the previous section for electrochemical inputs, the interaction between photons and molecules can both supply the energy necessary for the functioning of the machine and

DOI: 10.1021/acs.chemrev.9b00291
Chem. Rev. 2020, 120, 200−268

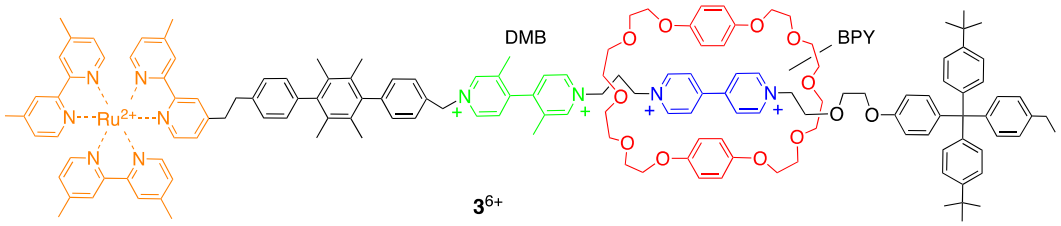

Figure 8. Structural formula of the photochemically driven molecular shuttle 3^{6+}.[135]

provide information about its state by means of spectroscopic techniques.[130,131]

A further element of interest about optical stimulation is that the use of reversible photochemical processes in appropriately designed molecules can enable the development of motors that function autonomously, that is, repeat their operating cycle under constant experimental conditions as long as the light source is available. This result is achieved by devising a mechanism based on a photoinduced sequence of processes that lead the system through transient electronic and (co)-conformational (mechanical) states, with the final deactivation of the system to the ground state providing an automatic reset and closing the cycle.[132] The successive absorption of another photon triggers a new cycle, and the process can be repeated indefinitely at a frequency that depends on the time scale of the transformations comprised in the operating cycle (unless irradiation is performed at such a low flux that the rate of incoming photons determines the reaction rate).

These concepts are exemplified by the [2]rotaxane 3^{6+} (Figure 8), a molecular machine designed to exploit the energy of visible light in an autonomous manner to repetitively shuttle a macrocycle back and forth along a track.[133] The ring component of 3^{6+} is a π-electron-rich crown ether, whereas the axle comprises several covalently linked units, namely, a Ru(II) polypyridine complex, a *p*-terphenyl-type rigid spacer, π-electron-poor 4,4′-bipyridinium (BPY) and 3,3′-dimethyl-4,4′-bipyridinium (DMB) units, and a tetraarylmethane group as the terminal stopper. The ruthenium-based moiety plays the dual role of a photosensitizer and a stopper, whereas the mechanical switch consists of the two electron-poor recognition sites and the electron-rich macrocycle. In the stable co-conformation of the rotaxane, the ring encircles the BPY site because it is a more efficient electron acceptor than the DMB one.

The photoinduced shuttling of the macrocyclic ring between the BPY and DMB sites is based on a four-step sequence of electron transfer and molecular rearrangement processes (Figure 9a). Visible-light excitation of 3^{6+} (process 1) generates the lowest singlet excited state (^{1}MLCT) of the Ru-based unit, which quickly deactivates to the lower-lying triplet level (^{3}MLCT). This triplet is relatively long lived (~1 μs in deoxygenated solution at room temperature), and the redox potential for its oxidation is ca. −0.8 V versus the standard calomel electrode (V vs SCE). As the monoelectronic reduction of BPY takes place at about −0.4 V vs SCE, the transfer of an electron from the excited Ru-based moiety to the BPY site (process 2) is thermodynamically downhill. This reaction is in competition with the inherent decay of the ^{3}MLCT state (process 3).

After the reduction of the BPY recognition site and its consequent deactivation, the macrocycle migrates by 1.3 nm to encircle the DMB unit (process 4). This process competes with the back electron-transfer from the reduced BPY site, still surrounded by the ring, to the oxidized photosensitizer (process

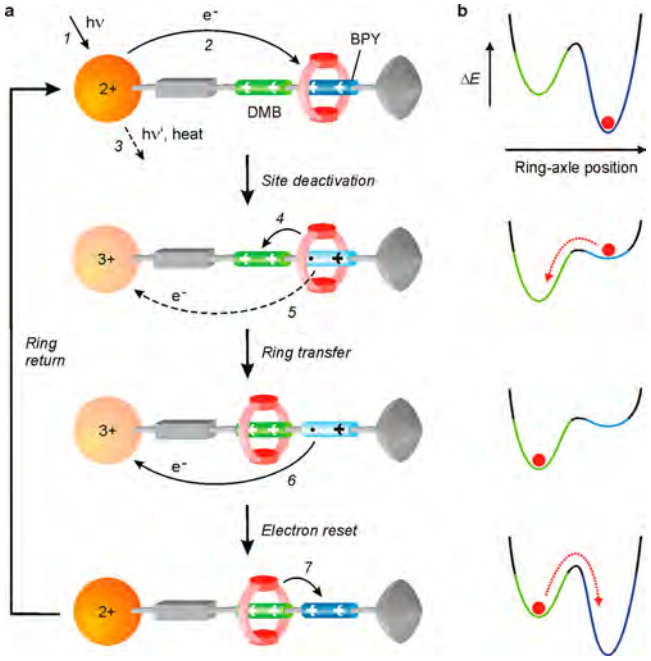

Figure 9. (a) Schematic representation of the autonomous light-driven shuttling of 3^{6+}.[133] Processes 2 and 4 are in competition with undesired reactions, represented by dashed lines. The mechanism is based solely on intramolecular processes and no waste is produced. (b) Simplified potential energy profiles for each structure in (a) as a function of the ring−axle relative position.

5). Once the macrocycle has moved away from its starting location, back electron-transfer from the reduced (and uncomplexed) BPY unit to the oxidized Ru-based unit (process 6) regenerates the primary recognition site by restoring its electron acceptor properties. As a consequence of such an "electronic reset", the ring moves from DMB to BPY by Brownian motion (process 7).[134] The cycle is thus completed, and the rotaxane is ready to process another photon. Therefore, the spontaneous thermally driven reset of the molecular machine enables its autonomous operation under the supply of light energy at a frequency of about 1 kHz at room temperature.

As happens for macroscopic motors, the successful operation of this nanomachine relies on a correct synchronization of the processes at the basis of the mechanism (Figure 9). Such a result implies fine control of the kinetics and can be achieved by careful structural design. Because of competition with undesirable energy-wasting processes (primarily the back electron-transfer process; step 5 in Figure 9), the overall quantum yield for ring shuttling is only 2%. The molecular shuttle 3^{6+} can also be operated with a higher quantum yield by a sacrificial mechanism involving irreversible reducing (triethanolamine, **tea**) and oxidizing (O_2) species (Figure 10a)[135] and by an intermolecular

DOI: 10.1021/acs.chemrev.9b00291
Chem. Rev. 2020, 120, 200−268

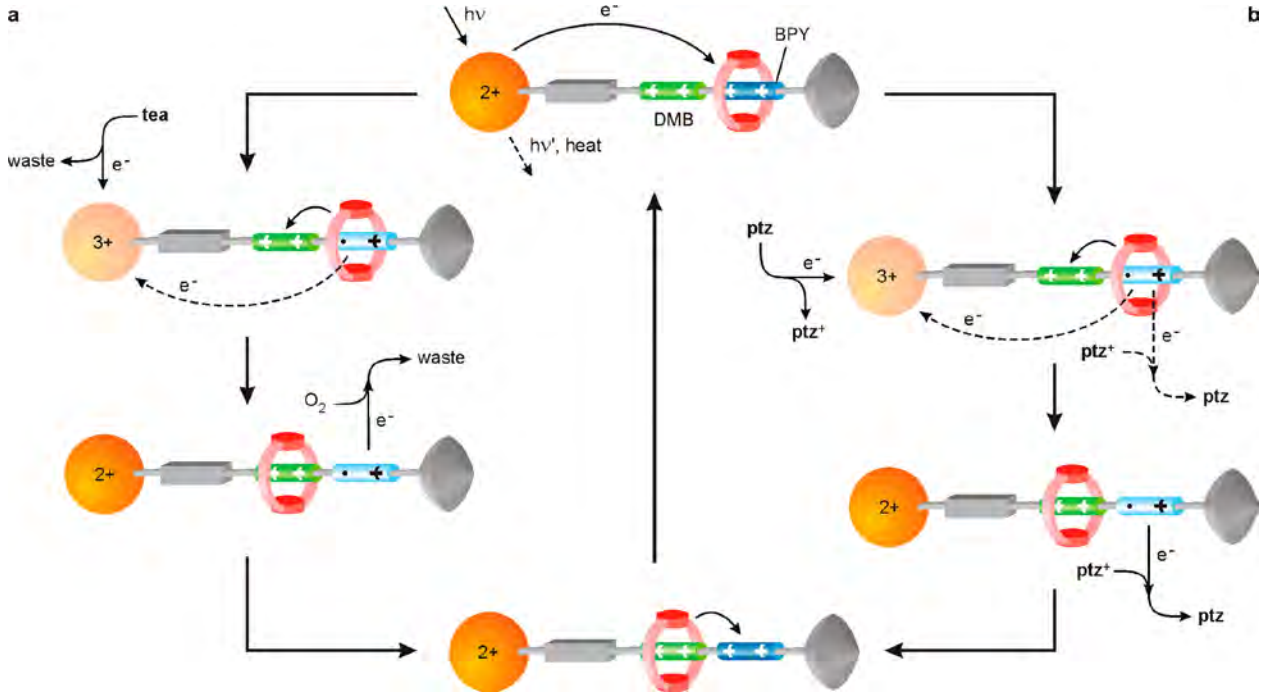

Figure 10. Alternative mechanisms for the photochemically triggered ring shuttling in $\mathbf{3}^{6+}$: (a) nonautonomous operation involving two sacrificial fuels; (b) photon-only autonomous operation assisted by an electron relay.

mechanism based on the kinetic assistance of a reversible electron relay (phenothiazine, **ptz**; Figure 10b).[133,136] The sacrificial mechanism, however, does not allow autonomous operation and leads to consumption of chemical fuels and concomitant formation of waste. On the other hand, the assistance by an electron relay affords autonomous behavior in which only photons are consumed, but the mechanism is no longer based solely on intrarotaxane processes and becomes concentration-dependent.

In summary, $\mathbf{3}^{6+}$ is a remarkable example of how optical inputs can be processed by a suitably designed molecule to achieve controlled motion. The result is a molecular machine (not a motor) that (i) consumes only visible photons, (ii) operates autonomously, (iii) follows a unimolecular mechanism, and (iv) does not produce waste. Alternatively, the ability of a molecular machine to exploit light energy in an autonomous fashion can arise from photoinduced switching between different forms of the photochromic compounds. Examples of this kind will be described in section 3.

In addition to the advantages discussed above, the use of light to power nanoscale devices and machines has a more profound justification. It is clear to (almost) everyone that the energy problem and climate change are the most critical issues that humankind has to face in the coming years, and it is clear that the products of a future nanotechnology-based industry will have to be powered by renewable and clean energy sources. In this context, the construction of molecular motors—including biomimetic[137] and artificial–natural hybrids[138,139]—that can harness solar energy in the form of visible or near-UV light is certainly an interesting possibility.

2. REDOX-DRIVEN MOTORS

2.1. General Considerations

As discussed in the previous sections, nature does not use redox reactions to directly power movement in biomolecular motors.[125] Nevertheless, electron transfer processes are of crucial importance in many biological processes, particularly in combination with proton transfer, for both energy transduction and signal transmission. For example, in photosynthesis the captured light energy is converted into chemical energy by means of electron transfer reactions.[123−125] Furthermore, in aerobic organisms the reduction of oxygen to water, catalyzed by cytochrome *c* oxidase, generates an electrochemical potential across the mitochondrial (or bacterial) membrane that results in proton pumping against a chemical gradient, ultimately driving the synthesis of ATP by the ATP synthase rotary motor.

From an artificial standpoint, redox reactions are an appealing option to power molecular motors because of the wide choice of molecular redox switches and their versatile application in multicomponent species.[42−46] Redox processes in solution can be accomplished by addition of chemical reactants, by exploiting photoactivated electron transfer processes, or by heterogeneous electron transfer reactions achieved by applying appropriate electrical potentials to conducting electrodes. The use of oxidizing or reducing agents enables the controlled oxidation or reduction of a bulk solution, but it brings about all the limitations related to the addition of chemical reagents (see section 1.3.1). Redox processes induced by light involve the transfer of an electron from (or to) an excited photosensitizer to (or from) the redox-active unit. The photosensitizer can be either integrated within the molecular components or added in solution to give a bimolecular reaction (see section 1.3.3). Molecular motors powered by photoinduced redox reactions will be described in section 3.

The advantages of using an electrochemical setup to trigger redox processes in the context of molecular machines have been discussed in section 1.3.2. It is worth recalling that electrical stimulation is also useful to afford redox processes in gels and solid materials, which can lead to mechanical actuation.[86,89,90] In general, the use of electrical energy to power mechanical

DOI: 10.1021/acs.chemrev.9b00291
Chem. Rev. 2020, 120, 200−268

nanoscale systems is very promising for prospective technological applications.

2.2. Useful Redox Processes

The majority of redox-driven molecular machines and motors[42−46] are based on catenane and rotaxane interlocked structures and rely on two general design approaches. The first one is based on redox control of the coordination geometry around transition metal ions.[25,26,32,66,140] Indeed, several transition metals can exist in different oxidation states and form a large variety of coordination complexes, whose nature (stoichiometry, geometry, ligand types) strongly depend on the oxidation state. Thus, a rearrangement of the coordination sphere can be induced by modifying the oxidation state of the metal ion with a redox stimulus. This strategy was originally developed by Sauvage and co-workers with a copper-containing [2]catenane.[141] One ring of the catenane contains a bidentate phenanthroline ligand, whereas the second macrocycle has two chelating sites, namely, a phenanthroline and a tridentate terpyridine ligand. As Cu(I) adopts a tetrahedral coordination geometry, in the Cu(I) catenane the rings are arranged in such a way that the metal ion is surrounded by the two phenanthroline ligands. On the other hand, Cu(II) prefers to be pentacoordinated, and therefore, upon oxidation of the Cu(I) to Cu(II), the catenane undergoes a rearrangement that enables coordination of the metal ion to one phenanthroline and one terpyridine ligand. The initial situation is restored upon successive reduction of Cu(II) to Cu(I).

This strategy[142] has also been successfully implemented with rotaxane-based systems, in which different polypyridine ligands are incorporated in either the axle or the ring component.[143−148] Interestingly, the metal ion plays the dual role of a templating element that enables the synthesis of the interlocked structure and a redox-switchable unit that drives the mechanical motion. Demetalation of the MIM and successive remetalation with a different ion (or the same ion in a different oxidation state) was also employed to bring about molecular rearrangements.[145,149,150]

The second approach to the design of redox-controlled mechanical devices is based on modulation of the electron donor−acceptor interactions that occur between the molecular components of the interlocked structure.[151−155] This strategy was originally developed by Stoddart, Kaifer, and co-workers[156] with a rotaxane comprising a CBPQT cyclophane[107] and an axle containing two π-electron-donor units, namely, biphenol and benzidine. This rotaxane exists as two translational isomers, wherein the macrocycle resides either on the benzidine station (84% occupancy) or the biphenol station (16% occupancy). Upon oxidation of the former unit, electrostatic repulsion is established between the positively charged macrocycle and the oxidized benzidine, and the CBPQT ring moves to encircle the biphenol station exclusively. Since this seminal work, a large variety of donor−acceptor pairs have been exploited in the design and construction of redox-switchable molecular machines.[42−46,157] Actually, a vastly exploited donor−acceptor combination is the one involving 4,4′-bipyridinium moieties[107,158] as electron acceptors and tetrathiafulvalene (TTF) derivatives[159−163] as electron donors (see, e.g., compound $\mathbf{1}^{4+}$ in Figure 3). This recognition motif, characterized by a clean and reversible dual switching mode (i.e., TTF oxidation or bipyridinium reduction),[164] has been included in several supramolecular complexes[165−167] and MIMs[105,168−170] with potential for applications.[171,172]

More recently, another class of redox reactions has proven useful for the design of artificial molecular machines, i.e., the supramolecular association of chemically or electrochemically generated radicals in solution. The prototypical example of this kind of reaction is the dimerization of bipyridinium-based radical cations, obtained by reduction of the corresponding dications, in aqueous media.[173] Such a process, also called pimerization, can be favored in the presence of a neutral host, such as a cucurbituril[174] or cyclodextrin,[175] whose cavity can encapsulate the dimer. The pimerization of bipyridinium radical cations has been exploited as an alternative recognition motif for new switchable host−guest complexes.[176] As a matter of fact, a two-electron-reduced CBPQT macrocycle (containing two bipyridinium radical cations) and a monoreduced bipyridinium-based axle can self-assemble,[177] forming strong host−guest complexes stabilized by radical−radical interactions. This strategy has been harnessed for the construction of (pseudo)-rotaxanes,[176,178,179] two- and three-station rotaxanes,[176] and catenanes.[180−183]

It is worth noting that in a supramolecular context, a redox reaction can be used to affect the minima and/or the maxima of the potential energy surface that determines the mutual arrangement of the molecular components. As an example, the pimerization reaction of bipyridinium units can be considered: upon reduction a stabilizing interaction is established between the radical cations, which means that an energy well is formed. On the other hand, reoxidation of the radicals to the doubly charged species installs an electrostatic repulsion, and the energy well is converted into a barrier. The possibility to tune the electrostatic interactions for modulation of the potential energy surface associated with the motion is particularly valuable when designing molecular motors that need to rely on energy ratchet mechanisms (see section 1.2.1).

Another process triggered by redox reactions that can be useful for molecular machines is the geometrical isomerization of double bonds such as C═C (e.g., in stilbene derivatives),[184−186] C═N (e.g., in imine and hydrazone derivatives),[187,188] and N═N (e.g., in azobenzene derivatives).[189,190] Oxidation or reduction of the molecule can lower the rotation barrier around a double bond by increasing its single-bond character; moreover, catalytic mechanisms involving radical species can be activated, leading to fast isomerization. Hence, molecular machines operated by photoinduced isomerization of C═C, C═N, and N═N double bonds (see section 3.2) could also be controlled, in principle, by redox stimulation.

It should be noted that although many examples of redox-driven molecular machines have been reported in the literature,[42−46] only a few of them can be considered as molecular motors (see section 1).

2.3. Supramolecular Pumps

Molecular pumps are linear motors in which a molecular substrate is directionally transported with respect to the motor component. The transport must be active, that is, intrinsically performed by the motor using its energy source, without relying on external concentration differences; in principle, it should take place *against* a concentration gradient. In this regard, molecular pumps are energy transducers capable of converting the energy input of the device into a chemical potential; in other words, they can use an external energy source to generate a nonequilibrium state.[191] This behavior is opposed to that of passive transporters, which simply facilitate the system to relax to equilibrium: the cargo moves down a concentration gradient,

DOI: 10.1021/acs.chemrev.9b00291
Chem. Rev. 2020, 120, 200−268

eventually exhausting it. It should be recalled that the controlled transport of molecular and ionic substrates across biological membranes that define and separate compartments is a fundamental task for living organisms.[1−4,191] The construction of artificial molecular devices capable of performing such a function is motivated by the high basic science value and the potential for technological and medical applications and constitutes a flourishing area of research in supramolecular chemistry.[37,192−195]

In recent years, artificial molecular pumps have been realized by following supramolecular design approaches based on (pseudo)rotaxane architectures. If the axle is defined as the "track" of the motor, then in these systems the ring component may be directionally moved (i.e., transported) along the track. It is worth noting, however, that in homogeneous solution, wherein none of the molecular components is connected to a fixed reference system, only relative movements can be considered, and the distinction between the "transporting" and "transported" components is purely conventional. Two different classes of pumps have been described, depending on the nature of the system.[196] On the one hand, in a pseudorotaxane complex, the ring and axle molecules may undergo unidirectional threading and dethreading. It can be envisaged that the ring becomes associated with the axle by passing over a specific extremity of the latter; successively, the ring dissociates by exiting from the opposite side (Figure 11a).

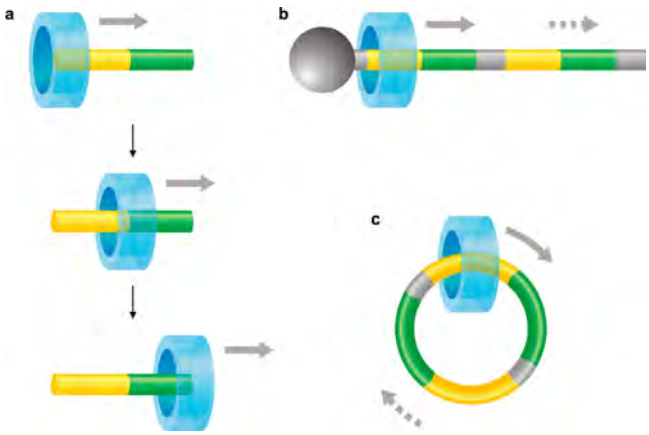

Figure 11. (a) Schematic representation of the relative unidirectional transit of a macrocycle along a nonsymmetric molecular axle. By incorporating the system shown in (a) into a rotaxane (b) or a catenane (c), linear or rotary motors may be obtained, respectively.

On the other hand, semirotaxane architectures have been reported in which a molecular ring passes over the unstoppered end of the axle, travels directionally along it, and is eventually blocked in the stopper-terminated portion of the axle. In both classes the pumping cycle can be repeated, resulting in the passage of successive rings along the axle in the pseudorotaxane species or the accumulation of more than one ring on the axle in the semirotaxane species. In the former case, the threading−dethreading cycle can produce a net effect only if the transport involves spatially separated "departure" and "arrival" compartments. This result could be achieved, for example, by a membrane that provides the boundary of the compartments and the fixed support for the "transporting" component of the pump.[197] Conversely, in the semirotaxane case the macrocycle(s) can be pumped energetically uphill along the axle, which thus acts as a "reservoir" of ring(s) in a metastable state. Therefore, chemical energy can in principle be stored in the system, even in homogeneous solution.

It should also be pointed out that the development of a pseudorotaxane motif capable of performing unidirectional threading and dethreading processes under the control of external stimuli (Figure 11a) would be useful for the construction of processive linear motors based on rotaxanes (Figure 11b) and rotary motors based on catenanes (Figure 11c).

The problem of obtaining directionally controlled threading−dethreading movements in pseudorotaxanes with appropriately designed nonsymmetric components has been discussed by several research groups.[198−204] Arduini, Credi, Venturi, and co-workers succeeded in directionally threading an oriented bipyridinium-containing axle into a calix[6]arene macrocycle and preventing back-dethreading by stoppering one end of the axle.[101] The electrochemical reduction of the bipyridinium unit did not cause dethreading, which was obtained, however, by changing the solvent. Although the challenge of realizing a stimuli-responsive molecular pump was met, the rather unpractical switching conditions and the need to perform a selective destoppering reaction to reset the device limited the interest of this approach.

The first example of a redox-driven molecular pump was reported by Stoddart and co-workers in 2013.[205] It is based on a pseudorotaxane consisting of a CBPQT macrocycle ($\mathbf{4}^{4+}$) and a nonsymmetric axle $\mathbf{5}^{+}$ that comprises a 1,5-dioxynapthalene (DNP) recognition site in the center and a neutral 2-isopropylphenyl (IPP) group and a positively charged 3,5-dimethylpyridinium (PY) unit at the two extremities (Figure 12a). The operating principle of the system is schematized in Figure 12b: $\mathbf{4}^{4+}$ encircles the axle on account of charge-transfer interactions with DNP (energy minimum). There are two possible paths for threading, but they are characterized by different energetic barriers. In fact, the Coulombic repulsion between $\mathbf{4}^{4+}$ and the charged PY unit is stronger than the steric interaction with the neutral IPP group.[206] Therefore, the passage of the ring is faster on the neutral group, and unidirectional threading is obtained. Upon reduction of the macrocycle, two effects are attained: (i) decreased stability of the complex (because the energy minimum is raised) and (ii) decreased Coulombic repulsion (with a drop of the energy barrier). Thus, an energy ratchet mechanism is effected (section 1.2.1): in the destabilized complex, the relative heights of the two kinetic barriers are reversed, and the reduced macrocycle passes over the PY end to dissociate, completing the unidirectional transit.

The redox processes were carried out by adding chemical reagents (Zn powder and oxygen as the reductant and oxidant, respectively), by performing an electrochemical reaction on a conducting electrode, and by exploiting photoinduced electron transfer from a ruthenium polypyridine complex used as a photosensitizer (section 3.3). Indeed, these results prove not only the solidity and flexibility of the reported system but also the general versatility of redox-controlled molecular devices. As pointed out above, this pump does not perform work because the ring is taken up from and released into the same solution. The operating cycle can be repeated, but the outcomes of successive cycles cannot sum up and lead to the buildup of an effect. Nevertheless, a system of this kind may prove useful for the realization of processive linear motors based on polymers or for "energy reservoir" rotaxanes. The latter systems consist of rotaxanes wherein the macrocycle is forced to surround a

DOI: 10.1021/acs.chemrev.9b00291
Chem. Rev. 2020, 120, 200−268

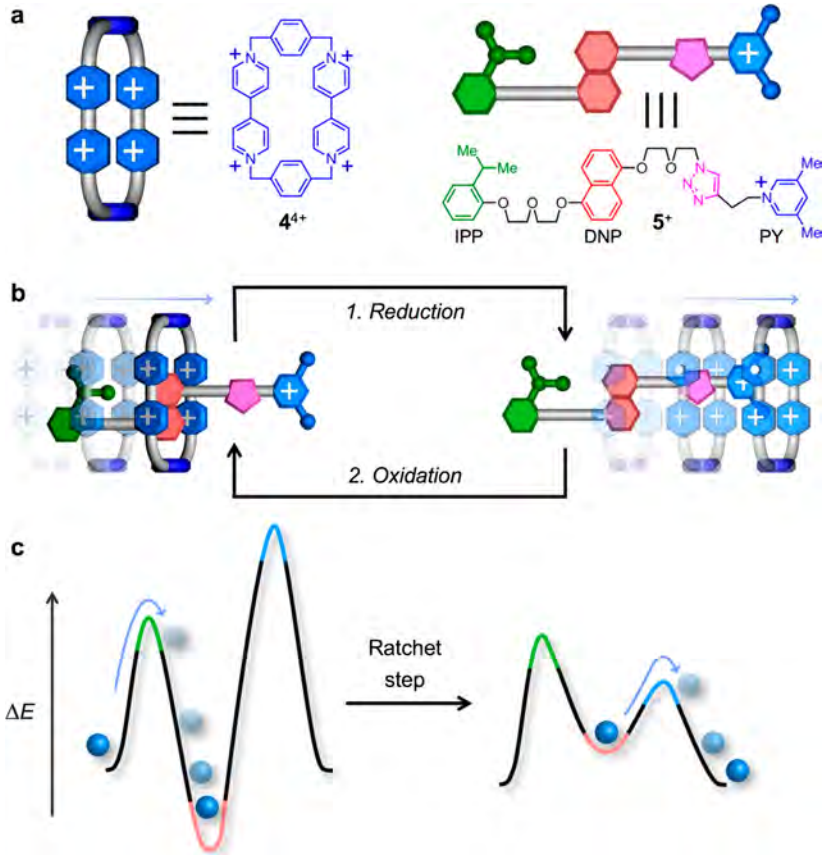

Figure 12. (a) Structural formulas of the molecular components $\mathbf{4}^{4+}$ and $\mathbf{5}^{+}$ of a redox-driven molecular pump. (b) Schematized operation mechanism of the molecular pump and (c) simplified potential energy surfaces. Unidirectional threading is accomplished by exploiting the electrostatic repulsion between CBPQT and PY; upon electrochemical reduction, the potential energy minimum increases and the potential energy maximum for the passage of CBPQT over PY decreases, thus forcing the macrocycle to dethread unidirectionally. Adapted from ref 205. Copyright 2013 American Chemical Society.

portion of the axle for which it has low or null affinity, forming a metastable state.[23,99,108]

The first attempt to realize a redox-driven version of such energetically demanding MIMs was based on a CBPQT ring ($\mathbf{4}^{4+}$ in Figure 12a) and a series of axle molecules $\mathbf{6a}-\mathbf{i}^{3+}$ (Figure 13) comprising in sequence a PY unit at one end, a short oligomethylene chain, a 4,4′-bipyridinium unit (BPY) as a recognition site for the macrocycle, a longer chain, and a bulky 2,6-diisopropylphenyl (DIP) stopper at the opposite end.[207] The operating principle, depicted in Figure 14, relies on modulation of the energy minima and maxima of the potential energy surfaces by tuning (i) the radical−radical interaction between the monoreduced bipyridinium moieties of CBPQT and BPY and (ii) the Coulombic repulsion between the oxidized macrocycle $\mathbf{4}^{4+}$ and the PY end unit. Upon electrochemical reduction, both the energy barrier for slipping through PY and the energy minimum are decreased, thus promoting the ring−axle association. Upon successive reoxidation, electrostatic repulsions are reinstalled, and both the barrier and the well increase again. The ring is forced to move away from BPY; as it cannot slip over PY, it has no choice but to reside on the oligomethylene chain. It was found that the half-life of this metastable state depends on the lengths of the spacers connecting the central BPY unit to the two different extremities. Interestingly, a longer chain on the side of the stopper stabilizes the complex by keeping BPY and CBPQT far apart, whereas a shorter chain on the PY side increases the Coulombic repulsion, thereby enhancing the chemical inactivity of the nonequilibrium state.

	m	n
$\mathbf{6a}^{3+}$	3	6
$\mathbf{6b}^{3+}$	3	8
$\mathbf{6c}^{3+}$	3	11
$\mathbf{6d}^{3+}$	4	8
$\mathbf{6e}^{3+}$	2	8
$\mathbf{6f}^{3+}$	2	6
$\mathbf{6g}^{3+}$	4	6

	n
$\mathbf{6h}^{3+}$	3
$\mathbf{6i}^{3+}$	4

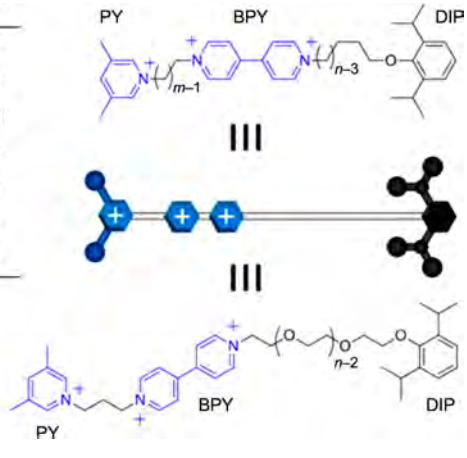

Figure 13. Structural formulas and cartoon representation of the axle components $\mathbf{6a}-\mathbf{i}^{3+}$ of a rotaxane that can pump one CBPQT macrocycle ($\mathbf{4}^{4+}$) energetically uphill. Adapted from ref 207. Copyright 2014 American Chemical Society.

Although these artificial supramolecular pumps can dissipate redox chemical energy to transport a molecular species to a high-energy state, their design did not allow the collection of more rings in the axle by repeating the operating cycle. Nevertheless,

DOI: 10.1021/acs.chemrev.9b00291
Chem. Rev. 2020, 120, 200−268

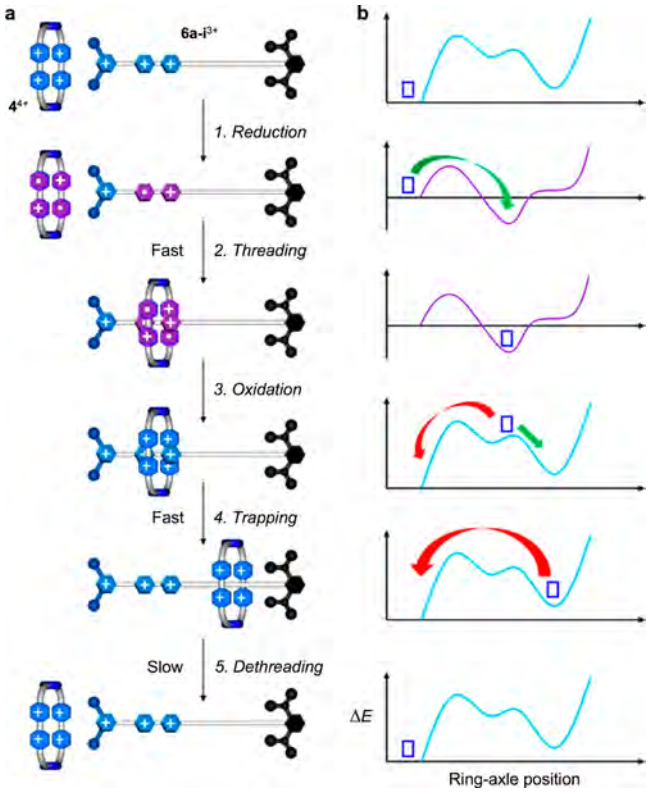

Figure 14. (a) Schematized mechanism and (b) potential energy curves for the pumping of macrocycle $\mathbf{4}^{4+}$ along axles $\mathbf{6a–i}^{3+}$ shown in Figure 13. Adapted from ref 207. Copyright 2014 American Chemical Society.

building upon these promising results, a more effective system was realized that is able to create a local concentration gradient by repetitively accumulating macrocyclic molecules along a portion of the axle.[208,209] The axle molecule $\mathbf{7}^{3+}$ (Figure 15) is derived from compounds $\mathbf{6a–i}^{3+}$ (Figure 13)[207] and is endowed with an IPP "steric speed bump"[206] between BPY and the collecting oligomethylene (OME) chain. The redox pumping mechanism is summarized in Figure 16. The first cycle of operation is similar to that of the previous example: the threading of the molecular components is triggered by electrochemical reduction of the axle and ring molecules, which enables the passage of the reduced CBPQT ring over PY and the formation of radical–radical stabilizing interactions. Upon reoxidation, the Coulombic repulsion between $\mathbf{4}^{4+}$ and the charged BPY and PY units destabilizes the complex and establishes an insurmountable kinetic barrier; consequently, the macrocycle overcomes the steric barrier exerted by IPP and moves toward the OME chain. In the second cycle of operation, a second ring is captured from the solution and transported into the collecting portion of the axle. Upon reduction, a competition for the monoreduced BPY site between a free and a complexed reduced CBPQT macrocycle is established. The IPP steric speed bump, however, provides a barrier for the return of the first entrapped ring onto the reduced BPY site, and threading of a second ring from the solution is kinetically favored. After reoxidation, the interaction is weakened and the electrostatic repulsion pushes the second ring onto the OME chain. Analysis of the kinetic and thermodynamic data for the systems suggested that the two ensnared CBPQT rings do not interact appreciably with one another; nevertheless, the number of cycles that can actually be performed depends on the length of the chain that collects the rings. Overall, this molecular pump can in principle operate repetitively, driving the system progressively further and further away from equilibrium.

Repetitive operation was demonstrated on an oligomeric dual pump[210] comprising two such modules[209] connected by a quaternary-ammonium-based carbon chain. By alternation of two constant potentials at −0.7 and +1.4 V, respectively, up to four CBPQT macrocycles could be loaded on the axle, thus forming a [5]rotaxane.

2.4. Molecular Rotary Motors

Two different architectures have been exploited for the realization of artificial rotary motors: interlocked structures based on catenanes[103,104,211,212] and molecular motors based on rotation around a covalent or coordination bond as the axis.[213] As a matter of fact, to date there are no examples of redox-driven molecular rotary motors based on catenanes, and only a few examples of rotation around single or double bonds triggered by electrochemical reactions are available.

Feringa and co-workers reported a series of molecular rotary motors based on overcrowded alkenes whose working principle is based on four alternating strokes of light and heat (see section 3.6.1).[213] By analogy to dithienylethene-based photochromic compounds, which can also be switched by electrochemical oxidation, the possibility to drive the rotary motor by redox stimulation has been explored.[214] The chosen structure, which belongs to the second generation of light-driven molecular rotary motors (see section 3.6.1),[215] contains sulfur atoms in both halves of the molecule. This structure is related to

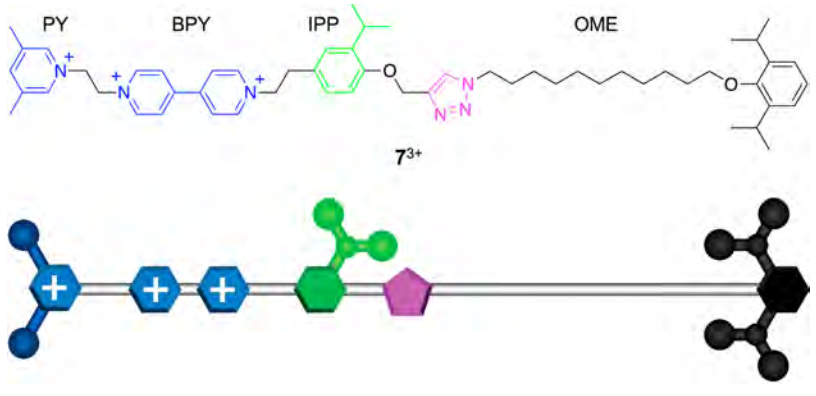

Figure 15. Structural formula and cartoon representation of the molecular axle $\mathbf{7}^{3+}$ that can collect more than one CBPQT macrocycle $\mathbf{4}^{4+}$ in its alkyl chain reservoir by redox pumping. Adapted with permission from ref 208. Copyright 2015 Springer Nature.

DOI: 10.1021/acs.chemrev.9b00291
Chem. Rev. 2020, 120, 200–268

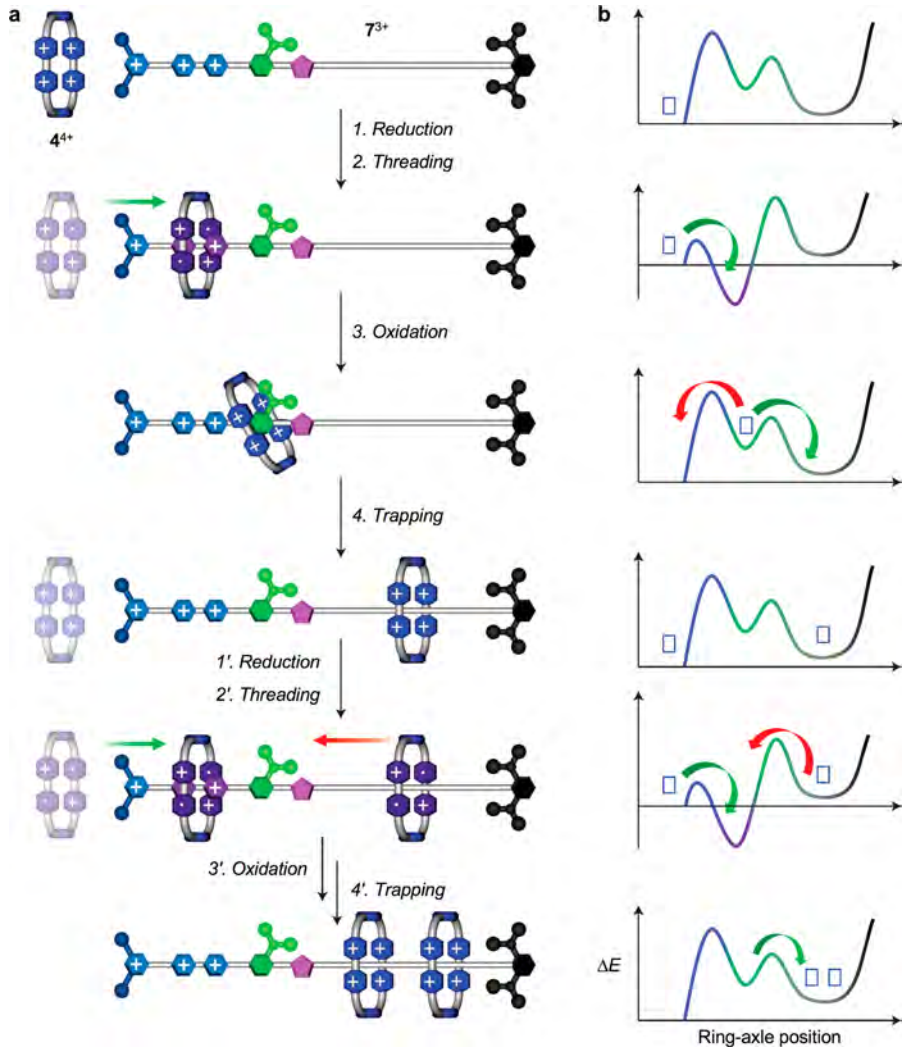

Figure 16. (a) Schematized mechanism and (b) potential energy curves for the pumping of macrocycle $\mathbf{4}^{4+}$ along axle $\mathbf{7}^{3+}$. Adapted with permission from ref 208. Copyright 2015 Springer Nature.

bis(thiaxanthylidene)s, which can be doubly oxidized, with loss of the double-bond character of the central C═C bond, and can subsequently undergo free rotation around the single bond. Indeed, upon oxidation of the molecular motor, an orthogonal conformation can be adopted; subsequent reduction restores the central double bond, possibly blocking the system in both stable and unstable conformations. Upon thermal helix inversion of the unstable conformation, a complete cycle would be accomplished. As a matter of fact, other redox-driven reactions prevent a full characterization of the system and its efficient operation; nevertheless, this study suggests a possible way to design redox-driven rotary motors.

Single bonds can intrinsically perform rotary motions, but in order make a motor, the random relative movements of the molecular components must be directionally biased by the intervention of an external input. The design of such motors[216] is based on a biaryl with three ortho substituents: A on the "lower" aryl unit and B and C on the "upper" aryl unit (Figure 17). Full rotation around the central axis is prevented by steric hindrance, and the molecule exists as two atropisomers (stations I and III in Figure 17). In order to obtain a rotary motor, the two aryl units must be able to perform a complete and unidirectional rotation. Two control elements are inserted in the system to fulfill these requirements: (i) a bridging unit that is able to bind to the ortho substituents in the upper and lower halves of the molecule, thus lowering the barrier for rotation, and (ii) a chiral element on group A, which converts the two atropisomers into two atrop-diastereomers with different energies. The structure of the molecular motor **8** is shown in Figure 18: A is a chiral sulfoxide, and B and C are a H and a Br atom, respectively; the bridging unit is palladium in two different oxidation states. The operation mechanism is schematized in Figure 18: Pd(II) reacts with the C−H ortho substituent of (*S*,*M*)-**8** to form the bridged complex Pd[(*R*,*P*)-**9**]XL, which is in equilibrium with the more stable Pd[(*R*,*M*)-**9**]XL isomer (X and L are anionic and neutral ligands, respectively). Subsequent transformation of the C−Pd bond into a C−H bond provides (*S*,*P*)-**8**, completing a 180° clockwise rotation. Treatment of (*S*,*P*)-**8** with a source of Pd(0) leads to the formation of the bridged complex Pd[(*R*,*P*)-**10**]BrL after an oxidative addition reaction on the C−Br bond. Again, the barrier to atropisomerization from Pd[(*R*,*P*)-**10**]BrL to Pd[(*R*,*M*)-**10**]BrL is lowered, and the equilibrium is shifted toward the latter compound. Reintroduction of the C−Br bond on Pd[(*R*,*M*)-**10**]BrL completes the 180° clockwise rotation, forming the starting compound (*S*,*M*)-**8**. It must be noted that in the first 180° rotation Pd(II) is converted into Pd(0) and in the second 180° rotation Pd(0) is converted into Pd(II); therefore,

DOI: 10.1021/acs.chemrev.9b00291
Chem. Rev. 2020, 120, 200−268

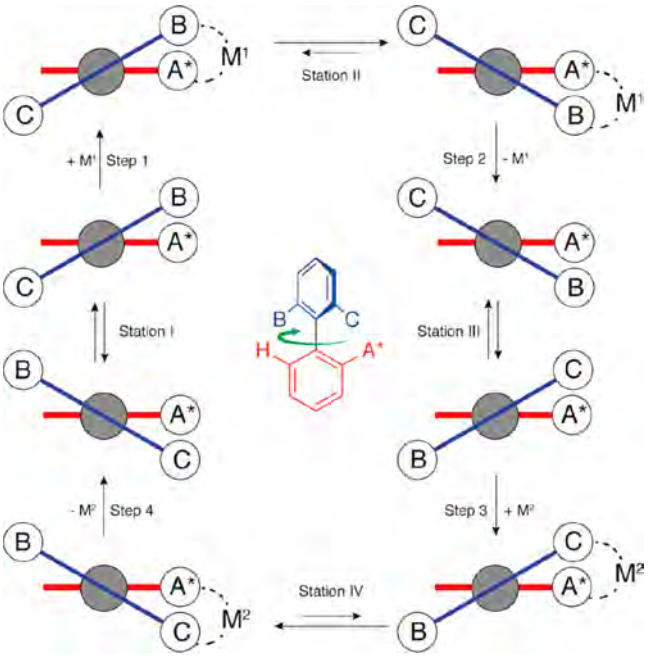

Figure 17. Schematic representation of the design principle of a molecular rotary motor based on a biaryl species and a metal redox cycle. Adapted with permission from ref 216. Copyright 2016 Springer Nature.

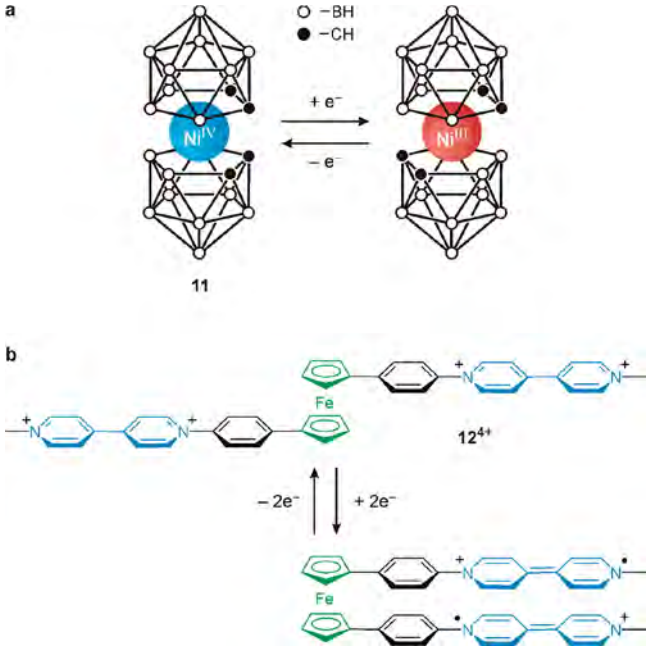

Figure 19. (a) Reversible conformational changes in nickelacarborane **11** upon changing the formal oxidation state of the central nickel ion.[217] (b) Reversible conformational changes in ferrocene–bipyridinium species $\mathbf{12}^{4+}$ upon redox-controlled intramolecular dimerization of the bipyridinium arms.[219]

the system could in principle operate autonomously by coupling of the unidirectional rotation to a redox cycle.

Sandwich-type compounds, such as metallocenes, metallocarboranes, and double-decker porphyrin complexes, have been proposed as prototypical species to construct molecular rotary motors because of the rotation around the metal ion.[27,28,33] For example, it was shown that changing the oxidation state of the nickel ion in carborane **11** (Figure 19a) causes reversible switching between the transoid and cisoid conformations.[217,218] Another strategy to achieve redox control of the rotation around a metal ion in a sandwich complex consists of functionalization of the two rotating halves with moieties that can undergo redox-induced dimerization, as illustrated by compound $\mathbf{12}^{4+}$ (Figure 19b).[219,220] A similar approach was employed in compounds comprising a binaphthyl hinge and bipyridinium arms to modulate the binaphthyl dihedral angle.[221,222] Rotary motors of this kind, however, are not available because complete unidirectional rotation has not yet been achieved.

A very interesting family of molecular rotors has been proposed in which unidirectional rotation is supposed to be powered by electron-transfer processes involving nanoscale electrodes (Figure 20).[28,223] Such a device would represent a nanoscale version of the electrostatic motor developed by

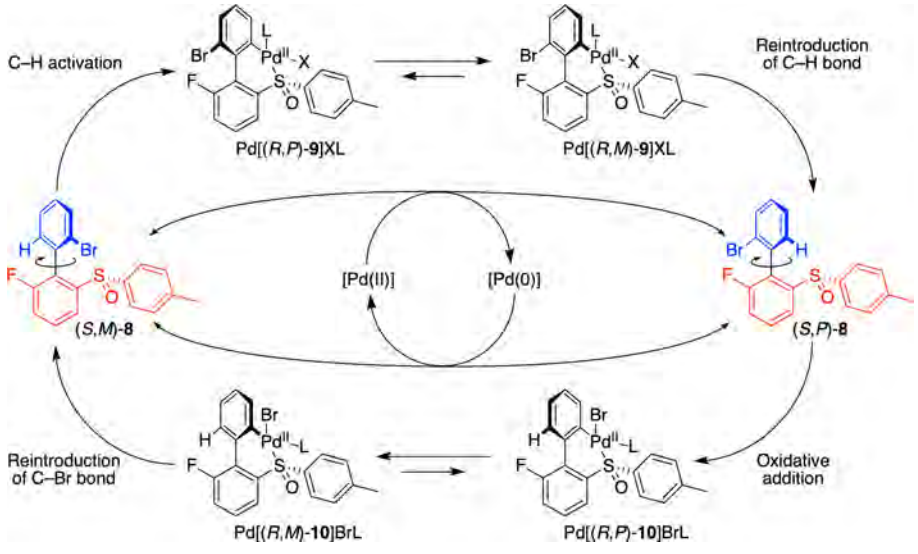

Figure 18. Molecular structures and operation mechanism of rotary motor **8**, corresponding to the general scheme depicted in Figure 17. Adapted with permission from ref 216. Copyright 2016 Springer Nature.

DOI: 10.1021/acs.chemrev.9b00291
Chem. Rev. 2020, 120, 200–268

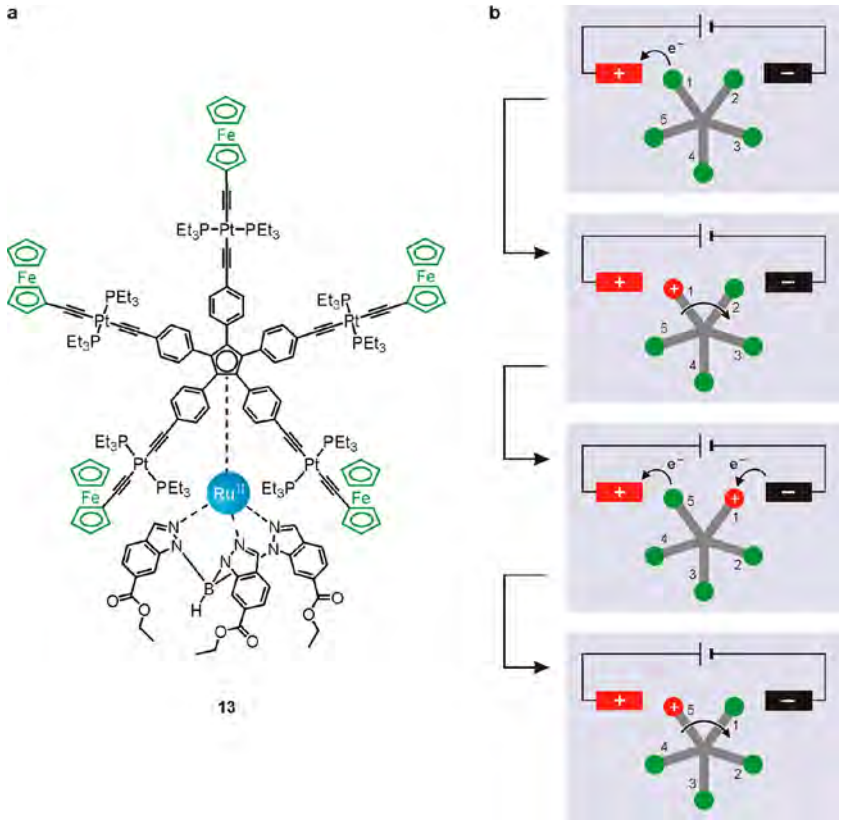

Figure 20. (a) Structural formula of molecular rotor **13**.[224] (b) Schematic representation of the mechanism of unidirectional rotation of the rotor powered by electron transfer across a nanoscale junction.[223]

Benjamin Franklin in 1748. The molecular rotor (e.g., compound **13** in Figure 20a)[224] has a piano-stool structure with a stator designed to be grafted on a surface, a Ru(II) ion as the hinge, and a rotor bearing redox-active ferrocene units. As shown schematically in Figure 20b, the molecule is placed off-center with respect to two facing nanoscale electrodes. A potential difference applied across the junction should cause oxidation of the ferrocene unit nearest the anode, which successively experiences an electrostatic repulsion toward the cathode. The oxidized unit close to the cathode is reduced, while the next ferrocene unit is oxidized at the anode. Overall, the passage of one electron across the junction should result in directional rotation of the rotor part of the molecule by one-fifth of a turn (Figure 20b). To prevent intramolecular electron transfer between two ferrocene units, which would compete with rotation, insulating spacers based on platinum acetylide units (as in **13**)[224] or bicyclo[2.2.2]octane[225] were introduced into the rotor arms. However, several problems, such as detection of the unidirectional motion, remain to be solved to complete this challenging project.[223]

3. PHOTOCHEMICALLY DRIVEN MOTORS

3.1. General Considerations

As discussed in section 1.3.3, nature does not typically use the energy of photons directly to produce mechanical movements but rather converts it into chemical fuels (e.g., ATP), which are more suitable energy vectors for powering natural molecular machines. Light energy, however, can bring about large-amplitude molecular reorganization processes or initiate chemical reactions that are conducive to molecular movement. Unlike chemical fuels, photoirradiation can power a molecular motor without the production of waste. Moreover, it is possible to exploit photons both to cause a transformation on a chemical system (i.e., "writing") and to monitor its state (i.e., "reading").[126−131]

3.2. Useful Photoinduced Processes

Light-driven molecular motors base their operation on molecular moieties that following the absorption of photons undergo a sequence of reversible transformations whose outcome is the relative movement of one portion of their (supra)molecular structure with respect to another. Therefore, it is not surprising that the development of photochemically operated molecular motors is closely related to research on reversible light-induced reactions and that most molecular motors activated by light are actually derived from a rather small number of intensely studied compounds that can support reversible and clean photoinduced processes.

The absorption of photons of opportune wavelength—usually in the range between 200 and 1000 nm—can promote a molecule to an electronically excited state, which is a transient species with profoundly different physical, chemical, and structural properties compared with the ground state. Because of their large excess of energy, excited states rapidly deactivate to the electronic ground state through different competitive processes, namely, radiative decay, nonradiative decay, and chemical reaction.[126,127] Among nonradiative decay processes, particularly significant in the present context is electronic energy transfer, by which the excited-state energy is transferred to another molecular unit either intramolecularly (in a multicomponent or supramolecular assembly) or through a bimolecular encounter. As a result, the energy acceptor becomes electronically excited without having directly absorbed a photon

DOI: 10.1021/acs.chemrev.9b00291
Chem. Rev. 2020, 120, 200−268

(see also section 1.2.2). Chemical reactions arising from an excited state include a large variety of different mechanisms such as isomerization, dimerization, additions, rearrangements, proton transfer, dissociation, and redox processes. Photoreactions can involve large structural changes in a molecular system that, when combined with an appropriate molecular design, can allow light energy to be directly translated into large-amplitude motion or chemical or electrochemical processes to be initiated in single molecules or multicomponent assemblies.

Of the different photoinduced processes that can be exploited in principle to operate a molecular device, only a few have actually been applied to molecular switches and motors.[128] In fact, to ensure repetitive operation in a molecular machine, clean and fatigue-resistant reactions are required. As discussed in section 1.3, autonomous light-driven molecular motors can be obtained by relying on reversible unimolecular photoreactions. It is therefore not surprising that photoisomerization reactions—a most studied class of photoprocesses—are at the basis of all light-driven molecular motors and most of the light-driven molecular devices developed to date.[130−132,226−230] Light-activated natural molecular motors and switches, such as bacteriorodopsin and halorhodopsin ion pumps present in Archea and retinal proteins involved in vision (e.g., rhodopsin), also rely on photoisomerization processes.[123]

In general, a photoisomerization reaction is a light-induced chemical transformation leading to an isomerization of the substrate by either bond rotation, skeletal rearrangement, or atom or group transfer. Although geometrical isomerization can also be achieved thermally and catalytically, the peculiarity of photochemical isomerization is that the composition of the photostationary state, in terms of the ratio between the different isomers, is not determined by ground-state thermodynamics but is instead controlled by the excited-state potential energy surface. In most cases, the absorption spectrum of the isomer formed after light irradiation is different from that of the starting compound. A color change may thus occur upon photoirradiation; this is why the adjective "photochromic" or "photochromatic" is often used to define such species.[226−229,231−233] However, some photoisomerizable compounds that have been widely used for the construction of molecular machines, such as stilbene, do not strictly adhere to this definition because neither isomer absorbs light in the visible region. More recently the term "molecular photoswitch" has come into use to identify molecular species that can be reversibly switched between two states with light.[94,95,228,230] This is a most useful addition to the chemical vocabulary that avoids the often superfluous or incorrect assumption of visible spectral changes upon photoswitching.

All molecular photoswitches share a number of common characteristics (Figure 21). In general terms, by irradiation with light of proper wavelength ($h\nu$), the A and B isomers of a photoswitchable moiety can be mutually interconverted. In addition, since in nearly all cases one of the two isomers has a significantly higher thermodynamic stability than the other, a thermally activated (dark) process by which the metastable isomer (B) reverts back to the stable one (A) can occur. While the photoinduced A → B transformation is usually very fast, the thermal B → A conversion may have a half-life as short as nanoseconds or as long as weeks, months, or even hundreds of years. Molecular photoswitches can thus be separated in two classes: thermally reversible (T-type), in which the photogenerated isomer thermally reverts to the initial form, and photochemically reversible (P-type), in which the back reaction

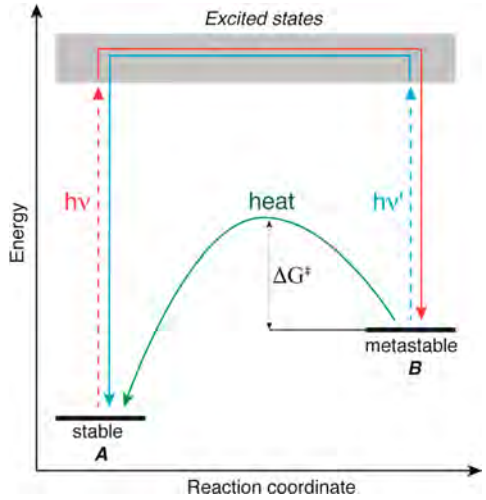

Figure 21. Simplified energy profile describing the light- and thermally induced conversion between the two isomeric forms of a molecular photoswitch.

is promoted only by light irradiation. Stilbenes, azobenzenes, and spiropyrans belong to the T-type class, while most diarylethenes are examples of the P-type class.

Usually, quantitative photochemical conversion to either A or B is prevented because of the overlap of the absorption spectra of the A and B forms, which are both photoreactive (Figure 21). A photostationary state enriched in one of the two forms is obtained, whose composition depends on the absorption coefficients of the isomers and the quantum yields of the forward and backward photoreactions at the irradiation wavelength and on the rate constant of the thermal back reaction.[126,127]

The photoinduced $E-Z$ configurational isomerization of organic compounds around an unsaturated bond is indeed the most commonly exploited photoreaction in the field of molecular devices and machines.[128,130−132,226−232] Representative categories of such compounds are alkenes, polyenes, azo compounds, and imines (Figure 22).

The photoisomerization of alkenes and polyenes around a C═C double bond (Figure 22a) has attracted much attention from theoretical, mechanistic, and synthetic points of view since the late 1960s, when Nobel laureate George Wald demonstrated that the fundamental process of vision is the photochemical $Z-E$ isomerization of the retinal chromophore in rhodopsin.[234] Because of its centrality for processes promoted by natural light and its mechanistic minimalism, retinal photoisomerization is one of the most investigated unimolecular photoreactions.[235] The prototypical example of this class is represented by the $E \rightarrow Z$ photoisomerization of stilbene and its derivatives, which was first described in 1946 by A. J. Henry.[236] Planar (E)-stilbene is readily converted to the nonplanar Z form upon irradiation with UV light. The latter, being 12 kJ mol^{-1} higher in energy compared to the E isomer, reverts almost quantitatively back to the E form in the dark.[231] The photoreaction of stilbene compounds can also be performed by using triplet sensitizers, a possibility vastly explored in different light-activated molecular machines. A photocyclization reaction leading to the formation of dihydrophenanthrene-type products, however, can also occur in this class of compounds, whose consequence—if not appropriately counteracted by functionalization of the stilbenoid

DOI: 10.1021/acs.chemrev.9b00291
Chem. Rev. 2020, 120, 200−268

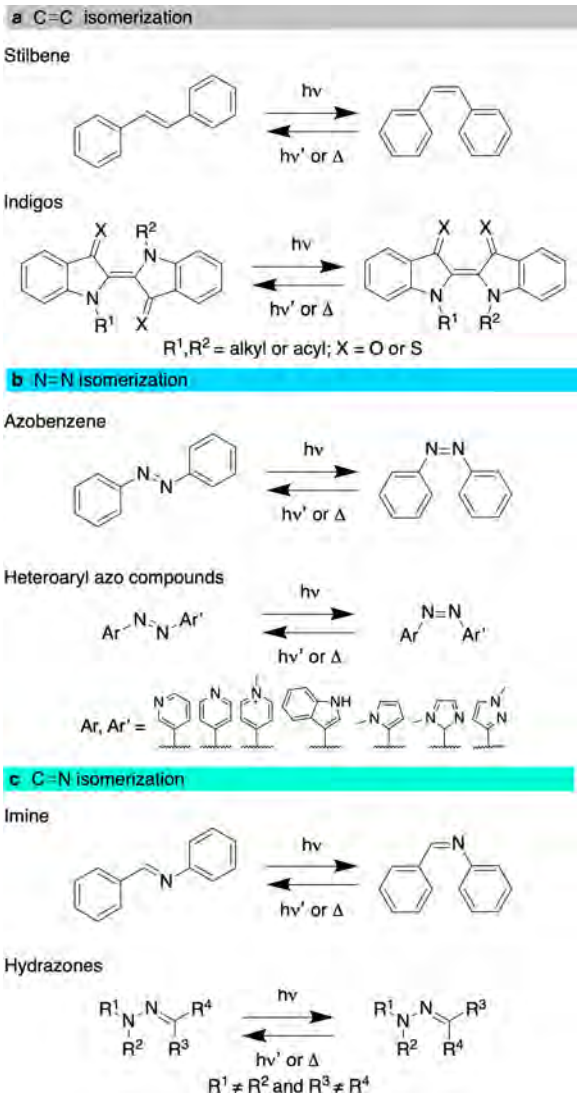

Figure 22. Main classes of molecular photoswitches based on the *E*–*Z* isomerization around (a) C═C, (b) N═N, and (c) C═N double bonds.

core aimed at frustrating cyclization—is a marked reduction of the fatigue resistance.

A family of compounds displaying a remarkably efficient photoisomerization reaction around a C═C double bond is that of indigoids and related moieties (Figure 22a). Indigo itself is not a photoswitch, but alkylation or acylation of the nitrogen atoms or substitution with sulfur (i.e., thioindigo) leads to photoswitchable compounds.[237−239] All of these derivatives exhibit absorption bands in the visible region of the spectrum that can be tuned by synthetic structural modifications, such that individual derivatives that absorb at nearly any portion of it can be prepared.[240−242] Moreover, the usually good separation between the absorption bands of the *E* and *Z* forms allows clean and quantitative photoswitching by the choice of proper irradiation wavelengths. Usually, the *Z* isomers of indigo compounds possess a very low rate of the thermally activated back reaction. Another most interesting and quite unique property that is often exploited as a tool to investigate the photoreactivity of indigo-type compounds and the operation of molecular devices relying on their photoisomerization is the strong room-temperature fluorescence of the *E* form. More details will be given in section 3.6.2.

The light-induced configurational switching of the N═N double bond in azobenzene and related derivatives (Figure 22b) is one of the oldest and most extensively investigated photochromic processes. The *Z* stereoisomer of azobenzene and the $E \rightarrow Z$ photoisomerization reaction were discovered in 1937 by G. S. Hartley.[243] Since then, the interest in and popularity of the photochemistry of azobenzene derivatives in the scientific community have continuously increased, establishing them as a common choice when photocontrol has to be achieved in chemical species and materials.[47−49,51−53,72,73,75,76,78,83−85,94,105,128,130,131,226−232,244−247] The *E* configuration of azobenzene is ca. 42 kJ mol^{-1} more stable that the *Z* form; thus, at equilibrium in the dark, azobenzene is present almost exclusively as its *E* stereoisomer. The latter is essentially planar, while the *Z* isomer exhibits a nonplanar structure with a C−N═N−C dihedral angle of about 45°. As the *E* and *Z* stereoisomers possess similar, largely overlapping absorption spectra in solution, the photostationary states of azobenzenes are mixtures of the two forms with a composition that is strongly dependent on the irradiation wavelength and on the presence of substituents around the azobenzene core.[231,232,244] Most of the simple azobenzenes (except those bearing amino or hydroxy substituents) are stable enough in the *Z* form to be isolated as pure species. In general, the thermally activated $Z \rightarrow E$ back reaction displays a strong dependence on the substitution pattern, with half-lives of the *Z* isomer ranging from days for unsubstituted azobenzene to a few microseconds in the case of push−pull azobenzenes. Heteroaryl azo compounds, because of their broad structural diversity that is reflected in their vast range of spectral properties, are emerging as a new class of highly efficient and versatile molecular photoswitches.[248,249]

Although compounds presenting an azomethine C═N double bond, such as oximes, Schiff bases, and hydrazones, have been known to exist in stereoisomeric forms for a long time,[250] their photochemical isomerization (Figure 22c) has been investigated in detail only in relatively recent times.[187,251] This is probably the case because the photogenerated stereoisomer, particularly in the case of Schiff bases, is very unstable, and therefore, the fast thermal back reaction hampered the recognition and investigation of the photoinduced isomerization. Indeed, the first reports on the reversible configurational photoisomerization of Schiff bases were conducted at very low temperature or in the solid state, where the thermal back reaction is significantly slowed down.[252] However, while there is still much debate on the mechanistic details, nowadays it is recognized that most compounds presenting an azomethine linkage are molecular photoswitches.[253] These species are characterized by rates of the (uncatalyzed) thermal back-isomerization spreading over more than nine powers of 10: N-heteroatom derivatives (i.e., oxime ethers and hydrazones) present high back conversion barriers and long-term stability, while *N*-alkylimines and *N*-arylimines are the least stable. Recent work, particularly from Aprahamian and co-workers, has unraveled a variety of hydrazone compounds exhibiting clean and reversible photoswitching both in solution and in complex matrices.[95,254]

Besides photoisomerization, another class of photoinduced processes that has found significant application in the development of molecular devices is that of light-induced proton-transfer reactions.[255] This is the case because in principle such

DOI: 10.1021/acs.chemrev.9b00291
Chem. Rev. 2020, 120, 200−268

reactions enable photocontrol of pH-responsive processes. Three main categories of photoinduced proton-transfer reactions can be identified: photoacid (or photobase) generators, excited-state proton transfer, and proton transfer from a metastable state. Photoacid (or photobase) generators[256] are molecules that undergo a reaction (e.g., dissociation) under irradiation that results in the release of an acidic (or basic) product. The photoinduced process is chemically irreversible, and photoacids are mainly used as initiators of polymerization reactions. In a recent proof-of-concept study, a compound of this kind was employed to operate a chemically driven mechanical molecular switch.[257]

In general terms, when the pK_a of the excited state of a molecule is different than that of its ground state, the molecule can undergo excited-state proton transfer.[258−260] The actual possibility to release or capture a proton depends on the competition among all of the processes taking place in the excited state.[261] A proton transfer back to the conjugate base (or from the conjugate acid) in the ground state resets the systems, thus enabling reversible and cyclic operation. Photoinduced proton transfer is a common process in nature[123] and has also been widely explored in chemistry and biology.[262] For example, the proton released after excitation of the photoacid can be taken up by an acid−base switch, thus triggering its protonation and deprotonation reactions.[263] The key requirement is that the pK_a of the switch is smaller than that of the photoacid in its ground state and larger than that of the photoacid in its excited state. Nevertheless, it is practically difficult to achieve large pH shifts with excited-state photoacids because of their fast relaxation to the ground state. Moreover, the mechanical movements of the machine should be faster than the reverse proton transfer reaction to the ground-state conjugate base. Indeed, the large difference between the time scales of excited-state processes and long-range molecular movements has to date prevented the effective application of excited-state photoacids to operate molecular machines.

A metastable state photoacid (or photobase) is a stronger acid (or base) with respect to the thermodynamically stable species. The frame is similar to that discussed earlier for excited states, but the lifetime of the metastable species is long enough to allow its accumulation. Therefore, one can obtain a pH jump large enough to affect other acid−base-responsive species present in the same solution (Figure 23). The metastable photoacid (or photobase) reverts to the stable species in the dark through reverse proton transfer with a half-life that can range from seconds to hours.[264]

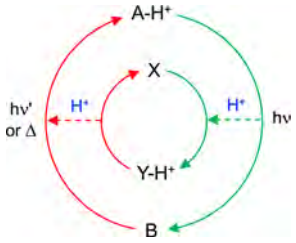

Figure 23. Schematic representation of the coupled operation of a metastable photoacid (outer cycle; $pK_{a,BH} \ll pK_{a,AH}$) and a pH-responsive switch (inner cycle). The "forward" and "backward" pathways of the overall switching cycle are shown in red and green, respectively; dashed lines denote the intramolecular proton transfer processes that enable the communication of the two systems.

One of the first examples of a light-induced reversible pH jump was based on a triphenylmethane leucohydroxide, which releases OH^- ions upon irradiation with a laser pulse.[265] Nevertheless, the most common design principle of metastable photoacids and photobases relies on the use of photochromic compounds: in fact, the structural rearrangement associated with the photoisomerization reaction can be accompanied by the emergence of new acid−base properties due to alteration of the electron distribution or intramolecular interactions.[266] A well-known class of compounds of this kind are the 2-hydroxyazobenzenes (Figure 24).[267,268] In the *E* configuration,

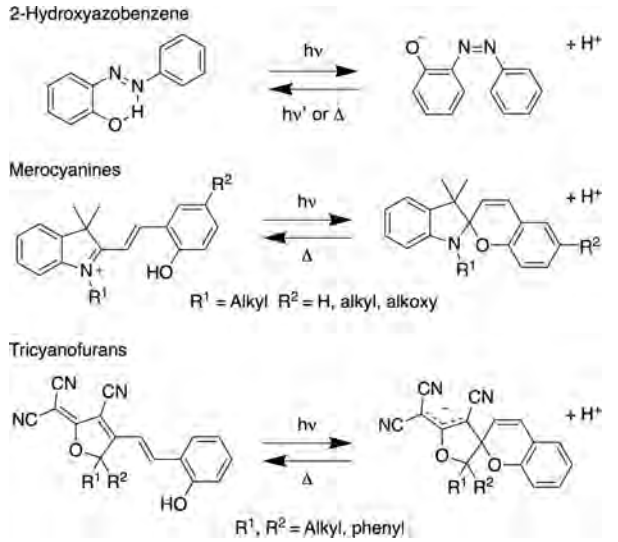

Figure 24. Molecular structures of three classes of metastable state photoacids: 2-hydroxyazobenzene,[268] merocyanines[269] and tricyanofurans.[270]

the acidity of the phenol unit is decreased by the hydrogen-bonding interaction with the nitrogen atoms; this interaction is lost upon $E \rightarrow Z$ isomerization, which thus causes an increase in the acidity of the compound. A general principle proposed for the design of metastable photoacids consists of an electron-accepting unit and a weakly acidic nucleophilic moiety connected by a double bond: upon $E \rightarrow Z$ isomerization a nucleophilic reaction takes place between the two units, with generation of a highly acidic metastable form.[264] In this frame, two classes of molecules have gained attention for their exploitation as photoacids, namely, merocyanine-based species[269] and switches based on the tricyanofuran unit[270,271] (Figure 24).

Merocyanine compounds have been employed in several examples of signal communication between molecular switches according to the scheme depicted in Figure 23.[272,273] With an appropriate selection of molecular components, the photoinduced proton exchange between merocyanine species and pH-controlled switches has been exploited to implement logic functions[274,275] or memory elements.[276] Credi, Raymo, and co-workers used a metastable photoacid to operate a molecular machine, showing that the threading−dethreading of a non-photoresponsive calixarene−bipyridinium pseudorotaxane[277] could be controlled by light via intermolecular proton transfer involving a merocyanine species.[278] The process is reversible, and unlike the operation of the same machine by addition of acid−base reactants, waste products are not generated upon cycling. With the same strategy, by an appropriate selection of

DOI: 10.1021/acs.chemrev.9b00291
Chem. Rev. 2020, 120, 200−268

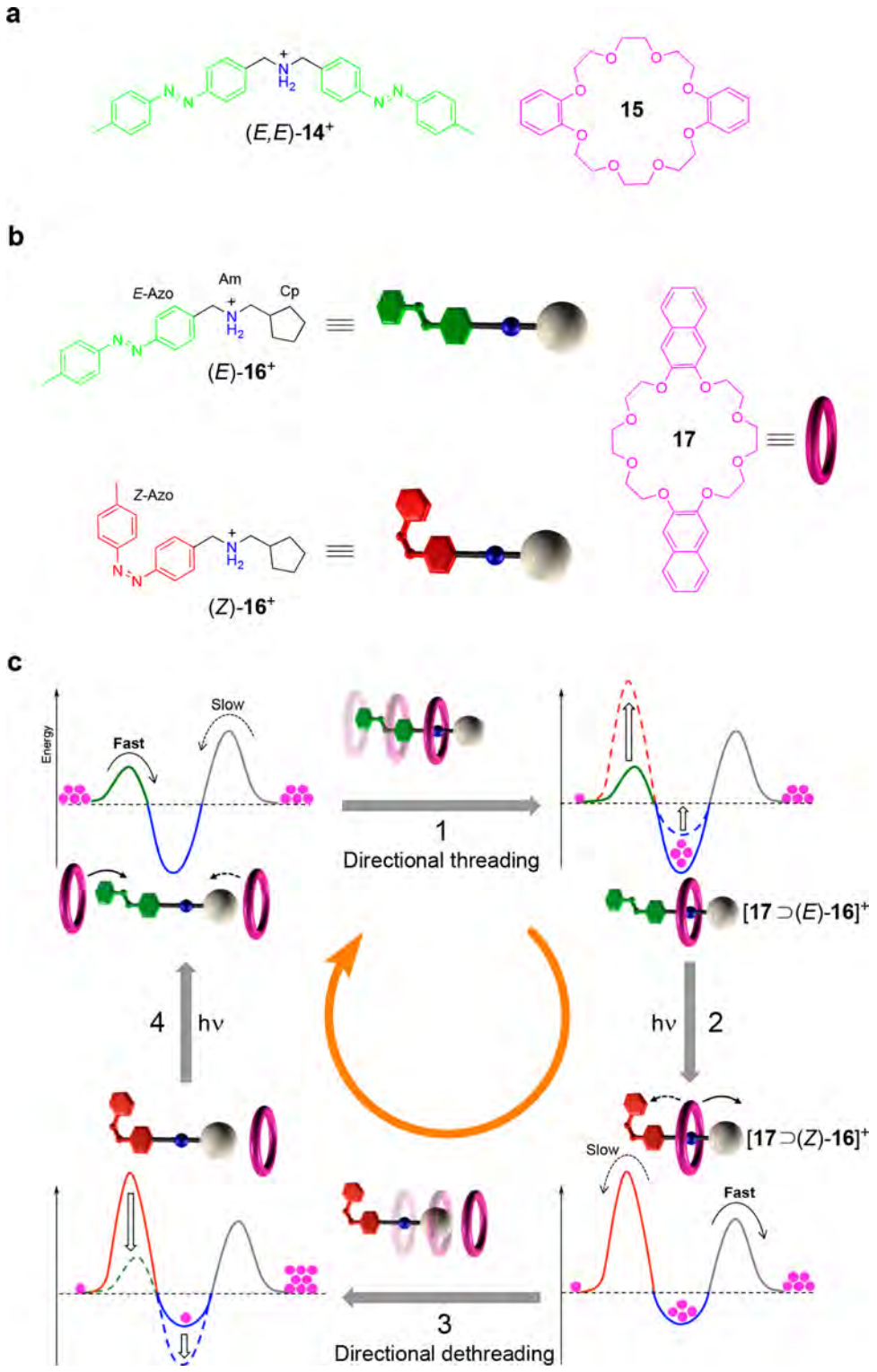

Figure 25. (a) Structural formulas of axle 14^+ in its *E*,*E* configuration and DB24C8 ring **15**. (b) Structural formulas and schematized representations of axle 16^+ in its *E* and *Z* configurations and ring **17**. (c) Schematic operation mechanism and simplified potential energy profiles, as functions of the ring–axle relative position, for each step (gray solid arrows) of the directional light-activated threading–dethreading motion (processes 1, 2, 3, and 4) of the ring and axle components. Dashed lines indicate processes that are kinetically prevented. The orange circular arrow shows the directional flux of species relevant in the operation of the system under steady-state out-of-equilibrium conditions.[291,293]

the photoacid, rotating hydrazone-based switches[279] and an acid–base-driven molecular shuttle[280] could be operated. These examples demonstrate the feasibility of such a general approach for activating a non-photoactive molecular machine with light by exploiting the intermolecular communication of chemical signals with a distinct photoswitch rather than integrating a photoresponsive unit into the device.[272]

It is well-known that the excess energy of an electronically excited state can be used to transfer electrons.[126,127] The fact that excited states are generally stronger oxidizing and reducing

DOI: 10.1021/acs.chemrev.9b00291
Chem. Rev. 2020, 120, 200–268

agents with respect to the ground state is at the basis of photoinduced electron transfer processes. These processes imply the interaction of the excited state with an electron donor or acceptor component, which can either be intramolecular in a supramolecular assembly or require a bimolecular encounter of separated partners. Indeed, as for excited-state proton transfer reactions, the charge transfer event is in competition with other processes taking place in the excited state, including primarily back electron-transfer. Most exploited candidates for the role of photosensitizers in light-induced electron transfer are transition metal complexes because in many instances they are excellent chromophores, exhibit tunable and reversible redox properties, and possess long-lived (and often emissive) excited states.[281] As noted above, however, the structural rearrangements associated with the operation of molecular machines are typically slower than excited-state processes, and their efficient competition with the relaxation to the ground state by back electron-transfer is a challenge. Hence, the latter process must be slowed down or, in a limiting case, totally prevented. For an analysis of this problem and its influence on the operation of the molecular machine, see the discussion on compound $\mathbf{3}^{6+}$ in section 1.3.3. Several studies in which redox-active mechanical molecular switches based on rotaxanes and catenanes are operated by light, taking advantage of photoinduced electron transfer, have been reported in the literature.[132−136,144,282−288]

3.3. Supramolecular Pumps

As discussed in section 2.3, the relative movement of the ring and axle components feasible in (pseudo)rotaxane-type architectures has been recently explored by different research groups for the construction of artificial supramolecular pumps. In order to make such a device work using light as the sole source of energy, a photoactive moiety has to be installed in one of the components of the (pseudo)rotaxane architecture, such that its light-induced transformation influences both the kinetics and thermodynamics of the ring−axle interaction. The scarcity of reported systems that conform to this scheme of operation is a clear indication of its challenging realization.

One of the most popular recognition motifs employed to build (pseudo)rotaxane-type architectures is that constituted by a crown ether encircling a secondary ammonium cation.[289] Venturi, Credi, and co-workers reported that the kinetics and thermodynamics of the self-assembly process that leads to the formation of a pseudorotaxane between the secondary ammonium axle $\mathbf{14}^+$ and dibenzo[24]crown-8 (DB24C8) ring **15** (Figure 25a) can be efficiently controlled via photoisomerization of the azobenzene units attached at both ends of $\mathbf{14}^+$.[290] Specifically, photoswitching of (*E*,*E*)-$\mathbf{14}^+$ to (*Z*,*Z*)-$\mathbf{14}^+$ results in both destabilization of the pseudorotaxane complex and a large decrease in the threading−dethreading rate constants. Moreover, because of the high fatigue resistance characteristic of azobenzene photoswitches, the process is fully reversible by irradiation with visible light or by heating. Thus, (*E*)-azobenzene was proved to operate as an efficient photoinduced inhibitor and negative catalyst for the self-assembly of ring **15** with axle $\mathbf{14}^+$.

Building on these preliminary results, the nonsymmetric axle $\mathbf{16}^+$ (Figure 25b) was synthesized with the objective of developing a system in which the ring would be forced to thread through the axle by following a specific direction.[291] Indeed, axle $\mathbf{16}^+$ accommodates a secondary ammonium station (Am) enclosed between an azobenzene unit (Azo) and a non-photoactive cyclopentyl moiety (Cp)[292] (Figure 25b), which exhibits a threading rate through the macrocycle that is intermediate between those of the Azo unit in the *E* and *Z* configurations.

Kinetic measurements proved that the slippage rate of the ring over the Cp end is nearly 2 orders of magnitude slower than that over the *E*-Azo end of (*E*)-$\mathbf{16}^+$, while it is still considerably faster than that over the *Z*-Azo moiety of (*Z*)-$\mathbf{16}^+$. Despite this observation, in acetonitrile at room temperature the photoisomerization of the Azo unit of $\mathbf{16}^+$ did not affect the affinity of the axle for the macrocycle; hence, the dissociation of ring **15** from the axle could not be obtained solely by light irradiation. A second pair of chemical stimuli had to be employed in order to complete a directionally controlled threading/dethreading cycle, which enabled the directionally controlled relative translation of the components but prevented the realization of an autonomous operating cycle.

To improve the system, in order to achieve autonomous light-driven operation, ring **15** was replaced with an analogous but strongly fluorescent macrocycle (compound **17** in Figure 25b),[293] with the dual aim of (i) enhancing the stability difference of the *E* and *Z* pseudorotaxanes and (ii) enabling the study the self-assembly process by luminescence spectroscopy, a more sensitive technique than NMR spectroscopy. To further strengthen the ring−axle interactions, dichloromethane was used as the solvent instead of acetonitrile. As anticipated, these rather simple changes enabled an increase in the ring−axle affinity by almost 3 orders of magnitude. Remarkably, the association constant of **17** with (*E*)-$\mathbf{16}^+$ turned out to be about 4 times larger than that with (*Z*)-$\mathbf{16}^+$, while the relative values of the rate constants and thus the energy barriers were unvaried. Hence, in the system composed of axle $\mathbf{16}^+$ and ring **17**, photoisomerization of the Azo unit of the axle is able to switch simultaneously both the kinetics and thermodynamics of the self-assembly process of the two components.

Under light irradiation, the system operates as a Brownian ratchet driven by photon energy that directionally transports rings from one end of the axle component to the opposite end, as represented in Figure 25c. During a cycle, at the start axle (*E*)-$\mathbf{16}^+$ and ring **17** efficiently self-assemble into the pseudorotaxane architecture $[\mathbf{17}\supset(E)\text{-}\mathbf{16}]^+$ (Figure 25c, process 1). The threading of the macrocycle occurs preferentially from the *E*-Azo end of the axle. Irradiation of the *E*-Azo unit of $[\mathbf{17}\supset(E)\text{-}\mathbf{16}]^+$ to yield $[\mathbf{17}\supset(Z)\text{-}\mathbf{16}]^+$ (Figure 25c, process 2), results in two simultaneous effects: a reduction in the affinity of **17** toward the Am station and an increase in the dethreading barrier at the Azo end of the axle. The reduced stability of the complex $[\mathbf{17}\supset(Z)\text{-}\mathbf{16}]^+$ forces the ring to slip past the Cp end, thus exiting the opposite side from which it had threaded initially (Figure 25c, process 3). Most important, since both isomers of the axle, namely, (*E*)-$\mathbf{16}^+$ and (*Z*)-$\mathbf{16}^+$, are photoreactive and absorb in the same spectral region, another photon of the same wavelength can trigger the $Z \rightarrow E$ photoisomerization of $\mathbf{16}^+$, thus restoring the initial state and completing the cycle (Figure 25c, process 4).

Upon light irradiation an out-of-equilibrium stationary state is reached, which establishes a clockwise net flux of species along the closed network of reactions (orange arrow in Figure 25c) that continues as long as photons are absorbed. Hence, in this system under constant illumination, light energy powers and controls not only the nanoscale directional motion of the ring and axle components (unidirectionality) but also the macroscopic flux of the species along the closed reaction network

DOI: 10.1021/acs.chemrev.9b00291
Chem. Rev. 2020, 120, 200−268

(termed "monodirectionality" in section 3.6.2). It is worth noting that the autonomous and out-of-equilibrium operation of this system is possible thanks to what is usually considered one of the major shortcomings of azobenzene photochromic compounds, that is, the spectral overlap between the *E* and *Z* stereoisomers (see section 3.2).

Interestingly, it was highlighted that the specific photo-induced ratcheting mechanism depends on the irradiation wavelength employed to induce the isomerization of the Azo unit of the axle.[294] If light with a wavelength $\lambda > 400$ nm is employed, the system operates according to an energy ratchet mechanism wherein the symmetry-breaking element that enables the autonomous operation is the difference in the association constants of the ring−axle complexes $[\mathbf{17}\supset(E)\text{-}\mathbf{16}]^+$ and $[\mathbf{17}\supset(Z)\text{-}\mathbf{16}]^+$. Conversely, if irradiation is conducted at 365 or 287 nm, the system operates according to a combination of energy and information ratcheting since at those wavelengths the photoisomerization efficiency of the axle depends on whether it is surrounded by the ring. It should also be noted, however, that the work done by the pumping motion is rapidly wasted by the free diffusion of the rings in the homogeneous solution. Nevertheless, the structural and synthetic simplicity of the components is expected to favor further development of this architecture[295] toward more advanced structures capable of generating concentration gradients or to transport chemical species along predetermined pathways.[296]

The only other reported example of a light-activated supramolecular pump is represented by the redox-activated system composed of axle $\mathbf{5}^+$ and ring $\mathbf{4}^{4+}$ (CBPQT), which was described earlier in section 2.3, when operated by photoinduced electron transfer from $[Ru(bpy)_3]^{2+}$ (bpy = 2,2′-bipyridine) in the presence of phenothiazine (**ptz**) as an electron relay (also see section 1.3.3).[205] The proposed operation mechanism is schematized in Figure 26: Upon irradiation of $[Ru(bpy)_3]^{2+}$ with visible light (process 1), intermolecular electron transfer from the long-lived ^{3}MLCT state of the ruthenium complex to ring $\mathbf{4}^{4+}$ occurs (process 2). The photogenerated $[Ru(bpy)_3]^{3+}$ species is reduced back to $[Ru(bpy)_3]^{2+}$ by **ptz**, which in its turn becomes oxidized (process 3), and the reduced macrocycle dethreads unidirectionally (process 4). Finally, $\mathbf{ptz}^+$ takes an electron from the free reduced CBPQT (process 5), thus regenerating the reactants, which upon unidirectional threading (process 6) regenerate the starting pseudorotaxane, and another working cycle can begin. The dethreading process is in competition with the back electron-transfer reactions from the reduced and still complexed CBPQT to $[Ru(bpy)_3]^{3+}$ or $\mathbf{ptz}^+$. Therefore, key requisites for efficient operation of the motor would be fast photoinduced electron transfer from $[Ru(bpy)_3]^{2+}$ to CBPQT and fast redox reaction between $[Ru(bpy)_3]^{3+}$ and **ptz** (processes 2 and 3, respectively). Electrochemical experiments on model compounds and on the pseudorotaxane indicate that the dissociation of the reduced CBPQT occurs on the millisecond time scale. This process should be faster than the recombination between $\mathbf{ptz}^+$ and the reduced CBPQT.

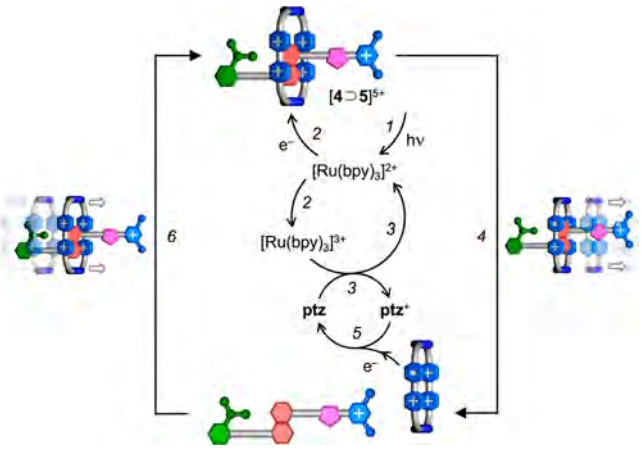

Figure 26. Proposed mechanism for the photochemically triggered operation of the redox-driven supramolecular pump based on macrocycle $\mathbf{4}^{4+}$ and axle $\mathbf{5}^+$ shown in Figure 12. The inner scheme depicts the photoinduced electron transfer cycle involving $[Ru(bpy)_3]^{2+}$ as the photosensitizer and phenothiazine (**ptz**) as the electron relay, while the outer scheme shows the unidirectional threading and dethreading reactions. Adapted from ref 205. Copyright 2013 American Chemical Society.

The operation of the supramolecular pump was investigated by following the absorption changes at 520 nm, where a charge transfer band arising from the interaction between CBPQT and DNP is diagnostic for the presence of the pseudorotaxane complex. After 5 min of irradiation with a laser at 450 nm (light mainly absorbed by the Ru photosensitizer), a small decrease in this absorption band was observed; when the irradiation was stopped, the band slowly recovered until the original spectrum was obtained.[205] These observations can be interpreted by assuming that after a fast photoinduced electron transfer process that generates the reduced pseudorotaxane and $\mathbf{ptz}^+$, dethreading takes place followed by slow rethreading after charge recombination. Unfortunately, key experiments in support of the mechanism shown in Figure 26, such as the observation of the transient electron transfer products $Ru(bpy)_3^{3+}$, $\mathbf{ptz}^+$, and reduced CBPQT and a kinetic investigation of the charge recombination between the two latter compounds, were not performed.

Also in this case, light energy can drive the system away from thermal equilibrium while forcing the unidirectional relative motion of the components, and this is the only example to date of a molecular motor that relies on photoinduced electron transfer. However, the delicate sequence of bimolecular reactions and the concentration dependence of the operation mechanism could hamper its practical application and fatigue resistance. In principle, the pump could be operated autonomously, but the very slow rethreading process would limit the turnover frequency.

3.4. Molecular Walkers

In the past few years, the large number of bipedal motor proteins found in nature belonging to the myosin, dynein, and kinesin superfamilies that "walk" down intracellular tracks to perform essential tasks in a variety of key biological processes in living cells[2−6] have inspired research on analogous artificial systems.[297] Although the mechanistic details at the base of the operation of natural "walking" motors are still not completely understood and their complexity precludes mere replication, the principal design paradigms they have in common with other types of molecular motors have been identified.[298] First, a molecular walker has to be processive; that is, it should always remain bonded to the track during its journey. In other words, the walking sequence must be repeated continuously with the walker never getting detached from the track. Moreover, the motion along the track must be directed by a ratcheting mechanism that enables the molecular walker to operate as a motor and not as a randomly

DOI: 10.1021/acs.chemrev.9b00291
Chem. Rev. 2020, 120, 200−268

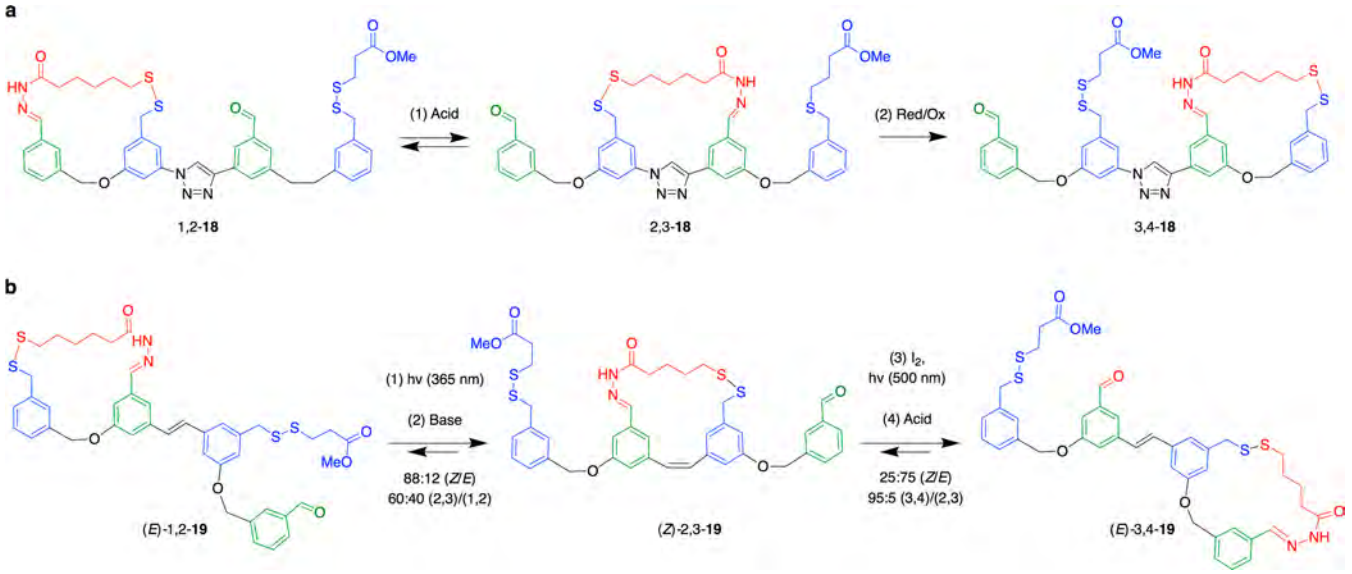

Figure 27. (a) Molecular walker (red) that moves along a four-station molecular track (stations are colored in green and blue) in response to (1) acidification and (2) chemical reduction and oxidation. An irreversible redox process (2) transports the walker predominantly to the right side of the track in compound **18** (away from the minimum-energy distribution).[100] (b) Light-driven small-molecule walker that moves along a four-station molecular track in response to the ring strain between the walker (red) and the track induced by the photoisomerization of the stilbene linker group. The reaction sequence transports the walker from the left end to the right end of the track in compound **19**; exchanging steps (2) and (4) causes the walker to be transported preferentially in the opposite direction.[305] The two numbers used in the descriptors of the molecules indicate the stations to which the walker is linked.

diffusing system. Finally, a highly desired property for a walker is the ability to process its "fuel" autonomously (see section 1.3).

Several examples of synthetic DNA-based walkers have been reported[299−302] that, thanks to the structural flexibility and highly predictable properties of nucleic acids,[303] fulfill all of the design elements detailed above. Conversely, fully artificial walkers based on small molecules are relatively rare. The design strategies that can be employed to realize light- or chemically fueled small-molecule walkers have been rationalized and reviewed.[304] However, despite the intense research on this type of system in the past decade, fully artificial molecular walkers with autonomous operations are still unrealized.

The first small-molecule walkers with the ability to operate in a processive, directional, and repetitive manner were described by Leigh and co-workers (Figure 27).[100,305] They are based on a molecular track with four attachments and a walker unit with two chemically different moieties that can be connected to the track. Such functional moieties can be orthogonally addressed in such a way that each "foot" acts as a temporarily fixed linkage while the other is engaged in a dynamic covalent exchange reaction. The chemical design is based on a hydrazone unit that joins the walker to the track and is labile under acidic conditions and a disulfide bridge as the second connection that through an irreversible redox disulfide exchange reaction transports the walker predominantly to the right-hand side of the track. The alternation between acidic conditions and the redox sequence forces the two-legged molecule to walk along the track with a significant directional bias by a Brownian information ratchet mechanism (see section 1.2).

Building on this result, Leigh and co-workers developed the first light-driven small-molecule walker, which is endowed with the unique possibility for the walker unit to move in either direction along a four-foothold track.[305] This result was achieved by installing a photoisomerizable stilbene moiety between the internal aldehyde and disulfide footholds of the track of the previously described chemically powered walker system.

The key to achieving directionality lies in photoisomerization of the stilbene unit, which allows the introduction of significant ring strain in the constitutional isomer in which the walker unit bridges the stilbene linkage (Figure 27b). $E \rightarrow Z$ isomerization provides a driving force for the walker to step onto the central stilbene unit, while subsequent $Z \rightarrow E$ isomerization causes a majority of the walkers to move away from the stilbene group in a direction determined by which foot−track interaction is labilized next. The overall direction in which the walker motion occurs is thus dependent on the sequence of the orthogonal applied stimuli: acid or base, which controls the dissociation of a "foot" of the walker from the track, and UV light or visible light (plus iodine), which controls the isomerization of the stilbene unit to increase or decrease the ring strain between the walker and the track.

The manipulation of the potential energy surface by altering the thermodynamic minima via changes in ring strain through stilbene photoisomerization and the kinetic barriers by either base or acid stimuli results in a Brownian energy ratchet mechanism. In particular, the energy that fuels the directional transport is supplied by the $E \rightarrow Z$ photoisomerization reaction of the stilbene unit by establishing a significant configurational strain in the track. The other three stimuli are all under thermodynamic control and dissipate the energy stored in the strained configuration in order to achieve the desired directional migration of the walker portion of the molecule.

This system is the first reported example of a molecular walker powered by light, with the added feature that its walking direction can be controlled by reversing the sequence of stimuli. These two combined features, which are not present in natural systems, represent a clever demonstration of the potential that well-designed artificial systems can attain. Besides these valuable characteristics, it should also be noted that the motor is slow and

DOI: 10.1021/acs.chemrev.9b00291
Chem. Rev. 2020, 120, 200−268

inefficient, with only a modest directional bias. Furthermore, as the track is short and relatively flexible, isomers can be formed in which the walker unit could bridge nonadjacent binding sites. Future studies on small-molecule walkers are likely to focus on new mechanisms for improved directional bias, different walker−track binding chemistries, and walker units that can migrate along tracks autonomously. Another stimulating task is the design of new tracks that are rigid or polymeric, have junctions, and/or may be tethered to surfaces.

3.5. Catenane Rotary Motors

As discussed in section 1.2.1, the topology inherent to catenanes presents key advantages for the realization of molecular motors compared with other supramolecular architectures. In fact, the interlocking of the ring components in a catenane enables ratcheting of the circulation of one ring with respect to the other, and even if a steady state in the distribution of the components is reached, directional motion can continue indefinitely without the need to compartmentalize the system. In a landmark study, Sauvage and co-workers observed the redox-controlled circumrotation of the molecular rings of a [2]catenane;[141] later, in collaboration with Balzani and co-workers, photochemically driven operation was also realized.[283] This system, however, is not a motor because of the absence of directionality in the motion.

In 2004 Leigh and co-workers designed and realized the first light-fueled catenane rotary motor that accomplishes directional biased circulation of one ring with respect to another via a photoactivated Brownian ratchet mechanism.[212] The system exploits a rather complex design based on a [3]catenane architecture, in which the presence of a third macrocycle helps in restricting the rotational freedom of the circumrotating rings (Figure 28). In catenane **20**, the larger macrocycle acts as a track for the two interlocked smaller rings by incorporating four different stations: fumaramide (A, green), methyl-substituted tertiary fumaramide (B, red), succinamide (C, orange), and amide (D, purple). The four binding sites on the large macrocycle were selected to display a relative affinity for the smaller amide macrocycles in the order A > B > C > D (Figure 28). As the fumaramide station A is positioned right next to a benzophenone unit, the isomerization of this station can be photosensitized by energy transfer, thus permitting the use of light of longer wavelength than that required for the non-sensitized photoisomerization of the fumaramide station, B. This design permits selective switching of the binding affinities of the A and B stations by irradiation with light of different wavelengths.

Initially, one of the macrocycles (Figure 28, blue ring) resides on the strongest binding station, A, while the second macrocycle (purple ring) encircles the second most favored station, B. The photosensitized selective $E \rightarrow Z$ isomerization of station A with 350 nm light weakens its interactions with the macrocycle and promotes the translocation of the latter toward the succinamide ester station, C (Figure 28, process 1). The presence of the second macrocycle residing around the tertiary fumaramide station, B, forces the translocation of the first ring (colored in purple in Figure 28) to occur in an anticlockwise direction by acting as a kinetic barrier to circumrotation in the opposite direction. Subsequent selective photoisomerization of the fumaramide station, B, with 250 nm light causes the second macrocycle to shuttle to its final resting position encircling the amide station, D (Figure 28, process 2). Again, the presence of a second macrocycle causes directionality in the movement of the

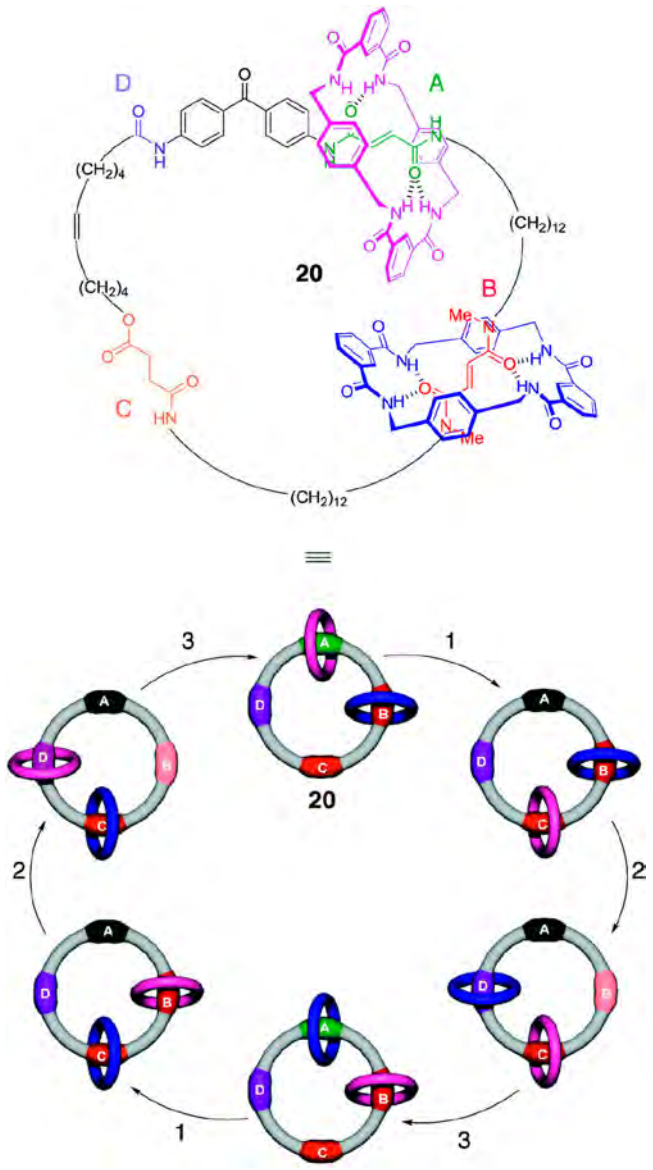

Figure 28. Directional circumrotation in [3]catenane **20** upon sequential light and chemical stimulation: (1) photosensitized isomerization of the fumaramide station (A, from light green to black) upon irradiation with 350 nm light; (2) photoisomerization of the tertiary fumaramide station (B, from red to pink) upon irradiation with 254 nm light; (3) back conversion of the A and B stations upon heating or by irradiation with light in the 400−670 nm range in the presence of a catalytic amount of Br_2. Adapted with permission from ref 38. Copyright 2017 Royal Society of Chemistry.

ring. Thermal back-isomerization, either in the presence of a catalytic amount of ethylenediamine or by irradiation with 400−670 nm light in the presence of a catalytic amount of Br_2, restores the initial configuration of the fumaramide stations (Figure 28, process 3).

It should be noted that in the course of this sequence the position of the two macrocycles is swapped; hence, a second sequence of the same stimuli is necessary to fully reset the system and bring the macrocycles back to their initial positions by completing a full directional rotation. In [3]catenane **20**, the combined control of the binding affinities of the stations by light irradiation and of the kinetic barrier presented by one macrocycle to the other allows the directional rotation; in

DOI: 10.1021/acs.chemrev.9b00291
Chem. Rev. 2020, 120, 200−268

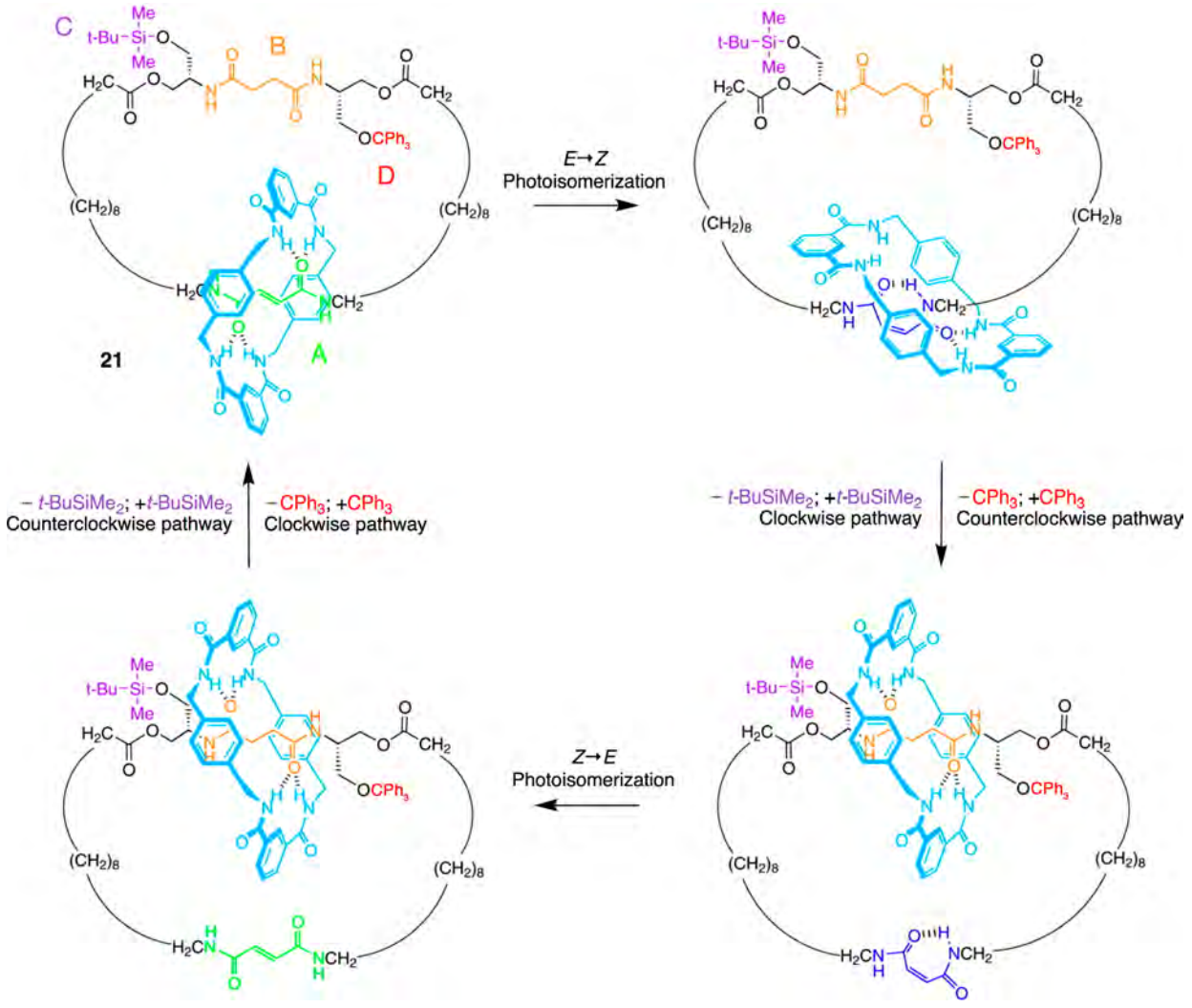

Figure 29. Photochemically and chemically driven directional circumrotation in [2]catenane **21**. A and B indicate the fumaramide and succinamide stations, respectively. C and D indicate the (*tert*-butyl)dimethylsilyl and triphenylmethyl kinetic barriers, respectively. Adapted with permission from ref 212. Copyright 2004 American Association for the Advancement of Science.

other words, a "follow the leader" process is established in which one small ring controls the direction of circumrotation of the other.

A rotary motor based on a simpler [2]catenane architecture and utilizing an alternative mode of operation was later reported by the same group.[212] In compound **21** (Figure 29) the larger ring presents only two binding sites for the smaller ring: a photoisomerizable fumaramide station (A) and a succinamide moiety (B). Station B is bordered by two bulky protective groups that act as kinetic barriers for the movement of the ring and can be orthogonally detached and reattached: a (*tert*-butyl)dimethylsilyl group (C) and a triphenylmethyl group (D). The ratcheting balance-breaking operation is based on the sequential application of successive light and chemical stimuli. In analogy with the previously described [3]catenane, light input induces the $E \rightarrow Z$ photoisomerization of the fumaramide station, A, thereby changing the relative binding affinities of the small ring for the two stations in favor of station B. Two orthogonal chemical inputs attach or detach the bulky protective groups around station A, thus switching the kinetic barrier experienced by the small ring during its movement along the larger "track" ring. By the application of these inputs in the correct sequence, the degeneracy of the two circumrotation pathways can be broken, resulting in directionality in the relative motion of the two rings.

In the starting state, the small ring encircles the fumaramide station, A. Upon $E \rightarrow Z$ isomerization promoted by 254 nm light and subsequent removal of the silyl protecting group, the small ring moves in a clockwise direction to encircle the succinamide station. Reattachment of the silyl protecting group and subsequent back-isomerization of the A station followed by removal of the trityl group results in a half-turn of the small ring that ends up surrounding the B station. Finally, tritylation of the free hydroxy group restores the initial state, thus concluding a full clockwise rotation powered by light irradiation and two orthogonal chemical stimuli. By inversion of the sequence of silylation and tritylation protection/deprotection reactions, the motion of the smaller ring can be reversed, affording counterclockwise circumrotation.

Catenanes **20** and **21** are the only examples of light-powered rotary motors based on mechanically interlocked molecules. Although both systems present some sophisticated features, such as the possibility to invert the direction of rotation, the complex sequence of stimuli required to operate them limits the efficiency of these systems and prevents autonomous operation. Another problem is related to the exploitation of the ring

DOI: 10.1021/acs.chemrev.9b00291
Chem. Rev. 2020, 120, 200–268

circumrotation to extract useful work or perform functions, because it is not easy to imagine covalent modifications of the components (e.g., for attaching a cargo moiety or linking the motor to a surface or to the backbone of a polymer) that would not block the movement. Surely this type of light-driven molecular motor is still underdeveloped, and there are opportunities for the design and construction of new prototypes relying on more practical and efficient operation schemes.

3.6. Molecular Rotary Motors

Rotary motion is intrinsic at room temperature in single bonds, but directional control of this motion is a highly challenging task. Initial attempts to develop molecular rotary motors were based on compounds endowed with sterically bulky groups and nonsymmetric moieties such that the free rotation around a single bond could be forced to occur along a preferential direction, in a way similar to a geared pawl device.[98] This system, which is the molecular implementation of Feynman's "ratchet and pawl" paradox,[306] cannot lead to directional motion because it lacks a ratcheting mechanism supported by an energy source.[307] In an outstanding proof-of-principle study, Kelly and co-workers introduced a chemically powered ratcheting step and demonstrated the occurrence of unidirectional 120° rotation.[308] Complete and repetitive unidirectional rotation, however, remained an elusive goal.

A true molecular rotary motor was eventually developed by controlling the rotation around a double bond—a fact that seems counterintuitive since rotation around double bonds is restricted. It is well-known, however, that light can cause such a rotation in an extremely efficient manner in photoisomerization processes (see section 3.2). Definitely, the totality of present-day light-powered molecular rotary motors is based on the photochemically driven *E*−Z isomerization of carbon−carbon or carbon−nitrogen double bonds. Photoisomerization is combined with specific stereochemical elements that, by breaking the symmetry of the potential energy surface, cause a directional bias in the relative sense of rotation of a "rotor" with respect to a "stator" portion of the molecule.[213]

Three main classes of molecular rotary motors have been developed in the last 20 years (Figure 30): (i) overcrowded

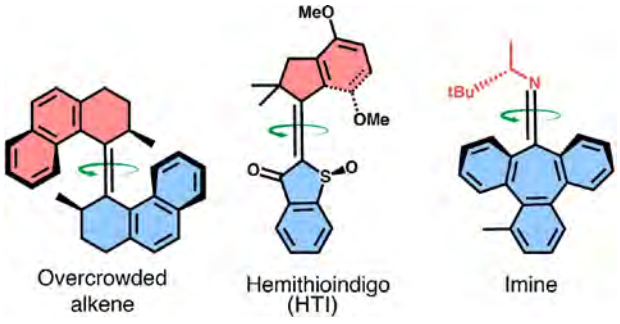

Figure 30. Chemical structures of the three main classes of molecular rotary motors. The "stator" and "rotor" moieties are colored in blue and red, respectively.[38]

alkenes, which represent the first and most investigated family of molecular rotary motors and one of the most advanced and extensively applied classes of molecular motors in general (see section 5);[68] (ii) hemithioindigos, which have several analogies with the previous class but can be natively powered with visible light and exhibit extremely high rotational speed;[239] and (iii) imines, which are highly promising candidates for the development of motors with made-to-order characteristics because of their straightforward synthesis.[213]

3.6.1. Overcrowded Alkenes. The first example of a light-driven single-molecule motor capable of performing repetitive unidirectional 360° rotation, thus converting light energy into a controlled directional rotary motion, was reported in 1999 by Feringa and co-workers (Figure 31).[309] The motor system is

Figure 31. Structure and mechanism for unidirectional rotation of Feringa's first-generation light-driven molecular rotary motor **22**.[309] Steps (1) and (3) are *E*/*Z* photoisomerization steps, and steps (2) and (4) are thermal helix inversion (THI) steps. The "stator" and "rotor" moieties are colored in black and red, respectively.

based on chiral overcrowded alkene **22** featuring a carbon−carbon double bond connecting two identical halves. The steric hindrance between the two rotating halves, installed in the system by the relatively short double bond, forces an out-of-plane arrangement of these two portions, thus conveying a helical shape (*P* or *M*) to the molecule, which proved to be a fundamental prerequisite for the operation of these systems.[310]

For each enantiomer of the first-generation molecular motor, four different stereoisomers exist, which can be interconverted following a sequence of four discrete alternating reactions activated by light and heat that results in the unidirectional rotation around the carbon−carbon double bond (the rotation axle). Starting from the stereoisomer (*P*,*P*)-(*E*)-**22**, light irradiation at 280 nm induces *E* → *Z* photoisomerization of the double bond, resulting in the inversion of the helicity and formation of (*M*,*M*)-(*Z*)-**22**. This species is metastable because of the strain caused by the methyl substituents that are forced in an equatorial conformation. The excess energy present in (*M*,*M*)-(*Z*)-**22** is released in a thermally activated step in the ground state in which one half of the molecule flips over the other half, thus inverting the helicity of the molecule and reorienting the methyl groups in their energetically favored position, affording (*P*,*P*)-(*Z*)-**22**. This thermal relaxation reaction, named "thermal helix inversion" (THI), is practically irreversible because of its large driving force and is responsible for the bias in the rotation direction. A second photoisomerization reaction transforms (*P*,*P*)-(*Z*)-**22** into the metastable (*M*,*M*)-(*E*) form, which undergoes a second THI step and concludes a 360° cycle of rotation around the carbon−carbon double bond by reforming the starting stereoisomer (*P*,*P*)-(*E*)-**22**. This mechanism of operation shows an elegant

DOI: 10.1021/acs.chemrev.9b00291
Chem. Rev. 2020, 120, 200−268

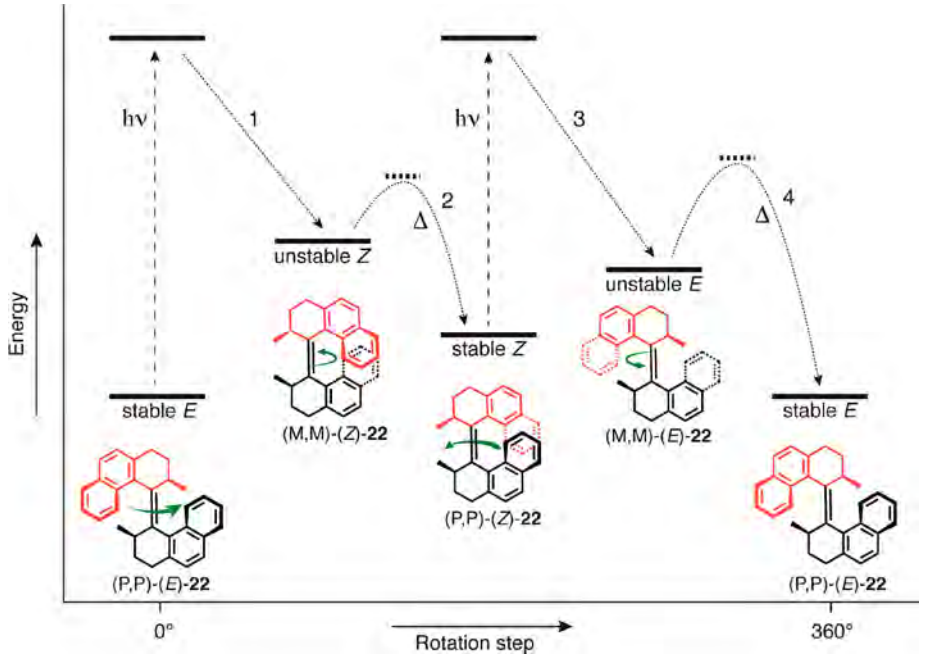

Figure 32. Simplified energy profile for the 360° rotation of the first-generation overcrowded alkene rotary motor **22**. Steps (1) and (3) are the *E*−*Z* photoisomerization steps, while steps (2) and (4) are the THI steps. The "stator" and "rotor" moieties are colored in black and red, respectively. Adapted with permission from ref 38. Copyright 2017 Royal Society of Chemistry.

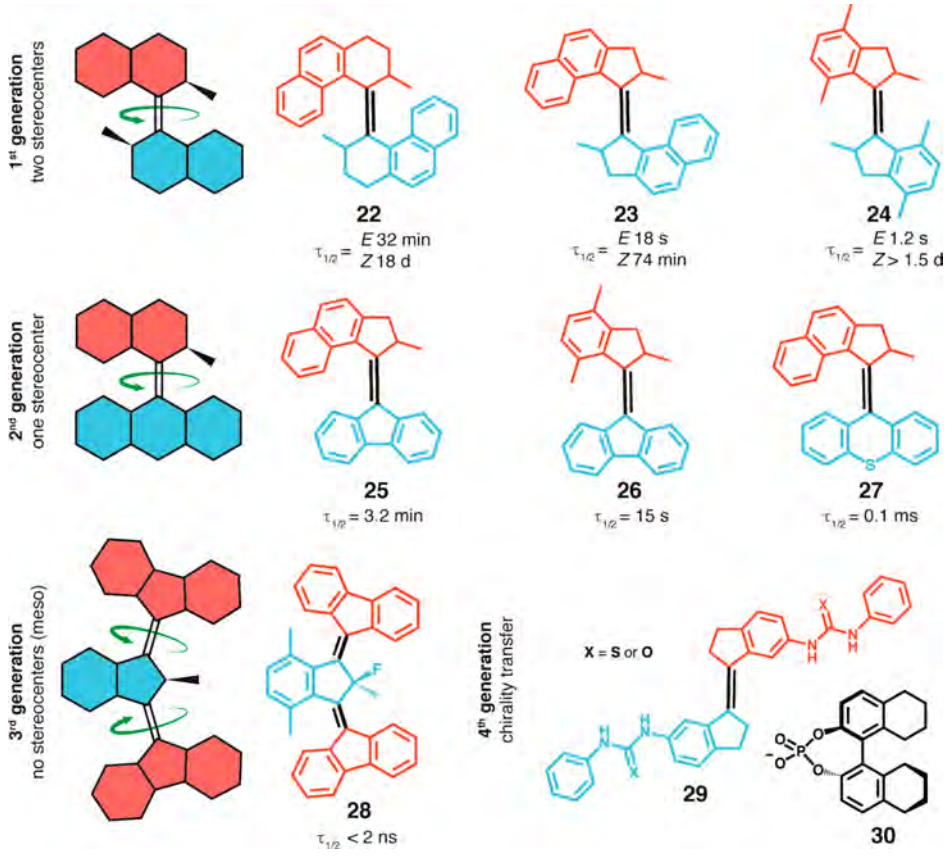

Figure 33. (left) Cartoon representation of the general structure ("stator" in blue, "rotor" in red) of light-activated rotary motors of the overcrowded alkene family.[38] Right: structural variations of the different motor generations and their effect on $t_{1/2}$ (at 25 °C) of the THI processes, which is inversely related to the rotational speed.[213]

interplay between the dynamic helical chirality established in the molecule by the bulky substituents attached to the double bond and the fixed point chirality of the stereogenic centers decorating the two rotating halves. As shown schematically in Figure 32, the configuration of the stereogenic centers biases the direction of rotation during the photoisomerization step that inverts the

DOI: 10.1021/acs.chemrev.9b00291
Chem. Rev. 2020, 120, 200−268

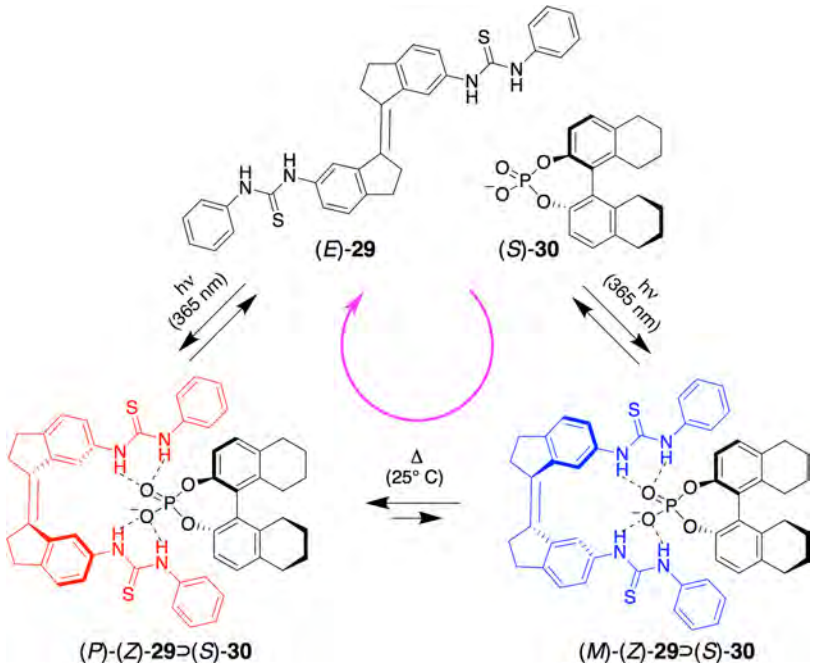

Figure 34. Structure and mechanism for unidirectional rotation of the fourth-generation light-driven molecular rotary motor **29** in the presence of the chiral guest **30**. Adapted from ref 315.

helicity of the molecule, while the irreversible energetically downhill THI ensures that the motor returns to its stable form, from which it can be excited again, leading to autonomous light-driven operation.[309]

The main shortcoming of the first-generation molecular motor is that the activation barriers for the two THI steps are not equal (Figure 32). Thus, the rotational motion proceeds with an irregular speed, and one half of the 360° rotation can be considerably slower than the other, depending on the difference between the activation energies of the two THI steps. In fact, because of the low rate of the (*M*,*M*)-(*E*) → (*P*,*P*)-(*E*) transformation at room temperature, motor **22** could perform full rotation cycles in an autonomous fashion only at temperatures higher than 60 °C.[310] The second-generation overcrowded alkene molecular motors developed by Feringa and co-workers addressed this issue by replacing one of the two halves of the first-generation motor with a symmetrical moiety (e.g., compounds **25**−**27** in Figure 33).[311] While the same mechanistic steps illustrated in Figure 32 account for the functioning of the second-generation motors, the simple and elegant structural modification results in very similar barriers for the two THI steps, allowing more uniform and controllable rotational motion. Moreover, the new overcrowded alkene molecular motors proved that the presence of a single stereogenic element is sufficient to achieve unidirectional rotation.[312]

The amount of "chiral information" necessary to achieve directionally controlled rotation was further reduced in the so-called third generation (compound **28** in Figure 33).[313,314] The design of the third generation is based on two second-generation overcrowded alkene motors joined together in such a way that the single stereocenter present in the two motors becomes a pseudo-asymmetric center in **28**, thus making the whole molecule achiral. The mode of operation is analogous to two rotary motors operating together; it should be noted that the two rotor moieties rotate in opposing directions relative to the middle stator unit. For an external observer, both rotor parts move in the same direction, in analogy to the wheels of a car connected by the axle. Besides reducing the amount of structural asymmetry required to achieve unidirectional rotation, in this generation of motors the computationally determined THI rate—which regulates the rotational speed—is one of the highest ever reported for an overcrowded alkene molecular motor, thus making compound **28** one of the fastest rotary motors developed to date. Moreover, the unique rotational dynamics displayed by this generation of motors could in principle be applied to obtain a directional movement on a surface, fostering the development of a new generation of autonomous light-powered nanocars.[116,313]

In a continued effort to reach a minimal amount of chiral information for dictating the direction of rotation in overcrowded alkenes, Feringa and co-workers developed a new type of molecular rotary motor that is completely devoid of stereocenters in the photoactive portion of the system.[315] In this "fourth-generation" motor (compound **29** in Figure 33), the preferential direction of rotation is enforced by a chiral guest molecule that can bind non-covalently to a light-activated switch. In other words, it is a supramolecular transfer of chirality from the optically active guest that induces the unidirectional rotation around the double bond of the photoswitchable receptor. Under the operational conditions (Figure 34), irradiation of motor **29** with 365 nm light results in equal rates of formation of the *P* and *M* stereoisomers of the photoswitchable moiety at the photostationary state. Binding of chiral phosphate anion **30** induces the preferential formation of one of the helical isomers, (*P*)-(*Z*)-**29**⊃(*S*)-**30**, over the other, (*M*)-(*Z*)-**29**⊃(*S*)-**30**, by a THI reaction. In this situation, the reverse *Z* → *E* photoisomerization takes place predominantly from the (*P*)-(*Z*)-**29**⊃(*S*)-**30** isomer, thus concluding a full cycle with a net unidirectional rotation of the two halves of the photoswitchable host around the joining double bond (Figure 34).

The mechanism of operation of the fourth-generation rotary motor closely resembles that of the first-generation one:

DOI: 10.1021/acs.chemrev.9b00291
Chem. Rev. 2020, 120, 200−268

ultimately, it is the formation of a metastable diastereomeric supramolecular complex during the photochemical step that drives the unidirectional rotation. Since the direction of rotation is enforced by the chirality of the guest, which can be easily exchanged in situ with a guest of opposite chirality, this generation of motors offers the unique possibility to switch the sense of rotation of the motor by means of chemical input.

Numerous studies aimed at increasing the rotational speed of the first- and second-generation rotary motors by analyzing in depth the effect of structural modifications on the mechanism of their operation were also carried out.[316−318] Since the photochemical isomerization is vastly faster (picosecond time scale) than the THI steps,[319] these studies mainly focused their attention on possible ways to reduce the barrier of the thermal steps to increase the rate of rotation. Experimental screening of different substitution patterns, aided by high-level computational studies, culminated in the development of modified first- and second-generation motors that can operate in the megahertz regime. This level, however, does not yet represent the speed limit predicted by theoretical calculations.[312,320]

Dynamic control of the rotational speed was a successive logical step to obtain a higher level of control in the operation of overcrowded alkene molecular motors. Preliminary investigations proved that the speed of the rotary motors is dependent on the nature of the solvent. In a series of systematic studies on first-generation motors with pendent arms of variable flexibility and length (Figure 35a), it was observed that the dynamics of the

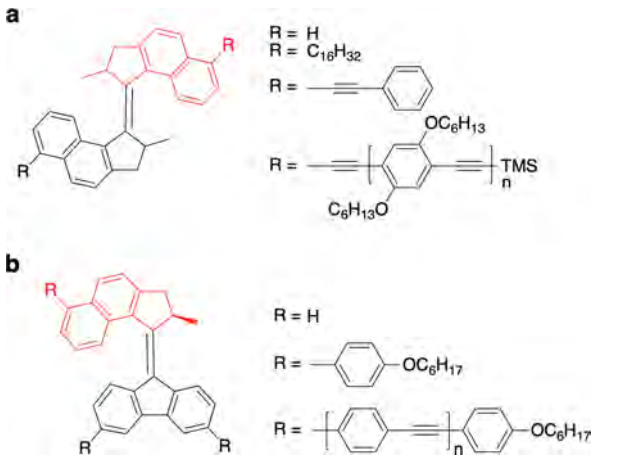

Figure 35. General structure and variations of (a) first-generation[321] and (b) second-generation[322] molecular motors developed to study the solvent viscosity dependence of the rotational dynamics. The "stator" and "rotor" moieties are colored in black and red, respectively.

THI steps are a function of both the size and rigidity of the substituents and the solvent viscosity, while the solvent polarity plays a minor role.[321] Interestingly, analogous studies conducted on second-generation motors decorated with similar substituents (Figure 35b) evidenced that for this class of motors the THI step is independent of the viscosity of the medium and size of the substituents. The rate of the photochemical step, which was revealed to be a complex stepwise excited-state reaction by fast spectroscopy studies,[319] is influenced by the viscosity of the solvent but is independent of the size of the substituents.[322] This implies that in the second-generation motors the evolution of the excited state toward the ground state is dominated by structural changes in the inner core of the motor, without large-scale reorientation of the motor and its substituents. These contrasting results suggest that while the mechanism of operation is at first sight similar for first- and second-generation motors, the details of the rotation mechanisms in the two generations of motors are different, and their comprehension deserves further research efforts.

While the dynamic control of the rotational rate by medium effects evidenced unexpected complexities, different systems have been developed with the purpose of modulating the rotational motion with chemical or light stimuli. In the second-generation motor **31** (Figure 36a), functionalized on the rotor

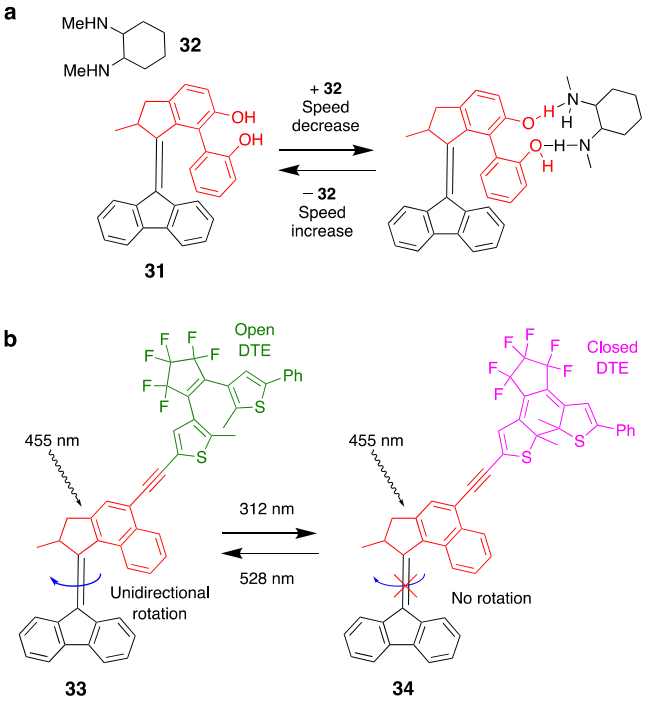

Figure 36. Structures and mode of operation of (a) chemically[323] and (b) photochemically[325] controllable light-activated second-generation molecular rotary motors.

half with a biphenol moiety, the rotational speed could be decreased by more than 2 orders of magnitude upon complexation with diamine **32**.[323] The binding of the diamine effectively decreases the rate of the THI step by forcing the rotor portion of the motor into a rigid planar conformation. The binding affinity of the amine guest can be tuned by the addition of either methanol or acetic acid, thus allowing the behavior of the molecular motor to be reversibly modulated through a combination of different chemical triggers. Along the same direction, by functionalization of the motor with a crown ether moiety, the rotary speed could be modulated by complexation with different metal cations.[324] More recently, in second-generation motor **33** bearing a photochromic dithienylethene (DTE) moiety attached to its rotor portion (Figure 36b), the possibility of light-gating of the rotational motion was demonstrated.[325] The photochromic DTE unit can be switched from an open form to a closed form by irradiation with a different wavelength from the one applied to operate the motor. In the closed form (compound **34** in Figure 36b), the DTE moiety completely inhibits the rotation of the motor unit. While the detailed mechanism of inhibition of the rotary motion by the closed form of DTE is not completely understood, the result achieved is remarkable, representing the first case of a phototriggered light-powered molecular rotary motor (see

DOI: 10.1021/acs.chemrev.9b00291
Chem. Rev. 2020, 120, 200−268

section 3.7 for examples of phototriggered chemically powered motors). Moreover, the extension of the conjugation brought by the functionalization with the DTE unit contributes to red-shifting the wavelength of light used to operate the motor into the visible region.

In order to employ light-driven artificial rotary motors in biological systems, two key requirements have to be fulfilled: (i) solubility in water and (ii) operation by excitation with light that can deeply penetrate living tissues without damaging them.[228,245] To reach these goals, first- and second-generation motors were rendered water-soluble by functionalization with appropriate hydrophilic substituents (see, e.g., compounds **35** and **36** in Figure 37), and their operation was investigated in aqueous buffers, verifying that the modified motors could function also in complex media.[326] The operation of second-generation motors has also been demonstrated inside micelles, whose lipophilic core closely mimics the environment present in cellular membranes and other biologically relevant hydrophobic regions.

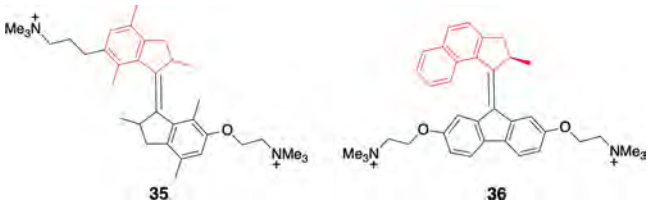

Figure 37. Structure of water-soluble molecular rotary motors of the first (**35**) and second (**36**) generations.[326] The "stator" and "rotor" moieties are colored in black and red, respectively.

Visible-light-powered rotation in overcrowded-alkene-based motors was first accomplished by triplet sensitization from an appended porphyrin with 530 nm light.[327] More recently it was shown that by extension of the aromatic core of a second-generation molecular motor with a dibenzofluorene lower half (compound **37** in Figure 38), the excitation wavelength is significantly red-shifted (down to 490 nm) without impairing the motor function.[328] The straightforward design makes extension of the conjugation of the stator moiety a promising and easily applicable strategy to tune the wavelength of the light used to operate this class of motors.

In a radically different design, the stator portion of a second-generation motor was substituted with a 4,5-diazafluorenyl coordination motif.[329] Upon complexation with bis-(bipyridine)ruthenium(II) (compound **38** in Figure 38), the rotation process can be driven with visible light with a wavelength of 450 nm. This observation was tentatively attributed to energy transfer from the metal complex to the motor. Furthermore, a large increase in the speed of rotation was observed that was shown by theoretical calculations to be the result of slight modifications of the conformation of the stator portion of the motor as a result of metal complexation. Very recently it was shown that second-generation rotary motors can also be operated by visible light by modification of the rotor half. For example, in compounds **39**[330] and **40**[331] (Figure 38), the rotor contains pyrenyl and *N*-methyloxyindole moieties, respectively.

A key aspect of overcrowded alkene motors is their ample potential for further chemical modification. This is clearly evidenced by the large variety of different structures described so far, that enabled not only fine-tuning of their operation but also their application in different chemical environments, encompassing surfaces, membranes, and nanoarchitectures (also see section 5).[332] A recent example is the functionalization of a quartz surface with the second-generation motor **41** bearing a fluorescent perylenebis(imide) (PBI) moiety on the rotor portion (Figure 39).[333] Light-driven rotation and fluorescent

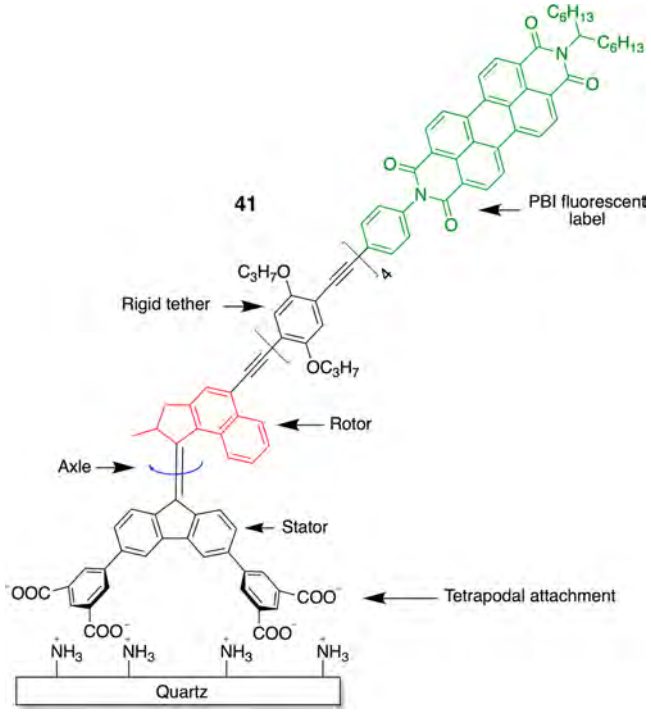

Figure 39. Structure of the second-generation molecular rotary motor **41** bound to a quartz surface. The rotor portion (in red) was functionalized with a long rigid tether bearing a fluorescent perylenebis(imide) unit (green). Adapted from ref 333. Copyright 2018 American Chemical Society.

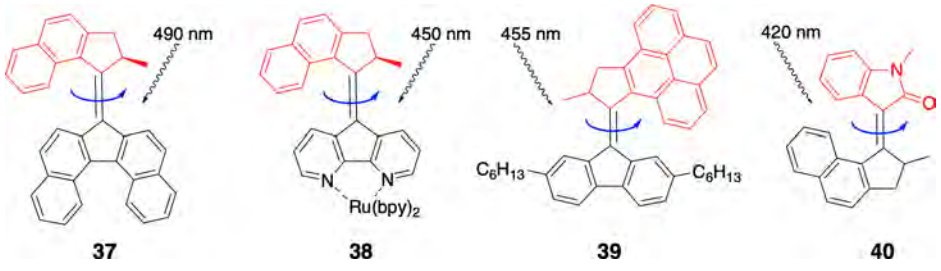

Figure 38. Structures of second-generation molecular motors **37**,[328] **38**,[329] **39**,[330] and **40**,[331] whose rotary movement can be driven by visible light. The "stator" and "rotor" moieties are colored in black and red, respectively.

DOI: 10.1021/acs.chemrev.9b00291
Chem. Rev. 2020, 120, 200−268

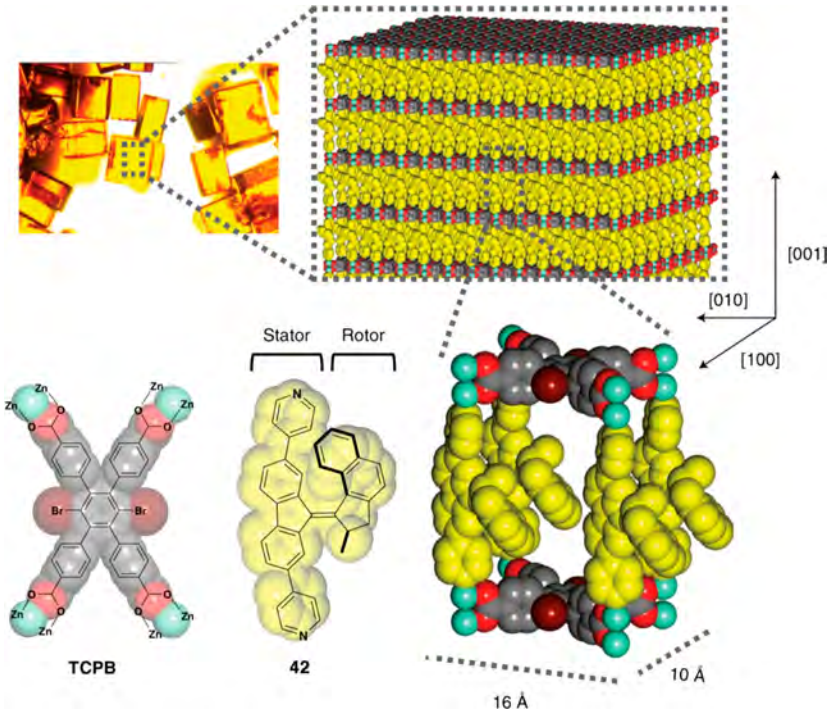

Figure 40. Schematic representation of the 3D architecture of a "moto-MOF". The packing of the crystal, the elementary cell, and the structure of the linkers, tetracarboxylic acid (**TCPB**), and molecular motor (**42**) are shown. The stator of the motor (that is, the fluorene unit) is used to bridge the 2D layers constructed from Zn paddlewheel clusters and **TCPB**, while the rotor moiety (the naphthyl unit) can rotate freely with respect to the other half under light irradiation. Adapted with permission from ref 335. Copyright 2019 Springer Nature.

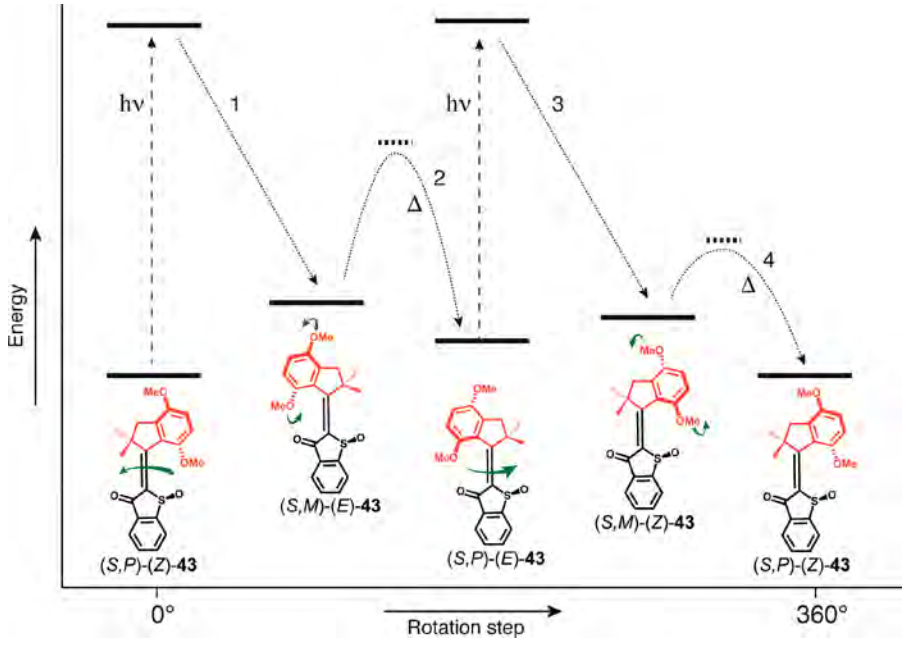

Figure 41. Simplified energy profile for the 360° rotation of the HTI-based molecular motor **43**.[3371] and[3] are the *E*−*Z* photoisomerization steps, while[2] and[4] are the thermal helix inversion (THI) steps. The "stator" and "rotor" moieties are colored in black and red, respectively.

detection were achieved with the multicomponent assembly grafted onto an amine-coated quartz substrate.[334] A key structural feature of **41** is that the PBI unit is connected to the motor with a rigid tether that is long enough (ca. 3.2 nm) to prevent photoinduced electron transfer that would impair motor operation. This system enabled imaging of the unidirectional rotation of individual molecular motors on a surface via defocused wide-field microscopy, thus revealing the mechanistic details of their operation at the single-molecule level in unprecedented detail.

Very recently, second-generation molecular motors were arranged in a crystalline metal−organic framework (MOF), as illustrated in Figure 40.[335] The motor units were installed in the three-dimensional (3D) structure as part of the organic linker (compound **42** in Figure 40). A combination of X-ray analysis and optical and Raman microscopy provided proof of

DOI: 10.1021/acs.chemrev.9b00291
Chem. Rev. 2020, 120, 200−268

unhindered unidirectional rotation in the solid state, permitted by the large free volume of the chosen framework, with a rotary speed (estimated from the rate of THI) comparable to that measured in solution. These so-called "moto-MOFs" hold high promise in applications aimed at controlling dynamic functions in crystalline materials, such as the diffusion of gases and the mass transport of adsorbed molecules, or as miniature light-powered pumps in microfluidic devices.[336]

In summary, the exceptional synthetic flexibility, together with a deep understanding of their functioning, definitely makes this category of rotary motors one of the most developed and widely applied classes of light-powered molecular motors in nanoscience (see section 5).

3.6.2. Hemithioindigos. The first example of a hemithioindigo (HTI)-based molecular rotary motor was designed by implementing additional stereochemical elements to the HTI framework (Figure 41):[337] a stereocenter on the sulfur atom (oxidized to a sulfoxide) and helical twisting around the double bond (by introducing steric crowding on the stilbene fragment). Therefore, molecule **43** can assume *Z* and *E* configurations with respect to the C═C double bond, *R* and *S* configurations on the sulfur atom, and *P* and *M* helicities around the double bond. The racemic mixtures of *S* and *R* enantiomers were analyzed; for the sake of conciseness, only one isomer will be discussed (see Figure 41). The (*S*,*P*)-(*Z*) isomer is the thermodynamically stable form of motor **43**, in thermodynamic equilibrium with the (*S*,*P*)-(*E*) isomer, which in turn is the most stable isomer of the metastable *E* configuration. Irradiation experiments on rotary motor **43** can be summarized as follows: upon irradiation with visible light, (*S*,*P*)-(*Z*) is converted into (*S*,*M*)-(*E*) (process 1 in Figure 41), which upon THI becomes (*S*,*P*)-(*E*) (process 2 in Figure 41). Irradiation of this compound transforms it into (*S*,*P*)-(*Z*) again, but without the formation of the metastable (*S*,*M*)-(*E*). Actually, another metastable state must be formed, i.e., (*S*,*M*)-(*Z*) (process 3 Figure 41), which could not be evidenced experimentally. The two coupled photochemical and thermal reactions consist respectively of 180° rotations, but they follow two different pathways: this result is only compatible with an overall 360° rotation. The operation of the rotary motor under irradiation is schematized by the energy profiles in Figure 41, which were also confirmed by theoretical calculations. Moreover, the theoretical description gives a calculated energetic barrier for helix inversion from (*S*,*M*)-(*Z*) to (*S*,*P*)-(*Z*) of only 5.54 kcal mol^{-1}, which corresponds to a half-life of 0.75 μs at 90 °C, a time range not accessible with conventional techniques.

In order to get evidence of the elusive (*S*,*M*)-(*Z*) isomer, fast spectroscopy measurements and theoretical calculations were performed.[338] Three important results emerged from that complete investigation. First of all, the formation of all four stable states was experimentally proven. Moreover, theoretical investigation evidenced that after photoexcitation both (*S*,*P*)-(*Z*) and (*S*,*P*)-(*E*) can reach triplet states, which then deactivate to the ground state without leading to isomerization; the triplet state of (*S*,*P*)-(*E*) was also evidenced and characterized with time-resolved spectroscopy. Triplet pathways are in competition with the isomerization reactions and are therefore unproductive for motor rotation. Nevertheless, these pathways are not the major factor responsible for reduced performance—the high quantum yields of the unproductive internal conversions are much more important. Finally, analysis of the kinetic and thermodynamic parameters associated with the operation of the molecular motor established a 95% unidirectionality for this motor and a kilohertz theoretical maximum speed of rotation, which would be quite remarkable performance. As a matter of fact, the speed of rotation is limited by the slowest thermal process (which is the (*S*,*M*)-(*E*) to (*S*,*P*)-(*E*) helix inversion, process 2 in Figure 41) only if the photochemical reactions are able to keep the system in the (*S*,*M*)-(*E*) state. Actually, under normal irradiation conditions, because of the low quantum yield of photoisomerization, the rate-limiting step is the light-driven population of (*S*,*M*)-(*E*) (process 1 in Figure 41), which reduces the maximum rotation rate to 0.01−1 Hz. All of these results taken together are extremely valuable for the proper design of molecular motors.

A more crowded HTI derivative was also investigated with conventional spectroscopic techniques at room temperature. Indeed, upon insertion of greater steric hindrance on the rotor (stilbene) fragment, the kinetics of rotation can be slowed down, thus enabling characterization of all four stable states.[339]

An original strategy for developing rotary motors was implemented with hemithioindigo derivative **44** shown in Figure 42.[340] Also in this case a stereocenter on the sulfur atom and a chiral axis confer asymmetry to the molecule, which can exist in four different states (Figure 42). These isomers differ either by the *Z* (A and B) or *E* (C and D) configuration or by the S_a (A and C) or R_a (B and D) axial chirality, and the atropisomers are thermally stable. The first consequence is that all four species can be separated and characterized. Each species, when irradiated, is converted into the others, following three possible reaction pathways: single-bond rotation, double-bond isomerization, or hula twist,[341,342] i.e., coupled double- and single-bond rotations. As an example, isomer A can convert into B via single-bond rotation, to C via double-bond isomerization, and to D via hula twist. Overall, 12 photoreactions could take place, which would interconvert each isomer with all of the others. The photochemical quantum yields of all the reactions under irradiation at 442 nm were determined via NMR spectroscopy, and the probability of each reaction over the others could then be estimated. In order to operate as a

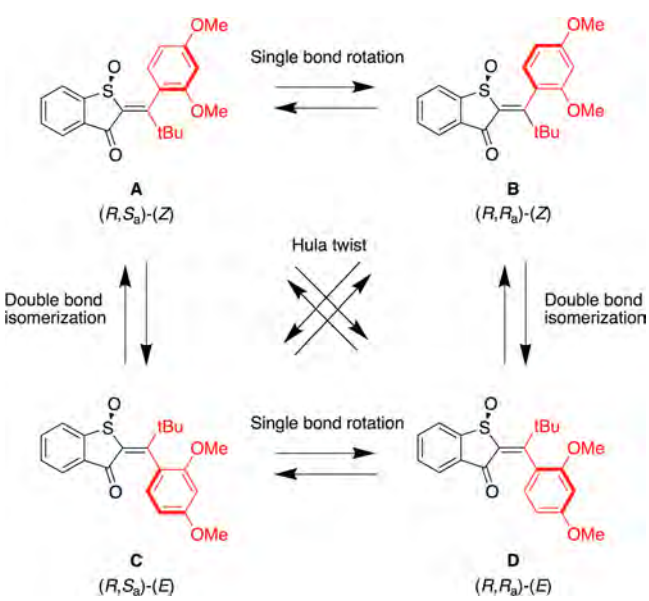

Figure 42. Molecular structures and interconversion pathways of the four stable diastereoisomers of **44**.[340] The "stator" and "rotor" moieties are colored in black and red, respectively.

DOI: 10.1021/acs.chemrev.9b00291
Chem. Rev. 2020, 120, 200−268

molecular motor, at least three steps must be performed without any reversal process (the probabilities of cycles involving more than three steps were low, so such cycles could be neglected). Therefore, eight different three-step cycles (four forward and four backward) can take place: ABC, ABD, ACD, and BCD are the forward cycles, and ACB, ADB, ADC, and BDC are the backward ones. Among all these possibilities, the ABC cycle is the most probable one at 20 °C, with a preference over the other cycles (i.e., monodirectionality) of 81% and 100% unidirectionality. Nevertheless, the propensities of the different photochemical reactions, and therefore the reaction pathway, can be modulated by changing the temperature. In the present system, to improve the monodirectionality (i.e., the preference for one cycle over the others), the probability of the B to C hula twist photoreaction should increase relative to the B to D double-bond isomerization, which is accomplished by decreasing the temperature to −50 °C. Indeed, under those experimental conditions, the monodirectionality of the ABC cycle is 98%. This is an unprecedented result in molecular motors, and it is clearly related to the absence of thermal steps in the sequence of reactions. Thermal steps in molecular motors are usually the ratcheting steps of the unidirectional rotation. Indeed, the unidirectionality, speed, and efficiency of the rotary motor depend on these processes. When the temperature is decreased, these thermal reactions are slowed down or suppressed, and the molecular motor is converted into a molecular switch. This molecular motor relies on a new strategy and unique rotation mechanism that is controlled solely by photons. Recently the HTI motor was functionalized with thioether feet for attachment on metal surfaces.[343]

3.6.3. Imines. Compounds containing a C═N double bond, such as imines, oximes, and hydrazones, combine the features of C═C bonds present in alkenes with the fluxional stereochemical possibilities intrinsic to a nitrogen atom. Lehn was the first one to hypothesize, in the otherwise deeply explored chemistry of the C═N double bond, the possibility to develop a novel class of rotary molecular motors.[344] The key aspect was identified in the possibility of C═N double bonds to follow two different independent *E*−*Z* isomerization pathways depending on whether the configurational switching is initiated by light or heat. Earlier experimental and theoretical studies indicated that while the thermal isomerization proceeds by an in-plane nitrogen inversion, the light-induced *E*−*Z* isomerization proceeds through an out-of-plane rotation around the C═N double bond (Figure 43).[252,253] The distinct trajectories of the thermal and photochemical pathways suggested that a combination of light and thermal energy could lead to a particularly simple and versatile molecular motor. In fact, it was argued that under chiral symmetry-breaking conditions, achieved by introducing a stereogenic center near the nitrogen atom, the photoinduced rotation could be forced to occur preferentially along a specific direction (either clockwise or anticlockwise). Such a photoinduced motion, together with the thermally activated in-plane isomerization, would result in the unidirectional rotation of the substituents attached to the carbon and nitrogen atoms around the double-bond axis. Thus, the directional light-driven rotation in one direction stores energy, which is then released by thermal nitrogen inversion.

The vast amount of research on the chemical properties of C═N double bonds helped in the choice of the best combination of substituents to realize this conjecture.[345] The design of the working prototype of the first amine-based rotary motor was based on diaryl-*N*-alkylimines, which are known to

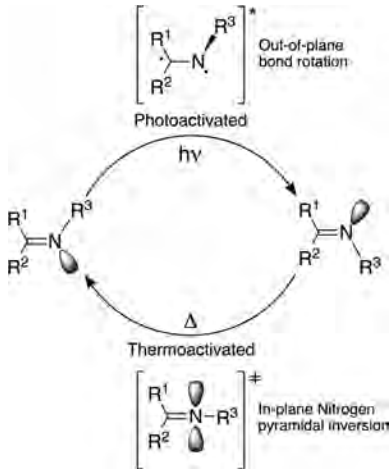

Figure 43. General schemes for the (top) photochemically and (bottom) thermally activated isomerization processes of imines.[213]

exhibit slow thermal *E*−*Z* isomerization at ambient temperature.[346]

Figure 44a shows the structure and operational cycle of the imine-based motor **45**. Irradiation of (*P*)-(*Z*)-**45** leads to *Z* → *E* photoisomerization through rotation around the C═N double bond, resulting in the metastable (*M*)-(*E*) stereoisomer. Interestingly, it was discovered that this high-energy strained species relaxes to the more stable (*P*)-(*E*) form not through pyramidal inversion of the substituents on the nitrogen atom but rather by a faster ring inversion process reminiscent of the thermal helix inversion observed in overcrowded alkene rotary motors (section 3.6.1). This additional process can occur because of the flexibility of the aromatic skeleton of the stator portion of the motor, which is able to flip in and out of the plane. The successive absorption of a photon triggers another half-rotation around the C═N double bond to yield (*M*)-(*E*)-**45**, and a final ring inversion step completes a full 360° rotation of the substituents around the double-bond axis. The operation mechanism proceeds through four distinct steps and is very similar to that of overcrowded alkene motors.

With an extremely elegant modification of the aromatic stator unit, rigidified by the introduction of a fused benzene ring that reduces the flexibility of the heptenyl aromatic core, Lehn and co-workers developed a motor molecule that, despite its similarity with **45**, operates in a different fashion.[346] Upon light irradiation, (*M*)-(*Z*)-**46** (Figure 44b) undergoes *Z* → *E* photoisomerization of the double bond through bond rotation; the so-formed high-energy (*P*)-(*E*) form undergoes pyramidal inversion at the nitrogen atom, as ring inversion is now a more energetically demanding path because of the rigidification of the aryl moiety. The pyramidal inversion proceeds through an in-plane rotation that leads to the starting stereoisomer by completion of a 360° rotation in only two elementary steps. Thus, it was nicely demonstrated that fine-tuning of the conformational flexibility of the aryl "stator" can alter the mode of operation of this class of motors from a four-step sequence of processes (alternating light power strokes and thermal relaxation steps via ring inversion) to a two-step sequence (a light power stroke and a thermal relaxation step via nitrogen inversion).

It is important to highlight that the possibility of installing a wide variety of substituents at the nitrogen and carbon termini, together with the straightforward synthetic accessibility of

DOI: 10.1021/acs.chemrev.9b00291
Chem. Rev. 2020, 120, 200−268

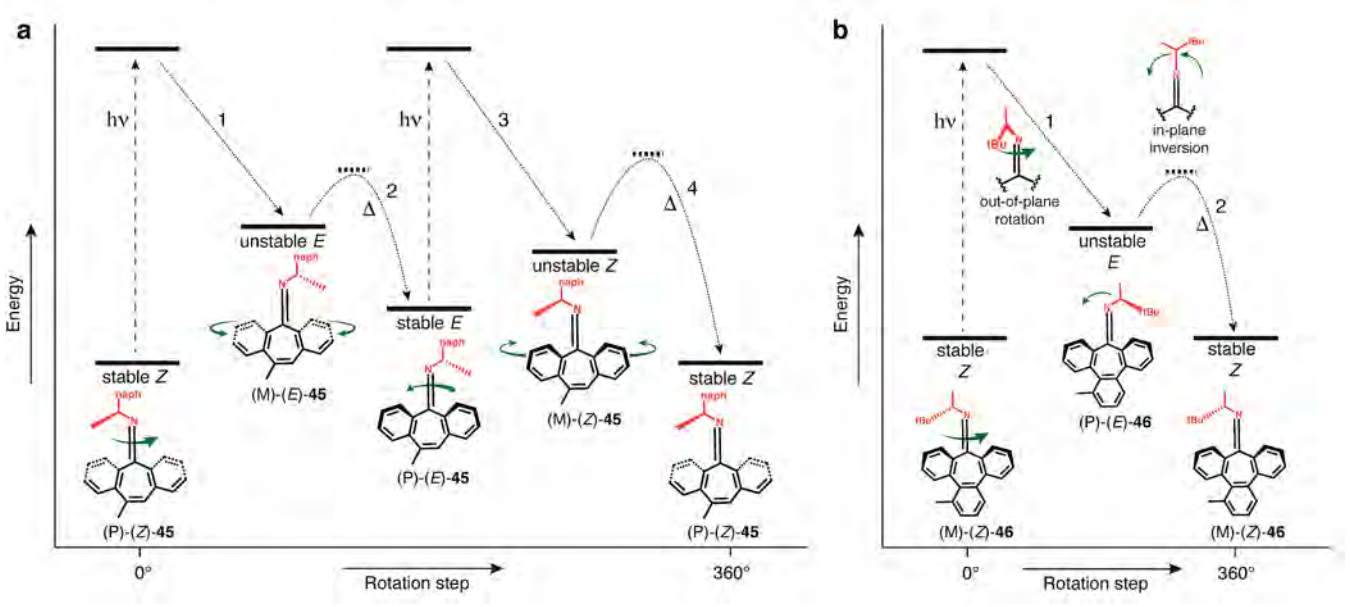

Figure 44. Structural formulas, operating mechanisms, and simplified energy profiles for 360° rotation of imine-based light-driven molecular rotary motors.[346] (a) Four-stroke motor **45**. Steps (1) and (3) denote *E*−*Z* photoisomerization, and steps (2) and (4) denote ring inversion. (b) Two-stroke motor **46**. Steps (1) and (2) denote *E*−*Z* photoisomerization and thermal nitrogen pyramidal inversion, respectively.

imines, enables the exploration of a wide range of possible structural modifications[347] and the preparation of this class of molecular motors in large amounts. The main drawback compared to overcrowded-alkene-based motors is that while the mechanistic details of the latter have been experimentally and computationally established in detail, in the case of imine-based motors the precise stereochemical dynamics of the motion, in particular for the photochemical steps, has been mostly determined only by means of computational studies.[348] Considerable experimental work still needs to be performed to fully clarify the details of the working mechanism of this fascinating new class of rotary motors.

A significant step forward toward the experimental demonstration of unidirectional rotation in chiral imine motors was reported in a follow-up study on camphor-based imines.[349] In camphorquinone-derived imine **47** (Figure 45), because of the rigidity of the stator portion of the motor, the rotational mechanism was expected to operate via a two-step pathway consisting of photoinduced rotation followed by thermal inversion. Direct experimental evidence of the photoinduced unidirectional rotation, however, has proven to be extremely difficult to obtain because of the ultrafast dynamics of the excited-state reactions.[350] Thus, to gain insight into the directionality of the C═N bond photoisomerization, a clever experiment was designed that was based on the trapping of the two different diastereotopic biradicals formed upon excitation of **47** to the S_2 state with 254 nm light. Specifically, excitation to the S_2 state leads to opening of the cyclopropyl ring and formation of a biradical species that can undergo C═N rotation (as happens in the S_1 state reached by 365 nm excitation). Before reaching the S_1 state, some of the biradical S_2 excited molecules undertake a rearrangement reaction, yielding two diastereomeric derivatives (exo- and endo-trapped states) whose ratio is indicative of the preference between the two diastereotopic excited-state trajectories that are responsible for the preferential sense of rotation (Figure 45). Indeed, a significant difference in the yields of the exo and endo stereoisomers upon prolonged light irradiation at 254 nm was observed. Although the rotational

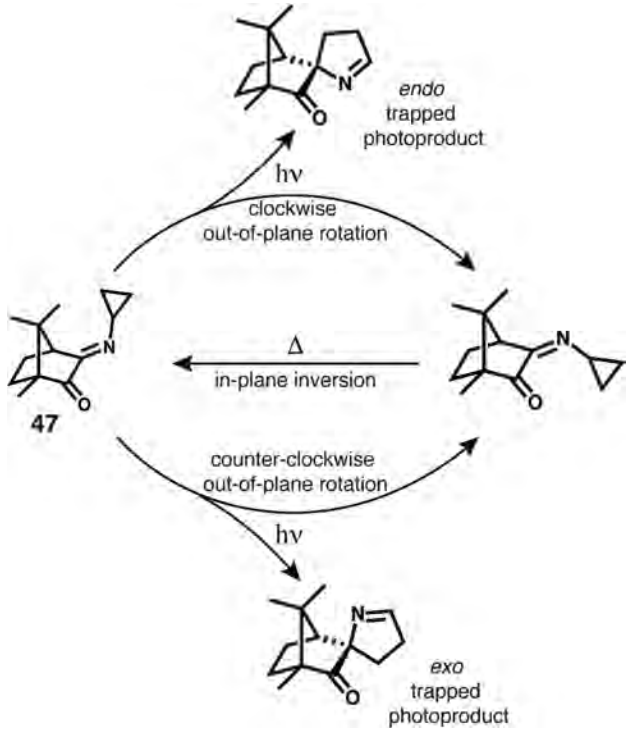

Figure 45. Structure and mechanism of directional rotation in camphorimine-based rotary motor **47**[349] and structures of the trapped endo and exo photoproducts.

preference in the biradical species (S_2 state) may differ from that of the pure C═N bond rotation (S_1 state), this result is an indirect yet convincing experimental proof of the unidirectional rotation in these chiral imines.[349]

As a general message conveyed by such experimental and computational studies, it is reasonable to anticipate that all chiral imines are potentially molecular rotary motors that can be driven by light and thermal energy. This is a striking consideration if

DOI: 10.1021/acs.chemrev.9b00291
Chem. Rev. 2020, 120, 200−268

one considers the large variety of imine intermediates that are formed along metabolic pathways of living cells. A most interesting and still unexplored possibility is to combine the motional dynamics of imines with their constitutional dynamics, which could in principle lead to dynamic libraries of motor moieties. All of these aspects make imine-based rotary motors some of the most interesting and promising molecular machines that chemistry has to offer.

3.6.4. Other Systems. On the basis of the knowledge acquired by studying the three main classes of molecular rotary motors described in the previous sections, different research groups have proposed or developed molecular systems able to exhibit unidirectional rotation. Most of them are the result of high-level computational studies on simple molecular systems. Indeed, nowadays through accurate modeling of the shapes and the critical points of the ground- and excited-state potential energy surfaces, one can identify the presence of deactivation pathways of photogenerated states that lead to the unidirectional rotation of a portion of a molecule with respect to another.

Recently, Filatov and co-workers proposed that the well-known photochromic fulgides have the proper characteristics to operate as molecular rotary motors under light irradiation.[351,352] Quantum-chemical calculations and molecular dynamics simulations support the hypothesis that chiral fulgide-based moieties (compounds **48** and **49** in Figure 46) are able to rotate

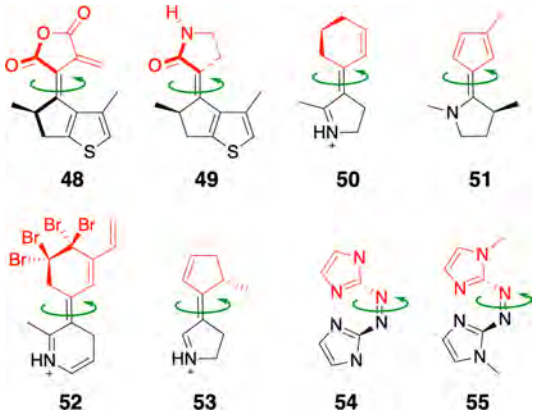

Figure 46. Molecular structures of different classes of computationally investigated rotary molecular motors. The "stator" and "rotor" moieties are colored in black and red, respectively.

unidirectionally around the central carbon double bond with high quantum efficiencies and dynamics on the femtosecond time scale. The synthetic accessibility of fulgides makes this finding interesting for applications, although the anticipated fast dynamics of the rotational motion will likely pose a significant problem for its experimental validation.

Durbeej and co-workers carried out a computational investigation of different structures of chiral bicyclic imines (**50**) and enamines (**51**), thereby finding possible novel mechanisms to enhance the directionality of rotation[353] and proposing an elegant minimalistic design for a visible-light-driven rotary motor constituted by a simple protonated imine conjugated to five C═C double bonds (**52**).[354,355]

In an even more extreme attempt to design the simplest light-activated molecular rotary motor, the groups of Olivucci, Léonard, and Gindensperger reported a computational study of the photoisomerization of the biomimetic indanylidene–pyrrolinium framework.[356] The results proved that in imine **53** the single stereogenic center in the allylic position with respect to the reactive double bond is sufficient to introduce unidirectional rotation in the photoisomerization process. Moreover, the calculations revealed that even a very small amount of pretwist (less than 2°) or helicity in the equilibrium ground state of the reactive double bond is sufficient to promote unidirectionality in the rotation, thus quantifying the minimal amount of "chiral information" that has to be contained in a molecular motor.

The photochemistry of simple chiral azoheteroarenes (compounds **54** and **55** in Figure 46) has also been computationally investigated, proving that in contrast to their homoaromatic counterparts such as azobenzenes, the *Z*–*E* photoisomerization mechanisms can display a high bias toward unidirectional rotary dynamics.[357] The proposed design is very interesting both from a theoretical perspective, as it represents the first proposed rotary motor exploiting light-activated rotation around an azo double bond, and a practical perspective, because the photoisomerization around the N═N bond is one of the best photoreactions in terms of fatigue resistance. This is an important characteristic for practical applications that is not always taken into proper consideration in the development of novel molecular motors.

The only example of an experimentally realized rotary motor exploiting the *E*–*Z* photoisomerization of azobenzene was reported by Haberhauer and co-workers (compound **56** in Figure 47a).[358] The structure is rather complex, and the motion sequence follows a pattern of movements resembling that of motile cilia. The authors speculate that since motile cilia are exploited in nature for the transport of particles and the locomotion of cells, their motor system should in principle be able to push surrounding molecules in a definite direction during its operating cycle. The central part of the motor is a chiral macrocycle. The pyridine rings attached to the central macrocycle of the bipyridine units are forced into a fixed position during a cycle and adopt a *P* configuration with respect to each other. One of the bipyridine units is functionalized with an azobenzene photoswitch that is the light-driven pushing blade of the motor. The other bipyridine unit acts as a stopper and controls the direction of the movement. By alternating irradiation with visible and UV light and complexation of the bypiridine ring with zinc(II) and decomplexation by addition of cyclam, the phenyl group of the azobenzene unit completes a 360° rotation around a virtual axis.

The whole rotation cycle consists of an alternating combination of light-induced folding and opening and rotational movement of the azobenzene blade (Figure 47b). The unidirectionality of the movement was supported by computational studies that evidenced the large difference in the energy barriers experienced by the bipyridine blades upon clockwise or anticlockwise rotation of the azobenzene blade. Even though the structure of this motor is quite complex and difficult to generalize and its operating cycle is not autonomous, as it requires four successive chemical and light stimuli in a precise sequence, the novel and unique motional dynamics obtained makes it an interesting platform for further development.

3.7. Photochemically Triggered Chemically Driven Motors

There are a few examples in the literature of molecular motors whose activity is reversibly triggered by a light stimulus. The fundamental difference between these and the photochemically *driven* motors described in the preceding sections is that in photochemically *triggered* motors light energy is not employed

DOI: 10.1021/acs.chemrev.9b00291
Chem. Rev. 2020, 120, 200–268

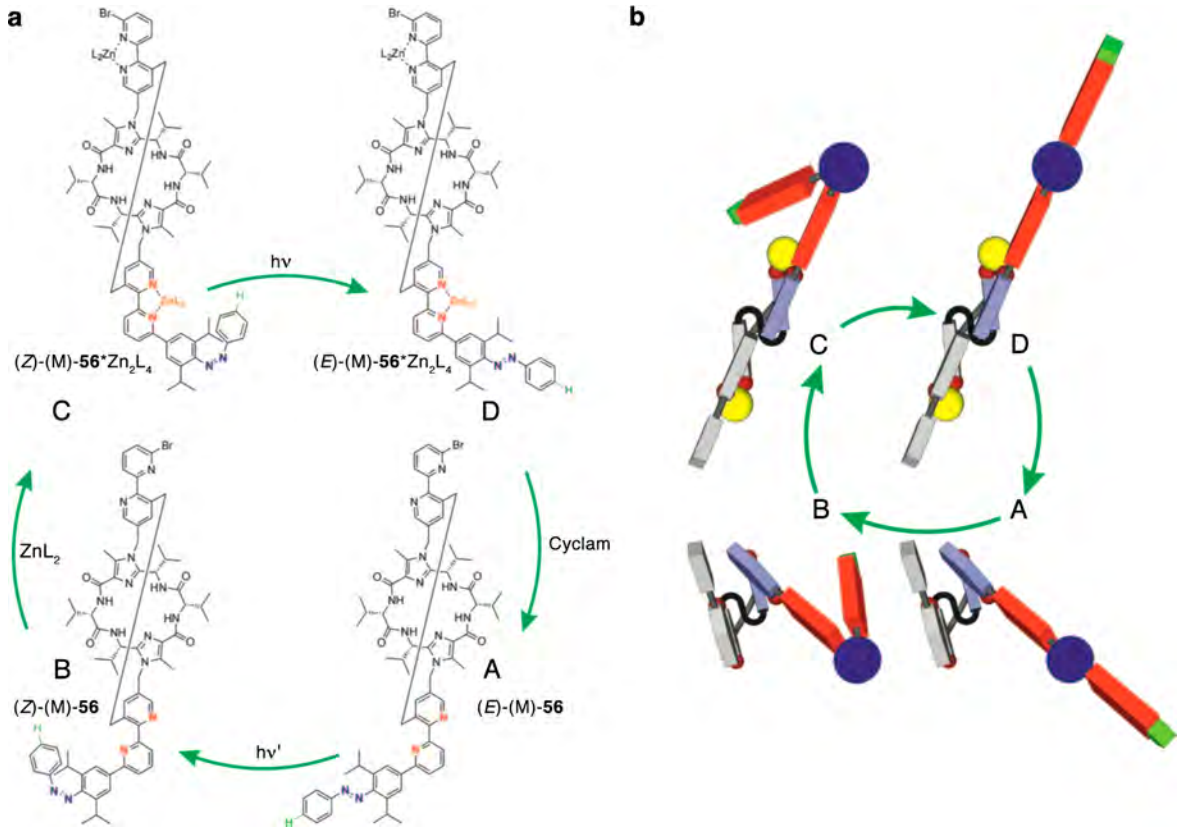

Figure 47. (a) Structural formula and operating cycle of four-stroke molecular motor **56**. (b) Schematic representation of the different motor states. The bipyridine unit bound to the azobenzene (red) pushing blade is colored light blue, and the other one is colored gray. The azo double bond is the dark-blue pivot, and the hydrogen atom that performs a 360° rotation during the operating cycle is highlighted in green. Adapted with permission from ref 358. Copyright 2011 Wiley-VCH Verlag GmbH & Co. KGaA, Weinheim.

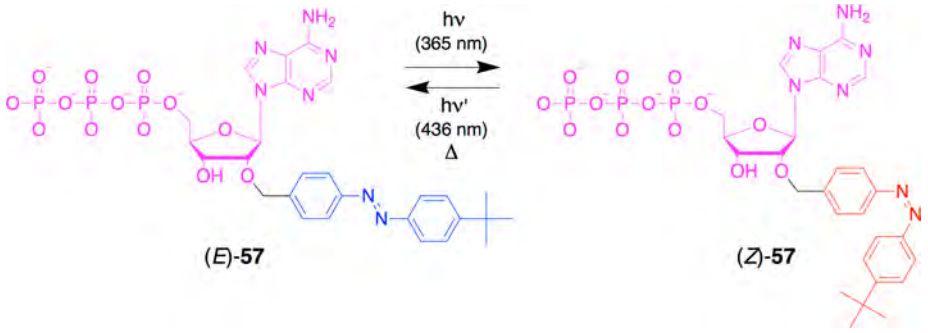

Figure 48. Photoisomerization reaction of the azobenzene-derivatized ATP species **57** applied as a phototriggerable fuel for driving a kinesin molecular motor. The ATP moiety is colored in magenta, and azobenzene in the *E* and *Z* configurations is shown in blue and red, respectively. Adapted with permission from ref 359. Copyright 2012 Royal Society of Chemistry.

to power the system but only to trigger the start and stop of its motion, which is instead powered by another source of energy. The main advantage of using light to start the operation of a motor is related to the high spatiotemporal resolution achievable with a light stimulus in comparison with other types of stimuli.

An efficient strategy to realize light-triggered motors that has been applied in both natural and small artificial molecular systems is the development of chemical fuels that can be interconverted between an active form and an inactive form by a reversible photochemical modification of their structure.[257] The system developed by Tamaoki and co-workers,[359] in which dynamic photocontrol of kinesin-driven microtubule motility is achieved, highlights the possibilities offered by this approach. Kinesin is an ATPase motor protein that converts chemical energy in the form of ATP into mechanical work.[2,6] The force generated enables kinesin to actively transport nanoscale cargos such as vesicles, chromosomes, organelles, etc. along microtubules. The latter are tubular polymeric protein assemblies that are about 24 nm in diameter and up to 50 μm in length and act as platforms for intracellular transport and also provide structure and shape to living cells.[1]

The approach, illustrated in Figure 48, is based on **57**, an ATP analogue possessing an azobenzene photochromic unit that strongly reduces its affinity toward ATPase kinesin upon light-triggered $E \rightarrow Z$ isomerization.[359] The photoisomerization of the azobenzene moiety thus acts as a switch that reversibly transforms the ATP−azobenzene conjugate from a fuel to an inert substrate for kinesin, thus enabling the reversible

DOI: 10.1021/acs.chemrev.9b00291
Chem. Rev. 2020, 120, 200−268

photocontrol of its motile activity. The activity of kinesin motor protein was assessed by a gliding motility assay, a well-established and versatile technique in which the gliding motility of fluorophore-labeled microtubules driven by biomolecular motors (typically kinesin or myosin) bound to a glass surface is visualized and monitored by fluorescence microscopy.

Different azobenzene−ATP conjugates were developed, and their interaction with kinesin was studied in detail to optimize the difference in affinity between the *E* and *Z* stereoisomers.[360,361] Despite the simplicity and elegance of this strategy, only a decrease of up to 79% of the gliding velocity of the microtubules, and not complete arrest, was achieved. This result was attributed to residual *E* isomer present at the photostationary state as a result of the incomplete $E \rightarrow Z$ conversion of the phototriggerable ATP fuel, which is sufficient to sustain the residual motility.

Tamaoki and co-workers proposed another strategy to overcome this limitation, by developing a library of photo-triggered inhibitors for kinesin activity based on a family of small peptides functionalized with an azobenzene group (Figure 49).[362] Extensive screening of different azobenzene−peptide

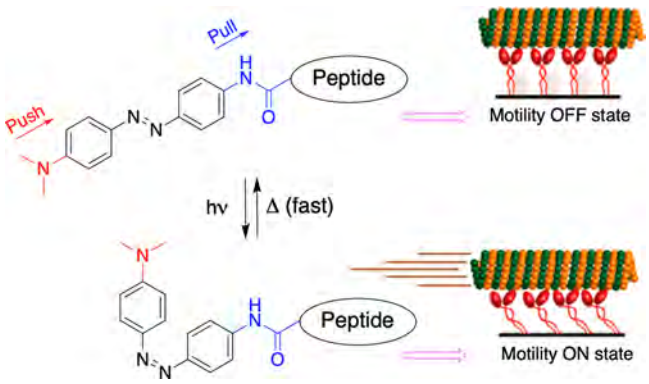

Figure 49. Photoisomerization of push−pull-azobenzene-tethered inhibitory peptides and schematization of their effect on microtubule motility. Adapted from ref 362. Copyright 2014 American Chemical Society.

derivatives enabled elucidation of the structure−property relationships among the sequence of the peptide, the structure of the linked azobenzene unit, and the inhibition activity.[363] A short peptide sequence was identified that once linked to an azobenzene group in the *E* form displays strong inhibition activity toward kinesin and is thus able to completely stop kinesin-driven gliding motility of microtubules. The inhibiting effect is strongly reduced upon $E \rightarrow Z$ photoisomerization of the azo moiety, and gliding motility with relatively high velocity is observed. With this strategy, the complete and reversible switching of the activity of a kinesin motor protein was achieved, using UV light to activate the motion and visible light to stop it.

By introducing push−pull substituents on the azobenzene group, which increase the thermal $Z \rightarrow E$ relaxation rate and shift the absorption maximum into the visible range, an inhibitor moiety for controlling the gliding motion with a single visible wavelength was developed (Figure 49). With this kind of inhibitor, the translocation, bending, and breaking of a single microtubule while the surrounding microtubules were kept at rest was demonstrated, showcasing the high level of spatial and temporal control affordable by such a method.[364] This study is one of the few examples of photoregulation of a selected single motor unit in an ensemble, and it is a highly desirable result for applications requiring controlled cargo manipulations in bionanodevices and advanced soft materials. Considering the large number of different motor systems present in living cells, the increasing knowledge of their operation mechanism, and the intense effort in the development of new molecular photoswitches and related techniques, this field of research has significant future perspectives.

4. MOTORS WITH COMBINED PHOTO- AND REDOX ACTIVATION

If a molecular motor does not operate autonomously, it needs a sequence of (orthogonal) inputs to operate, and therefore, more than one source of energy could be used to drive a motor. If one of these inputs consists of a chemical reaction, accumulation of waste products, dilution effects, or interference with the motor molecule could affect the long-term operation of the device. For this reason, the design of a molecular machine that operates solely by photochemical and redox reversible reactions would in principle be able to operate indefinitely as long as the correct sequence of inputs is administered to the system.

To date, only one example of a molecular motor activated by light and electrons has been reported.[365] Its design is partially based on the pushing motor developed by Haberhauer and co-workers, which was described in section 3.6.4.[358] In compound **58** (Figure 50), two moving parts—an azobenzene and a thianthrene—are connected to a macrocyclic clamp that acts as a support (Figure 50). Azobenezene is the photoswitch, whose *E*−*Z* isomerization corresponds to an up-and-down movement of the motor. Thianthrene is the redox switch: upon electrochemical oxidation, the molecular structure is converted from a bent conformation to an almost planar one; therefore, redox processes are responsible for the stretching and bending movements of the motor. The state of compound **58** is thus characterized by the *E*−*Z* configuration of the azobenzene unit and the neutral/radical state of the thianthrene moiety. The unidirectionality of the movement is guaranteed by the chirality of the macrocyclic scaffold and is conditional on the transformation of the (*E*)-azobenzene into only the corresponding (*P*)-(*Z*) isomer and not the (*M*)-(*Z*) one. In fact, quantum-chemical calculations and circular dichroism (CD) measurements confirmed that only the (*P*)-(*Z*) isomer is present in solution.

The operation mechanism of motor **58** is schematized in Figure 50: the cycle starts from bent (*E*)-**58** (state A). Oxidation affords the stretched (*E*)-**58**$^+$ form (state B), and subsequent irradiation at 365 nm generates (*P*)-(*Z*)-**58**$^+$ (state C). Reduction leads to the formation of (*P*)-(*Z*)-**58** (state D), and irradiation at 405 nm resets the system to state A. In analogy with the light-driven four-stroke motor reported by the same author,[358] it is hypothesized that as the stretched planar thianthrene can push more molecules in one direction with respect to its bent neutral counterpart, compound **58** should be able to push the surrounding molecules directionally when operated cyclically.

5. FROM MOVEMENTS TO FUNCTIONS

The examples illustrated in the previous sections showcase the types of artificial redox- and photodriven molecular motors available to date and highlight the level of sophistication reached in their design, synthesis, and investigation. The time is ripe to start developing systems in which the movement performed by

DOI: 10.1021/acs.chemrev.9b00291
Chem. Rev. 2020, 120, 200−268

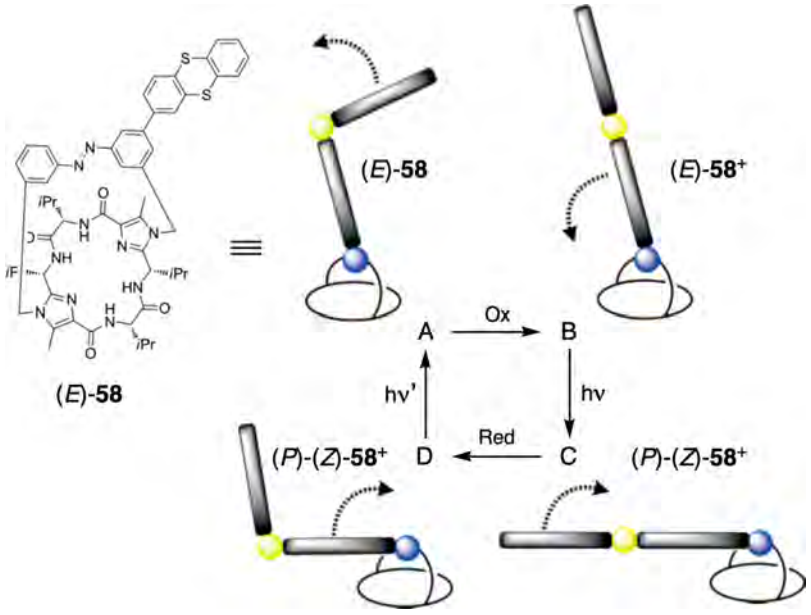

Figure 50. Structural formula and schematic representation of the molecular pushing motor **58** and its operating mechanism. Adapted with permission from ref 365. Copyright 2017 Wiley-VCH Verlag GmbH & Co. KGaA, Weinheim.

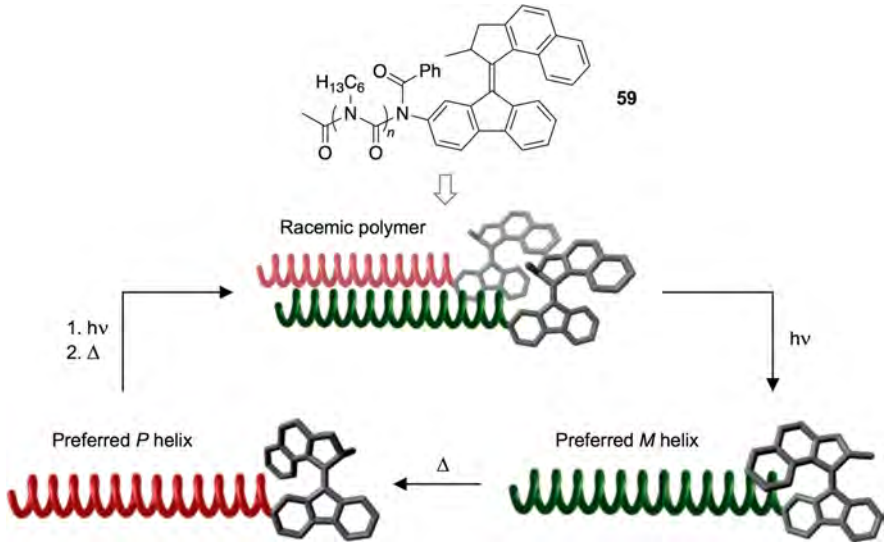

Figure 51. Structural formula of compound **59** and schematic representation of the photoinduced control of the helicity of the polyisocyanate polymer chain with a covalently linked second-generation overcrowded alkene molecular rotary motor. Adapted with permission from ref 367. Copyright 2007 Wiley-VCH Verlag GmbH & Co. KGaA, Weinheim.

molecular motors is not an end in itself but is exploited to accomplish a function. This is what happens in biomolecular motors, which utilize the motion to perform useful tasks across different length scales, encompassing molecular (e.g., the making of other molecules), microscopic (e.g., intracellular transport), and macroscopic (e.g., muscle-based actuation and locomotion) settings.

In this section we will describe experiments in which the redox- or light-powered motion of synthetic molecular motors is harnessed, transmitted, or collected such that a sizable change is observed beyond the motors themselves. We would like to point out that some of the systems described in the following are based on molecular switches rather than motors or contain a molecular motor that is used as a switch. Nevertheless, we find it appropriate to include them in this review because they show how redox- or photoinduced tasks can be achieved by harnessing controlled molecular movements in suitably designed systems and materials. The examples are categorized according to the type of functionality enabled by the molecular movement.

5.1. Control of Chemical and Physical Properties

5.1.1. Transfer of Chirality. The transfer of chiral information and its amplification from the molecular to the supramolecular or macromolecular level is an interesting research objective that can lead to applications in responsive materials, sensing, and catalysis.[366] To this aim, molecular rotary motors of the overcrowded alkene family (section 3.6.1) appear to be suitable control elements because they operate according to a sequence of photo- and thermally induced transformations involving diastereoisomers with a well-defined helicity. A first step forward toward dynamic intramolecular transmission of chirality triggered by light is represented by compound **59**

DOI: 10.1021/acs.chemrev.9b00291
Chem. Rev. 2020, 120, 200−268

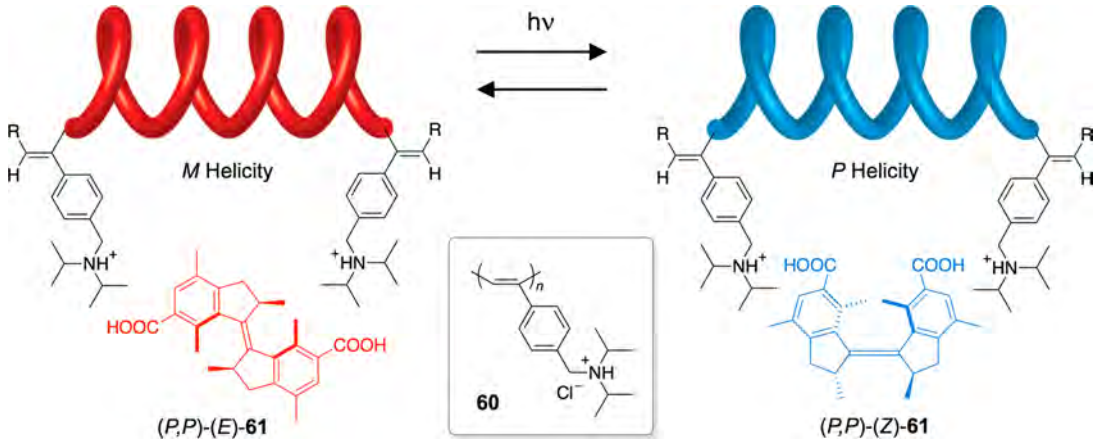

Figure 52. Photocontrol of the helicity of cationic poly(phenylacetylene)-type polymer **60** by chiral induction from molecular motor **61** bound non-covalently. Adapted with permission from ref 368. Copyright 2017 Royal Society of Chemistry.

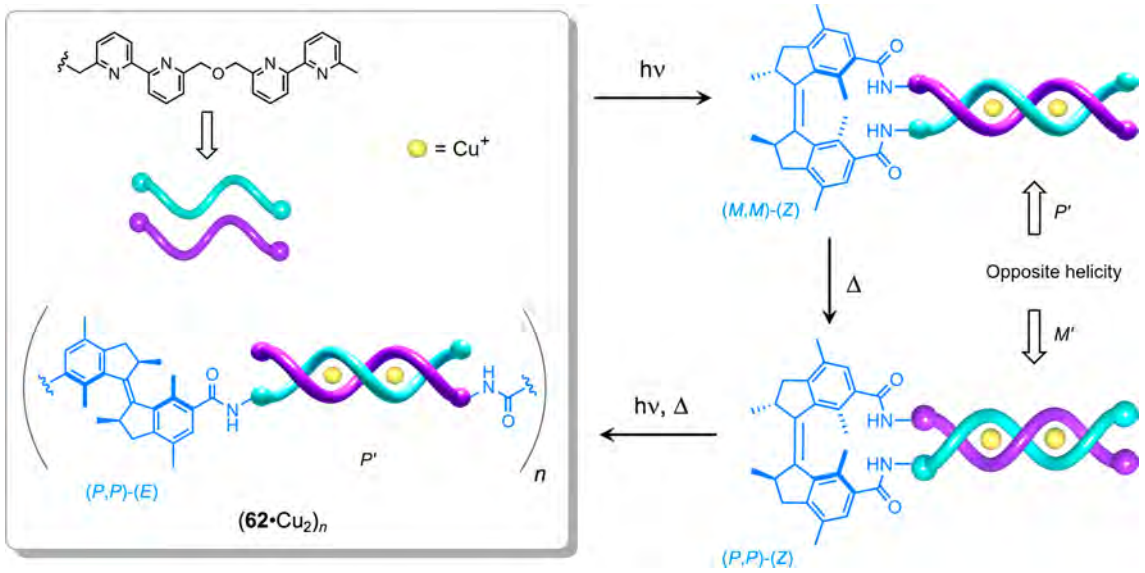

Figure 53. Formula of compound **62** combining molecular motor and bis(bipyridine) ligand components and schematic representation of the photoinduced switching between oligomeric and monomeric double-stranded Cu(I) helicates of distinct handedness. Adapted with permission from ref 369. Copyright 2016 Springer Nature.

(Figure 51), consisting of a poly(hexylisocyanate) polymer functionalized at one end with a second-generation molecular rotary motor moiety.[367] In solution, the polymer chain assumes a helical conformation and is dynamically racemic—that is, the compound contains equal amounts of interconverting right-handed and left-handed helices. This behavior is maintained in **59** when the molecular motor, appended as its *S* enantiomer, is in the form of its stable (*M*)-(*E*) isomer, which exerts little influence on the polyisocyanate chain. Upon photoisomerization to the unstable (*P*)-(*Z*) form, the *M*-helical polymer is exclusively obtained. Successive thermal relaxation to the stable (*M*)-(*Z*) isomer of the motor results in the formation of the opposite helical conformation of the polymer (that is, the *P* helix). The racemic state of the polymer can be restored by completing the motor cycle and return to the starting (*M*)-(*E*) form. Therefore, the chirality transfer from the molecular motor to the polymer dictates the preferred helical sense of the latter and enables reversible switching between the racemic, *M*, and *P* states.

More recently, the same concept was extended to a water-soluble poly(phenylacetylene) dynamic helical polymer bearing ammonium side groups (**60**; Figure 52).[368] In this case the molecular motor (**61**) was not covalently linked to the polymer but rather intermolecularly associated with it through hydrophobic and electrostatic interactions. The chirality transfer from **61** to **60** was investigated by CD spectroscopy; the effects of pH, salt concentration, and amount of motor dopant were studied. The results showed that the chirality of the motor can be transferred to the non-covalently bound polymer and that the helical conformation of the latter can be switched by light.

In another study, both halves of an overcrowded alkene motor were functionalized with oligo(bipyridine) ligand strands, which are known to self-assemble into double-helicate complexes in the presence of Cu(I) ions (Figure 53).[369] When the motor moiety of compound **62** is in the stable (*P*,*P*)-(*E*) form, addition of Cu(I) results in the formation of coordination oligomers. Photoswitching to the unstable (*M*,*M*)-(*Z*) isomer leads to disassembly of the oligomers to yield intramolecular helicates with defined handedness (*P*′). The successive thermal helix

DOI: 10.1021/acs.chemrev.9b00291
Chem. Rev. 2020, 120, 200−268

inversion of the motor, affording the stable (*P*,*P*)-(*Z*) isomer, causes inversion of the chirality of the copper helicate (from *P*′ to *M*′). Further irradiation and thermal helix inversion to complete the rotary cycle of the motor regenerates the oligomeric *E* state, and the switching scheme can be repeated. Examples of intramolecular transfer of chirality in rotary motors with tightly conformationally coupled rotors will be discussed in sections 5.1.2 and 5.2. Chirality transfer and amplification in liquid crystals doped with overcrowded alkene molecular motors has also been investigated (see section 5.5).

5.1.2. Catalytic Properties. In biological systems, chemical reactions are precisely controlled by means of sophisticated catalytic mechanisms mastered by enzymes. Indeed, the making of other molecules is a major task of biomolecular machinery.[1−4] Using synthetic molecular motors to obtain dynamic stimuli-responsive catalytic effects is a fascinating goal for molecular machines.

The photoswitchable stereochemical features of overcrowded alkene molecular rotary motors were exploited to develop catalysts for enantioselective transformations whose efficiency can be controlled by light.[370−373] It was envisaged that the individual chiral forms obtained during the unidirectional rotary cycle could dictate the ability of the catalyst to induce a preferred handedness in the product of an asymmetric reaction. In an initial study, a first-generation molecular motor bearing 4-dimethylaminopyridine and thiourea units (**63** in Figure 54a) was employed as an organocatalyst in the asymmetric Michael addition of 2-methoxythiophenol to 2-cyclohexen-1-one.[374] The *E* isomer, wherein the functional substituents that can coordinate the substrates are far apart, exhibits low catalytic activity and leads to a racemic product. Upon photoisomerization to the *Z* form, the two substituents become close enough to act cooperatively, and a significant enhancement of the reaction rate and enantioselection is observed. The chirality of the product is determined by the relative helical orientation of the aminopyridine and thiourea substituents, which in turn depends on the helical configuration of the motor. Thus, the photogenerated unstable (*M*,*M*)-(*Z*) isomer affords the product in the *S* configuration, while the *R* configuration is obtained upon subsequent thermal relaxation to the stable (*P*,*P*)-(*Z*) form (Figure 54b). The last two isomerization steps of the full rotary cycle reset the catalyst to its initial state. In summary, **63** behaves as a photochemically and thermally responsive catalyst that can trigger the formation of the racemate or either of the enantiomers of the product in a well-defined sequence.[375]

The system was later redesigned by removal of the phenyl spacers connecting the motor to the catalytically active moieties (**64** in Figure 55).[376] It was envisaged that such moieties could come into closer proximity in the new catalyst, thereby forming a more constrained pocket and leading to enhanced activity and stereoselectivity. This expectation was experimentally confirmed by using **64** as a catalyst in the Henry reaction between nitromethane and trifluoroketones. Along the same line, a molecular motor was equipped with two thiourea units; the resulting compound (**65** in Figure 55) also exhibited photoswitchable organocatalytic activity and stereoselectivity in an asymmetric Henry reaction.[377]

Compound **66** was prepared by attaching a phosphine group to each half of the motor, thus obtaining a chiral biphosphine that could function as a ligand for transition metal catalysis.[378] The behavior of **66** was tested in the palladium-catalyzed desymmetrization of *meso*-cyclopent-2-en-1,4-diol bis(carbamate), a well-known model reaction to study the enantioselectivity of chiral ligands. When the (*P*,*P*)-(*E*) isomer was used as the ligand for Pd, a nearly racemic product (enantiomeric ratio 53:47) was obtained in 65% yield. Upon

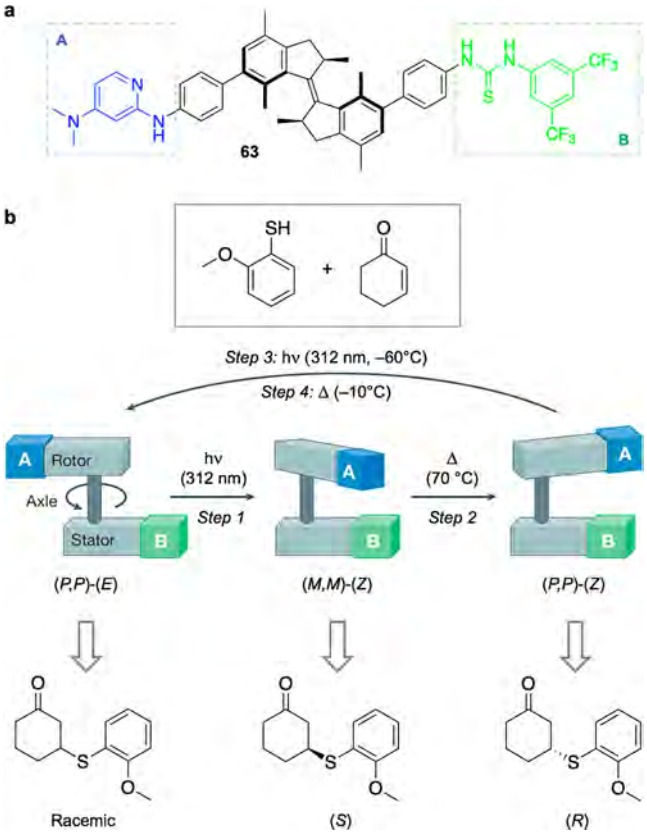

Figure 54. (a) Structural formula of switchable catalyst **63** derived from a first-generation molecular rotary motor, in its (*P*,*P*)-(*E*) form. (b) Schematic representation of the photochemical and thermal control of the activity and enantioselectivity of **63** in the Michael addition of 2-methoxythiophenol to 2-cyclohexen-1-one.[374] Adapted with permission from ref 54. Copyright 2017 Springer Nature.

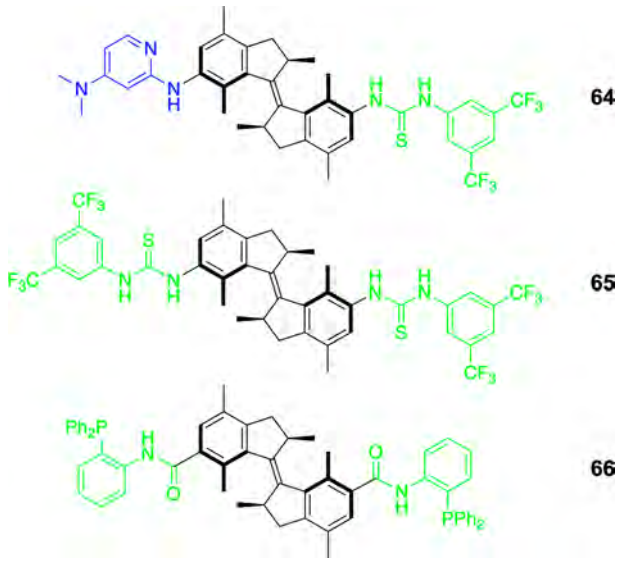

Figure 55. Structural formulas of switchable catalysts **64**−**66** in their (*P*,*P*)-(*E*) forms.

DOI: 10.1021/acs.chemrev.9b00291
Chem. Rev. 2020, 120, 200−268

photoisomerization to the (*M*,*M*)-(*Z*) isomer, the palladium complex of **66** was shown to catalyze the reaction in 90% yield with an enantiomeric ratio of 93:7 in favor of the (3*R*,4*S*)-oxazolidinone product. Conversely, after isomerization to the (*P*,*P*)-(*Z*) isomer, the opposite enantiomer, (3*S*,4*R*), was obtained with an enantiomeric ratio of 6:94 in 85% yield. Unfortunately, the palladium catalyst could not be switched in situ because of the poor stability of the species generated by UV irradiation and heating, which leads to a decrease in selectivity.

In a more recent work, a second-generation molecular rotary motor was combined with a 2,2′-biphenol unit to yield compound **67** (Figure 56).[379] The biphenol moiety was selected

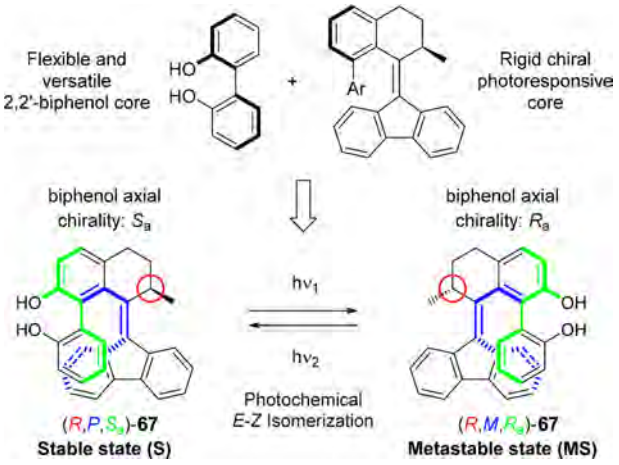

Figure 56. Design strategy, structural formula, and photoinduced switching of compound **67**. Acting as a catalyst in an enantioselective addition, this compound features point-to-helical-to-axial-to-point transfer of chirality. Reproduced from ref 379. Copyright 2018 American Chemical Society.

because of its ability to function as a bidentate ligand for a metal center, thus forming a complex with potential catalytic activity. Because of the tight steric coupling of the motor and biphenol moieties, it was envisaged that the preferred axial chirality of the biaryl (highlighted in green in Figure 56) would be dictated by the helicity of the overcrowded alkene core (blue), which in turn is determined by the configuration of the stereogenic carbon atom (red). The photoswitching properties of **67** and the related stereochemical changes were studied by detailed NMR, UV, and CD spectroscopy experiments. The results showed that light irradiation affords reversible switching between the (*R*,*P*,S_a) and (*R*,*M*,R_a) stereoisomers, indicating that changing the helicity of the motor changes the chirality of the biphenol. The behavior of **67** as a catalyst was tested in an asymmetric addition reaction of diethylzinc to aromatic aldehydes. The active catalyst is formed upon coordination of **67** to a zinc ion through the biphenol ligand. Interestingly, reversal of the enantioselectivity upon photoirradiation was observed for several substrates, suggesting that the metastable (*R*,*M*,R_a) isomer of the catalyst resembles the enantiomer of the stable (*R*,*P*,S_a) isomer as far as the chiral induction is concerned. This study demonstrates that switchable chiral catalysts can be obtained by the designed integration of functional elements with well-defined stereochemical properties. The tight conformational coupling at the basis of the transmission of chiral information from the motor to the catalyst is reminiscent of the function of a mechanical gear—a concept that will be illustrated in more detail in section 5.2.

It should be pointed out that all of the systems described above, as well as several examples presented in the next sections, do not harness the photoinduced directional, repetitive, and autonomous rotary movement characteristic of the motor, which is therefore used as a light-responsive switch. Molecular rotary motors, however, offer a higher degree of control with respect to conventional bistable photochromic compounds because they act as multistate switches in which the various states exhibit different structures (e.g., size, shape, helicity) and features (e.g., polarity, optical properties).

5.1.3. Biological Functions. Stimuli-induced change of structural features is a powerful means to regulate the functions of biomolecules. In the attempt to develop biohybrid systems that can exhibit similar behavior, molecular machines are promising candidates to play the role of mechanical control elements. A first step along this direction is the recently reported functionalization of a DNA hairpin with a first-generation motor of the overcrowded alkene family.[380] The motor, whose halves were functionalized with rigid connectors to render it a bifunctional linker, was incorporated into a 16-mer strand of self-complementary DNA via solid-phase synthesis. The results showed that the presence of the motor as a bridgehead does not hamper the formation of the eight-base-pair hairpin and that the photoisomerization and thermal helix inversion steps at the basis of the motor function are retained in the hairpin. The *E*/*Z* configuration of the motor was found to affect the stability of the duplex, as reflected in different melting temperatures (T_m) of the *E* and *Z* hairpins. Contrary to what expected from the design of the system, aided by DFT calculations, the *E* hairpin is more stable than the *Z* one. UV irradiation experiments performed over a temperature range around the melting temperature of the hybrids indicated that the duplex stability of the oligonucleotide can be adjusted by light stimulation. The overcrowded alkene switch exhibits a number of advantages—such as efficiency, structural rigidity, multistate behavior, and helicity inversion—over azobenzene species used in earlier studies of photocontrolled DNA hybridization,[381] highlighting the potential of molecular rotary motors to engineer photoregulated processes in biological systems.

Overcrowded alkene rotary motors bearing either dye units (cyanine for **68**, boron dipyrromethene (BODIPY) for **69**; Figure 57) or oligopeptide chains (in the case of **70**−**73**) on the stator were physisorbed on either synthetic lipid bilayers or cell membranes, and the effect of photochemical irradiation on the membrane stability was assessed.[382] Remarkably, the presence of the dyes in **68** and **69** does not quench the photoreactivity of the motor core.[383] Molecular motors with smaller substituents (**74** and **75**) were also considered, as well as a number of control compounds. The latter include **76**, a switch that can undergo only *E*−*Z* photoisomerization without a full rotation, i.e., it can only exhibit a flapping (reciprocating) motion; **77**, a molecule derived from **74** but lacking the allylic methyl group, which exhibits light-induced random (not unidirectional) rotation; **78**, a stator with no rotor; and **79**, a photochemically inactive chromophore mimicking the absorption properties of the motors. In a first series of experiments, compound **68** and a BODIPY dye were coencapsulated into large unilamellar vesicles (LUVs) self-assembled from phospholipids. Upon irradiation of the LUV suspension at 365 nm, a decrease in the BODIPY-based luminescence intensity of the vesicles was detected by confocal fluorescence microscopy. Control experiments confirmed that such a decrease can be attributed to the destabilization of the membrane caused by the photoactivated motion of **68** within

DOI: 10.1021/acs.chemrev.9b00291
Chem. Rev. 2020, 120, 200−268

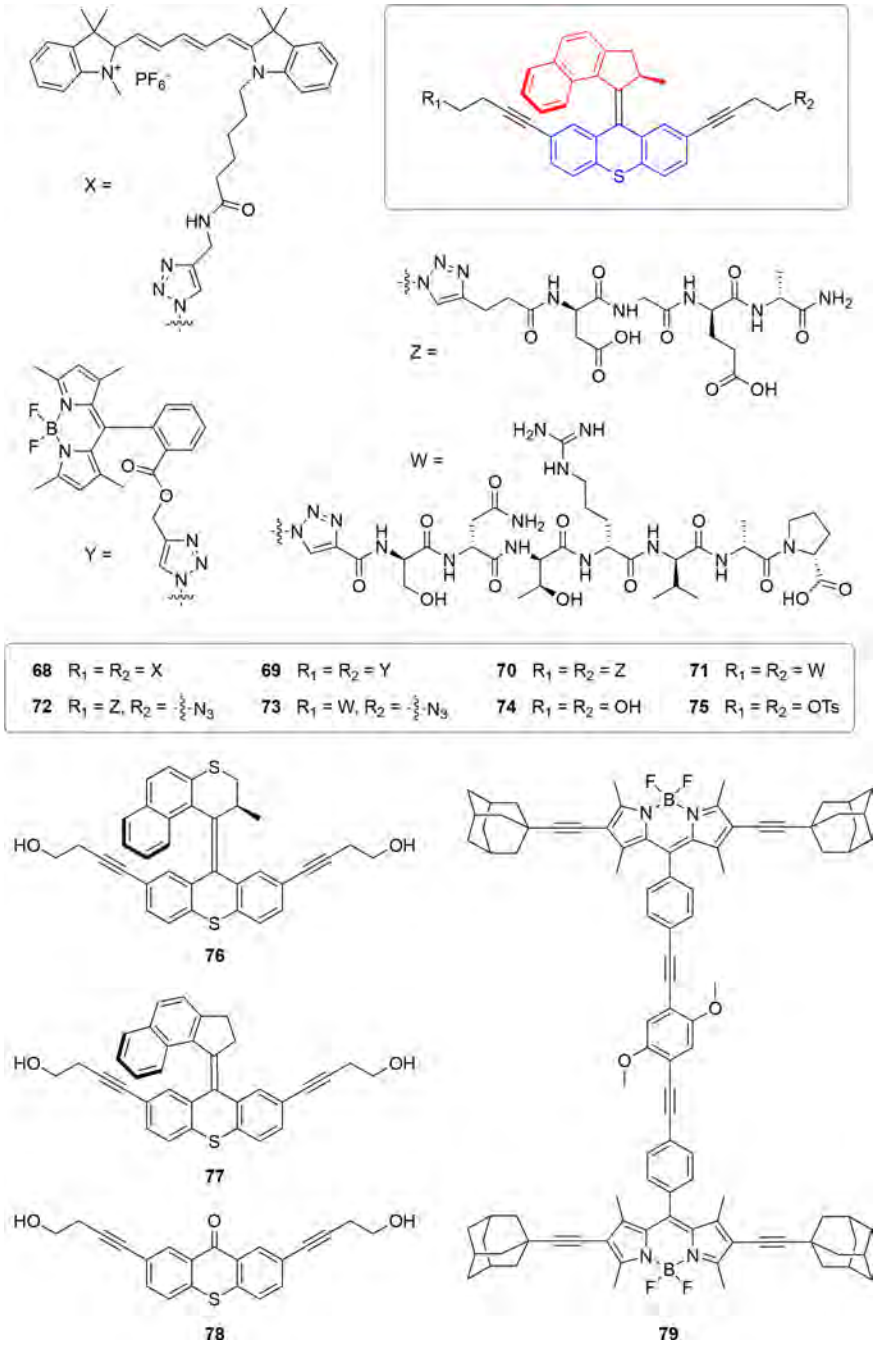

Figure 57. Structural formulas of molecular rotary motors **68**–**75** and control compounds **76**–**79** used in investigations of the photodestabilization of bilayer membranes.[382]

the bilayer, thus enabling the escape of BODIPY dye molecules. This kind of phenomenon, although interesting, is not unprecedented for molecular photoswitches;[384−386] moreover, a connection between the membrane perturbation and the unidirectional rotation of the motor was not clearly established.

Successively, compounds **68** and **69** were introduced into living cells, and their behavior with and without UV irradiation was studied in vitro by optical microscopy.[382] The observations showed that the cell internalization of these species is significantly accelerated upon light irradiation to cause rotation of the molecular motors. The same experiments performed with motors **74** and **75** indicated a photoinduced perturbation of the cell membrane, resulting in membrane blebbing and necrosis. The addition of peptide substituents to the molecular motors, as in compounds **70**–**73**, allowed the targeting of specific cells. Little or no cell death was observed upon UV irradiation in control experiments performed with compounds **76**–**79**, suggesting that the nonreciprocating unidirectional rotation of the molecular motors is crucial to afford their efficient light-induced penetration through the lipid bilayer. It is hypothesized that membrane rupture and pore formation are induced by a tangential mechanical force exerted by the rotating nanomotors embedded in the bilayer (Figure 58). The disruption of external or internal cellular membranes can be used to introduce species into cells or to expedite cell death. Appropriate functionalization of the motors enables fluorescence tracking of the molecular motors within cells or targeting of specific cells by exploiting surface recognition elements. All of these features offer

DOI: 10.1021/acs.chemrev.9b00291
Chem. Rev. 2020, 120, 200−268

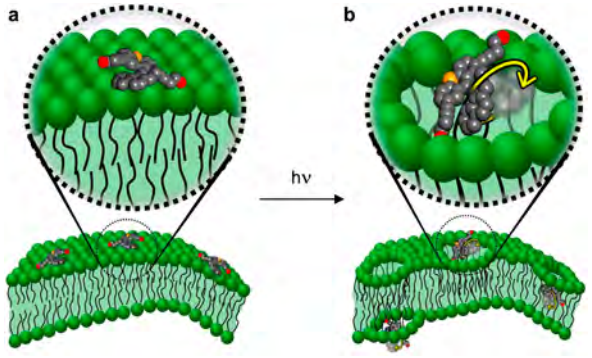

Figure 58. (a) Schematic representation of molecular motors physisorbed on a cell membrane. (b) UV-induced rotation of the motors induces membrane rupture and pore formation. Reproduced with permission from ref 382. Copyright 2017 Springer Nature.

opportunities for the application of molecular motors to solve biomedical problems.

5.2. Transmission of Directed Motion within Molecular Systems

In macroscopic mechanical machines, the movement produced by a motor component—that is, an active device that uses an energy source to generate forces—is transmitted and processed by means of other passive elements—e.g., gears, belts, and joints—that are mechanically coupled to the motor. Biological systems show that the mechanical coupling of molecular motors with other molecular components of the surrounding environment is essential also for molecular machinery performing tasks.[1−4]

Concerted movements were observed in ingeniously designed synthetic molecules consisting of sterically coupled moieties, leading to nanoscale versions of mechanical devices[24,27,62,63,387] such as cogwheels,[388,389] bevel gears[390,391] and drive chains[392]

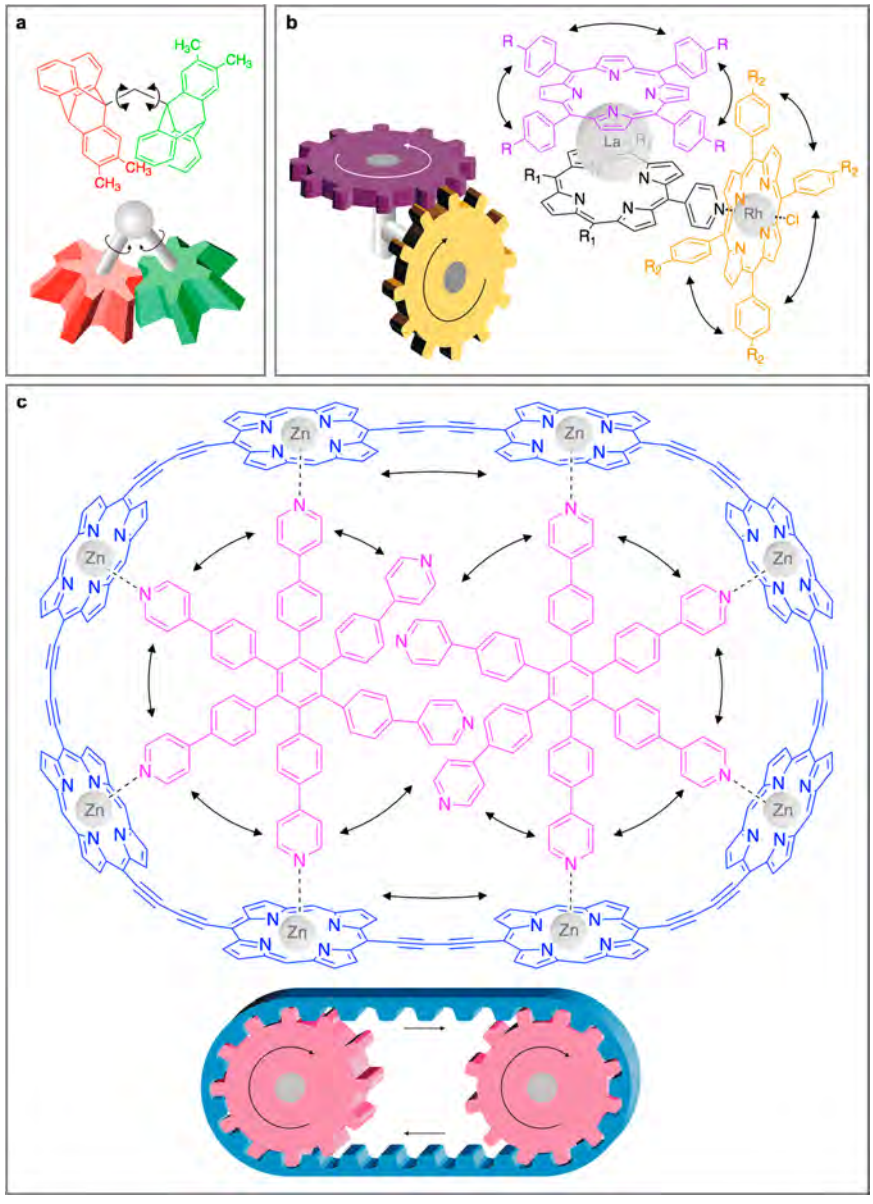

Figure 59. Mechanical coupling of molecular components: (a) cogwheels,[389] (b) bevel gear,[391] and (c) drive chain.[392] These molecular devices are based on passive rotors and thus exhibit random nondirectional motion driven by thermal energy.

DOI: 10.1021/acs.chemrev.9b00291
Chem. Rev. 2020, 120, 200−268

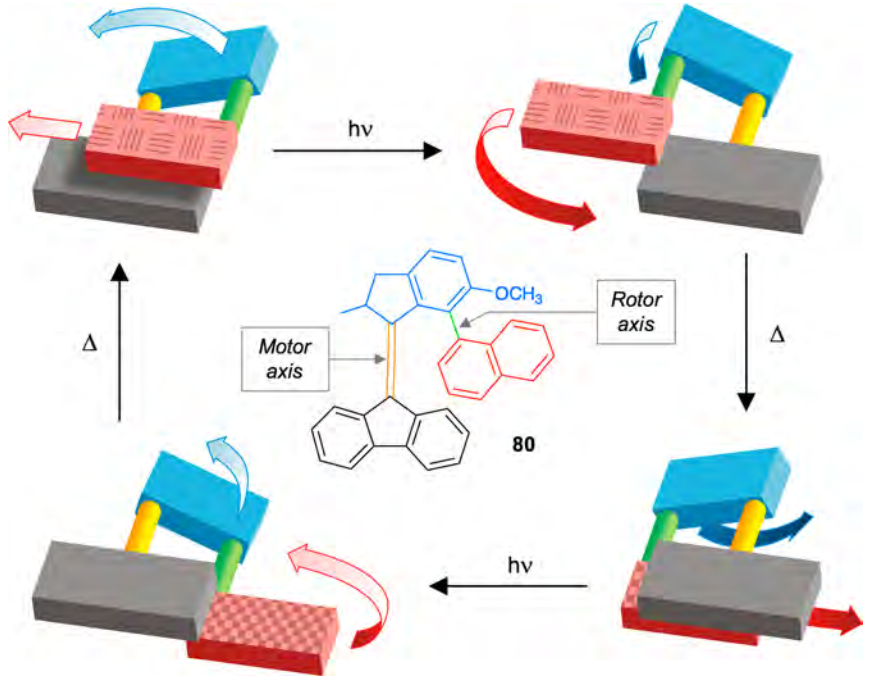

Figure 60. Structural formula of compound **80** and schematic representation of its four-stage photochemical and thermal switching cycle that affords the transfer of a directionally controlled rotary movement from the motor to the rotor.[393] Upon unidirectional rotation of the overcrowded alkene core (blue rotor and gray stator), the appended naphthyl paddle (red) revolves around the motor axis (orange) and rotates around the rotor axis (green). The different faces of the naphthyl paddle are marked to highlight the tidal locking.

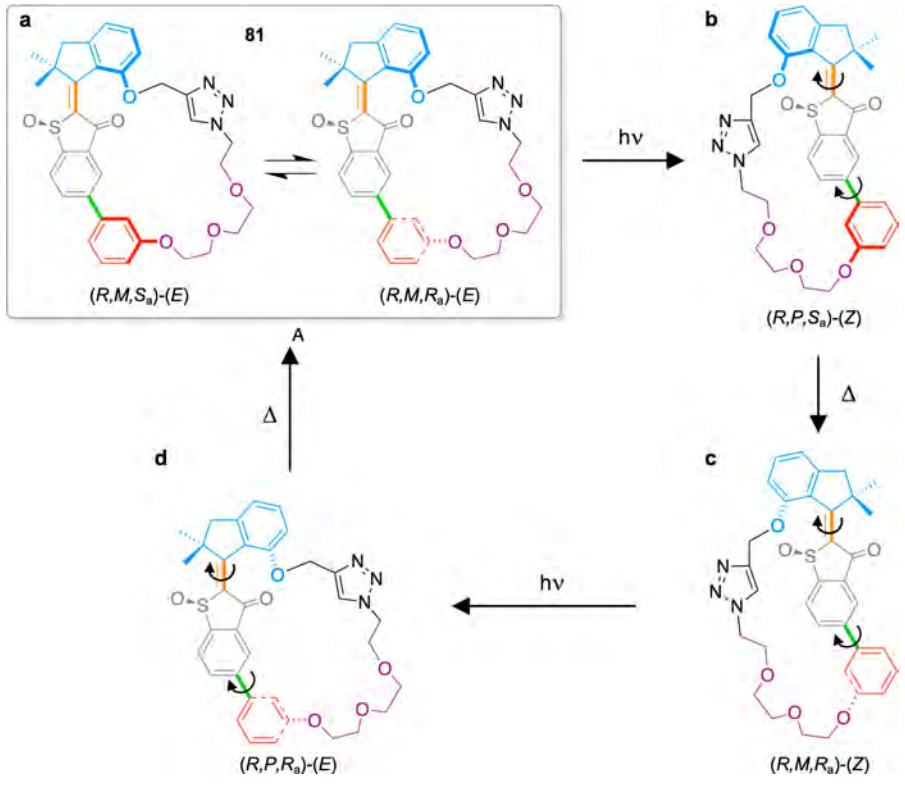

Figure 61. Structural formula of macrocycle **81** and representation of the photochemically and thermally driven steps at the basis of the transmission of directional rotation from the hemithioindigo motor (blue rotor and gray stator) to an aryl paddle (red) by means of an ethylene glycol linker (purple).[394] The rotation axes of the motor and the passive rotor are colored in orange and green, respectively.

(Figure 59). These movements, however, have a Brownian origin and therefore lack the directionality necessary to perform stimuli-induced functions.

Feringa and co-workers recently reported the first example of synchronous transmission of photoactivated directional motion from a second-generation overcrowded alkene motor to a

DOI: 10.1021/acs.chemrev.9b00291
Chem. Rev. 2020, 120, 200−268

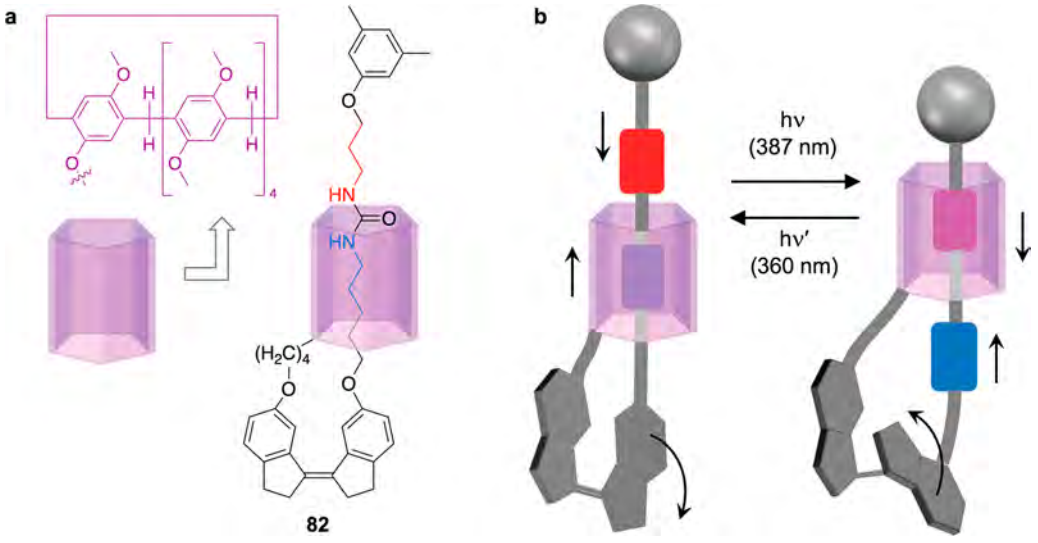

Figure 62. (a) Structural formula of [1]rotaxane **82** and (b) schematic representation of its photoinduced switching that converts the flapping motion of the stilbenoid unit into linear translation of the pillararene ring along the axle.[396]

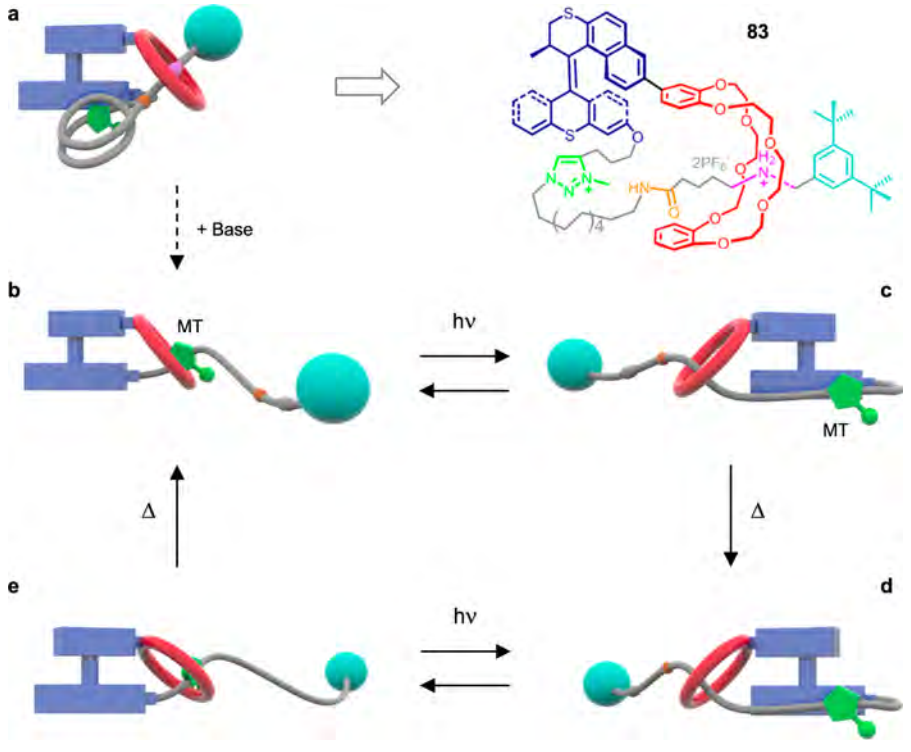

Figure 63. (a) Structural formula and cartoon representation of [1]rotaxane **83** comprising a photochemically driven molecular rotary motor. As shown in (b–e), the light-driven rotation of the motor results in concomitant translation of the ring with respect to the axle. Adapted from ref 397. Copyright 2019 American Chemical Society.

coupled rotor.[393] Compound **80** (Figure 60) consists of a naphthyl rotor covalently appended to the indanyl half of the rotary motor, such that the motion of the rotor is locked with the light-triggered rotation of the motor. NMR and CD spectroscopies were employed to identify unambiguously all of the structures involved in the operating cycle and to study the kinetics of the transitions between them. The results demonstrated that during a full rotation of the motor, the naphthyl paddle slides along and rotates around the fluorenyl unit of the core, always facing it with the same side (Figure 60). Thus, the rotations around the rotor and motor axes are locked and synchronized, as happens for the tidally locked movement of the Moon around the Earth. The precision in the transmission of the motion relies on an appropriate tuning of the energy barriers associated with the different rotary movements, which was obtained by clever molecular design.

An alternative approach for the intramolecular transmission of unidirectional rotary motion from a molecular motor to a passive rotor was recently reported by Dube and co-workers.[394] Compound **81** (Figure 61) consists of a biaryl unit, acting as the passive rotor, incorporated within the stator half of a light-driven hemithioindigo motor (section 3.6.2). In this macrocyclic

DOI: 10.1021/acs.chemrev.9b00291
Chem. Rev. 2020, 120, 200–268

species, an ethylene glycol chain links the rotor half of the motor with the aryl paddle of the passive rotor in an off-axis manner with respect to the biaryl rotation axis. It was envisaged that the ethylene glycol tether could transfer the photochemically driven unidirectional rotation of the motor to the remote biaryl rotor by exploiting the steric strain created in the different stereoisomers involved in the operating cycle of the device. The behavior of **81** was investigated by CD and NMR spectroscopies together with quantum-chemical calculations and crystallographic analyses.

Like **80** and the related compound **67** discussed in section 5.1.2, compound **81** contains three stereogenic elements, namely, point chirality around the sulfoxide unit, helicity around the motor double bond, and axial chirality around the biaryl axis. The starting state of the device is the (*R*,*M*,S_a/R_a)-(*E*) isomer, in which the flexible ethylene glycol chain allows the interconversion between the R_a and S_a atropisomers in dichloromethane solution at room temperature (Figure 61a). Irradiation of this species at 470 nm affords the (*R*,*M*,R_a)-(*Z*) stereoisomer (Figure 61c), whose CD spectrum is consistent with the biaryl unit occurring in the R_a configuration. Indirect evidence suggests that this transformation takes place through the formation of the unstable (*R*,*P*,S_a)-(*Z*) intermediate (Figure 61b); although this isomer could not be experimentally observed, only minimum-energy structures in which the biaryl unit is in the S_a configuration were found in a computational analysis. Successive irradiation of the (*R*,*M*,R_a)-(*Z*) stereoisomer with 470 nm light affords the (*R*,*P*,R_a)-(*E*) form (Figure 61d), which successively undergoes thermal relaxation to the starting state. Thus, the biaryl rotor of **81** experiences a spatially restricted rotational freedom because of the covalent constraints, and its configuration reflects that of the motor core; as a result, the light-driven unidirectional rotation of the hemithioindigo moiety is transferred to the passive rotor.

An important feature of the systems described above, in comparison with the previously reported transfer of controlled movements within artificial molecular machines,[395] is that the rotation generated by the motor is autonomous and unidirectional and that such extremely valuable properties are preserved upon transmission.[387]

Attempts to couple rotary and translational movements have also been reported. Yang and co-workers synthesized compound **82** consisting of a [1]rotaxane in which the axle and ring components are linked by means of an overcrowded alkene (or "stiff stilbene") moiety (Figure 62a).[396] The stilbenoid unit can undergo *E*−*Z* photoisomerization, but it does not exhibit unidirectional rotation. As shown schematically in Figure 62b, the change in the distance between the two aromatic halves of the switch, caused by their relative rotation, results in linear movement of the pillararene macrocycle along the axle. Although this system contains no molecular motors (both movements are reciprocating), it represents an interesting example of combining rotary and linear mechanical devices.

Very recently, along the same idea, a second-generation overcrowded alkene rotary motor was covalently combined with a rotaxane-based molecular shuttle architecture[397] according to a design previously exploited to achieve chemical gating of a photochemically driven molecular rotary motor.[398] In compound **83** (Figure 63a), the rotor and stator moieties of the molecular motor are functionalized with a DB24C8-type ring and an ammonium-containing axle, respectively, which are in turn interlocked together to yield a [1]rotaxane. The working cycle begins with deprotonation of **83** to "unlock" the crown ether from the ammonium center (which has become an amine) and transfer it to the methyltriazolium (MT) site (Figure 63b). Upon UV irradiation, the motor begins its rotation cycle, which causes the ring to dissociate from the MT unit of the axle and slide along the hydrocarbon chain (Figure 63c). The thermal helix inversion of the motor affords the stable *E* form (Figure 63d). The successive absorption of another UV photon drives the second half-turn of the motor, which pushes the ring back to the MT site (Figure 63e); a final helix inversion affords the stable *Z* form of the motor, thus completing the cycle. Apart from the transmission of movement (it should be noted, though, that the unidirectional rotation is transformed into a reciprocating shuttling motion), this study is interesting because it highlights that the molecular rotary motor can function against the non-covalent interactions that occur between the DB24C8 ring and the MT site.

5.3. Locomotion at the Nanoscale

5.3.1. Molecular Swimmers. Some kinds of bacteria (e.g., *Escherichia coli*) use the biomolecular motor-powered rotation[8] of a lashlike appendage (the flagellum) protruding from the cell body to move across a fluid medium.[3,4] Achieving the propulsion of a micro- or nanoscale object is a major challenge because at these length scales inertial forces, which are at the basis of swimming at the macroscopic scale, are absent, and motion is dominated by the viscosity of the medium.[64,96,97] The ratio of the inertial and viscous forces for a given object can be expressed by a dimensionless parameter, the Reynolds number (*Re*). A large *Re* indicates that inertia dominates, whereas very low values of *Re* could be due to the small dimension of the object and/or high viscosity and indicate that motion is governed by viscous forces. It is easy to show that the extremely small size of nanoscale objects results in very low Reynold numbers. In such a regime, propulsion based on conventional swimming mechanisms, which rely on time-reversible strategies (Figure 64a), is impossible; any net displacement must involve a nonreciprocating motion to break the time-reversal symmetry (Figure 64b,c).[399,400] Another significant issue is represented by Brownian motion (i.e., thermally driven collisions with solvent molecules), which tends to randomize the trajectory of small

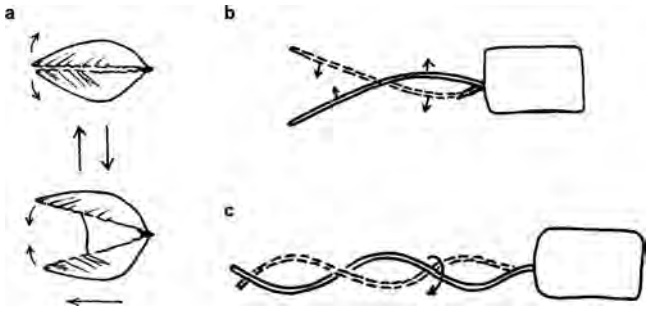

Figure 64. (a) "Scalloplike" motion, which relies on reciprocating flapping of two halves connected by a hinge, is ineffective at very low Reynolds numbers. Because of the high viscosity of the medium, any directional displacement achieved in the first half-cycle would be canceled by the opposite displacement caused by the second half-cycle. (b) In the flexible oar mechanism, the oar bends one way during the first half-cycle and the other way during the second half, thus avoiding time-reversal symmetry. (c) The corkscrew mechanism exploits the coupling of rotational and translational motion around the axis of a helicoidal filament. Mechanisms (b) and (c) are both employed in bacterial swimming. Adapted from ref 399, with the permission of the American Association of Physics Teachers.

DOI: 10.1021/acs.chemrev.9b00291
Chem. Rev. 2020, 120, 200−268

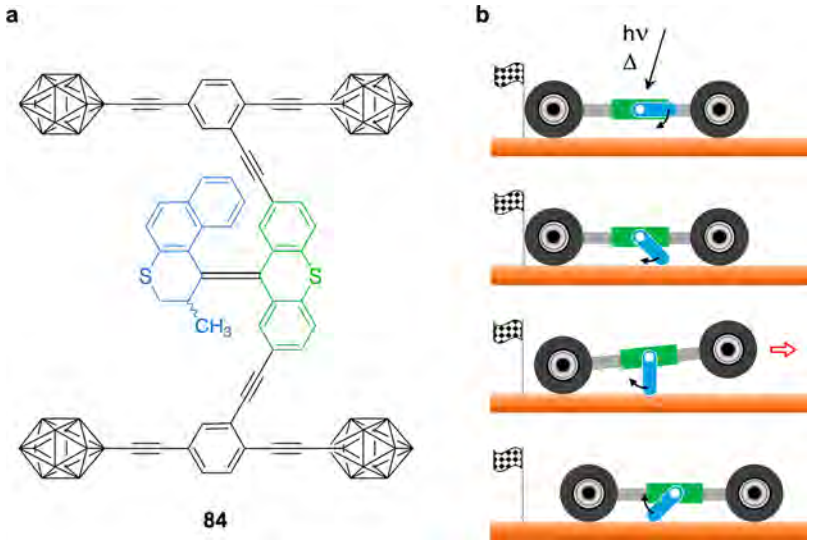

Figure 65. (a) Structural formula of nanocar **84** incorporating a light-powered molecular rotary motor in its chassis.[404] (b) Schematization of the proposed propulsion mechanism: irradiation with 365 nm light, together with thermal activation, operates the motor (green stator and blue rotor), whose unidirectional rotation causes the forward movement of the nanocar relative to the surface.

moving particles and hampers imparting directionality to their displacement.

The unidirectional (nonreciprocating) rotation of a molecular motor could in principal be exploited to achieve propulsion. A crucial problem in this regard is performing the motion repetitively with a frequency high enough to produce observable effects against random Brownian motion. Molecular rotary motors of the overcrowded alkene family, because of their ability to carry out fast and autonomous unidirectional rotation cycles, seem to be a suitable choice. An attempt along this direction was reported by Tour and co-workers, who investigated the solution behavior of compound **68** (Figure 57) and other related model compounds by fluorescence correlation spectroscopy.[383] As discussed in section 5.1.3, **68** comprises a photochemically driven molecular motor and a cyanine fluorophore that can be optically tracked. The results showed that UV irradiation of **68** causes an increase of the apparent diffusion coefficient by 26% in acetonitrile. Model compounds analogous to **68** but bearing either a slowly rotating motor or a stator with no rotor (akin to **76** and **78**, respectively, in Figure 57) do not exhibit any UV-induced increase in diffusivity. However, a molecule related to **68** equipped with a non-unidirectional photoswitch in the place of the motor (akin to compound **77** in Figure 57) also showed an enhanced diffusion coefficient under light irradiation. Thermal effects associated with light irradiation were ruled out by experiments; nevertheless, the mechanism at the basis of the photoinduced enhancement of diffusion remains unclear.

5.3.2. Surface-Roving Nanovehicles. One of the most imaginative applications of artificial molecular motors is certainly as engine components in nanometer-sized vehicles that can move directionally and autonomously across a surface. Nanovehicles consisting of rotating molecular wheels connected to a rigid molecular chassis have been synthesized and investigated.[116−119] The first prototypes, developed by Tour and co-workers, were devoid of a motor and thus not capable of controllable autonomous movement.[401,402] These nanovehicles, however, could be deposited on a metal surface and pulled/pushed using the tip of a scanning probe microscope.[403] Later, with the objective of constructing a motorized nanocar, the same group incorporated an overcrowded alkene molecular rotary motor into the chassis of a carborane-wheeled vehicle (**84** in Figure 65a).[404] The use of only one motor per vehicle removes the need for chiral resolution in the synthesis because a given motor can only rotate in a specific direction. It was envisaged that the unidirectional rotation of the motor could cause directed translational motion on the surface according to a paddlewheel-like mechanism (Figure 65b). While single molecules of **84** could be deposited and imaged on a copper surface, no lateral motion was observed upon light irradiation or STM manipulation, presumably because of strong molecule−surface interactions.[405]

More recently, the photoinduced displacement of a motorized nanovehicle on a metal surface was described.[406] Compound **85** (Figure 66a) looks like a roadster and consists of a second-generation overcrowded alkene motor attached to a phenylene ethynylene axle terminated with two adamantane wheels. The molecules were deposited on an atomically flat Cu[111] surface under ultrahigh vacuum, and an STM was used to follow the motion of individual objects. The influence of light on the behavior of surface-deposited **85** was assessed by (i) imaging individual molecules in their initial positions, (ii) retracting the STM tip to allow in situ illumination of the sample, and (iii) approaching the STM tip again to image the same surface area and determine the molecular positions after illumination. As thermal helix inversion steps are necessary for the rotation of the motor, the effect of temperature was also investigated.

At temperatures above ∼150 K, the molecules begin to diffuse across the surface (Figure 66b). STM imaging combined with in situ illumination performed at 161 K revealed that the nanoroadsters can diffuse for rather long distances upon irradiation with light of a wavelength absorbed by the motor (Figure 66c,d). Analysis of the individual behaviors of a statistically significant group of molecules not only confirmed this observation but also indicated that the enhancement of the diffusion steps was larger for 355 nm light (Figure 66d), which is closer to the absorption maximum of the motor, than for 266 nm light (Figure 66c). Irradiation at a wavelength not absorbed by the motor (635 nm) caused only a very minor effect, and illumination experiments performed on a motorless control compound resulted in no diffusion enhancement. Taken

DOI: 10.1021/acs.chemrev.9b00291
Chem. Rev. 2020, 120, 200−268

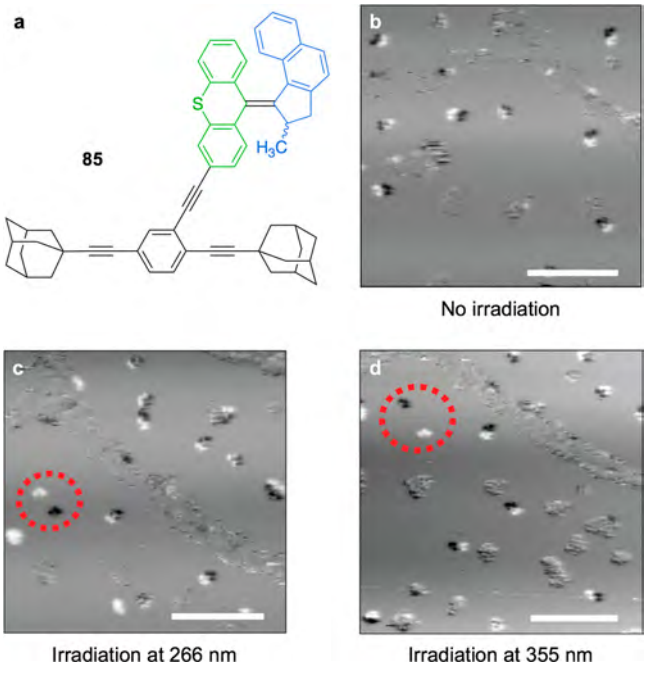

Figure 66. (a) Structural formula of motorized nanoroadster **85**. (b–d) Difference images obtained from STM experiments at 161 K showing the roadsters at their starting position (dark) and after (white) either thermally induced diffusion (b), irradiation at 266 nm (c), or irradiation at 355 nm (d). The red circles in (c) and (d) highlight a molecule that underwent a long-distance displacement. Scale bars, 20 nm. Adapted from ref 406. Copyright 2016 American Chemical Society.

together, these results indicate that a light-driven process due to the presence of the molecular motor enables long-distance translation steps across the surface. However, the observations are not sufficient to confirm that a paddlewheel-like mechanism such as that shown in Figure 65b is at the basis of the motion. It could happen that the stereoisomers of the motor populated by light irradiation exhibit different diffusion properties, possibly because of changes in the molecule–surface interaction, thus resulting in a photoinduced increase in the observed diffusion. A similar behavior was recently observed for photoactive azobenzene tetrapods adsorbed on a silver surface.[407]

It is worth pointing out the crucial role played by temperature in these experiments. In studies carried out at 6 K, the nanoroadsters did not move, whereas at temperatures above 170 K, thermally driven diffusion became faster than STM imaging. At low temperatures it can be presumed that the thermal energy is not sufficient to enable the thermal helix inversion of the motor; conversely, if the temperature of the surface is too high, then random Brownian diffusion dominates the motion.

Nanocars derived from **84** (Figure 65) were equipped with BODIPY fluorescent dyes to allow tracking of the movements of individual molecules by fluorescence microscopy.[408] Scanning tunneling microscopy outperforms single-molecule fluorescence microscopy in terms of imaging resolution, but the latter technique does not require the use of conductive surfaces and ultrahigh-vacuum conditions. Indeed, individual fluorescent nanocars lacking the motor component were successfully located and tracked by fluorescence microscopy.[409]

As mentioned in section 1.3.2, examples of surface-mounted single-molecule motors activated by means of the tunneling current provided locally by the STM tip[113−119,405]—including Feringa's famous four-wheel-drive nanocar[116]—are not reviewed here because their operation does not rely on redox or photochemical excitation.

5.4. Controlled Transport of Molecular Cargos

A crucial task performed by biomolecular machines is controlled directional transport of substrates within cells.[1−6] In fact, ions and small molecules can diffuse to where they are needed, but larger entities such as vesicles and organelles would move too slowly across the cytosol and need to be transported by motor proteins. These machines comprise a motor domain, which is capable of moving directionally along a track by consuming ATP, and a docking domain, to which appropriate cargos may be attached and detached on demand.[5,6] The design and construction of artificial molecular machines that can actively transport molecular or ionic substrates along specific directions or across membranes is a fascinating goal for nanoscientists and may disclose unconventional routes in catalysis, smart materials, energy conversion and storage, and medical therapy.[410−413] While outstanding examples of molecular robots[414] capable of transporting and sorting cargos have been developed by engineering of DNA architectures,[415−419] the development of fully synthetic systems is still in its infancy.[420]

5.4.1. Systems Based on Linear Molecular Switches. Multicomponent rotaxane **86** (Figure 67a) was designed to achieve the controlled capture, transport, and release of ruthenium(II) polypyridine complex **87** under chemical and photochemical stimulation.[421] The rotaxane is composed of a dibenzo[24]crown-8-type macrocycle and a molecular axle that contains a dibenzylammonium site (primary station) and a 4,4′-

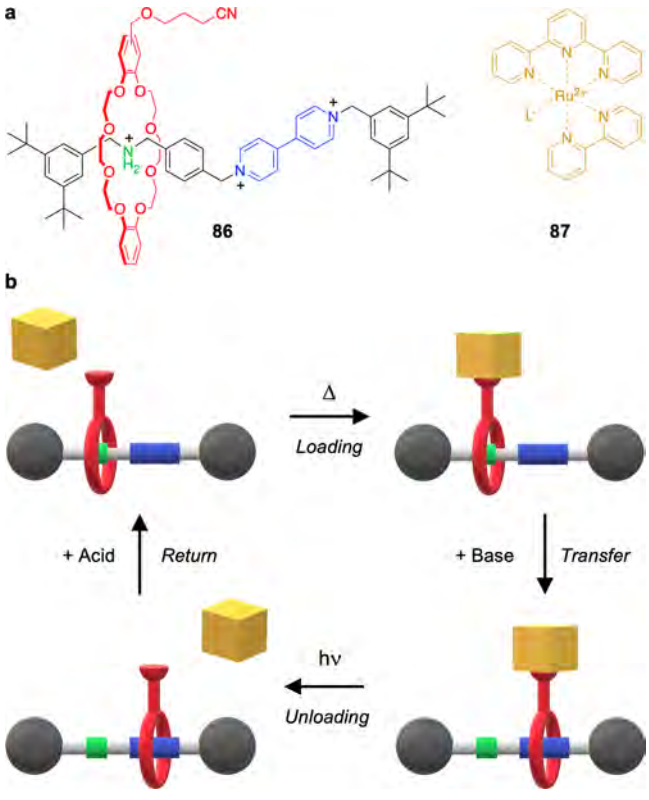

Figure 67. (a) Structural formulas of rotaxane transporter **86** and cargo **87**. (b) Schematic representation of the transport cycle. The cargo loading/unloading is performed by a thermally reversible photoinduced ligand dissociation, while the ring transfer/return is achieved by addition of basic and acidic reactants.[421]

DOI: 10.1021/acs.chemrev.9b00291
Chem. Rev. 2020, 120, 200−268

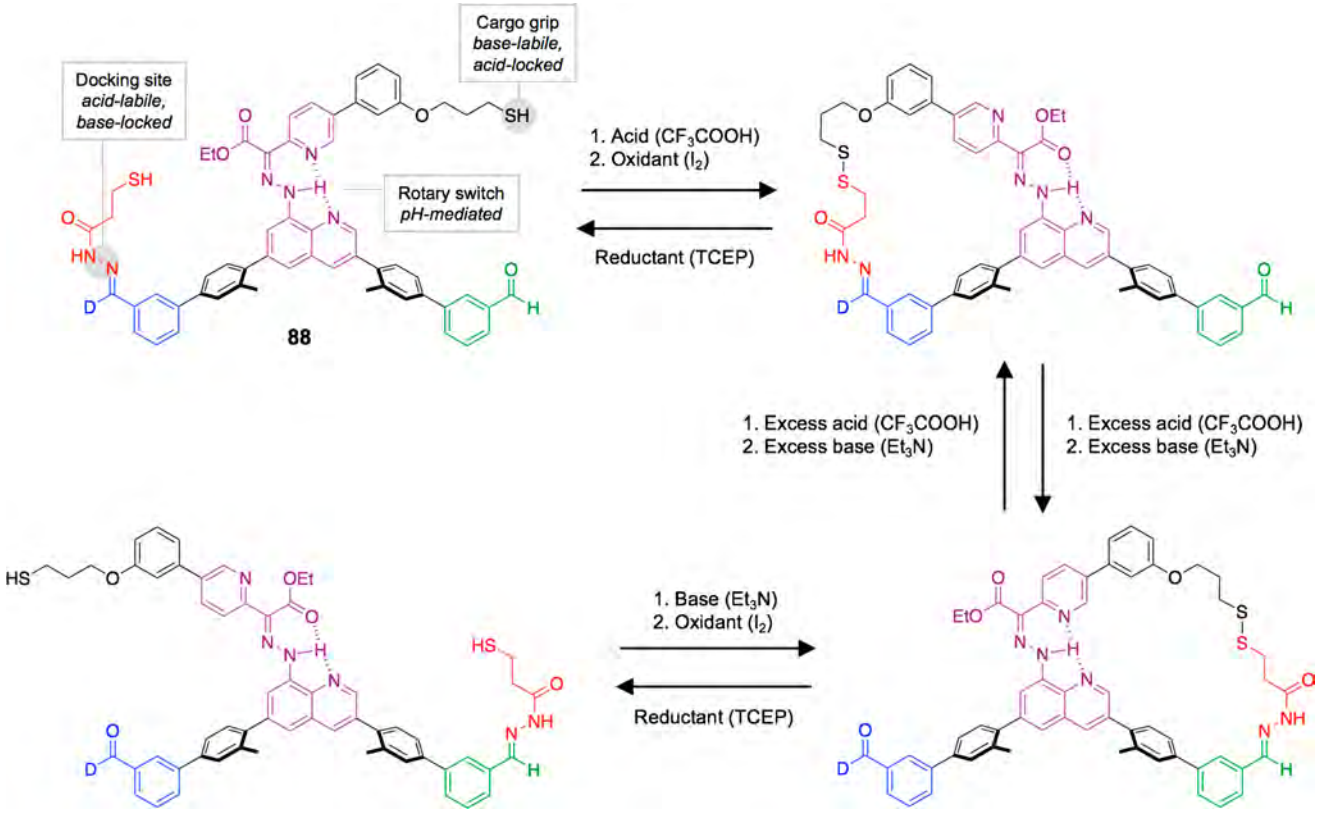

Figure 68. Reversible intramolecular transport of a cargo (red) between two distant chemically equivalent sites (blue and green) in compound **88** containing a hydrazone-based rotary switch (purple).[426] TCEP = tris(2-carboxyethyl)phosphine.

bipyridinium unit (secondary station). In this kind of compound, the ring selectively encircles the ammonium site; deprotonation of the latter with a base causes transfer of the macrocycle to the bipyridinium station. The initial situation is restored by adding an acid to regenerate the ammonium site. Therefore, the movement of the ring in **86** can be controlled reversibly by chemical acid–base stimulation.[422] The macrocycle is functionalized with a short chain ending with a nitrile group that serves as an anchoring point for the cargo. Specifically, the latter is a $[Ru(tpy)(bpy)L]^{2+}$ complex in which tpy and bpy are chelating ligands (tpy = 2,2′;6′,2″-terpyridine; bpy = 2,2′-bipyridine) and L is a monodentate ancillary ligand (e.g., an acetonitrile solvent molecule). Under appropriate conditions, in a solution containing **86** and **87**, the monodentate ligand of the ruthenium complex can be replaced by the nitrile terminus of **86**, leading to coordination of the cargo to the transporter, whose ring is initially located on the ammonium station (Figure 67b). Addition of a base causes the transfer of the ring toward the bipyridinium station and does not affect the cargo, which thus remains attached to the ring. At this point, irradiation with visible light induces the decoordination of the Ru(II) complex from the nitrile tether of the rotaxane;[281,423,424] this reaction has no effect on the position of the ring. Upon successive addition of acid, the (unloaded) ring returns to its initial position, and in principle the cycle can be repeated; in practice, thermal recoordination of the rotaxane to the cargo was not observed in situ, presumably because the vacant coordination position at the ruthenium center is occupied by a ligand (e.g., an anion or an adventitious water molecule) stronger than the −CN moiety of **86**.

It is worth noting that in this device the translocation of the macrocycle between the stations and the capture/release of the cargo rely on orthogonal switching processes and can be controlled by noninterfering stimuli. Furthermore, the use of a kinetically inert coordination bond ensures that the cargo remains docked to the machine during ring shuttling. These are both essential requirements to carry out the transport correctly.[421] It should also be pointed out that the time-reversal symmetry of ring shuttling between the two stations is broken by the (stimuli-controlled) presence or absence of the cargo. Hence, the sequential operation of the two distinct molecular switches can lead to the net performance of a task. In the present case the transport is unproductive because the cargo is captured and released in the same homogeneous solution; appropriately designed rotaxanes, however, could be embedded in membranes and used to shuttle cargos across physically separated compartments. A passive molecular transporter of this kind, which transports K^+ ions across a membrane down a concentration gradient, has recently been described.[195,425]

5.4.2. Systems Based on Rotary Molecular Switches. Intramolecular transport of a molecular cargo between two distinct sites at the extremities of a molecular platform has been realized in prototypical devices. They use molecular rotary switches to move a robotic "arm" in such a way that its distances from the different extremities of the platform can be changed in response to external stimuli. Another orthogonal stimulus is employed to control the docking of the cargo at the robotic arm and at either site on the platform, enabling controllable transport in either direction. The cargo never detaches from the machine, thus preventing the exchange with other molecules in the solution.

The first example, reported by Leigh and co-workers,[426] consists of a hydrazone rotary switch[427] whose "stator" is functionalized at either end with two chemically equivalent (but

DOI: 10.1021/acs.chemrev.9b00291
Chem. Rev. 2020, 120, 200−268

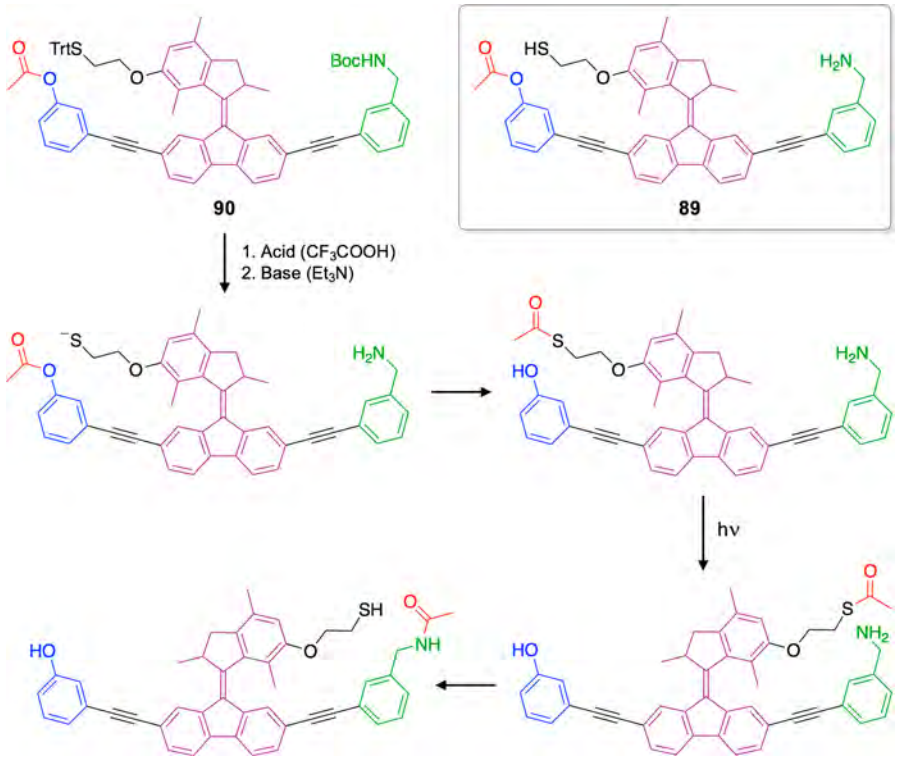

Figure 69. Structural formulas of molecular transporter **89** and its protected precursor **90** and operating scheme underlying the chemically and photochemically triggered transport of an acetyl cargo (red) from a phenoxy "departure" site (blue) to a benzylamine "arrival" site (green).[428] The light-driven motor unit used as the rotary switch is colored in purple.

experimentally distinguishable) docking stations for a 3-mercaptopropionyl hydrazide cargo while the "rotor" is terminated with a thiol unit (**88** in Figure 68). The distance between the two extremities of the rigid platform is approximately 2 nm. The redox-triggered reversible formation of disulfide bonds controls the capture and release of the cargo from the rotor "arm", whereas acid−base-sensitive dynamic hydrazone bonds are employed to control the docking to the platform. Acid−base stimuli also mediate the operation of the rotary switch.[427] As shown schematically in Figure 68, the cargo is initially mounted on the left-hand side of the platform. The sequential addition of CF_3COOH and I_2 as an oxidant results in the formation of a disulfide bond between the arm and the cargo. Successive treatment with a large excess of CF_3COOH followed by an excess of Et_3N leads to release of the cargo from the left-hand site and its repositioning on the right-hand site. Finally, cleavage of the disulfide bond by reduction with tris(2-carboxyethyl)phosphine (TCEP) detaches the cargo from the arm, and the left-to-right transport is accomplished in 79% yield. Backward transport of the cargo can also be obtained with an overall efficiency of 85% by I_2-promoted disulfide formation, acid-catalyzed rotation of the hydrazone switch, neutralization with trimethylamine, and reduction of the disulfide with TCEP. A similar design scheme was later applied to develop an artificial molecular assembler that can be programmed to make any one of four stereoisomers of the product using a given set of reactants.[420] This remarkable nanodevice is not described here because although it involves reductive bond cleavage, it does not make use of redox stimulation.

More recently, Feringa and co-workers used an overcrowded alkene rotary motor to construct a device operated by light that can transfer an acetyl group between distant sites within the molecule.[428] The activated transporter (**89** in Figure 69) is a first-generation motor endowed with three distinct appendages: (i) a phenoxy moiety on one side of the stator, to which the cargo is initially bound; (ii) a benzylamine moiety on the other side of the stator, where the cargo may be delivered after rotation; and (iii) a thiol-terminated arm in the rotor that can grip the cargo. The operation (Figure 69) begins with acid-catalyzed cleavage of the trityl and Boc groups that protect the thiol and amine moieties, respectively, in precursor **90** (Figure 69), followed by treatment with a base. The cargo is picked up by the rotor arm via the reaction of the thiolate moiety with the phenolic ester to form a thioacetate. Subsequent irradiation at 312 nm causes rotation around the C═C axis, bringing the thioacetate close to the benzylamine unit. Acetyl transfer to the amine then occurs, transferring the cargo from the rotor arm to the stator. The net result of this series of reactions is the intramolecular transport of the acetyl cargo from one extremity of the stator to the other, covering a distance of about 2 nm.

5.5. Amplification of Motion by Collective Strategies

In skeletal muscles, the forces exerted by single myosin molecules (ca. 10^{-12} N) are collected over a huge number of individuals and summed up, such that macroscopic forces can be eventually generated.[2] Such a tremendous amplification effect is achieved by means of a precise, multistage hierarchical organization that, starting from the molecular scale, involves increasingly larger and complex structures. The smallest functional element of the muscle is the sarcomere, in which filaments made of many myosin molecules are interdigitated with actin filaments. The ATP-fueled gliding of these filaments with respect to one another causes contraction of the sarcomere. Many thousands of sarcomeres are connected in series to yield myofibrils, which in turn are aggregated into fascicles and thicker fibers. Thanks to this stunning organization, the motion of

DOI: 10.1021/acs.chemrev.9b00291
Chem. Rev. 2020, 120, 200−268

individual molecular motors can be accumulated in space and time, leading to macroscopic actuation.

In the past few years, amplification of motion from the molecular scale to the microscopic[170,429,430] and macroscopic[73,431,432] scales has been obtained in proof-of-principle studies in which carefully designed mechanical molecular switches are deposited on surfaces,[433−437] incorporated into polymeric materials[436,438−441] or arranged in crystalline structures.[442−444] In this section we discuss recent investigations aimed at collecting the action of many artificial molecular motors in organized assemblies in order to achieve effects at larger length scales.

5.5.1. Doped Liquid Crystals. As discussed in section 5.1.1, the chirality present in small-molecule rotary motors of the overcrowded alkene family can be scaled up to the macromolecular level. Another way to transfer and amplify structural information from individual molecules to extended supramolecular assemblies is to exploit liquid crystal (LC) phases.[445] Feringa and co-workers showed that doping a nematic LC with enantiopure second-generation molecular motors such as **91** (Figure 70a) induces the formation of a cholesteric phase in which the helical pitch of the cholesteric LC is determined by the helicity of the motor units.[446,447] As every step in the rotary process of the motor is accompanied by a change in helicity, irradiation of the dopant in the sample causes a reorganization of the liquid crystal. When a thin film of this LC is placed on top of an aligned polyimide layer, the photoinduced rearrangement determines a clockwise rotation of the typical "fingerprint" cholesteric texture, which can be visualized with the aid of a microscopic glass rod lying on the surface. Indeed, irradiation with 365 nm light triggered the clockwise rotation of the rod, which could be imaged with an optical microscope (Figure 70b−e). The motion gradually stopped after a few minutes, when a photostationary distribution of the motor isomers was reached. When the irradiation was turned off, reverse rotation was observed as the initial isomer distribution was restored. The use of the other enantiomer of the motor caused the rod to rotate in the opposite direction. It is worth noting that the rotation of the rod is not the result of the unidirectional rotation of the molecular motor molecules but rather a consequence of their switched helicity. Nevertheless, the amplification of the movement from the molecular world to a scale on which an object could be seen to rotate was a landmark accomplishment in the field of molecular machines.

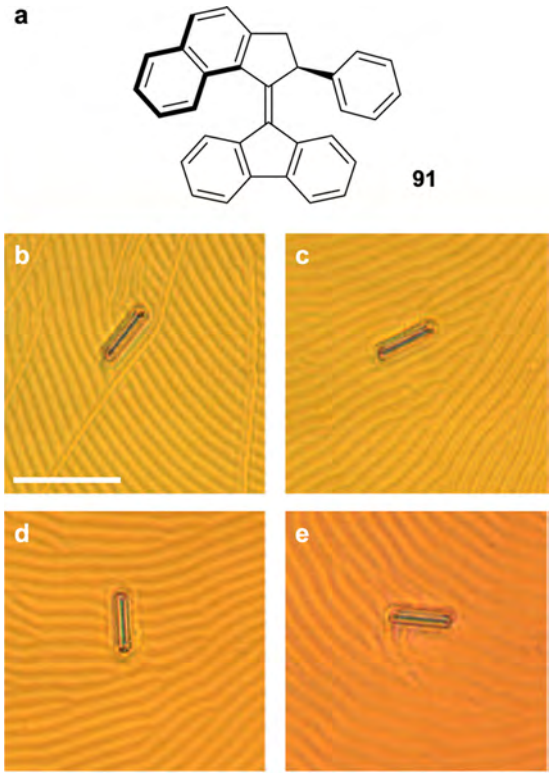

Figure 70. (a) Structural formula of molecular motor dopant **91**. (b−e) Optical micrographs of a microscopic glass rod lying on a liquid-crystalline thin film doped with 1% w/w **91**: (b) starting state (before irradiation); clockwise rotation of the glass rod by (c) 28° after 15 s of irradiation, (d) 141° after 30 s, and (e) 226° after 45 s. The scale bar is 50 μm. Adapted with permission from ref 446. Copyright 2006 Springer Nature.

The photoinduced change in the helical organization of cholesteric LC phases induced by molecular rotary motor dopants was exploited by Yang, Yang, and co-workers to construct diffraction gratings that could be configured by light irradiation and erased thermally.[448] These devices are based on a cholesteric liquid crystal doped with enantiopure molecular motor **92** (Figure 71a); the planar texture of the LC is stabilized by in situ photopolymerization. The UV-induced twist of the cholesteric helix arising from isomerization of the molecular motor is accompanied by disruption of the planar alignment in favor of a focal conic state characterized by strong light scattering (Figure 71b). By performing the UV irradiation through a mask (Figure 71c), diffraction gratings consisting of alternating lines of planar alignment and focal conic structures could be constructed (Figure 71d). The gratings showed a

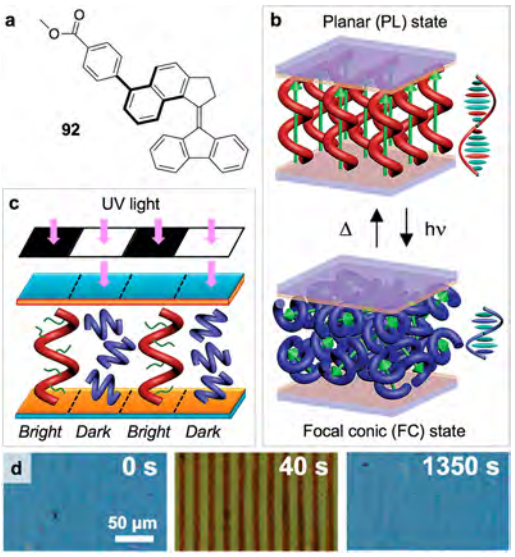

Figure 71. (a) Structural formula of compound **92** used as a dopant in cholesteric liquid crystals. (b) Scheme of the photoinduced and thermoreversible transition between the planar alignment and focal conic state of the LC helical superstructures. (c) Construction of a diffraction grating by the photoinduced local transition from the planar state to the focal conic state obtained by UV irradiation through a mask. Stabilizing polymer molecules are shown in green. (d) Polarized optical micrographs of a polymer-stabilized LC film as-prepared (left), after UV irradiation for 40 s (center), and after successive relaxation in the dark at room temperature for 1350 s (right). Adapted from ref 448.

DOI: 10.1021/acs.chemrev.9b00291
Chem. Rev. 2020, 120, 200−268

diffraction efficiency of up to 35% and were erased within minutes at room temperature because of the thermal reset of the motor dopant.

Katsonis, Lacaze, de Pablo, and collaborators studied the light-responsive behavior of cholesteric LC droplets doped with alkene molecular motors.[449] Such droplets exhibit peculiar topological features, such as microcavities, determined by the ratio between the cholesteric pitch and the droplet radius. Experiments performed on a large number of micrometer-sized droplets, together with simulations, revealed that the photo-induced change of the cholesteric pitch driven by switching of the helicity of the molecular motor dopant can be used to control the position of topological defects and the handedness of the radial spherical structure of the droplet. These results are thought to be of interest for optoelectronic applications involving the processing of polarized light.[450]

In the examples described above, the light-triggered LC rearrangement ceases as soon as the concentrations of the isomeric forms of the molecular motor reach a photostationary state. In general, this limitation can be circumvented by modulating the irradiation conditions in time and space at the macroscopic scale in order to obtain an oscillating behavior.[71,72,75,76,78,80−85,87,88,451] An LC-based system was recently reported in which the emergence of oscillations under photostationary conditions results from molecular-level behavior.[452] The liquid crystal, doped with overcrowded alkene molecular rotary motors and with a bridged 1,1′-bi-2-naphthol derivative as a photoinactive shape-persistent codopant, was confined between two glass slides spaced by a gap smaller than the pitch of the cholesteric helix. Second-generation molecular motors **25** (Figure 33) and **91** (Figure 70) were employed. At low irradiation power, axially symmetric chiral patterns were observed by polarized optical microscopy (Figure 72a). Above a certain irradiation power, structural symmetry breaking took place spontaneously, leading to non-axisymmetric patterns featuring a kink (Figure 72b). The patterns were seen to rotate continuously, with both the handedness and direction of rotation dictated by the axisymmetric pattern from which they arose. The unidirectional rotation was attributed to the interplay between the twist of the supramolecular LC arrangement and the diffusion of the chiral molecular motors away from a localized illumination area. It was also shown that a particle-like LC structure can orbit around the center of the revolving pattern when it is trapped in the periphery of the latter. In other words, the light-fueled rotation of the LC is harnessed to move a cargo. A significant feature of this assembly is that it can use the energy of light to establish and maintain nonequilibrium conditions at length scales that are typically 4 orders of magnitude larger than their molecular components.

5.5.2. Self-Assembled Systems. Control over the orientation and mutual alignment of molecules in order to obtain cooperative effects can be achieved by taking advantage of supramolecular association phenomena such as gelation and amphiphilic self-assembly. For example, overcrowded alkene photochromic switches, structurally related to the molecular rotary motors discussed in section 3.6.1, have been utilized to exert photocontrol over solvent gelation processes.[453,454] In another study, an amphiphilic overcrowded alkene switch was found to self-assemble into vesicles that can shrink in response to light irradiation and expand upon thermal relaxation.[455] Such materials are appealing for intelligent drug release or control of biological phenomena.[227]

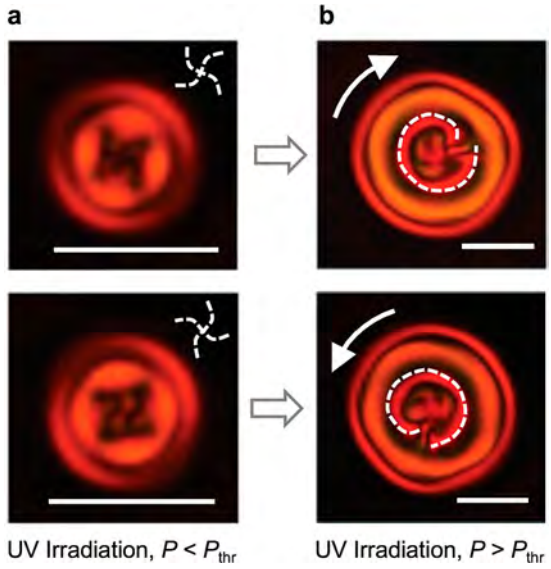

Figure 72. (a) Polarized optical micrographs showing axially symmetric chiral patterns with opposite handedness (highlighted by the dashed twisted crosses) observed when a liquid crystal doped with an enantiopure molecular rotary motor and a chiral codopant is embedded within two closely spaced glass slides and irradiated with low-intensity 375 nm light. No rotation of the patterns is observed. (b) Upon increasing the irradiation power (P) above a certain threshold (P_{thr}), larger and non-axisymmetric patterns are formed and rotate continuously and unidirectionally. Both the handedness (evidenced by the dashed spirals) and the direction of rotation (marked by solid white arrows) depend on the chirality of the starting axisymmetric pattern. Scale bars, 20 μm. Adapted with permission from ref 452. Copyright 2018 Springer Nature.

The self-assembly in water of second-generation overcrowded alkene motors rendered amphiphilic by appropriate substituents was investigated by Feringa and co-workers.[456] Compounds **93** and **94** (Figure 73a) form tubular structures when coassembled with the phospholipid DOPC, as observed by cryogenic transmission electron microscopy. While the nanotubes containing **93** did not exhibit morphological changes upon light irradiation, a transition from a tubular shape (nanotubes) to a spherical shape (vesicles) was observed upon irradiation of the nanotubes containing **94** as a consequence of the transformation from the stable E isomer to the unstable Z one (Figure 73b). Heating the system induces the isomerization of the molecular motor back to the starting isomer without the observation of a change in the morphology of the vesicles. However, the original nanotubes are obtained after freeze−thawing of the sample. The results indicate that the rotary motor function of **94** is preserved when this compound forms aggregates in water, thus opening the way to the operation of light-driven molecular motors in aqueous media.

Amphiphilic overcrowded alkene motors were found to undergo hierarchical self-organization in water, yielding nanofibers that can be further assembled into aligned bundles that eventually make up centimeter-long strings.[457] Compound **95** (Figure 74) resembles amphiphile **94** (Figure 73a) and consists of a second-generation motor functionalized with a dodecyl chain on the rotor side and two carboxyl-terminated alkyl chains on the stator side. The initial stage, self-assembly of **95** in aqueous NaOH at a concentration of 5% w/w, affords micrometer-long nanofibers with a diameter of about 5−6 nm (Figure 74a). Spectroscopic studies demonstrated that the

DOI: 10.1021/acs.chemrev.9b00291
Chem. Rev. 2020, 120, 200−268

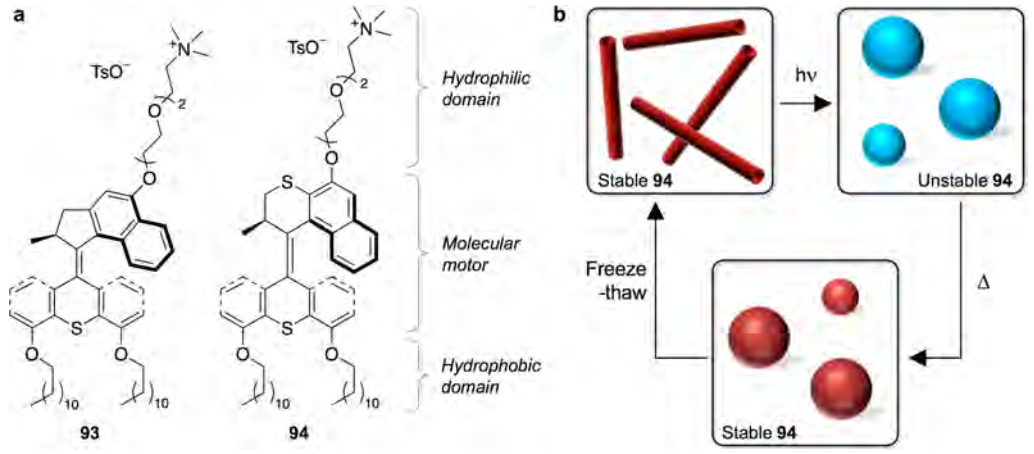

Figure 73. (a) Structural formulas of molecular rotary motors **93** and **94** highlighting their amphiphilic design. (b) Schematic representation of the photochemically and thermally induced changes in morphology of the corresponding self-assembled aggregates. Adapted from ref 456. Copyright 2015 American Chemical Society.

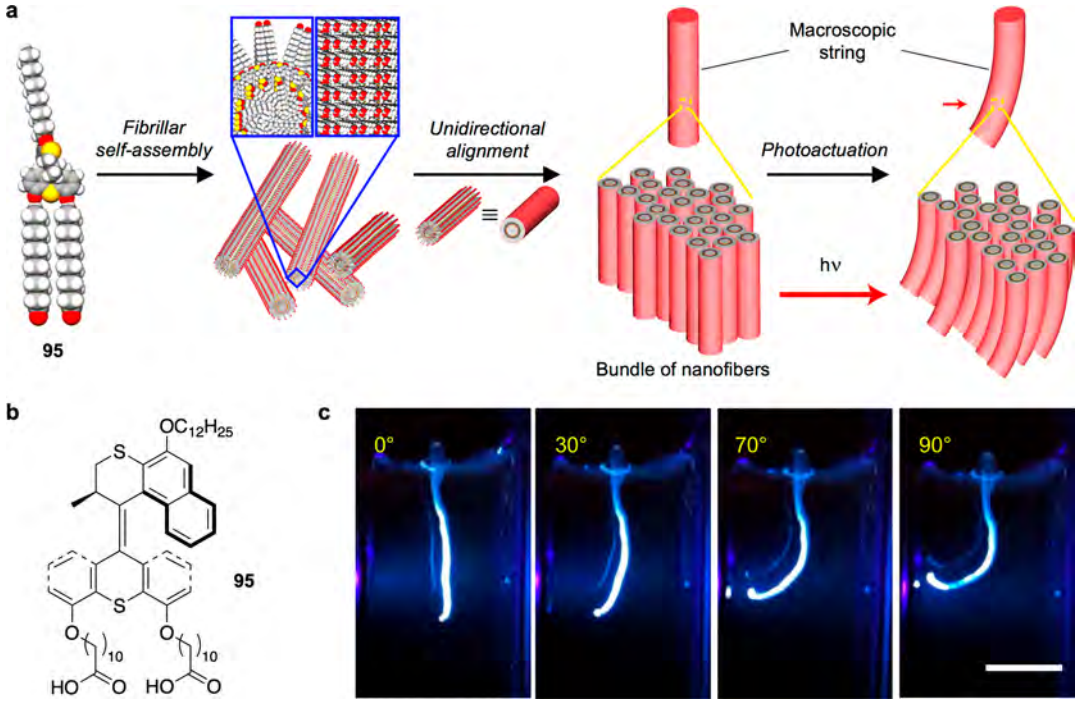

Figure 74. (a) Schematic representation of the hierarchical self-organization of amphiphilic molecular rotary motor **95** into nanofibers and bundles that make up macroscopic soft strings. (b) Structural formula of the molecular motor. (c) Photographic snapshots of a supramolecular string in water during UV irradiation from the left. Bending toward the source from 0 to 90° occurs within 60 s. Scale bar, 5 mm. Adapted with permission from ref 457. Copyright 2017 Springer Nature.

photoinduced motor function of **95** is preserved in the self-assembled fibers. Manually drawing the fiber solution into a concentrated aqueous solution of $CaCl_2$ afforded a noodlelike string of arbitrary length. Because of the electrostatic screening of the calcium ions and the shear flow, the nanofibers became directionally aligned in the bundles that constitute the string (Figure 74a). Remarkably, the string readily bent toward the light source upon 365 nm illumination in water (Figure 74c) and returned to its original state after 3 h at 50 °C. The process could also be carried out in air on a suspended string, which was shown to lift a 0.4 mg piece of paper adhered to its end. In situ small-angle X-ray scattering (SAXS) experiments were employed to investigate the photoactuation mechanism. It is hypothesized that the photoisomerization of the motor from the stable isomer to the unstable isomer causes an increase in the excluded volume around the motor, which in turn causes a perturbation of the local packing arrangement. Eventually, the effect of light irradiation is that of thickening and shortening the fibers; considering the thickness of the string (~300 μm) and its optical density at the irradiation wavelength (due to the absorbance of the motor), the contraction occurs only at the photoirradiated side of the string, thus causing its bending toward the light source.[457] The fact that macroscopic actuation by collection and amplification of molecular movements can be achieved under ambient conditions with a self-assembled system consisting of 95% water is very promising for the realization of mechanically active soft materials.

DOI: 10.1021/acs.chemrev.9b00291
Chem. Rev. 2020, 120, 200−268

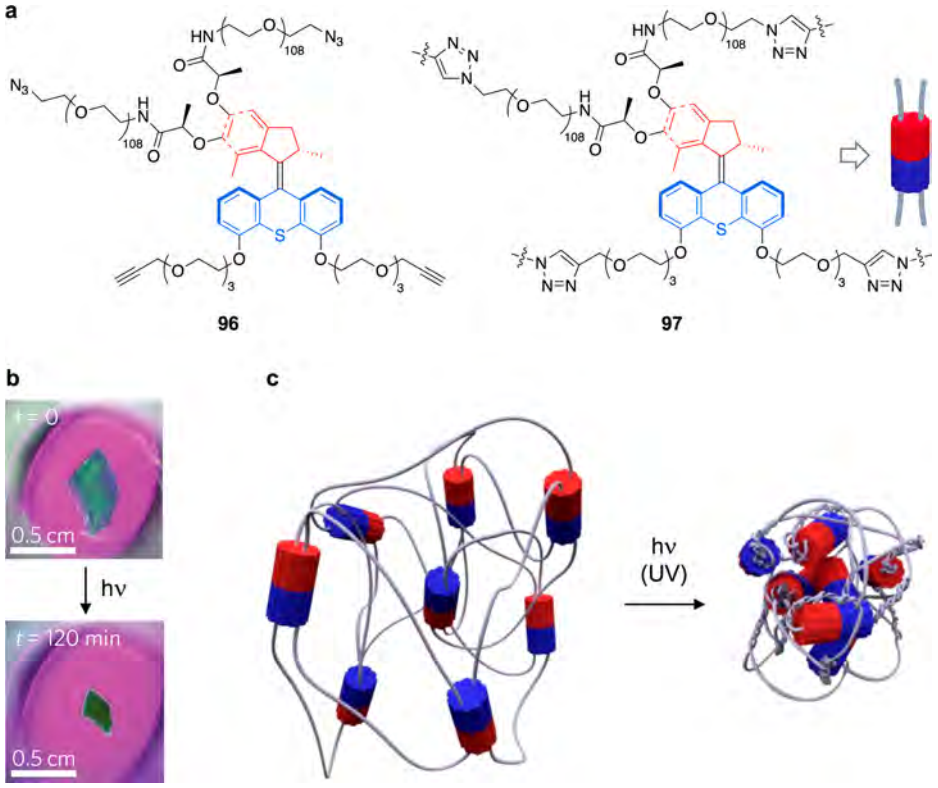

Figure 75. (a) The intermolecular "click" reaction between molecules of **96** yields polymer−motor conjugate **97**. (b) Photographs showing the contraction of a piece of gel consisting of **97** swollen with toluene upon UV light irradiation. (c) Schematic representation of the braiding of the polymer chains of **97** caused by the photoinduced rotation of the molecular motor units at the branching points, which results in the shrinkage of the gel. Adapted with permission from ref 460. Copyright 2015 Springer Nature.

5.5.3. Systems with Covalently Linked Molecular Motor Units. The incorporation of molecular machines into covalent polymers has been proposed for several years as a promising way to collect and amplify motion from the nanometer scale to the macroscopic scale.[434,436,439] Remarkable examples in this regard are polymers obtained by the head-to-tail connection of [c2]daisy chain rotaxane dimers.[458,459] Recent investigations have shown that the synchronous collective mechanical switching between contracted and expanded forms of the monomers, triggered by pH changes[432] or light irradiation,[73] can bring about a change in the size of a macroscopic fragment of material.

Studies of polymers with covalently embedded molecular motor elements are very rare. Giuseppone and co-workers incorporated second-generation overcrowded alkene rotary motors into a polymeric gel and investigated the effect of UV irradiation on the resulting material.[460,461] Compound **96** (Figure 75a) was obtained by functionalizing the stator and rotor halves of the enantiopure motor with two alkyne-terminated oligomeric ethylene glycol chains and two azide-terminated poly(ethylene glycol) chains, respectively. The successive copper-catalyzed alkyne−azide cycloaddition ("click" reaction) performed with **96** under high-concentration conditions afforded the cross-linked polymer **97** (Figure 75a), in which the ethylene glycol chains attached to different motors are connected together by means of triazole units. The polymer was found to form a gel in toluene at 10% w/w, which was characterized by SAXS and atomic force microscopy (AFM) supported by DFT calculations. The contraction of a millimeter-sized piece of the gel caused by UV irradiation could be clearly seen (Figure 75b). Such a behavior was explained by assuming that the entangled polymer chains are coiled up because of the light-driven unidirectional rotation of the motor components (Figure 75c). This interpretation is consistent with the results of experiments performed on model compounds obtained by the intramolecular reaction of the arms of **96** (achieved under dilute conditions) to yield eight-shaped macromolecules. AFM imaging revealed that individual eight-shaped objects exhibit a transition to a collapsed, more compact shape under UV illumination, a result consistent with the motor-driven formation of a wound structure.

It is worth noting that this system exploits the unidirectional movement of a molecular motor driven autonomously by a single stimulus and is therefore substantially different from materials based on molecular mechanical switches, which are interconverted between two thermodynamic minima by different stimuli.[73,429−432,459] As a matter of fact, the continuous photoinduced rotation of the motor units in **97** drives the system progressively away from thermal equilibrium; the energy of incident photons is thus converted into free energy of the entangled polymer chains (whose entropy decreases) and stored in the gel, with an overall estimated efficiency of about 0.15%. This energy, however, could not be retrieved because the light-driven braiding of the polymer was irreversible.

To address this issue, the design depicted in Figure 75 was improved by introducing diarylethene photoswitches in the gel as "modulator" elements[462] that act as on-demand elastic releasers by unbraiding the polymer chains in the cross-linked network. For this purpose, compound **98** (similar to **96** but containing only alkyne ends) was copolymerized with azide-terminated diarylethene derivative **99** (Figure 76a) to yield a polymeric gel analogous to **97** (Figure 75a) containing both

DOI: 10.1021/acs.chemrev.9b00291
Chem. Rev. 2020, 120, 200−268

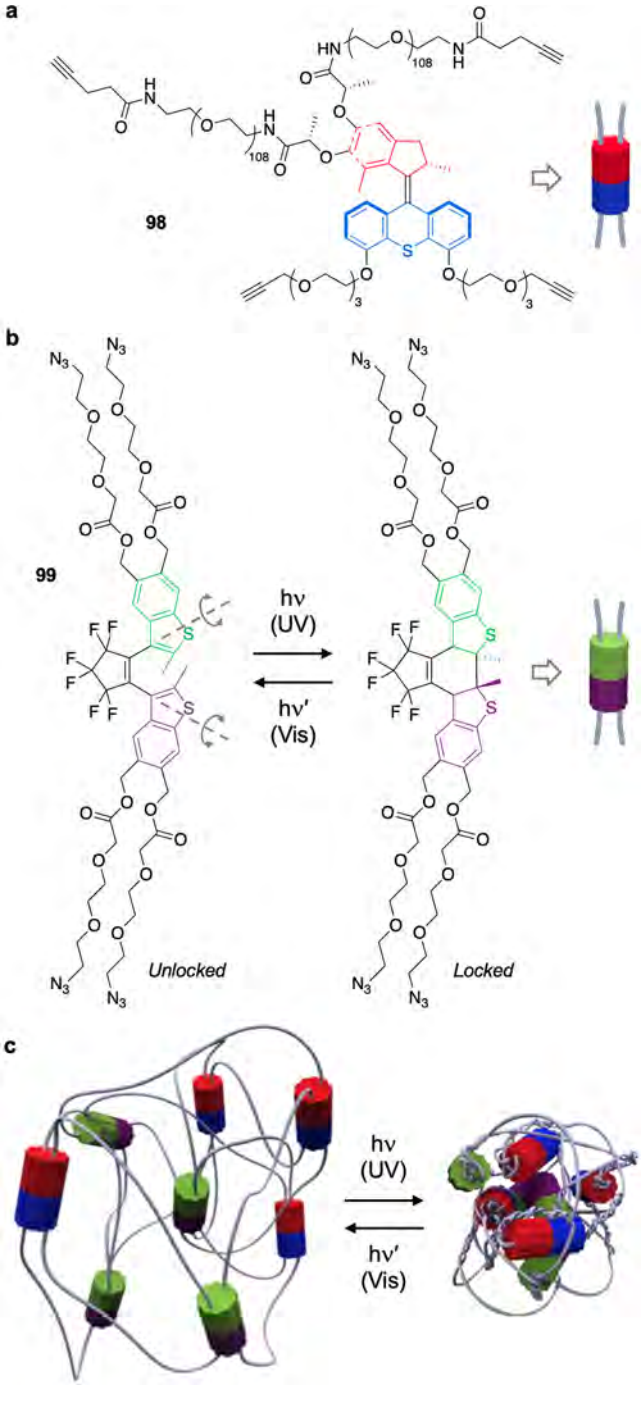

Figure 76. (a) Structural formula of alkyne-terminated molecular rotary motor **98**. (b) Structural formula of the diarylethene-based compound **99** that by a quadruple intermolecular "click" reaction with **98** yields a cross-linked polymer similar to **97** (Figure 75a) containing both molecular motor and modulator units. The open form (modulator unlocked; rotation axes shown in gray) and closed form (modulator locked) can be interconverted by UV and visible-light irradiation. (c) Schematic representation of the gel obtained by copolymerization of **98** and **99** and of the UV-induced braiding and visible-light-induced unbraiding of its chains. Adapted with permission from ref 462. Copyright 2017 Springer Nature.

modulator and motor subunits. A key feature of this design is that the modulators can be activated at a wavelength different from that employed to operate the rotary motors. In particular, irradiation with UV light promotes the unidirectional rotation of the motors (Figure 75c) while the diarylethene units are in their closed (locked) form, thereby sustaining the coiling of the polymer chains caused by the motors. Conversely, visible-light irradiation switches the modulators to their open (unlocked) form but is ineffective for actuation of the motors (Figure 76). Free rotation around C−C single bonds in the diarylethene units can thus release the torsional energy accumulated in the braided polymer until thermodynamic equilibrium is reached. It is important to note that the reversibility of the process relies on the elastic properties of the polymer.

Upon irradiation with both UV and visible light, the motors coil the polymer chains and the modulators allow their unwinding. By adjusting the relative intensities of the UV and visible light, one can tune the winding and unwinding rates and overall determine whether the gel is contracting or expanding. When these rates are equal, a photostationary out-of-equilibrium state is reached. Hence, the energy stored in the material and its mechanical output can be tuned by optical modulation of the braiding and unbraiding frequencies. As discussed in section 1, unidirectional motion is necessary for a molecular machine to bring its surroundings away from equilibrium; collection and accumulation of the effects of such movements in a material, however, may lead to irreversible changes that prevent the exploitation of the harvested energy (see above). The strategy devised by Giuseppone and co-workers[462] provides a general solution to this problem by precise molecular design and paves the way toward the development of more complex molecular-motor-based systems capable of converting light energy into potential and mechanical energy.

6. CONCLUSIONS AND OUTLOOK

After billions of years of evolution, nature has managed to produce amazingly beautiful and sophisticated molecule-based motors that oversee the most important aspects of the operation of living organisms. In a few decades, chemists have learned how to design, synthesize, and activate artificial molecular motors, thus fulfilling—at least in part—Feynman's prophecy on nanotechnology.[12] Although human-made molecular machines and motors cannot rival biological ones in terms of functionality, efficiency, and structural complexity, much progress has been made from both theoretical and experimental standpoints. The research in this field has evolved from an initial stage in which scientists were sharpening their wits to build simple prototypes of molecular machines by emulating the structure or movements of macroscopic counterparts to a more mature period in which researchers have gained more awareness of the fundamental concepts at the basis of nanoscale motion and begun to focus on issues such as energy supply, directional control, and interaction with the environment. The amazing growth of this area is evident also from a quantitative point of view if one considers the increase in the number of books, articles, and scientific meetings in the subject. More and more scientists are eager to tackle the many challenges related to the utilization of artificial molecular machines to perform tasks and ultimately their exploitation in the real world. In fact, the 2016 Nobel Prize in Chemistry recognized not only the huge and largely unexplored applicative potential of these tiny devices but also the very significant conceptual and technical leaps forward achieved in chemistry and neighboring disciplines by applying an engineering mentality, synthesis-driven creativity, and bioinspired ingenuity to molecular sciences.

In the context of molecular motors, the development of systems driven by light- or redox-induced processes is

DOI: 10.1021/acs.chemrev.9b00291
Chem. Rev. 2020, 120, 200−268

particularly interesting because while the vast majority of biomolecular motors are powered by chemical reactions, the use of photonic or electrical stimuli is more appealing from a technological perspective. As illustrated by the examples in this review, the evolution from proof-of-principle designs to more advanced prototypes has led to the construction of artificial molecular motors capable of exploiting an energy source autonomously to produce directional motion that through judicious interfacing of the motor with its surrounding environment can be used to accomplish a function. Nevertheless, analysis of the state of the art of photo- and redox-driven molecular motors also highlights that there are still several gaps to be filled, problems to be solved, and challenges to be faced. In the following we try to identify the most significant issues that in our opinion should be addressed in the near future; many of them are not necessarily limited to redox- and photoactivated systems.

- **Expanding the variety of molecular architectures.** Most of the molecular rotary motors developed to date are based on a single class of molecules, and some types of devices—for example, redox-driven rotary motors based on catenanes—are still missing. The construction of linear motors capable of directed long-range translation is at a very early stage. Thus, promoting fundamental research on new types of molecular motors is essential to strengthen the scientific ground of the field and enrich the "toolbox" available to "molecular machinists". While synthetic minimalism for motor modules is surely a plus, modern chemical synthesis can indeed be called to arms for incorporating the motors into large and sophisticated architectures.
- **Precise mechanistic and operational understanding.** Detailed knowledge of the processes at the basis of the operating mechanism and the way they are affected by the environment (temperature, solvent/matrix, presence of counterions and other species, etc.) is not always available for the systems reported to date. This information is particularly important for the thoughtful design of new generations of motors. Moreover, investigating the thermodynamic and kinetic aspects of the working cycle of a motor is essential to assess its ability to function away from thermodynamic equilibrium and identify appropriate operational conditions. To advance in this direction, a strong effort in terms of high-level physicochemical experimental and computational techniques is required.
- **Autonomous exploitation of the energy source.** This feature, which enables the motor to repeat a working cycle by continuously dissipating energy from a single source rather than requiring an operator-dependent sequence of different inputs, is crucial for practical operation. This is how motor proteins operate, by constantly consuming ATP as a fuel. Artificial molecular motors that dissipate light energy in an autonomous manner are available, but they belong to a restricted category of chemical compounds. For example, autonomous light-fueled catenane rotary motors have not been realized yet, and autonomous operation of redox-driven molecular machines has not been achieved.
- **Advanced regulation of the motor activation.** The construction of molecular motors whose operation can be turned on/off or modulated by physical or chemical stimuli (other than the energy source) is an important step forward toward the realization of adaptive systems that can dynamically respond to environmental changes. It may be envisaged, for example, that molecular motors could adjust their working mode according to a given combination of substrates (i.e., to the result of a logic operation between them) or that self-regulating nanomechanical devices could be constructed by implementing feedback loops within their operating mechanism. The sporadic examples of stimuli-gated autonomous light-driven molecular motors described in section 3.6.1 are a good starting point, but more research is required to reach the above-mentioned goals.
- **Taking full advantage of directed motion.** In several examples described in section 5, molecular rotary motors are employed as bistable photoswitches or, at best, as multistate switches. In these cases, the task performed by the motor does not arise from the oriented sequence of transitions between states that leads to unidirectional motion. On another front, the potential effect of relative directional transport of one molecular component with respect to another vanishes if they eventually dissociate in a homogeneous fluid medium. Thus, although supramolecular pumps capable of directional and autonomous light-driven motion are available (section 3.3), they need to be introduced in compartmentalized environments to take advantage of the active transport. In general, from a functional point of view there is much to be gained from the full exploitation of directed movements, particularly with regard to the conversion and storage of the energy inputs.
- **Connecting active and passive molecular mechanical parts.** Macroscopic machines usually comprise a motor component that drives passive moving parts such as gears, chains, and shafts. A similar situation can be envisioned for future nanomechanical devices. The construction of artificial multicomponent systems in which molecular motors are mechanically coupled with other movable molecular-level parts is a fascinating and delicate task. The transmission of motion requires a fine balance of the steric interactions: if the fit is too tight, the device is blocked, but if it is too loose, the coupling is lost. Recent proof-of-principle studies aimed at combining molecular rotary motors with passive rotors or pistons (section 5.2) have paved the way for further investigations.
- **Single-molecule operation.** The realization of molecular machines that can be operated and monitored individually at the nanometer scale is one of the most thrilling and imaginative goals of nanoscience. Besides the construction of "nanocars", such an objective is also relevant for high-density data processing and storage.[172] The main problems are the identification of appropriate supports—typically, surfaces—to afford a desired degree of (im)-mobilization of the molecular machines and the solution to the technical difficulties related to excitation/addressing and imaging/readout at the single-molecule level.
- **Harvesting collective effects.** Natural systems show that macroscopic work can be performed by harnessing the motion of many molecular motors that are appropriately organized in space and operated synchronously. Indeed, the amplification of movement from the nanometer world up to larger scales requires the arrangement of artificial

DOI: 10.1021/acs.chemrev.9b00291
Chem. Rev. 2020, 120, 200−268

molecular machines with a controlled orientation into an extended framework. From an operational viewpoint, such a structure should not only preserve the motion but also enable the parallel stimulation of large number of individual devices. Although recent attempts based on both soft matter (liquid crystals, supramolecular polymers, and covalent gels; see section 5.5) and hard matter (covalent frameworks; see section 3.6.1) are promising, the preparation and characterization of hybrid materials of this kind remain considerably difficult tasks.

In conclusion, research on photo- and redox-driven artificial molecular motors, despite its relatively young age, is characterized by a past of exciting discoveries, a present of outstanding achievements, and a future of astonishing challenges for both fundamental and applied science. Indeed, constructing functional devices and materials based on artificial molecular motors is an extremely complex endeavor. Nevertheless, these systems have the potential to revolutionize entire sectors of technology and medicine by disclosing radically innovative solutions to problems in fine chemistry, solar energy conversion and storage, information and communication technology, medical diagnostics and therapy, robotics, etc. The opportunity to go well beyond the incremental improvement of existing paradigms to address key societal challenges justifies the high risks and long times inherent to this research and motivates more and more scientists to join it.

AUTHOR INFORMATION

Corresponding Authors

*E-mail: massimo.baroncini@unibo.it.
*E-mail: serena.silvi@unibo.it.
*E-mail: alberto.credi@unibo.it.

ORCID

Massimo Baroncini: 0000-0002-8112-8916
Serena Silvi: 0000-0001-9273-4148
Alberto Credi: 0000-0003-2546-9801

Notes

The authors declare no competing financial interest.

Biographies

Massimo Baroncini received his M.Sc. in Chemistry in 2006 at the University of Bologna under the supervision of Prof. Vincenzo Balzani and his Ph.D. in Chemical Sciences in 2010, which was awarded with the Springer-Verlag Theses Award in 2011. He is currently an assistant professor in the Department of Agricultural and Food Sciences (DISTAL) at the University of Bologna and an associate researcher at the Center for Light Activated Nanostructures (CLAN), a UNIBO–National Research Council joint laboratory for research in photochemistry, supramolecular chemistry, materials science, and nanoscience. He has coauthored over 50 scientific publications, six book chapters, and one monograph. His main research activity deals with the synthesis and investigation of photoactive molecular and supramolecular systems and materials with tailored physicochemical functionalities.

Serena Silvi got her M.Sc. in 2002 at the University of Bologna with Prof. Vincenzo Balzani, and in 2006 she earned her Ph.D. under the supervision of Prof. Alberto Credi with a thesis on artificial molecular machines. From 2006 to 2008 she collaborated with the research in the Photochemistry and Supramolecular Chemistry laboratory, and since 2008 she has been an assistant professor at the Chemistry Department "Giacomo Ciamician" of the University of Bologna. Her research activity is focused on the design and characterization of artificial molecular machines based on interlocked structures, photochromic compounds and photoactive molecular materials, and complex systems for signal processing.

Alberto Credi is Professor of Chemistry at the University of Bologna and an associate research director at the National Research Council. He is the founder and director of CLAN. His research deals with the development of stimuli-responsive molecular-based systems, with a particular focus on logic devices, machines, and motors. He has authored four books and over 280 scientific publications, and he is the principal investigator of an Advanced Grant of the European Research Council for the development of light-driven molecular motors. Since the beginning of his career he has been engaged in the popularization of chemistry disciplines and scientific culture in general.

ACKNOWLEDGMENTS

Financial support from the European Union's Horizon 2020 research and innovation program (ERC Advanced Grants "Leaps" 692981 and FET-OPEN "Magnify" 801378) and the Ministero dell'Istruzione, Università e Ricerca (FARE Grant "Ampli" R16S9XXKX3) is gratefully acknowledged.

REFERENCES

(1) Mann, S. Life as a Nanoscale Phenomenon. *Angew. Chem., Int. Ed.* **2008**, *47*, 5306–5320.
(2) *Molecular Motors*; Schliwa, M., Ed.; Wiley-VCH: Weinheim, Germany, 2003.
(3) Goodsell, D. S. *Bionanotechnology—Lessons from Nature*; Wiley-Liss: Hoboken, NJ, 2004.
(4) Jones, R. A. L. *Soft Machines—Nanotechnology and Life*; Oxford University Press: Oxford, U.K., 2008.
(5) Foth, B. J.; Goedecke, M. C.; Soldati, D. New Insights into Myosin Evolution and Classification. *Proc. Natl. Acad. Sci. U. S. A.* **2006**, *103*, 3681–3686.
(6) Hirokawa, N.; Noda, Y.; Tanaka, Y.; Niwa, S. Kinesin Superfamily Motor Proteins and Intracellular Transport. *Nat. Rev. Mol. Cell Biol.* **2009**, *10*, 682–696.
(7) von Ballmoos, C.; Cook, G. M.; Dimroth, P. Unique Rotary ATP Synthase and its Biological Diversity. *Annu. Rev. Biophys.* **2008**, *37*, 43–64.
(8) Minamino, T.; Imada, K. The Bacterial Flagellar Motor and its Structural Diversity. *Trends Microbiol.* **2015**, *23*, 267–274.
(9) Hübscher, U.; Maga, G.; Spadari, S. Eukaryotic DNA Polymerases. *Annu. Rev. Biochem.* **2002**, *71*, 133–163.
(10) Sengupta, S.; Spiering, M. M.; Dey, K. K.; Duan, W.; Patra, D.; Butler, P. J.; Astumian, R. D.; Benkovic, S. J.; Sen, A. DNA Polymerase as a Molecular Motor and Pump. *ACS Nano* **2014**, *8*, 2410–2418.
(11) Saibil, H. Chaperone Machines for Protein Folding, Unfolding and Disaggregation. *Nat. Rev. Mol. Cell Biol.* **2013**, *14*, 630–642.
(12) Feynman, R. P. There's Plenty of Room at the Bottom. *Eng. Sci.* **1960**, *23*, 22–36.
(13) Joachim, C.; Launay, J.-P. Sur la Possibilité d'un Traitement Moleculaire du Signal. *Nouv. J. Chim.* **1984**, *8*, 723–728.
(14) Balzani, V.; Moggi, L.; Scandola, F. Towards a Supramolecular Photochemistry. Assembly of Molecular Components To Obtain Photochemical Molecular Devices. In *Supramolecular Photochemistry*; Balzani, V., Ed.; Reidel: Dordrecht, The Netherlands, 1987; pp 1–28.
(15) Balzani, V.; Credi, A.; Venturi, M. The Bottom-up Approach to Molecular-Level Devices and Machines. *Chem. - Eur. J.* **2002**, *8*, 5524–5532.
(16) Lehn, J.-M. *Supramolecular Chemistry—Concepts and Perspectives*; Wiley-VCH: Weinheim, Germany, 1995.
(17) Dietrich-Buchecker, C. O.; Sauvage, J.-P. Interlocking of Molecular Threads – From the Statistical Approach to the Templated Synthesis of Catenands. *Chem. Rev.* **1987**, *87*, 795–810.

DOI: 10.1021/acs.chemrev.9b00291
Chem. Rev. 2020, 120, 200–268

(18) Amabilino, D. B.; Stoddart, J. F. Interlocked and Intertwined Structures and Superstructures. *Chem. Rev.* **1995**, *95*, 2725−2828.
(19) Noji, H.; Yasuda, R.; Yoshida, M.; Kinosita, K. Direct Observation of the Rotation of F_1-ATPase. *Nature* **1997**, *386*, 299−302.
(20) Astumian, R. D. Thermodynamics and Kinetics of a Brownian Motor. *Science* **1997**, *276*, 917−922.
(21) Astumian, R. D.; Hänggi, P. Brownian Motors. *Phys. Today* **2002**, *55* (11), 33−39.
(22) Bustamante, C.; Keller, D.; Oster, G. The Physics of Molecular Motors. *Acc. Chem. Res.* **2001**, *34*, 412−420.
(23) Chatterjee, M. N.; Kay, E. R.; Leigh, D. A. Beyond Switches: Ratcheting a Particle Energetically Uphill with a Compartmentalized Molecular Machine. *J. Am. Chem. Soc.* **2006**, *128*, 4058−5073.
(24) Balzani, V.; Credi, A.; Raymo, F. M.; Stoddart, J. F. Artificial Molecular Machines. *Angew. Chem., Int. Ed.* **2000**, *39*, 3348−3391.
(25) Collin, J.-P.; Dietrich-Buchecker, C.; Gaviña, P.; Jimenez-Molero, M. C.; Sauvage, J.-P. Shuttles and Muscles: Linear Molecular Machines Based on Transition Metals. *Acc. Chem. Res.* **2001**, *34*, 477−487.
(26) Sauvage, J.-P. Transition Metal-Complexed Catenanes and Rotaxanes as Molecular Machine Prototypes. *Chem. Commun.* **2005**, 1507−1510.
(27) Kottas, G. S.; Clarke, L. I.; Horinek, D.; Michl, J. Artificial Molecular Rotors. *Chem. Rev.* **2005**, *105*, 1281−1376.
(28) Rapenne, G. Synthesis of Technomimetic Molecules: Towards Rotation Control in Single-Molecular Machines and Motors. *Org. Biomol. Chem.* **2005**, *3*, 1165−1169.
(29) Kinbara, K.; Aida, T. Toward Intelligent Molecular Machines: Directed Motions of Biological and Artificial Molecules and Assemblies. *Chem. Rev.* **2005**, *105*, 1377−1400.
(30) Browne, W. R.; Feringa, B. L. Making Molecular Machines Work. *Nat. Nanotechnol.* **2006**, *1*, 25−35.
(31) Kay, E. R.; Leigh, D. A.; Zerbetto, F. Synthetic Molecular Motors and Mechanical Machines. *Angew. Chem., Int. Ed.* **2007**, *46*, 72−191.
(32) Champin, B.; Mobian, P.; Sauvage, J.-P. Transition Metal Complexes as Molecular Machine Prototypes. *Chem. Soc. Rev.* **2007**, *36*, 358−366.
(33) Michl, J.; Sykes, E. C. H. Molecular Rotors and Motors: Recent Advances and Future Challenges. *ACS Nano* **2009**, *3*, 1042−1048.
(34) Coskun, A.; Banaszak, M.; Astumian, R. D.; Stoddart, J. F.; Grzybowski, B. A. Great Expectations: Can Artificial Molecular Machines Deliver on Their Promise? *Chem. Soc. Rev.* **2012**, *41*, 19−30.
(35) van Dongen, S. F. M.; Cantekin, S.; Elemans, J. A. A. W.; Rowan, A. E.; Nolte, R. J. M. Functional Interlocked Systems. *Chem. Soc. Rev.* **2014**, *43*, 99−122.
(36) Erbas-Cakmak, S.; Leigh, D. A.; McTernan, C. T.; Nussbaumer, A. L. Artificial Molecular Machines. *Chem. Rev.* **2015**, *115*, 10081−10206.
(37) Watson, M. A.; Cockroft, S. L. Man-Made Molecular Machines: Membrane Bound. *Chem. Soc. Rev.* **2016**, *45*, 6118−6129.
(38) Kassem, S.; van Leeuwen, T.; Lubbe, A. S.; Wilson, M. R.; Feringa, B. L.; Leigh, D. A. Artificial Molecular Motors. *Chem. Soc. Rev.* **2017**, *46*, 2592−2621.
(39) Pezzato, C.; Cheng, C.; Stoddart, J. F.; Astumian, R. D. Mastering the Non-Equilibrium Assembly and Operation of Molecular Machines. *Chem. Soc. Rev.* **2017**, *46*, 5491−5507.
(40) Zhang, L.; Marcos, V.; Leigh, D. A. Molecular Machines with Bio-Inspired Mechanisms. *Proc. Natl. Acad. Sci. U. S. A.* **2018**, *115*, 9397−9404.
(41) Baroncini, M.; Casimiro, L.; de Vet, C.; Groppi, J.; Silvi, S.; Credi, A. Making and Operating Molecular Machines: A Multidisciplinary Challenge. *ChemistryOpen* **2018**, *7*, 169−179.
(42) Nijhuis, C. A.; Ravoo, B. J.; Huskens, J.; Reinhoudt, D. N. Electrochemically Controlled Supramolecular Systems. *Coord. Chem. Rev.* **2007**, *251*, 1761−1780.
(43) Credi, A.; Semeraro, M.; Silvi, S.; Venturi, M. Redox Control of Molecular Motion in Switchable Artificial Nanoscale Devices. *Antioxid. Redox Signaling* **2011**, *14*, 1119−1165.
(44) Venturi, M.; Credi, A. Electroactive [2]Catenanes. *Electrochim. Acta* **2014**, *140*, 467−475.
(45) Le Poul, N.; Colasson, B. Electrochemically and Chemically Induced Redox Processes in Molecular Machines. *ChemElectroChem* **2015**, *2*, 475−496.
(46) Ragazzon, G.; Baroncini, M.; Ceroni, P.; Credi, A.; Venturi, M. Electrochemically Controlled Supramolecular Switches and Machines. In *Comprehensive Supramolecular Chemistry II*; Atwood, J. L., Ed.; Elsevier: Oxford, U.K., 2017; Vol. *2*, pp 343−368.
(47) Credi, A. Artificial Molecular Motors Powered by Light. *Aust. J. Chem.* **2006**, *59*, 157−169.
(48) Saha, S.; Stoddart, J. F. Photo-Driven Molecular Devices. *Chem. Soc. Rev.* **2007**, *36*, 77−92.
(49) Credi, A.; Venturi, M. Molecular Machines Operated by Light. *Cent. Eur. J. Chem.* **2008**, *6*, 325−339.
(50) Bonnet, S.; Collin, J.-P. Ruthenium-Based Light-Driven Molecular Machine Prototypes: Synthesis and Properties. *Chem. Soc. Rev.* **2008**, *37*, 1207−1217.
(51) Balzani, V.; Credi, A.; Venturi, M. Light Powered Molecular Machines. *Chem. Soc. Rev.* **2009**, *38*, 1542−1550.
(52) Ma, X.; Tian, H. Bright Functional Rotaxanes. *Chem. Soc. Rev.* **2010**, *39*, 70−80.
(53) Silvi, S.; Venturi, M.; Credi, A. Light Operated Molecular Machines. *Chem. Commun.* **2011**, *47*, 2483−2489.
(54) van Leeuwen, T.; Lubbe, A. S.; Štacko, P.; Wezenberg, S. J.; Feringa, B. L. Dynamic Control of Function by Light-Driven Molecular Motors. *Nat. Rev. Chem.* **2017**, *1*, No. 0096.
(55) Stoddart, J. F. Molecular Machines. *Acc. Chem. Res.* **2001**, *34*, 410−411.
(56) Credi, A.; Tian, H. Big Challenges for Tiny Machines. *Adv. Funct. Mater.* **2007**, *17*, 679−682.
(57) Browne, W. R.; Woolley, G. A.; Qu, D.-H. Molecular Machines. *ChemPhysChem* **2016**, *17*, 1713−1714.
(58) Sluysmans, D.; Stoddart, J. F. Growing Community of Artificial Molecular Machinists. *Proc. Natl. Acad. Sci. U. S. A.* **2018**, *115*, 9359−9361.
(59) *Molecular Machines*; Kelly, T. R., Ed.; Springer: Berlin, 2005.
(60) *From Non-Covalent Assemblies to Molecular Machines*; Sauvage, J.-P., Gaspard, P., Eds.; Wiley-VCH: Weinheim, Germany, 2011.
(61) *Molecular Machines and Motors—Recent Advances and Perspectives*; Credi, A., Silvi, S., Venturi, M., Eds.; Springer: Cham, Switzerland, 2014.
(62) Balzani, V.; Credi, A.; Venturi, M. *Molecular Devices and Machines—A Journey in the Nano World*; Wiley-VCH: Weinheim, Germany, 2003.
(63) Balzani, V.; Credi, A.; Venturi, M. *Molecular Devices and Machines—Concepts and Perspectives for the Nanoworld*; Wiley-VCH: Weinheim, Germany, 2008.
(64) Wang, J. *Nanomachines—Fundamentals and Applications*; RSC Publishing: Cambridge, U.K., 2012.
(65) Bruns, C.; Stoddart, J. F. *The Nature of the Mechanical Bond: From Molecules to Machines*; Wiley: Hoboken, NJ, 2016.
(66) Sauvage, J.-P. From Chemical Topology to Molecular Machines (Nobel Lecture). *Angew. Chem., Int. Ed.* **2017**, *56*, 11080−11093.
(67) Stoddart, J. F. Mechanically Interlocked Molecules (MIMs) - Molecular Shuttles, Switches, and Machines (Nobel Lecture). *Angew. Chem., Int. Ed.* **2017**, *56*, 11094−11125.
(68) Feringa, B. L. The Art of Building Small: From Molecular Switches to Motors (Nobel Lecture). *Angew. Chem., Int. Ed.* **2017**, *56*, 11060−11078.
(69) Leigh, D. A. Genesis of the Nanomachines: the 2016 Nobel Prize in Chemistry. *Angew. Chem., Int. Ed.* **2016**, *55*, 14506−14508.
(70) Peplow, M. March of the Machines. *Nature* **2015**, *525*, 18−21.
(71) Eremin, A.; Hirankittiwong, P.; Chattham, N.; Nádasi, H.; Stannarius, R.; Limtrakul, J.; Haba, O.; Yonetake, K.; Takezoe, H. Optically Driven Translational and Rotational Motions of Microrod Particles in a Nematic Liquid Crystal. *Proc. Natl. Acad. Sci. U. S. A.* **2015**, *112*, 1716−1720.

DOI: 10.1021/acs.chemrev.9b00291
Chem. Rev. 2020, 120, 200−268

(72) Kumar, K.; Knie, C.; Bléger, D.; Peletier, M. A.; Friedrich, H.; Hecht, S.; Broer, D. J.; Debije, M. G.; Schenning, A. P. H. J. A Chaotic Self-Oscillating Sunlight-Driven Polymer Actuator. *Nat. Commun.* **2016**, *7*, 11975.
(73) Iwaso, K.; Takashima, Y.; Harada, A. Fast Response Dry-Type Artificial Molecular Muscles with [c2]Daisy Chains. *Nat. Chem.* **2016**, *8*, 625−633.
(74) Tu, Y.; Peng, F.; Sui, X.; Men, Y.; White, P. B.; van Hest, J. C. M.; Wilson, D. A. Self-Propelled Supramolecular Nanomotors with Temperature-Responsive Speed Regulation. *Nat. Chem.* **2017**, *9*, 480−486.
(75) Gelebart, A. H.; Mulder, D. J.; Varga, M.; Konya, A.; Vantomme, G.; Meijer, E. W.; Selinger, R. L. B.; Broer, D. J. Making Waves in a Photoactive Polymer Film. *Nature* **2017**, *546*, 632−636.
(76) Aßhoff, S. J.; Lancia, F.; Iamsaard, S.; Matt, B.; Kudernac, T.; Fletcher, S. P.; Katsonis, N. High-Power Actuation from Molecular Photoswitches in Enantiomerically Paired Soft Springs. *Angew. Chem., Int. Ed.* **2017**, *56*, 3261−3265.
(77) Liles, K. P.; Greene, A. F.; Danielson, M. K.; Colley, N. D.; Wellen, A.; Fisher, J. M.; Barnes, J. C. Photoredox-Based Actuation of an Artificial Molecular Muscle. *Macromol. Rapid Commun.* **2018**, *39*, 1700781.
(78) Lahikainen, M.; Zeng, H.; Priimagi, A. Reconfigurable Photo-actuator through Synergistic Use of Photochemical and Photothermal Effects. *Nat. Commun.* **2018**, *9*, 4148.
(79) Xuan, M.; Shao, J.; Gao, C.; Wang, W.; Dai, L.; He, Q. Self-Propelled Nanomotors for Thermomechanically Percolating Cell Membranes. *Angew. Chem., Int. Ed.* **2018**, *57*, 12463−12467.
(80) Inaba, H.; Uemura, A.; Morishita, K.; Kohiki, T.; Shigenaga, A.; Otaka, A.; Matsuura, K. Light-Induced Propulsion of a Giant Liposome Driven by Peptide Nanofiber Growth. *Sci. Rep.* **2018**, *8*, 6243.
(81) Yuan, Y.; Abuhaimed, G. N.; Liu, Q.; Smalyukh, I. I. Self-Assembled Nematic Colloidal Motors Powered by Light. *Nat. Commun.* **2018**, *9*, 5040.
(82) Zhang, D.; Sun, Y.; Li, M.; Zhang, H.; Song, B.; Dong, B. A Phototactic Liquid Micromotor. *J. Mater. Chem. C* **2018**, *6*, 12234−12239.
(83) Bléger, D.; Yu, Z.; Hecht, S. Toward Optomechanics: Maximizing the Photodeformation of Individual Molecules. *Chem. Commun.* **2011**, *47*, 12260−12266.
(84) Priimagi, A.; Barrett, C. J.; Shishido, A. Recent Twists in Photoactuation and Photoalignment Control. *J. Mater. Chem. C* **2014**, *2*, 7155−7162.
(85) Hu, Y.; Li, Z.; Lan, T.; Chen, W. Photoactuators for Direct Optical-to-Mechanical Energy Conversion: From Nanocomponent Assembly to Macroscopic Deformation. *Adv. Mater.* **2016**, *28*, 10548−10556.
(86) Ohtake, T.; Tanaka, H. Redox-Induced Actuation in Macromolecular and Self-Assembled Systems. *Polym. J.* **2016**, *48*, 25−37.
(87) Lin, X.; Wu, Z.; Wu, Y.; Xuan, M.; He, Q. Self-Propelled Micro-/Nanomotors Based on Controlled Assembled Architectures. *Adv. Mater.* **2016**, *28*, 1060−1072.
(88) Xu, L.; Mou, F.; Gong, H.; Luo, M.; Guan, J. Light-Driven Micro/Nanomotors: From Fundamentals to Applications. *Chem. Soc. Rev.* **2017**, *46*, 6905−6926.
(89) Fukino, T.; Yamagishi, H.; Aida, T. Redox-Responsive Molecular Systems and Materials. *Adv. Mater.* **2017**, *29*, 1603888.
(90) Otero, T. F. Structural and Conformational Chemistry from Electrochemical Molecular Machines. Replicating Biological Functions. *Chem. Rec.* **2018**, *18*, 788−806.
(91) Wang, J.; Xiong, Z.; Zheng, J.; Zhan, X.; Tang, J. Light-Driven Micro/Nanomotor for Promising Biomedical Tools: Principle, Challenge, and Prospect. *Acc. Chem. Res.* **2018**, *51*, 1957−1965.
(92) *Oxford English Dictionary*; Oxford University Press: Oxford, U.K., 1989.
(93) Coffey, T. S.; Krim, J. C_{60} Molecular bearings and the Phenomenon of Nanomapping. *Phys. Rev. Lett.* **2006**, *96*, 186104.
(94) *Molecular Switches*, 2nd ed.; Feringa, B. L., Browne, W. R., Eds.; Wiley-VCH: Weinheim, Germany, 2011.
(95) Harris, J. D.; Moran, M. J.; Aprahamian, I. New Molecular Switch Architectures. *Proc. Natl. Acad. Sci. U. S. A.* **2018**, *115*, 9414−9422.
(96) Astumian, R. D. Design Principles for Brownian Molecular Machines: How to Swim in Molasses and Walk in a Hurricane. *Phys. Chem. Chem. Phys.* **2007**, *9*, 5067−5083.
(97) Hoffman, P. M. *Life's Ratchet. How Molecular Machines Extract Order from Chaos*; Basic Books: New York, 2012.
(98) Kelly, T. R.; Tellitu, I.; Sestelo, J. P. In Search of Molecular Ratchets. *Angew. Chem., Int. Ed. Engl.* **1997**, *36*, 1866−1868.
(99) Alvarez-Pérez, M.; Goldup, S. M.; Leigh, D. A.; Slawin, A. M. Z. A Chemically-Driven Molecular Information Ratchet. *J. Am. Chem. Soc.* **2008**, *130*, 1836−1838.
(100) von Delius, M.; Geertsema, E. M.; Leigh, D. A. A Synthetic Small Molecule that Can Walk Down a Track. *Nat. Chem.* **2010**, *2*, 96−101.
(101) Arduini, A.; Bussolati, R.; Credi, A.; Monaco, S.; Secchi, A.; Silvi, S.; Venturi, M. Solvent- and Light-Controlled Unidirectional Transit of a Nonsymmetric Molecular Axle Through a Nonsymmetric Molecular Wheel. *Chem. - Eur. J.* **2012**, *18*, 16203−16213.
(102) Meng, Z.; Xiang, J.-F.; Chen, C.-F. Directional Molecular Transportation Based on a Catalytic Stopper-Leaving Rotaxane System. *J. Am. Chem. Soc.* **2016**, *138*, 5652−5658.
(103) Erbas-Cakmak, S.; Fielden, S. D. P.; Karaca, U.; Leigh, D. A.; McTernan, C. T.; Tetlow, D. J.; Wilson, M. R. Rotary and Linear Molecular Motors Driven by Pulses of a Chemical Fuel. *Science* **2017**, *358*, 340−343.
(104) Wilson, M. R.; Sola, J.; Carlone, A.; Goldup, S. M.; Lebrasseur, N.; Leigh, D. A. An Autonomous Chemically Fueled Small-Molecule Motor. *Nature* **2016**, *534*, 235−240.
(105) Avellini, T.; Li, H.; Coskun, A.; Barin, G.; Trabolsi, A.; Basuray, A. N.; Dey, S. K.; Credi, A.; Silvi, S.; Stoddart, J. F.; et al. Photoinduced Memory Effect in a Redox Controllable Bistable Mechanical Molecular Switch. *Angew. Chem., Int. Ed.* **2012**, *51*, 1611−1615.
(106) Choi, J. W.; Flood, A. H.; Steuerman, D. W.; Nygaard, S.; Braunschweig, A. B.; Moonen, N. N. P.; Laursen, B. W.; Luo, Y.; DeIonno, E.; Peters, A. J.; et al. Ground-state Equilibrium Thermodynamics and Switching Kinetics of Bistable [2]Rotaxanes Switched in Solution, Polymer Gels, and Molecular Electronic Devices. *Chem. - Eur. J.* **2006**, *12*, 261−279.
(107) Odell, B.; Reddington, M. V.; Slawin, A. M. Z.; Spencer, N.; Stoddart, J. F.; Williams, D. J. Cyclobis(paraquat-*p*-phenylene). A Tetracationic Multipurpose Receptor. *Angew. Chem., Int. Ed. Engl.* **1988**, *27*, 1547−1550.
(108) Serreli, V.; Lee, C.-F.; Kay, E. R.; Leigh, D. A. A Molecular Information Ratchet. *Nature* **2007**, *445*, 523−527.
(109) Parrondo, J. M. R.; Horowitz, J. M.; Sagawa, T. Thermodynamics of Information. *Nat. Phys.* **2015**, *11*, 131−139.
(110) Kaifer, A. E.; Gómez-Kaifer, M. *Supramolecular Electrochemistry*; Wiley-VCH: Weinheim, Germany, 1999.
(111) *Electrochemistry of Functional Supramolecular Systems*; Venturi, M., Ceroni, P., Credi, A., Eds.; Wiley: Hoboken, NJ, 2010.
(112) Amemiya, S.; Bard, A. J.; Fan, F. R. F.; Mirkin, M. V.; Unwin, P. R. Scanning Electrochemical Microscopy. *Annu. Rev. Anal. Chem.* **2008**, *1*, 95−131.
(113) Grill, L. Functionalized Molecules Studied by STM: Motion, Switching and Reactivity. *J. Phys.: Condens. Matter* **2008**, *20*, No. 053001.
(114) Tierney, H. L.; Murphy, C. J.; Jewell, A. D.; Baber, A. E.; Iski, E. V.; Khodaverdian, H. Y.; McGuire, A. F.; Klebanov, N.; Sykes, E. C. H. Experimental Demonstration of a Single-Molecule Electric Motor. *Nat. Nanotechnol.* **2011**, *6*, 625−629.
(115) Perera, U. G. E.; Ample, F.; Kersell, H.; Zhang, Y.; Vives, G.; Echeverria, J.; Grisolia, M.; Rapenne, G.; Joachim, C.; Hla, S. W. Controlled Clockwise and Anticlockwise Rotational Switching of a Molecular Motor. *Nat. Nanotechnol.* **2013**, *8*, 46−51.
(116) Kudernac, T.; Ruangsupapichat, N.; Parschau, M.; Maciá, B.; Katsonis, N.; Harutyunyan, S. R.; Ernst, K.-H.; Feringa, B. L. Electrically Driven Directional Motion of a Four-Wheeled Molecule on a Metal Surface. *Nature* **2011**, *479*, 208−211.

DOI: 10.1021/acs.chemrev.9b00291
Chem. Rev. 2020, 120, 200−268

(117) Joachim, C.; Rapenne, G. Molecule Concept Nanocars: Chassis, Wheels, and Motors? *ACS Nano* **2013**, *7*, 11−14.
(118) Simpson, G. J.; García-López, V.; Petermeier, P.; Grill, L.; Tour, J. M. How to Build and Race a Fast Nanocar. *Nat. Nanotechnol.* **2017**, *12*, 604−606.
(119) Rapenne, G.; Joachim, C. The First Nanocar Race. *Nat. Rev. Mater.* **2017**, *2*, 17040.
(120) Vacek, J.; Michl, J. Artificial Surface-Mounted Molecular Rotors: Molecular Dynamics Simulations. *Adv. Funct. Mater.* **2007**, *17*, 730−739.
(121) Zheng, X.; Mulcahy, M. E.; Horinek, D.; Galeotti, F.; Magnera, T. F.; Michl, J. Dipolar and Nonpolar Altitudinal Molecular Rotors Mounted on an Au(111) Surface. *J. Am. Chem. Soc.* **2004**, *126*, 4540−4542.
(122) Kobr, L.; Zhao, K.; Shen, Y.; Comotti, A.; Bracco, S.; Shoemaker, R.; Sozzani, P.; Clark, N.; Price, J.; Rogers, C.; Michl, J. Inclusion Compound Based Approach to Arrays of Artificial Dipolar Molecular Rotors. A Surface Inclusion. *J. Am. Chem. Soc.* **2012**, *134*, 10122−10131.
(123) *Photobiology - The Science of Life and Light*; Björn, L. O., Ed.; Springer: New York, 2008.
(124) Balzani, V.; Credi, A.; Venturi, M. Photochemical Conversion of Solar Energy. *ChemSusChem* **2008**, *1*, 26−58.
(125) *Mechanisms of Primary Energy Transduction in Biology*; Wikström, M., Ed.; RSC Publishing: Cambridge, U.K., 2018.
(126) Turro, N. J.; Ramamurthy, V.; Scaiano, J. C. *Modern Molecular Photochemistry of Organic Molecules*; University Science Books: Sausalito, CA, 2010.
(127) Balzani, V.; Ceroni, P.; Juris, A. *Photochemistry and Photophysics: Concepts, Research, Applications*; Wiley-VCH: Weinheim, Germany, 2014.
(128) Baroncini, M.; Canton, M.; Casimiro, L.; Corra, S.; Groppi, J.; La Rosa, M.; Silvi, S.; Credi, A. Photoactive Molecular-Based Devices, Machines and Materials: Recent Advances. *Eur. J. Inorg. Chem.* **2018**, *2018*, 4589−4603.
(129) Astumian, R. D. Optical *vs.* Chemical Driving for Molecular Machines. *Faraday Discuss.* **2016**, *195*, 583−579.
(130) Ceroni, P.; Credi, A.; Venturi, M. Light to Investigate (Read) and Operate (Write) Molecular Devices and Machines. *Chem. Soc. Rev.* **2014**, *43*, 4068−4083.
(131) Kathan, M.; Hecht, S. Photoswitchable Molecules as Key Ingredients To Drive Systems Away from the Global Thermodynamic Minimum. *Chem. Soc. Rev.* **2017**, *46*, 5536−5550.
(132) Credi, A.; Venturi, M.; Balzani, V. Light on Molecular Machines. *ChemPhysChem* **2010**, *11*, 3398−3403.
(133) Balzani, V.; Clemente-Leon, M.; Credi, A.; Ferrer, B.; Venturi, M.; Flood, A. H.; Stoddart, J. F. Autonomous Artificial Nanomotor Powered by Sunlight. *Proc. Natl. Acad. Sci. U. S. A.* **2006**, *103*, 1178−1183.
(134) Raiteri, P.; Bussi, G.; Cucinotta, C. S.; Credi, A.; Stoddart, J. F.; Parrinello, M. Unravelling the Shuttling Mechanism in a Photoswitchable Multicomponent Bistable Rotaxane. *Angew. Chem., Int. Ed.* **2008**, *47*, 3536−3539.
(135) Ashton, P. R.; Ballardini, R.; Balzani, V.; Credi, A.; Dress, K. R.; Ishow, E.; Kleverlaan, C. J.; Kocian, O.; Preece, J. A.; Spencer, N.; et al. A Photochemically Driven Molecular-level Abacus. *Chem. - Eur. J.* **2000**, *6*, 3558−3574.
(136) Brouwer, A. M.; Frochot, C.; Gatti, F. G.; Leigh, D. A.; Mottier, L.; Paolucci, F.; Roffia, S.; Wurpel, G. W. H. Photoinduction of Fast, Reversible Translational Motion in a Hydrogen-bonded Molecular Shuttle. *Science* **2001**, *291*, 2124−2128.
(137) For example, see: Xie, G.; Li, P.; Zhao, Z.; Kong, X.-Y.; Zhang, Z.; Xiao, K.; Wang, G.; Wen, L.; Jiang, L. Bacteriorhodopsin-Inspired Light-Driven Artificial Molecule Motors for Transmembrane Mass Transportation. *Angew. Chem., Int. Ed.* **2018**, *57*, 16708−16712.
(138) Steinberg-Yfrach, G.; Rigaud, J.-L.; Durantini, E. N.; Moore, A. L.; Gust, D.; Moore, T. A. Light-Driven Production of ATP Catalysed by F_0F_1-ATP Synthase in an Artificial Photosynthetic Membrane. *Nature* **1998**, *392*, 479−482.
(139) Bennett, I. M.; Farfano, H. M. V.; Bogani, F.; Primak, A.; Liddell, P. A.; Otero, L.; Sereno, L.; Silber, J. J.; Moore, A. L.; Moore, T. A.; Gust, D. Active Transport of Ca^{2+} by an Artificial Photosynthetic Membrane. *Nature* **2002**, *420*, 398−401.
(140) Durot, S.; Heitz, V.; Sour, A.; Sauvage, J.-P. Transition-Metal-Complexed Catenanes and Rotaxanes: From Dynamic Systems to Functional Molecular Machines. *Top. Curr. Chem.* **2014**, *354*, 35−70.
(141) Livoreil, A.; Dietrich-Buchecker, C. O.; Sauvage, J.-P. Electrochemically Triggered Swinging of a [2]-Catenate. *J. Am. Chem. Soc.* **1994**, *116*, 9399−9400.
(142) Cardenas, D. J.; Livoreil, A.; Sauvage, J.-P. Redox Control of the Ring-Gliding Motion in a Cu-Complexed Catenane: A Process Involving Three Distinct Geometries. *J. Am. Chem. Soc.* **1996**, *118*, 11980−11981.
(143) Collin, J.-P.; Gaviña, P.; Sauvage, J.-P. Electrochemically Induced Molecular Motions in a Copper(I) Complex Pseudorotaxane. *Chem. Commun.* **1996**, 2005−2006.
(144) Armaroli, N.; Balzani, V.; Collin, J.-P.; Gaviña, P.; Sauvage, J.-P.; Ventura, B. Rotaxanes Incorporating Two Different Coordinating Units in Their Thread: Synthesis and Electrochemically and Photochemically Induced Molecular Motions. *J. Am. Chem. Soc.* **1999**, *121*, 4397−4408.
(145) Poleschak, I.; Kern, J.-M.; Sauvage, J.-P. A Copper-Complexed Rotaxane in Motion: Pirouetting of the Ring on the Millisecond Timescale. *Chem. Commun.* **2004**, 474−476.
(146) Durola, F.; Sauvage, J.-P. Fast Electrochemically Induced Translation of the Ring in a Copper-Complexed [2]Rotaxane: The Biisoquinoline Effect. *Angew. Chem., Int. Ed.* **2007**, *46*, 3537−3540.
(147) Collin, J.-P.; Durola, F.; Lux, J.; Sauvage, J.-P. A Rapidly Shuttling Copper-Complexed [2]Rotaxane with Three Different Chelating Groups in Its Axis. *Angew. Chem., Int. Ed.* **2009**, *48*, 8532−8535.
(148) Joosten, A.; Trolez, Y.; Collin, J.-P.; Heitz, V.; Sauvage, J.-P. Copper(I)-Assembled [3]Rotaxane Whose Two Rings Act as Flapping Wings. *J. Am. Chem. Soc.* **2012**, *134*, 1802−1809.
(149) Jiménez, M. C.; Dietrich-Buchecker, C.; Sauvage, J.-P. Towards Synthetic Molecular Muscles: Contraction and Stretching of a Linear Rotaxane Dimer. *Angew. Chem., Int. Ed.* **2000**, *39*, 3284−3287.
(150) Niess, F.; Duplan, V.; Sauvage, J.-P. Interconversion Between a Vertically Oriented Transition Metal-Complexed Figure-of-Eight and a Horizontally Disposed One. *J. Am. Chem. Soc.* **2014**, *136*, 5876−5879.
(151) Ashton, P. R.; Bissell, R. A.; Spencer, N.; Stoddart, J. F.; Tolley, M. S. Towards Controllable Molecular Shuttles-1. *Synlett* **1992**, *1992*, 914−918.
(152) Ashton, P. R.; Bissell, R. A.; Gorski, R.; Philp, D.; Spencer, N.; Stoddart, J. F.; Tolley, M. S. Towards Controllable Molecular Shuttles-2. *Synlett* **1992**, *1992*, 919−922.
(153) Ashton, P. R.; Bissell, R. A.; Spencer, N.; Stoddart, J. F.; Tolley, M. S. Towards Controllable Molecular Shuttles-3. *Synlett* **1992**, *1992*, 923−926.
(154) Anelli, P. L.; Asakawa, M.; Ashton, P. R.; Bissell, R. A.; Clavier, G.; Gorski, R.; Kaifer, A. E.; Langford, S. J.; Mattersteig, G.; Menzer, S.; et al. Toward Controllable Molecular Shuttles. *Chem. - Eur. J.* **1997**, *3*, 1113−1135.
(155) Ballardini, R.; Balzani, V.; Credi, A.; Brown, C. L.; Gillard, R. E.; Montalti, M.; Philp, D.; Stoddart, J. F.; Venturi, M.; White, A. J. P.; et al. Controlling Catenations, Properties and Relative Ring-Component Movements in Catenanes with Aromatic Fluorine Substituents. *J. Am. Chem. Soc.* **1997**, *119*, 12503−12513.
(156) Bissell, R. A.; Cordova, E.; Kaifer, A. E.; Stoddart, J. F. A chemically and electrochemically switchable molecular shuttle. *Nature* **1994**, *369*, 133−137.
(157) Fahrenbach, A. C.; Bruns, C. J.; Cao, D.; Stoddart, J. F. Ground-State Thermodynamics of Bistable Redox-Active Donor-Acceptor Mechanically Interlocked Molecules. *Acc. Chem. Res.* **2012**, *45*, 1581−1592.
(158) Striepe, L.; Baumgartner, T. Viologens and Their Application as Functional Materials. *Chem. - Eur. J.* **2017**, *23*, 16924−16940.

DOI: 10.1021/acs.chemrev.9b00291
Chem. Rev. 2020, 120, 200−268

(159) Philp, D.; Slawin, A. M.; Spencer, N.; Stoddart, J. F.; Williams, D. J. The Complexation of Tetrathiafulvalene by Cyclobis(Paraquat-*p*-Phenylene). *J. Chem. Soc., Chem. Commun.* **1991**, 1584−1586.
(160) Ashton, P. R.; Balzani, V.; Becher, J.; Credi, A.; Fyfe, M. C. T.; Mattersteig, G.; Menzer, S.; Nielsen, M. B.; Raymo, F. M.; Stoddart, J. F.; et al. A Three-Pole Supramolecular Switch. *J. Am. Chem. Soc.* **1999**, *121*, 3951−3957.
(161) Nielsen, M. B.; Lomholt, C.; Becher, J. Tetrathiafulvalenes as Building Blocks in Supramolecular Chemistry II. *Chem. Soc. Rev.* **2000**, *29*, 153−164.
(162) Jana, A.; Bahring, S.; Ishida, M.; Goeb, S.; Canevet, D.; Salle, M.; Jeppesen, J. O.; Sessler, J. L. Functionalised Tetrathiafulvalene- (TTF-) Macrocycles: Recent Trends in Applied Supramolecular Chemistry. *Chem. Soc. Rev.* **2018**, *47*, 5614−5645.
(163) Schröder, H. V.; Schalley, C. A. Tetrathiafulvalene − A Redox-Switchable Building Block to Control Motion in Mechanically Interlocked Molecules. *Beilstein J. Org. Chem.* **2018**, *14*, 2163−2185.
(164) Asakawa, M.; Ashton, P. R.; Balzani, V.; Credi, A.; Mattersteig, G.; Matthews, O. A.; Montalti, M.; Spencer, N.; Stoddart, J. F.; Venturi, M. Electrochemically Induced Molecular Motions in Pseudorotaxanes: A Case of Dual-Mode (Oxidative and Reductive) Dethreading. *Chem. - Eur. J.* **1997**, *3*, 1992−1996.
(165) Devonport, W.; Blower, M. A.; Bryce, M. R.; Goldenberg, L. M. A Redox-active Tetrathiafulvalene [2]Pseudorotaxane: Spectroelectrochemical and Cyclic Voltammetric Studies of the Highly-reversible Complexation/Decomplexation Process. *J. Org. Chem.* **1997**, *62*, 885−887.
(166) Credi, A.; Montalti, M.; Balzani, V.; Langford, S. J.; Raymo, F. M.; Stoddart, J. F. Simple Molecular-level Machines. Interchange between Different Threads in Pseudorotaxanes. *New J. Chem.* **1998**, *22*, 1061−1065.
(167) Balzani, V.; Credi, A.; Mattersteig, G.; Matthews, O. A.; Raymo, F. M.; Stoddart, J. F.; Venturi, M.; White, A. J. P.; Williams, D. J. Switching of Pseudorotaxanes and Catenanes Incorporating a Tetrathiafulvalene Unit by Redox and Chemical Inputs. *J. Org. Chem.* **2000**, *65*, 1924−1936.
(168) Ashton, P. R.; Belohradsky, M.; Philp, D.; Spencer, N.; Stoddart, J. F. The Self-Assembly of [2]- and [3]Rotaxanes by Slippage. *J. Chem. Soc., Chem. Commun.* **1993**, *0*, 1274−1277.
(169) Collier, C. P.; Jeppesen, J. O.; Luo, Y.; Perkins, J.; Wong, E. W.; Heath, J. R.; Stoddart, J. F. Molecular-Based Electronically Switchable Tunnel Junction Devices. *J. Am. Chem. Soc.* **2001**, *123*, 12632−12641.
(170) Liu, Y.; Flood, A. H.; Bonvallet, P. A.; Vignon, S. A.; Northrop, B. H.; Tseng, H.-R.; Jeppesen, J. O.; Huang, T. J.; Brough, B.; Baller, M.; et al. Linear Artificial Molecular Muscles. *J. Am. Chem. Soc.* **2005**, *127*, 9745−9759.
(171) Steuerman, D. W.; Tseng, H. R.; Peters, A. J.; Flood, A. H.; Jeppesen, J. O.; Nielsen, K. A.; Stoddart, J. F.; Heath, J. R. Molecular-Mechanical Switch-Based Solid-State Electrochromic Devices. *Angew. Chem., Int. Ed.* **2004**, *43*, 6486−6491.
(172) Green, J. E.; Choi, J. W.; Boukai, A.; Bunimovich, Y.; Johnston-Halperin, E.; DeIonno, E.; Luo, Y.; Sheriff, B. A.; Xu, K.; Shin, Y. S.; et al. A 160-Kilobit Molecular Electronic Memory Patterned at 10^{11} Bits per Square Centimetre. *Nature* **2007**, *445*, 414−417.
(173) Geuder, W.; Hünig, S.; Suchy, A. Single and Double Bridged Viologens and Intramolecular Pimerization of Their Cation Radicals. *Tetrahedron* **1986**, *42*, 1665−1677.
(174) Jeon, W. S.; Kim, H.-J.; Lee, C.; Kim, K. Control of the Stoichiometry in Host-Guest Complexation by Redox Chemistry of Guests: Inclusion of Methylviologen in Cucurbit[8]uril. *Chem. Commun.* **2002**, 1828−1829.
(175) Park, J. W.; Choi, N. H.; Kim, J. H. Facile Dimerization of Viologen Radical Cations Covalently Bonded to β-Cyclodextrin and Suppression of the Dimerization by β-Cyclodextrin and Amphiphiles. *J. Phys. Chem.* **1996**, *100*, 769−774.
(176) Trabolsi, A.; Khashab, N.; Fahrenbach, A. C.; Friedman, D. C.; Colvin, M. T.; Cotí, K. K.; Benítez, D.; Tkatchouk, E.; Olsen, J.-C.; Belowich, M. E.; et al. Radically Enhanced Molecular Recognition. *Nat. Chem.* **2010**, *2*, 42−49.
(177) Li, H.; Fahrenbach, A. C.; Dey, S. K.; Basu, S.; Trabolsi, A.; Zhu, Z. X.; Botros, Y. Y.; Stoddart, J. F. Mechanical Bond Formation by Radical Templation. *Angew. Chem., Int. Ed.* **2010**, *49*, 8260−8265.
(178) Li, H.; Zhu, Z.; Fahrenbach, A. C.; Savoie, B. M.; Ke, C.; Barnes, J. C.; Lei, J.; Zhao, Y.-L.; Lilley, L. M.; Marks, T. J.; et al. Mechanical Bond-Induced Radical Stabilization. *J. Am. Chem. Soc.* **2013**, *135*, 456−467.
(179) Wang, Y.; Sun, J.; Liu, Z.; Nassar, M. S.; Botros, Y. Y.; Stoddart, J. F. Radically Promoted Formation of a Molecular Lasso. *Chem. Sci.* **2017**, *8*, 2562−2568.
(180) Barnes, J. C.; Fahrenbach, A. C.; Cao, D.; Dyar, S. M.; Frasconi, M.; Giesener, M. A.; Benítez, D.; Tkatchouk, E.; Chernyashevskyy, O.; Shin, W. H.; et al. A Radically Configurable Six-State Compound. *Science* **2013**, *339*, 429−433.
(181) Gibbs-Hall, I. C.; Vermeulen, N. A.; Dale, E. J.; Henkelis, J. J.; Blackburn, A. J.; Barnes, J. C.; Stoddart, J. F. Catenation through a Combination of Radical Templation and Ring-Closing Metathesis. *J. Am. Chem. Soc.* **2015**, *137*, 15640−15643.
(182) Nguyen, M. T.; Ferris, D. P.; Pezzato, C.; Wang, Y.; Stoddart, J. F. Densely Charged Dodecacationic [3]- and Tetracosacationic Radial [5]Catenanes. *Chem.* **2018**, *4*, 2329−2344.
(183) Sun, J.; Liu, Z.; Liu, W.-G.; Wu, Y.; Wang, Y.; Barnes, J. C.; Hermann, K. R.; Goddard, W. A., III; Wasielewski, M. R.; Stoddart, J. F. Mechanical-Bond-Protected, Air-Stable Radicals. *J. Am. Chem. Soc.* **2017**, *139*, 12704−12709.
(184) Majima, T.; Tojo, S.; Ishida, A.; Takamuku, S. *Cis*−*Trans* Isomerization and Oxidation of Radical Cations of Stilbene Derivatives. *J. Org. Chem.* **1996**, *61*, 7793−7800.
(185) Majima, T.; Tojo, S.; Ishida, A.; Takamuku, S. Reactivities of Isomerization, Oxidation, and Dimerization of Radical Cations of Stilbene Derivatives. *J. Phys. Chem.* **1996**, *100*, 13615−13623.
(186) Browne, W. R.; Pollard, M. M.; de Lange, B.; Meetsma, A.; Feringa, B. L. Reversible Three-State Switching of Luminescence: A New Twist to Electro and Photochromic Behavior. *J. Am. Chem. Soc.* **2006**, *128*, 12412−12413.
(187) Gordillo, M. A.; Soto-Monsalve, M.; Carmona-Vargas, C. C.; Gutiérrez, G.; D'vries, R. F.; Lehn, J.-M.; Chaur, M. N. Photochemical and Electrochemical Triggered Bis(Hydrazone) Switch. *Chem. - Eur. J.* **2017**, *23*, 14872−14882.
(188) Cvrtila, I.; Fanlo-Virgós, H.; Schaeffer, G.; Monreal Santiago, G.; Otto, S. Redox Control Over Acyl Hydrazone Photoswitches. *J. Am. Chem. Soc.* **2017**, *139*, 12459−12465.
(189) Goulet-Hanssens, A.; Utecht, M.; Mutruc, D.; Titov, E.; Schwarz, J.; Grubert, L.; Bléger, D.; Saalfrank, P.; Hecht, S. Electrocatalytic Z→E Isomerization of Azobenzenes. *J. Am. Chem. Soc.* **2017**, *139*, 335−341.
(190) Goulet-Hanssens, A.; Rietze, C.; Titov, E.; Abdullahu, L.; Grubert, L.; Saalfrank, P.; Hecht, S. Hole Catalysis as a General Mechanism for Efficient and Wavelength-Independent *Z* → *E* Azobenzene Isomerization. *Chem.* **2018**, *4*, 1740−1755.
(191) Gadsby, D. C. Ion Channels Versus Ion Pumps: The Principal Difference, in Principle. *Nat. Rev. Mol. Cell Biol.* **2009**, *10*, 344−352.
(192) Matile, S.; Vargas Jentzsch, A.; Montenegro, J.; Fin, A. Recent Synthetic Transport Systems. *Chem. Soc. Rev.* **2011**, *40*, 2453−2474.
(193) Chen, J.-Y.; Hou, J.-L. Controllable Synthetic Ion Channels. *Org. Chem. Front.* **2018**, *5*, 1728−1736.
(194) Wu, X.; Howe, E. N. W.; Gale, P. A. Supramolecular Transmembrane Anion Transport: New Assays and Insights. *Acc. Chem. Res.* **2018**, *51*, 1870−1879.
(195) Credi, A. A Molecular Cable Car for Transmembrane Ion Transport. *Angew. Chem., Int. Ed.* **2019**, *58*, 4108−4110.
(196) Cheng, C.; McGonigal, P. R.; Stoddart, J. F.; Astumian, R. D. Design and Synthesis of Nonequilibrium Systems. *ACS Nano* **2015**, *9*, 8672−8688.
(197) For example, see: Zappacosta, R.; Fontana, A.; Credi, A.; Arduini, A.; Secchi, A. Incorporation of Calix[6]Arene Macrocycles and (Pseudo)Rotaxanes in Bilayer Membranes: Towards Controllable Artificial Liposomal Channels. *Asian J. Org. Chem.* **2015**, *4*, 262−270.

DOI: 10.1021/acs.chemrev.9b00291
Chem. Rev. 2020, 120, 200−268

(198) Park, J. W.; Song, H. J. Isomeric [2]Rotaxanes and Unidirectional [2]Pseudorotaxane Composed of α-Cyclodextrin and Aliphatic Chain-Linked Carbazole-viologen Compounds. *Org. Lett.* **2004**, *6*, 4869−4872.
(199) Park, J. W. Kinetics and Mechanism of Cyclodextrin Inclusion Complexation Incorporating Bidirectional Inclusion and Formation of Orientational Isomers. *J. Phys. Chem. B* **2006**, *110*, 24915−24922.
(200) Oshikiri, T.; Takashima, Y.; Yamaguchi, H.; Harada, A. Face-Selective [2]- and [3]Rotaxanes: Kinetic Control of the Threading Direction of Cyclodextrins. *Chem. - Eur. J.* **2007**, *13*, 7091−7098.
(201) Park, J. W.; Song, H. J.; Cho, Y. J.; Park, K. K. Thermodynamics and Kinetics of Formation of Orientationally Isomeric [2]-Pseudorotaxanes between α-Cyclodextrin and Aliphatic Chain-Linked Aromatic Donor-Viologen Acceptor Compounds. *J. Phys. Chem. C* **2007**, *111*, 18605−18614.
(202) Oshikiri, T.; Takashima, Y.; Yamaguchi, H.; Harada, A. Kinetic Control of Threading of Cyclodextrins onto Axle Molecules. *J. Am. Chem. Soc.* **2005**, *127*, 12186−12187.
(203) Arduini, A.; Bussolati, R.; Credi, A.; Faimani, G.; Garaudee, S.; Pochini, A.; Secchi, A.; Semeraro, M.; Silvi, S.; Venturi, M. Towards Controlling the Threading Direction of a Calix[6]arene Wheel by Using Nonsymmetric Axles. *Chem. - Eur. J.* **2009**, *15*, 3230−3242.
(204) Arduini, A.; Bussolati, R.; Credi, A.; Secchi, A.; Silvi, S.; Semeraro, M.; Venturi, M. Toward Directionally Controlled Molecular Motions and Kinetic Intra- and Intermolecular Self-Sorting: Threading Processes of Nonsymmetric Wheel and Axle Components. *J. Am. Chem. Soc.* **2013**, *135*, 9924−9930.
(205) Li, H.; Cheng, C.; McGonigal, P. R.; Fahrenbach, A. C.; Frasconi, M.; Liu, W.-G.; Zhu, Z.; Zhao, Y.; Ke, C.; Lei, J.; Young, R. M.; et al. Relative Unidirectional Translation in an Artificial Molecular Assembly Fueled by Light. *J. Am. Chem. Soc.* **2013**, *135*, 18609−18620.
(206) McGonigal, P. R.; Li, H.; Cheng, C.; Schneebeli, S. T.; Frasconi, M.; Witus, L. S.; Stoddart, J. F. Controlling Association Kinetics in the Formation of Donor-Acceptor Pseudorotaxanes. *Tetrahedron Lett.* **2015**, *56*, 3591−3594.
(207) Cheng, C.; McGonigal, P. R.; Liu, W.-G.; Li, H.; Vermeulen, N. A.; Ke, C.; Frasconi, M.; Stern, C. L.; Goddard, W. A., III; Stoddart, J. F. Energetically Demanding Transport in a Supramolecular Assembly. *J. Am. Chem. Soc.* **2014**, *136*, 14702−14705.
(208) Cheng, C.; McGonigal, P. R.; Schneebeli, S. T.; Li, H.; Vermeulen, N. A.; Ke, C.; Stoddart, J. F. An Artificial Molecular Pump. *Nat. Nanotechnol.* **2015**, *10*, 547−553.
(209) Pezzato, C.; Nguyen, M. T.; Cheng, C.; Kim, D. J.; Otley, M. T.; Stoddart, J. F. An Efficient Artificial Molecular Pump. *Tetrahedron* **2017**, *73*, 4849−4857.
(210) Pezzato, C.; Nguyen, M. T.; Kim, D. J.; Anamimoghadam, O.; Mosca, L.; Stoddart, J. F. Controlling Dual Molecular Pumps Electrochemically. *Angew. Chem., Int. Ed.* **2018**, *57*, 9325−9329.
(211) Leigh, D. A.; Wong, J. K. Y.; Dehez, F.; Zerbetto, F. Unidirectional Rotation in a Mechanically Interlocked Molecular Rotor. *Nature* **2003**, *424*, 174−179.
(212) Hernández, J. V.; Kay, E. R.; Leigh, D. A. A Reversible Synthetic Rotary Molecular Motor. *Science* **2004**, *306*, 1532−1537.
(213) Roke, D.; Wezenberg, S. J.; Feringa, B. L. Molecular Rotary Motors: Unidirectional Motion Around Double Bonds. *Proc. Natl. Acad. Sci. U. S. A.* **2018**, *115*, 9423−9431.
(214) Logtenberg, H.; Areephong, J.; Bauer, J.; Meetsma, A.; Ferigna, B. L.; Browne, W. R. Towards Redox-Driven Unidirectional Molecular Motion. *ChemPhysChem* **2016**, *17*, 1895−1901.
(215) Koumura, N.; Geertsema, E. M.; van Gelder, M. B.; Meetsma, A.; Feringa, B. L. Second Generation Light-Driven Molecular Motors. Unidirectional Rotation Controlled by a Single Stereogenic Center with Near-Perfect Photoequilibria and Acceleration of the Speed of Rotation by Structural Modification. *J. Am. Chem. Soc.* **2002**, *124*, 5037−5051.
(216) Collins, B. S. L.; Kistemaker, J. C. M.; Otten, E.; Feringa, B. L. A Chemically Powered Unidirectional Rotary Molecular Motor Based on a Palladium Redox Cycle. *Nat. Chem.* **2016**, *8*, 860−866.
(217) Hawthorne, M. F.; Zink, J. I.; Skelton, J. M.; Bayer, M. J.; Liu, C.; Livshits, E.; Baer, R.; Neuhauser, D. Electrical or Photocontrol of the Rotary Motion of a Metallacarborane. *Science* **2004**, *303*, 1849−1851.
(218) Safronov, A. B.; Shlyakhtina, N. I.; Everett, T. A.; vanGordon, M. R.; Sevryugina, Y. V.; Jalisatgi, S. S.; Hawthorne, M. F. Direct Observation of Bis(dicarbollyl)nickel Conformers in Solution by Fluorescence Spectroscopy: An Approach to Redox-Controlled Metallacarborane Molecular Motors. *Inorg. Chem.* **2014**, *53*, 10045−10053.
(219) Iordache, A.; Oltean, M.; Milet, A.; Thomas, F.; Baptiste, B.; Saint-Aman, E.; Bucher, C. Redox Control of Rotary Motions in Ferrocene-Based Elemental Ball Bearings. *J. Am. Chem. Soc.* **2012**, *134*, 2653−2671.
(220) Takai, A.; Yasuda, T.; Ishizuka, T.; Kojima, T.; Takeuchi, M. A Directly Linked Ferrocene-Naphthalenediimide Conjugate: Precise Control of Stacking Structures of π-Systems by Redox Stimuli. *Angew. Chem., Int. Ed.* **2013**, *52*, 9167−9171.
(221) Gao, C.; Silvi, S.; Ma, X.; Tian, H.; Venturi, M.; Credi, A. Reversible Modulation of Helicity in a Binaphthyl-Bipyridinium Species and its Cucurbit[8]uril Complexes. *Chem. Commun.* **2012**, *48*, 7577−7579.
(222) Gao, C.; Silvi, S.; Ma, X.; Tian, H.; Credi, A.; Venturi, M. Chiral Supramolecular Switches Based on (*R*)-Binaphthalene-Bipyridinium Guests and Cucurbituril Hosts. *Chem. - Eur. J.* **2012**, *18*, 16911−16921.
(223) Vives, G.; Jacquot de Rouville, H.-P.; Carella, A.; Launay, J.-P.; Rapenne, G. Prototypes of Molecular Motors Based on Star-Saped Organometallic Ruthenium Complexes. *Chem. Soc. Rev.* **2009**, *38*, 1551−1561.
(224) Vives, G.; Sistach, S.; Carella, A.; Launay, J.-P.; Rapenne, G. Synthesis of Triester-Functionalized Molecular Motors Incorporating Bis-Acetylide Trans-Platinum Insulating Fragments. *New J. Chem.* **2006**, *30*, 1429−1438.
(225) Vives, G.; Gonzalez, A.; Jaud, J.; Launay, J.-P.; Rapenne, G. Synthesis of Molecular Motors Incorporating para-Phenylene-Conjugated or Bicyclo[2.2.2]octane-Insulated Electroactive Groups. *Chem. - Eur. J.* **2007**, *13*, 5622−5631.
(226) Special Issue on Photochromism: Memories and Switches: *Chem. Rev.* **2000**, *100*, 1683−1890.
(227) Zhang, J.; Zou, Q.; Tian, H. Photochromic Materials: More than Meets the Eye. *Adv. Mater.* **2013**, *25*, 378−399.
(228) Bléger, D.; Hecht, S. Visible-Light-Activated Molecular Switches. *Angew. Chem., Int. Ed.* **2015**, *54*, 11338−11349.
(229) Wang, L.; Li, Q. Photochromism Into Nanosystems: Towards Lighting Up the Future Nanoworld. *Chem. Soc. Rev.* **2018**, *47*, 1044−1097.
(230) Pianowski, Z. L. Recent Implementations of Molecular Photoswitches into Smart Materials and Biological Systems. *Chem. - Eur. J.* **2019**, *25*, 5128−5144.
(231) *Photochromism: Molecules and Systems*; Dürr, H., Bouas-Laurent, H., Eds.; Elsevier: Amsterdam, 2003.
(232) *New Frontiers in Photochromism*; Irie, M., Yokoyama, Y., Seki, T., Eds.; Springer: Tokyo, 2013.
(233) Nakagawa, T.; Ubukata, T.; Yokoyama, Y. Chirality and Stereoselectivity in Photochromic Reactions. *J. Photochem. Photobiol., C* **2018**, *34*, 152−191.
(234) Wald, G. The Molecular Basis of Visual Excitation. *Nature* **1968**, *219*, 800−807.
(235) Waldeck, D. H. Photoisomerization Dynamics of Stilbenes. *Chem. Rev.* **1991**, *91*, 415−436.
(236) Henry, A. J. The Photochemical Instability of *cis*- and *trans*-4:4′-Diamidinostilbene. *J. Chem. Soc.* **1946**, *12*, 1156−1164.
(237) Yamaguchi, T.; Seki, T.; Tamaki, T.; Ichimura, K. Photochromism of Hemithioindigo Derivatives. I. Preparation and Photochromic Properties in Organic Solvents. *Bull. Chem. Soc. Jpn.* **1992**, *65*, 649−656.
(238) Wiedbrauk, S.; Dube, H. Hemithioindigo−An Emerging Photoswitch. *Tetrahedron Lett.* **2015**, *56*, 4266−4274.
(239) Petermayer, C.; Dube, H. Indigoid Photoswitches: Visible Light Responsive Molecular Tools. *Acc. Chem. Res.* **2018**, *51*, 1153−1163.

DOI: 10.1021/acs.chemrev.9b00291
Chem. Rev. 2020, 120, 200−268

(240) Cordes, T.; Schadendorf, T.; Rück-Braun, K.; Zinth, W. Chemical Control of Hemithioindigo-photoisomerization − Substituent-effects on different molecular parts. *Chem. Phys. Lett.* **2008**, *455*, 197−201.
(241) Maerz, B.; Wiedbrauk, S.; Oesterling, S.; Samoylova, E.; Nenov, A.; Mayer, P.; de Vivie-Riedle, R.; Zinth, W.; Dube, H. Making Fast Photoswitches Faster—Using Hammett Analysis to Understand the Limit of Donor−Acceptor Approaches for Faster Hemithioindigo Photoswitches. *Chem. - Eur. J.* **2014**, *20*, 13984−13992.
(242) Wiedbrauk, S.; Maerz, B.; Samoylova, E.; Reiner, A.; Trommer, F.; Mayer, P.; Zinth, W.; Dube, H. Twisted Hemithioindigo Photoswitches: Solvent Polarity Determines the Type of Light-Induced Rotations. *J. Am. Chem. Soc.* **2016**, *138*, 12219−12227.
(243) Hartley, G. S. The *Cis*-Form of Azobenzene. *Nature* **1937**, *140*, 281.
(244) Bandara, H. M. D.; Burdette, S. C. Photoisomerization in Different Classes of Azobenzene. *Chem. Soc. Rev.* **2012**, *41*, 1809−1825.
(245) Szymanski, W.; Beierle, J. M.; Kistemaker, H. A. V.; Velema, W. A.; Feringa, B. L. Reversible Photocontrol of Biological Systems by the Incorporation of Molecular Photoswitches. *Chem. Rev.* **2013**, *113*, 6114−6178.
(246) Baroncini, M.; Ragazzon, G.; Silvi, S.; Venturi, M.; Credi, A. The Eternal Youth of Azobenzene: New Photoactive Molecular and Supramolecular Devices. *Pure Appl. Chem.* **2015**, *87*, 537−545.
(247) Baroncini, M.; Bergamini, G. Azobenzene: a Photoactive Building Block for Supramolecular Architectures. *Chem. Rec.* **2017**, *17*, 700−712.
(248) Calbo, J.; Weston, C. E.; White, A. J. P.; Rzepa, H. S.; Contreras-García, J.; Fuchter, M. J. Tuning Azoheteroarene Photoswitch Performance through Heteroaryl Design. *J. Am. Chem. Soc.* **2017**, *139*, 1261−1274.
(249) Crespi, S.; Simeth, N. A.; König, B. Heteroaryl Azo Dyes as Molecular Photoswitches. *Nat. Rev. Chem.* **2019**, *3*, 133−146.
(250) Fischer, E.; Frei, Y. Photoisomerization Equilibria Involving the C═N Double Bond. *J. Chem. Phys.* **1957**, *27*, 808−809.
(251) Dugave, C.; Demange, L. *Cis*−*Trans* Isomerization of Organic Molecules and Biomolecules: Implications and Applications. *Chem. Rev.* **2003**, *103*, 2475−2532.
(252) Pratt, A. C. The Photochemistry of Imines. *Chem. Soc. Rev.* **1977**, *6*, 63−81.
(253) Fanghänel, D.; Timpe, G.; Orthman, V. Photochromic Compounds with N═N and C═N Chromophores. In *Organic Photochromes*; El'tsov, A. V., Ed.; Springer: Boston, 1990; pp 105−175.
(254) Su, X.; Aprahamian, I. Hydrazone-Based Switches, Metallo-Assemblies and Sensors. *Chem. Soc. Rev.* **2014**, *43*, 1963−1981.
(255) Kumpulainen, T.; Lang, B.; Rosspeintner, A.; Vauthey, E. Ultrafast Elementary Photochemical Processes of Organic Molecules in Liquid Solution. *Chem. Rev.* **2017**, *117*, 10826−10939.
(256) Martin, C. J.; Rapenne, G.; Nakashima, T.; Kawai, T. Recent progress in development of photoacid generators. *J. Photochem. Photobiol., C* **2018**, *34*, 41−51.
(257) Biagini, C.; Di Pietri, F.; Mandolini, L.; Lanzalunga, O.; Di Stefano, S. Photoinduced Release of a Chemical Fuel for Acid-Base-Operated Molecular Machines. *Chem. - Eur. J.* **2018**, *24*, 10122−10127.
(258) Arnaut, L. G.; Formosinho, S. J. Excited-State Proton-Transfer Reactions. I. Fundamentals and Intermolecular Reactions. *J. Photochem. Photobiol., A* **1993**, *75*, 1−20.
(259) Arnaut, L. G.; Formosinho, S. J. Excited-State Proton-Transfer Reactions. II. Intramolecular Reactions. *J. Photochem. Photobiol., A* **1993**, *75*, 21−48.
(260) Tolbert, L. M.; Solntsev, K. M. Excited-State Proton Transfer: From Constrained Systems to "Super" Photoacids to Superfast Proton Transfer. *Acc. Chem. Res.* **2002**, *35*, 19−27.
(261) Harris, C. M.; Selinger, B. K. Proton-Induced Fluorescence Quenching of 2-Naphthol. *J. Phys. Chem.* **1980**, *84*, 891−898.
(262) Photoinduced Proton Transfer in Chemistry and Biology Symposium Special Issue: *J. Phys. Chem. B* **2015**, *119*, 2089−2768.
(263) Forster, T.; Volker, S. Laser Flash Spectroscopy of Rapid Proton-Transfer Processes. 2. Reactions with Weak Acids. *Z. Phys. Chem.* **1975**, *97*, 275−284.
(264) Liao, Y. Design and Applications of Metastable-State Photoacids. *Acc. Chem. Res.* **2017**, *50*, 1956−1964.
(265) Irie, M. Light-Induced Reversible pH Change. *J. Am. Chem. Soc.* **1983**, *105*, 2078−2079.
(266) Peters, M. V.; Stoll, R. S.; Kühn, A.; Hecht, S. Photoswitching of Basicity. *Angew. Chem., Int. Ed.* **2008**, *47*, 5968−5972.
(267) Haberfield, P. Phototropic Molecules. 1. Phase Transfer as a Method for Detecting Transient Species. *J. Am. Chem. Soc.* **1987**, *109*, 6177−6178.
(268) Emond, M.; Le Saux, T.; Maurin, S.; Baudin, J.-B.; Plasson, R.; Jullien, L. 2-Hydroxyazobenzenes to Tailor pH Pulses and Oscillations with Light. *Chem. - Eur. J.* **2010**, *16*, 8822−8831.
(269) Shi, Z.; Peng, P.; Strohecker, D.; Liao, Y. Long-Lived Photoacid Based upon a Photochromic Reaction. *J. Am. Chem. Soc.* **2011**, *133*, 14699−14703.
(270) Johns, V. K.; Peng, P.; DeJesus, J.; Wang, Z.; Liao, Y. Visible-Light-Responsive Reversible Photoacid Based on a Metastable Carbanion. *Chem. - Eur. J.* **2014**, *20*, 689−692.
(271) Yang, C.; Khalil, T.; Liao, Y. Photocontrolled Proton Transfer in Solution and Polymers Using a Novel Photoacid with Strong C−H Acidity. *RSC Adv.* **2016**, *6*, 85420−85426.
(272) Remón, P.; Pischel, U. Chemical Communication between Molecules. *ChemPhysChem* **2017**, *18*, 1667−1677.
(273) Wojtyk, J. T. C.; Wasey, A.; Xiao, N.-N; Kazmaier, P. M.; Hoz, S.; Yu, C.; Lemieux, R. P.; Buncel, E. Elucidating the Mechanisms of Acidochromic Spiropyran-Merocyanine Interconversion. *J. Phys. Chem. A* **2007**, *111*, 2511−2516.
(274) Raymo, F. M.; Giordani, S. Signal Communication Between Molecular Switches. *Org. Lett.* **2001**, *3*, 3475−3478.
(275) Silvi, S.; Constable, E. C.; Housecroft, C. E.; Beves, J. E.; Dunphy, E. L.; Tomasulo, M.; Raymo, F. M.; Credi, A. All-Optical Integrated Logic Operations Based on Chemical Communication Between Molecular Switches. *Chem. - Eur. J.* **2009**, *15*, 178−185.
(276) Raymo, F. M.; Alvarado, R. J.; Giordani, S.; Cejas, M. A. Memory Effects Based on Intermolecular Photoinduced Proton Transfer. *J. Am. Chem. Soc.* **2003**, *125*, 2361−2364.
(277) Credi, A.; Dumas, S.; Silvi, S.; Venturi, M.; Arduini, A.; Pochini, A.; Secchi, A. Viologen-Calix[6]arene Pseudorotaxanes. Ion-Pair Recognition and Threading/Dethreading Molecular Motions. *J. Org. Chem.* **2004**, *69*, 5881−5887.
(278) Silvi, S.; Arduini, A.; Pochini, A.; Secchi, A.; Tomasulo, M.; Raymo, F. M.; Baroncini, M.; Credi, A. A Simple Molecular Machine Operated by Photoinduced Proton Transfer. *J. Am. Chem. Soc.* **2007**, *129*, 13378−13379.
(279) Tatum, L. A.; Foy, J. T.; Aprahamian, I. Waste Management of Chemically Activated Switches: Using a Photoacid To Eliminate Accumulation of Side Products. *J. Am. Chem. Soc.* **2014**, *136*, 17438−1744.
(280) Yang, L.-P.; Jia, F.; Cui, J.-S.; Lu, S.-B.; Jiang, W. Light-Controlled Switching of a Non-photoresponsive Molecular Shuttle. *Org. Lett.* **2017**, *19*, 2945−2948.
(281) *Photochemistry and Photophysics of Coordination Compounds*; Balzani, V., Campagna, S., Eds.; Springer: Heidelberg, Germany, 2007.
(282) Ashton, P. R.; Ballardini, R.; Balzani, V.; Boyd, S. E.; Credi, A.; Gandolfi, M. T.; Gómez-López, M.; Iqbal, S.; Philp, D.; Preece, J. A.; et al. Simple Mechanical Molecular and Supramolecular Machines: Photochemical and Electrochemical Control of Switching Processes. *Chem. - Eur. J.* **1997**, *3*, 152−170.
(283) Livoreil, A.; Sauvage, J.-P.; Armaroli, N.; Balzani, V.; Flamigni, L.; Ventura, B. Electrochemically and Photochemically Driven Ring Motions in a Disymmetrical Copper [2]-Catenate. *J. Am. Chem. Soc.* **1997**, *119*, 12114−12124.
(284) Ashton, P. R.; Ballardini, R.; Balzani, V.; Constable, E. C.; Credi, A.; Kocian, O.; Langford, S. J.; Preece, J. A.; Prodi, L.; Schofield, E. R.; et al. Ru(II) Polypyridine Complexes Covalently Linked to Electron

DOI: 10.1021/acs.chemrev.9b00291
Chem. Rev. 2020, 120, 200−268

Acceptors as Wires for Light-Driven Pseudorotaxane-Type Molecular Machines. *Chem. - Eur. J.* **1998**, *4*, 2413−2422.
(285) Ashton, P. R.; Balzani, V.; Kocian, O.; Prodi, L.; Spencer, N.; Stoddart, J. F. A Light-Fueled "Piston Cylinder" Molecular-Level Machine. *J. Am. Chem. Soc.* **1998**, *120*, 11190−11191.
(286) Chia, S. Y.; Cao, J. G.; Stoddart, J. F.; Zink, J. I. Working Supramolecular Machines Trapped in Glass and Mounted on a Film Surface. *Angew. Chem., Int. Ed.* **2001**, *40*, 2447−2451.
(287) Saha, S.; Johansson, E.; Flood, A. H.; Tseng, H.-R.; Zink, J. I.; Stoddart, J. F. A Photoactive Molecular Triad as a Nanoscale Power Supply for a Supramolecular Machine. *Chem. - Eur. J.* **2005**, *11*, 6846−6858.
(288) Scarpantonio, L.; Tron, A.; Destribats, C.; Godard, P.; McClenaghan, N. D. Concatenation of Reversible Electronic Energy Transfer and Photoinduced Electron Transfer to Control a Molecular Piston. *Chem. Commun.* **2012**, *48*, 3981−3983.
(289) Ashton, P. R.; Campbell, P. J.; Glink, P. T.; Philp, D.; Spencer, N.; Stoddart, J. F.; Chrystal, E. J. T.; Menzer, S.; Williams, D. J.; Tasker, P. A. Dialkylammonium Ion/Crown Ether Complexes: the Forerunners of a New Family of Interlocked Molecules. *Angew. Chem., Int. Ed. Engl.* **1995**, *34*, 1865−1869.
(290) Baroncini, M.; Silvi, S.; Venturi, M.; Credi, A. Reversible Photoswitching of Rotaxane Character and Interplay of Thermodynamic Stability and Kinetic Lability in a Self-Assembling Ring-Axle Molecular System. *Chem. - Eur. J.* **2010**, *16*, 11580−11587.
(291) Baroncini, M.; Silvi, S.; Venturi, M.; Credi, A. Photoactivated Directionally Controlled Transit of a Non-Symmetric Molecular Axle Through a Macrocycle. *Angew. Chem., Int. Ed.* **2012**, *51*, 4223−4226.
(292) Ashton, P. R.; Baxter, I.; Fyfe, M. C. T.; Raymo, F. M.; Spencer, N.; Stoddart, J. F.; White, A. J. P.; Williams, D. J. Rotaxane or Pseudorotaxane? That Is the Question! *J. Am. Chem. Soc.* **1998**, *120*, 2297−2307.
(293) Ragazzon, G.; Baroncini, M.; Silvi, S.; Venturi, M.; Credi, A. Light-Powered Autonomous and Directional Molecular Motion of a Dissipative Self-Assembling System. *Nat. Nanotechnol.* **2015**, *10*, 70−75.
(294) Ragazzon, G.; Baroncini, M.; Silvi, S.; Venturi, M.; Credi, A. Light-Powered, Artificial Molecular Pumps: A Minimalistic Approach. *Beilstein J. Nanotechnol.* **2015**, *6*, 2096−2104.
(295) Casimiro, L.; Groppi, J.; Baroncini, M.; La Rosa, M.; Credi, A.; Silvi, S. Photochemical Investigation of Cyanoazobenzene Derivatives as Components of Artificial Supramolecular Pumps. *Photochem. Photobiol. Sci.* **2018**, *17*, 734−740.
(296) Sevick, E. Nanomachines: A Light-driven Molecular Pump. *Nat. Nanotechnol.* **2015**, *10*, 18−19.
(297) Qu, D.-H.; Tian, H. Synthetic Small-Molecule Walkers at Work. *Chem. Sci.* **2013**, *4*, 3031−3035.
(298) von Delius, M.; Leigh, D. A. Walking Molecules. *Chem. Soc. Rev.* **2011**, *40*, 3656−3676.
(299) Bath, J.; Turberfield, A. J. DNA Nanomachines. *Nat. Nanotechnol.* **2007**, *2*, 275−284.
(300) Yin, P.; Yan, H.; Daniell, X. G.; Turberfield, A. J.; Reif, J. H. A Unidirectional DNA Walker that Moves Autonomously along a Track. *Angew. Chem., Int. Ed.* **2004**, *43*, 4906−4911.
(301) Wang, Z.-G.; Elbaz, J.; Willner, I. DNA Machines: Bipedal Walker and Stepper. *Nano Lett.* **2011**, *11*, 304−309.
(302) You, M.; Chen, Y.; Zhang, X.; Liu, H.; Wang, R.; Wang, K.; Williams, K. R.; Tan, W. An Autonomous and Controllable Light-Driven DNA Walking Device. *Angew. Chem.* **2012**, *124*, 2507−2510.
(303) Seeman, N. C.; Sleiman, H. F. DNA Nanotechnology. *Nat. Rev. Mater.* **2018**, *3*, 17068.
(304) Leigh, D. A.; Lewandowska, U.; Lewandowski, B.; Wilson, M. R. Synthetic Molecular Walkers. *Top. Curr. Chem.* **2014**, *354*, 111−138.
(305) Barrell, M. J.; Campaña, A. G.; von Delius, M.; Geertsema, E. M.; Leigh, D. A. Light-Driven Transport of a Molecular Walker in Either Direction Along a Molecular Track. *Angew. Chem., Int. Ed.* **2011**, *50*, 285−290.
(306) Feynman, R. P.; Leighton, R. B.; Sands, M. *The Feynman Lectures on Physics*; Addison-Wesley: Reading, MA, 1963; Vol. *I*, Chapter 46.
(307) Davis, A. P. Tilting at Windmills? the Second Law Survives. *Angew. Chem., Int. Ed.* **1998**, *37*, 909−910.
(308) Kelly, T. R.; De Silva, H.; Silva, R. A. Unidirectional Rotary Motion in a Molecular System. *Nature* **1999**, *401*, 150−152.
(309) Koumura, N.; Zijlstra, R. W. J.; van Delden, R. A.; Harada, N.; Feringa, B. L. Light-Driven Monodirectional Molecular Rotor. *Nature* **1999**, *401*, 152−155.
(310) Feringa, B. L.; Jager, W. F.; De Lange, B.; Meijer, E. W. Chiroptical Molecular Switch. *J. Am. Chem. Soc.* **1991**, *113*, 5468−5470.
(311) Pollard, M. M.; Meetsma, A.; Feringa, B. L. A Redesign of Light-Driven Rotary Molecular Motors. *Org. Biomol. Chem.* **2008**, *6*, 507−512.
(312) Pollard, M. M.; Klok, M.; Pijper, D.; Feringa, B. L. Rate Acceleration of Light-Driven Rotary Molecular Motors. *Adv. Funct. Mater.* **2007**, *17*, 718−729.
(313) Kistemaker, J. C. M.; Štacko, P.; Visser, J.; Feringa, B. L. Unidirectional Rotary Motion in Achiral Molecular Motors. *Nat. Chem.* **2015**, *7*, 890−896.
(314) Kistemaker, J. C. M.; Štacko, P.; Roke, D.; Wolters, A. T.; Heideman, G. H.; Chang, M.-C.; van der Meulen, P.; Visser, J.; Otten, E.; Feringa, B. L. Third-Generation Light-Driven Symmetric Molecular Motors. *J. Am. Chem. Soc.* **2017**, *139*, 9650−9661.
(315) Wezenberg, S. J.; Feringa, B. L. Supramolecularly Directed Rotary Motion in a Photoresponsive Receptor. *Nat. Commun.* **2018**, *9*, 1984.
(316) Hall, C. R.; Conyard, J.; Heisler, I. A.; Jones, G.; Frost, J.; Browne, W. R.; Feringa, B. L.; Meech, S. R. Ultrafast Dynamics in Light-Driven Molecular Rotary Motors Probed by Femtosecond Stimulated Raman Spectroscopy. *J. Am. Chem. Soc.* **2017**, *139*, 7408−7414.
(317) Beekmeyer, R.; Parkes, M. A.; Ridgwell, L.; Riley, J. W.; Chen, J.; Feringa, B. L.; Kerridge, A.; Fielding, H. H. Unravelling the Electronic Structure and Dynamics of an Isolated Molecular Rotary Motor in the Gas-Phase. *Chem. Sci.* **2017**, *8*, 6141−6148.
(318) Hall, C. R.; Browne, W. R.; Feringa, B. L.; Meech, S. R. Mapping the Excited-State Potential Energy Surface of a Photomolecular Motor. *Angew. Chem., Int. Ed.* **2018**, *57*, 6203−6207.
(319) Conyard, J.; Addison, K.; Heisler, I. A.; Cnossen, A.; Browne, W. R.; Feringa, B. L.; Meech, S. R. Ultrafast Dynamics in the Power Stroke of a Molecular Rotary Motor. *Nat. Chem.* **2012**, *4*, 547−551.
(320) Klok, M.; Boyle, N.; Pryce, M. T.; Meetsma, A.; Browne, W. R.; Feringa, B. L. MHz Unidirectional Rotation of Molecular Rotary Motors. *J. Am. Chem. Soc.* **2008**, *130*, 10484−10485.
(321) Chen, J.; Kistemaker, J. C. M.; Robertus, J.; Feringa, B. L. Molecular Stirrers in Action. *J. Am. Chem. Soc.* **2014**, *136*, 14924−14932.
(322) Conyard, J.; Štacko, P.; Chen, J.; McDonagh, S.; Hall, C. R.; Laptenok, S. P.; Browne, W. R.; Feringa, B. L.; Meech, S. R. Ultrafast Excited State Dynamics in Molecular Motors: Coupling of Motor Length to Medium Viscosity. *J. Phys. Chem. A* **2017**, *121*, 2138−2150.
(323) van Leeuwen, T.; Danowski, W.; Pizzolato, S. F.; Štacko, P.; Wezenberg, S. J.; Feringa, B. L. Braking of a Light-Driven Molecular Rotary Motor by Chemical Stimuli. *Chem. - Eur. J.* **2018**, *24*, 81−84.
(324) Dorel, R.; Miro, C.; Wei, Y.; Wezenberg, S. J.; Feringa, B. L. Cation-Modulated Rotary Speed in a Light-Driven Crown Ether Functionalized Molecular Motor. *Org. Lett.* **2018**, *20*, 3715−3718.
(325) Roke, D.; Stuckhardt, C.; Danowski, W.; Wezenberg, S. J.; Feringa, B. L. Light-Gated Rotation in a Molecular Motor Functionalized with a Dithienylethene Switch. *Angew. Chem., Int. Ed.* **2018**, *57*, 10515−10519.
(326) Lubbe, A. S.; Böhmer, C.; Tosi, F.; Szymanski, W.; Feringa, B. L. Molecular Motors in Aqueous Environment. *J. Org. Chem.* **2018**, *83*, 11008−11018.
(327) Cnossen, A.; Hou, L.; Pollard, M. M.; Wesenhagen, P. V.; Browne, W. R.; Feringa, B. L. Driving Unidirectional Molecular Rotary Motors with Visible Light by Intra- and Intermolecular Energy Transfer from Palladium Porphyrin. *J. Am. Chem. Soc.* **2012**, *134*, 17613−17619.

DOI: 10.1021/acs.chemrev.9b00291
Chem. Rev. 2020, 120, 200−268

(328) van Leeuwen, T.; Pol, J.; Roke, D.; Wezenberg, S. J.; Feringa, B. L. Visible-Light Excitation of a Molecular Motor with an Extended Aromatic Core. *Org. Lett.* **2017**, *19*, 1402−1405.
(329) Wezenberg, S. J.; Chen, K.-Y.; Feringa, B. L. Visible-Light-Driven Photoisomerization and Increased Rotation Speed of a Molecular Motor Acting as a Ligand in a Ruthenium(II) Complex. *Angew. Chem.* **2015**, *127*, 11619−11623.
(330) Roke, D.; Feringa, B. L.; Wezenberg, S. J. A Visible-Light-Driven Molecular Motor Based on Pyrene. *Helv. Chim. Acta* **2019**, *102*, No. e1800221.
(331) Roke, D.; Sen, M.; Danowski, W.; Wezenberg, S. J.; Feringa, B. L. Visible-Light-Driven Tunable Molecular Motors Based on Oxindole. *J. Am. Chem. Soc.* **2019**, *141*, 7622−7627.
(332) Kaleta, J.; Chen, J.; Bastien, G.; Dračínský, M.; Mašát, M.; Rogers, C. T.; Feringa, B. L.; Michl, J. Surface Inclusion of Unidirectional Molecular Motors in Hexagonal Tris(O-Phenylene)-Cyclotriphosphazene. *J. Am. Chem. Soc.* **2017**, *139*, 10486−10498.
(333) Chen, J.; Vachon, J.; Feringa, B. L. Design, Synthesis, and Isomerization Studies of Light-Driven Molecular Motors for Single Molecular Imaging. *J. Org. Chem.* **2018**, *83*, 6025−6034.
(334) Krajnik, B.; Chen, J.; Watson, M. A.; Cockroft, S. L.; Feringa, B. L.; Hofkens, J. Defocused Imaging of UV-Driven Surface-Bound Molecular Motors. *J. Am. Chem. Soc.* **2017**, *139*, 7156−7159.
(335) Danowski, W.; van Leeuwen, T.; Abdolahzadeh, S.; Roke, D.; Browne, W. R.; Wezenberg, S. J.; Feringa, B. L. Unidirectional Rotary Motion in a Metal−Organic Framework. *Nat. Nanotechnol.* **2019**, *14*, 488−494.
(336) Huang, H.; Aida, T. Towards Molecular Motors in Unison. *Nat. Nanotechnol.* **2019**, *14*, 407.
(337) Guentner, M.; Schildhauer, M.; Thumser, S.; Mayer, P.; Stephenson, D.; Mayer, P. J.; Dube, H. Sunlight-Powered kHz Rotation of a Hemithioindigo-Based Molecular Motor. *Nat. Commun.* **2015**, *6*, 8406.
(338) Wilcken, R.; Schildhauer, M.; Rott, F.; Huber, L. A.; Guentner, M.; Thumser, S.; Hoffmann, K.; Oesterling, S.; de Vivie-Riedle, R.; Riedle, E.; et al. Complete Mechanism of Hemithioindigo Motor Rotation. *J. Am. Chem. Soc.* **2018**, *140*, 5311−5318.
(339) Huber, L. A.; Hoffmann, K.; Thumser, S.; Böcher, N.; Mayer, P.; Dube, H. Direct Observation of Hemithioindigo-Motor Unidirectionality. *Angew. Chem., Int. Ed.* **2017**, *56*, 14536−14539.
(340) Gerwien, A.; Mayer, P.; Dube, H. Photon-Only Molecular Motor with Reverse Temperature-Dependent Efficiency. *J. Am. Chem. Soc.* **2018**, *140*, 16442−16445.
(341) Liu, R. S. H. Photoisomerization by Hula-Twist: A Fundamental Supramolecular Photochemical Reaction. *Acc. Chem. Res.* **2001**, *34*, 555−562.
(342) Gerwien, A.; Schildhauer, M.; Thumser, S.; Mayer, P.; Dube, H. Direct evidence for hula twist and single-bond rotation photoproducts. *Nat. Commun.* **2018**, *9*, 2510.
(343) Hoffmann, K.; Mayer, P.; Dube, H. A Hemithioindigo Molecular Motor for Metal Surface Attachment. *Org. Biomol. Chem.* **2019**, *17*, 1979−1983.
(344) Lehn, J.-M. Conjecture: Imines as Unidirectional Photodriven Molecular Motors−Motional and Constitutional Dynamic Devices. *Chem. - Eur. J.* **2006**, *12*, 5910−5915.
(345) Carbon−Nitrogen Double Bonds. In *Patai's Chemistry of Functional Groups*; Patai, S., Ed.; Wiley: Chichester, U.K., 1970.
(346) Greb, L.; Lehn, J.-M. Light-Driven Molecular Motors: Imines as Four-Step or Two-Step Unidirectional Rotors. *J. Am. Chem. Soc.* **2014**, *136*, 13114−13117.
(347) Hammerich, M.; Rusch, T.; Krekiehn, N. R.; Bloedorn, A.; Magnussen, O. M.; Herges, R. Imine-Functionalized Triazatriangulenium Platforms: Towards an Artificial Ciliated Epithelium. *ChemPhysChem* **2016**, *17*, 1870−1874.
(348) Amatatsu, Y. Computational Design of a Light-Driven Imine-Based Motor with Bulky Chiral Stator. *Chem. Phys.* **2018**, *508*, 51−60.
(349) Greb, L.; Eichhöfer, A.; Lehn, J.-M. Synthetic Molecular Motors: Thermal N Inversion and Directional Photoinduced C═N Bond Rotation of Camphorquinone Imines. *Angew. Chem.* **2015**, *127*, 14553−14556.
(350) Pollok, C. H.; Riesebeck, T.; Merten, C. Photoisomerization of a Chiral Imine Molecular Switch Followed by Matrix-Isolation VCD Spectroscopy. *Angew. Chem., Int. Ed.* **2017**, *56*, 1925−1928.
(351) Filatov, M.; Paolino, M.; Min, S. K.; Kim, K. S. Fulgides as Light-Driven Molecular Rotary Motors: Computational Design of a Prototype Compound. *J. Phys. Chem. Lett.* **2018**, *9*, 4995−5001.
(352) Filatov, M.; Paolino, M.; Min, S. K.; Choi, C. H. Design and Photoisomerization Dynamics of a New Family of Synthetic 2-Stroke Light Driven Molecular Rotary Motors. *Chem. Commun.* **2019**, *55*, 5247−5250.
(353) Oruganti, B.; Wang, J.; Durbeej, B. Excited-State Aromaticity Improves Molecular Motors: a Computational Analysis. *Org. Lett.* **2017**, *19*, 4818−4821.
(354) Wang, J.; Durbeej, B. Toward Fast and Efficient Visible-Light-Driven Molecular Motors: a Minimal Design. *ChemistryOpen* **2018**, *7*, 583−589.
(355) Wang, J.; Oruganti, B.; Durbeej, B. Light-Driven Rotary Molecular Motors Without Point Chirality: a Minimal Design. *Phys. Chem. Chem. Phys.* **2017**, *19*, 6952−6956.
(356) Marchand, G.; Eng, J.; Schapiro, I.; Valentini, A.; Frutos, L. M.; Pieri, E.; Olivucci, M.; Léonard, J.; Gindensperger, E. Directionality of Double-Bond Photoisomerization Dynamics Induced by a Single Stereogenic Center. *J. Phys. Chem. Lett.* **2015**, *6*, 599−604.
(357) Pang, X.; Jiang, C.; Qi, Y.; Yuan, L.; Hu, D.; Zhang, X.; Zhao, D.; Wang, D.; Lan, Z.; Li, F. Ultrafast Unidirectional Chiral Rotation in the Z−E Photoisomerization of two Azoheteroarene Photoswitches. *Phys. Chem. Chem. Phys.* **2018**, *20*, 25910−25917.
(358) Haberhauer, G. A Molecular Four-Stroke Motor. *Angew. Chem., Int. Ed.* **2011**, *50*, 6415−6418.
(359) Kamei, T.; Fukaminato, T.; Tamaoki, N. A Photochromic ATP Analogue Driving a Motor Protein with Reversible Light-Controlled Motility: Controlling Velocity and Binding Manner of a Kinesin−Microtubule System in an in Vitro Motility Assay. *Chem. Commun.* **2012**, *48*, 7625−7627.
(360) Islam, M. J.; Matsuo, K.; Menezes, H. M.; Takahashi, M.; Nakagawa, H.; Kakugo, A.; Sada, K.; Tamaoki, N. Substrate Selectivity and Its Mechanistic Insight of the Photo-Responsive Non-Nucleoside Triphosphate for Myosin and Kinesin. *Org. Biomol. Chem.* **2019**, *17*, 53−65.
(361) Perur, N.; Yahara, M.; Kamei, T.; Tamaoki, N. A Non-Nucleoside Triphosphate for Powering Kinesin-Microtubule Motility with Photo-Tunable Velocity. *Chem. Commun.* **2013**, *49*, 9935−9937.
(362) Kumar, K. R. S.; Kamei, T.; Fukaminato, T.; Tamaoki, N. Complete ON/OFF Photoswitching of the Motility of a Nano-biomolecular Machine. *ACS Nano* **2014**, *8*, 4157−4165.
(363) Amrutha, A. S.; Kumar, K. R. S.; Matsuo, K.; Tamaoki, N. Structure−Property Relationships of Photoresponsive Inhibitors of the Kinesin Motor. *Org. Biomol. Chem.* **2016**, *14*, 7202−7210.
(364) Amrutha, A. S.; Kumar, K. R. S.; Kikukawa, T.; Tamaoki, N. Targeted Activation of Molecular Transportation by Visible Light. *ACS Nano* **2017**, *11*, 12292−12301.
(365) Burkhart, C.; Haberhauer, G. A Light- and Electricity-Driven Molecular Pushing Motor. *Eur. J. Org. Chem.* **2017**, *2017*, 1308−1317.
(366) Morrow, S. M.; Bissette, A. J.; Fletcher, S. P. Transmission of Chirality Through Space and Across Length Scales. *Nat. Nanotechnol.* **2017**, *12*, 410−419.
(367) Pijper, D.; Feringa, B. L. Molecular Transmission: Controlling the Twist Sense of a Helical Polymer with a Single Light-Driven Molecular Motor. *Angew. Chem., Int. Ed.* **2007**, *46*, 3693−3696.
(368) Van Leeuwen, T.; Heideman, H.; Zhao, D.; Wezenberg, S. J.; Feringa, B. L. *In Situ* Control of Polymer Helicity with a Non-Covalently Bound Photoresponsive Molecular Motor Dopant. *Chem. Commun.* **2017**, *53*, 6393−6396.
(369) Zhao, D.; van Leeuwen, T.; Cheng, J.; Feringa, B. L. Dynamic Control of Chirality and Self-Assembly of Double-Stranded Helicates with Light. *Nat. Chem.* **2017**, *9*, 250−256.

DOI: 10.1021/acs.chemrev.9b00291
Chem. Rev. 2020, 120, 200−268

(370) Neilson, B. M.; Bielawski, C. W. Illuminating Phtoswitchable Catalysis. *ACS Catal.* **2013**, *3*, 1874−1885.
(371) Goestl, R.; Senf, A.; Hecht, S. Remote-Controlling Chemical Reactions by Light: Towards Chemistry with High Spatio-Temporal Resolution. *Chem. Soc. Rev.* **2014**, *43*, 1982−1996.
(372) Blanco, V.; Leigh, D. A.; Marcos, V. Artificial Switchable Catalysts. *Chem. Soc. Rev.* **2015**, *44*, 5341−5370.
(373) Vlatković, M.; Collins, B. S. L.; Feringa, B. L. Dynamic Responsive Systems for Catalytic Functions. *Chem. - Eur. J.* **2016**, *22*, 17080−17111.
(374) Wang, J.; Feringa, B. L. Dynamic Control of Chiral Space in a Catalytic Asymmetric Reaction Using a Molecular Motor. *Science* **2011**, *331*, 1429−1432.
(375) For a related example based on a photoswitchable helicene-type catalyst, see: Chen, C.-T.; Tsai, C.-C.; Tsou, P.-K.; Huang, G.-T.; Yu, C.-H. Enantiodivergent Steglich Rearrangement of O-Carboxylazlactones Catalyzed by a Chirality Switchable Helicene Containing a 4-Aminopyridine Unit. *Chem. Sci.* **2017**, *8*, 524−529.
(376) Vlatković, M.; Bernardi, L.; Otten, E.; Feringa, B. L. Dual Stereocontrol Over the Henry Reaction Using a Light- and Heat-Triggered Organocatalyst. *Chem. Commun.* **2014**, *50*, 7773−7775.
(377) Vlatković, M.; Volarić, J.; Collins, B. S. L.; Bernardi, L.; Feringa, B. L. Dynamic Control Over Catalytic Function Using Responsive Bisthiourea Catalysts. *Org. Biomol. Chem.* **2017**, *15*, 8285−8294.
(378) Zhao, D.; Neubauer, T. M.; Feringa, B. L. Dynamic Control of Chirality in Phosphine Ligands for Enantioselective Catalysis. *Nat. Commun.* **2015**, *6*, 6652.
(379) Pizzolato, S. F.; Štacko, P.; Kistemaker, J. C. M.; van Leeuwen, T.; Otten, E.; Feringa, B. L. Central-to-Helical-to-Axial-to-Central Transfer of Chirality with a Photoresponsive Catalyst. *J. Am. Chem. Soc.* **2018**, *140*, 17278−17289.
(380) Lubbe, A. S.; Liu, Q.; Smith, S. J.; de Vries, J. W.; Kistemaker, J. C. M.; de Vries, A. H.; Faustino, I.; Meng, Z.; Szymanski, W.; Hermann, A.; et al. Photoswitching of DNA Hybridization Using a Molecular Motor. *J. Am. Chem. Soc.* **2018**, *140*, 5069−5076.
(381) For example, see: Wu, L.; Koumoto, K.; Sugimoto, N. Reversible Stability Switching of a Hairpin DNA Via a Photo-Responsive Linker Unit. *Chem. Commun.* **2009**, *14*, 1915−1917.
(382) García-López, V.; Chen, F.; Nilewski, L. G.; Duret, G.; Aliyan, A.; Kolomeisky, A. B.; Robinson, J. T.; Wang, G.; Pal, R.; Tour, J. M. Molecular Machines Open Cell Membranes. *Nature* **2017**, *548*, 567−572.
(383) García-López, V.; Chiang, P.-T.; Chen, F.; Ruan, G.; Martí, A. A.; Kolomeisky, A. B.; Wang, G.; Tour, J. M. Unimolecular Submersible Nanomachines. Synthesis, Actuation, and Monitoring. *Nano Lett.* **2015**, *15*, 8229−8239.
(384) For example, see: Anzai, J.-I.; Osa, T. Photosensitive Artificial Membranes Based on Azobenzene and Spirobenzopyran Derivatives. *Tetrahedron* **1994**, *50*, 4039−4070.
(385) For example, see: Lei, Y.; Hurst, J. K. Photoregulated Potassium Ion Permeation through Dihexadecyl Phosphate Bilayers Containing Azobenzene and Stilbene Surfactants. *Langmuir* **1999**, *15*, 3424−3429.
(386) Wandera, D.; Wickramasinghe, S. R.; Husson, S. M. Stimuli-Responsive Membranes. *J. Membr. Sci.* **2010**, *357*, 6−35.
(387) Baroncini, M.; Credi, A. Gearing Up Molecular Rotary Motors. *Science* **2017**, *356*, 906−907.
(388) Kwart, H.; Alekman, S. A Cogwheel Effect in the Internal Rotations of Highly Hindered Systems. *J. Am. Chem. Soc.* **1968**, *90*, 4482−4483.
(389) Iwamura, H.; Mislow, K. Stereochemical Consequences of Dynamic Gearing. *Acc. Chem. Res.* **1988**, *21*, 175−182.
(390) Stevens, A. M.; Richards, C. J. A Metallocene Molecular Gear. *Tetrahedron Lett.* **1997**, *38*, 7805−7808.
(391) Ogi, S.; Ikeda, T.; Wakabayashi, R.; Shinkai, S.; Takeuchi, M. A Bevel-Gear-Shaped Rotor Bearing a Double-Decker Porphyrin Complex. *Chem. - Eur. J.* **2010**, *16*, 8285−8290.
(392) Liu, S.; Kondratuk, D. V.; Rousseaux, S. A. L.; Gil-Ramírez, G.; O'Sullivan, M. C.; Cremers, J.; Claridge, T. D. W.; Anderson, H. W. Caterpillar Track Complexes in Template-Directed Synthesis and Correlated Molecular Motion. *Angew. Chem., Int. Ed.* **2015**, *54*, 5355−5359.
(393) Štacko, P.; Kistemaker, J. C. M.; van Leeuwen, T.; Chang, M.-C.; Otten, E.; Feringa, B. L. Locked Synchronous Rotor Motion in a Molecular Motor. *Science* **2017**, *356*, 964−968.
(394) Uhl, E.; Thumser, S.; Mayer, P.; Dube, H. Transmission of Unidirectional Molecular Motor Rotation to a Remote Biaryl Axis. *Angew. Chem., Int. Ed.* **2018**, *57*, 11064−11068.
(395) For example, see: Muraoka, T.; Kinbara, K.; Aida, T. Mechanical Twisting of a Guest by a Photoresponsive Host. *Nature* **2006**, *440*, 512−515.
(396) Wang, Y.; Tian, T.; Chen, Y.-Z.; Niu, L.-Y.; Wu, L.-Z.; Tung, C.-H.; Yang, Q.-Z.; Boulatov, R. A Light-Driven Molecular Machine Based on Stiff Stilbene. *Chem. Commun.* **2018**, *54*, 7991−7994.
(397) Yu, J.-J.; Zhao, L.-Y.; Shi, Z.-T.; Zhang, Q.; London, G.; Liang, W.-J.; Gao, C.; Li, M.-M.; Cao, X.-M.; Tian, H.; et al. Pumping a Ring-Sliding Molecular Motion by a Light-Powered Molecular Motor. *J. Org. Chem.* **2019**, *84*, 5790−5802.
(398) Qu, D.-H.; Feringa, B. L. Controlling Molecular Rotary Motion with a Self-Complexing Lock. *Angew. Chem., Int. Ed.* **2010**, *49*, 1107−1110.
(399) Purcell, E. M. Life at Low Reynolds Number. *Am. J. Phys.* **1977**, *45*, 3−11.
(400) Locomotion of a microscopic object by reciprocating motion is possible in non-Newtonian fluids. For example, see: Qiu, T.; Lee, T.-C.; Mark, A. G.; Morozov, K. I.; Muenster, R.; Mierka, O.; Turek, S.; Leshansky, A. M.; Fischer, P. Swimming by Reciprocal Motion at Low Reynolds Number. *Nat. Commun.* **2014**, *5*, 5119.
(401) Shirai, Y.; Morin, J.-F.; Sasaki, T.; Guerrero, J. M.; Tour, J. M. Recent Progress on Nanovehicles. *Chem. Soc. Rev.* **2006**, *35*, 1043−1055.
(402) Shirai, F.; Osgood, A. J.; Zhao, Y.; Yao, Y.; Saudan, L.; Yang, H.; Yu-Hung, C.; Alemany, L. B.; Sasaki, T.; Morin, J.-F.; et al. Surface-Rolling Molecules. *J. Am. Chem. Soc.* **2006**, *128*, 4854−4864.
(403) Shirai, Y.; Osgood, A. J.; Zhao, Y.; Kelly, K. F.; Tour, J. M. Directional Control in Thermally Driven Single-Molecule Nanocars. *Nano Lett.* **2005**, *5*, 2330−2334.
(404) Morin, J.-F.; Shirai, Y.; Tour, J. M. En Route to a Motorized Nanocar. *Org. Lett.* **2006**, *8*, 1713−1716.
(405) Chiang, P.-T.; Mielke, J.; Godoy, J.; Guerrero, J. M.; Alemany, L. B.; Villagómez, C. J.; Saywell, A.; Grill, L.; Tour, J. M. Toward a Light-Driven Motorized Nanocar: Synthesis and Initial Imaging of Single Molecules. *ACS Nano* **2012**, *6*, 592−597.
(406) Saywell, A.; Bakker, A.; Mielke, J.; Kumagai, T.; Wolf, M.; García-López, V.; Chiang, P.-T.; Tour, J. M.; Grill, L. Light-Induced Translation of Motorized Molecules on a Surface. *ACS Nano* **2016**, *10*, 10945−10952.
(407) Nacci, C.; Baroncini, M.; Credi, A.; Grill, L. Reversible Photoswitching and Isomer-Dependent Diffusion of Single Azobenzene Tetramers on a Metal Surface. *Angew. Chem., Int. Ed.* **2018**, *57*, 15034−15039.
(408) García-López, V.; Chu, P.-L. E.; Chiang, P.-T.; Sun, J.; Martí, A. A.; Tour, J. M. Synthesis of a Light-Driven Motorized Nanocar. *Asian J. Org. Chem.* **2015**, *4*, 1308−1314.
(409) Chu, P.-L.; Wang, L.-Y.; Khatua, S.; Kolomeisky, A. B.; Link, S.; Tour, J. M. Synthesis and Single-Molecule Imaging of Highly Mobile Adamantane-Wheeled Nanocars. *ACS Nano* **2013**, *7*, 35−41.
(410) For example, see: Chao, S.; Romuald, C.; Fournel-Marotte, K.; Clavel, C.; Coutrot, F. A Strategy Utilizing a Recyclable Macrocycle Transporter for the Efficient Synthesis of a Triazolium-Based [2]Rotaxane. *Angew. Chem., Int. Ed.* **2014**, *53*, 6914−6919.
(411) De Bo, G.; Gall, M. A. Y.; Kitching, M. O.; Kuschel, S.; Leigh, D. A.; Tetlow, D. J.; Ward, J. W. Sequence-Specific beta-Peptide Synthesis by a Rotaxane-Based Molecular Machine. *J. Am. Chem. Soc.* **2017**, *139*, 10875−10879.
(412) O'Reilly, R. K.; Turberfield, A. J.; Wilks, T. R. The Evolution of DNA-Templated Synthesis as a Tool for Materials Discovery. *Acc. Chem. Res.* **2017**, *50*, 2496−2509.

DOI: 10.1021/acs.chemrev.9b00291
Chem. Rev. 2020, 120, 200−268

(413) De Bo, G.; Gall, M. A. Y.; Kuschel, S.; De Winter, J.; Gerbaux, P.; Leigh, D. A. An Artificial Molecular Machine That Builds an Asymmetric Catalyst. *Nat. Nanotechnol.* **2018**, *13*, 381−385.
(414) Hagiya, M.; Konagaya, A.; Kobayashi, S.; Saito, H.; Murata, S. Molecular Robots with Sensors and Intelligence. *Acc. Chem. Res.* **2014**, *47*, 1681−1690.
(415) Gu, H.; Chao, J.; Xiao, S.-J.; Seeman, N. C. A Proximity-Based Programmable DNA Nanoscale Assembly Line. *Nature* **2010**, *465*, 202−205.
(416) Muscat, R. A.; Bath, J.; Turberfield, A. J. A Programmable Molecular Robot. *Nano Lett.* **2011**, *11*, 982−987.
(417) Amir, Y.; Ben-Ishay, E.; Levner, D.; Ittah, S.; Abu-Horowitz, A.; Bachelet, I. Universal Computing by DNA Origami Robots in a Living Animal. *Nat. Nanotechnol.* **2014**, *9*, 353−357.
(418) Thubagere, A. J.; Li, W.; Johnson, R. F.; Chen, Z.; Doroudi, S.; Lee, Y. L.; Izatt, G.; Wittman, S.; Srinivas, N.; Woods, D. A Cargo-Sorting DNA Robot. *Science* **2017**, *357*, eaan6558.
(419) Wang, J.; Zhou, Z.; Yue, L.; Wang, S.; Willner, I. Switchable Triggered Interconversion and Reconfiguration of DNA Origami Dimers and Their Use for Programmed Catalysis. *Nano Lett.* **2018**, *18*, 2718−2724.
(420) For example, see: Kassem, S.; Lee, A. T. L.; Leigh, D. A.; Marcos, V.; Palmer, L. I.; Pisano, S. Stereodivergent Synthesis with a Programmable Molecular Machine. *Nature* **2017**, *549*, 374−378.
(421) Schäfer, C.; Ragazzon, B.; Colasson, B.; La Rosa, M.; Silvi, S.; Credi, A. An Artificial Molecular Transporter. *ChemistryOpen* **2016**, *5*, 120−124.
(422) Ashton, P. R.; Ballardini, R.; Balzani, V.; Baxter, I.; Credi, A.; Fyfe, M. C. T.; Gandolfi, M. T.; Gómez-López, M.; Martínez-Díaz, M. V.; Piersanti, A.; et al. Acid-base Controllable Molecular Shuttles. *J. Am. Chem. Soc.* **1998**, *120*, 11932−11942.
(423) Mobian, P.; Kern, J.-M.; Sauvage, J.-P. Light-Driven Machine Prototypes Based on Dissociative Excited States: Photoinduced Decoordination and Thermal Recoordination of a Ring in a Ruthenium(II)-Containing [2]Catenane. *Angew. Chem., Int. Ed.* **2004**, *43*, 2392−2395.
(424) Bonnet, S.; Limburg, B.; Meeldijk, J. D.; Klein Gebbink, R. J. M.; Killian, J. A. Ruthenium-Decorated Lipid Vesicles: Light-Induced Release of $[Ru(terpy)(bpy)(OH_2)]^{2+}$ and Thermal Back Coordination. *J. Am. Chem. Soc.* **2011**, *133*, 252−261.
(425) Chen, S.; Wang, Y.; Nie, T.; Bao, C.; Wang, C.; Xu, T.; Lin, Q.; Qu, D.-H.; Gong, X.; Yang, Y.; et al. An Artificial Molecular Shuttle Operates in Lipid Bilayers for Ion Transport. *J. Am. Chem. Soc.* **2018**, *140*, 17992−17998.
(426) Kassem, S.; Lee, A. T. L.; Leigh, D. A.; Markevicius, A.; Solà, J. Pick-up, Transport and Release of a Molecular Cargo Using a Small-Molecule Robotic Arm. *Nat. Chem.* **2016**, *8*, 138−143.
(427) Su, C.; Aprahamian, I. Switching Around Two Axles: Controlling the Configuration and Conformation of a Hydrazone-Based Switch. *Org. Lett.* **2011**, *13*, 30−33.
(428) Chen, J.; Wezenberg, S.; Feringa, B. L. Intramolecular Transport of Small-Molecule Cargo in a Nanoscale Devices Operated by Light. *Chem. Commun.* **2016**, *52*, 6765−6768.
(429) Huang, T. J.; Brough, B.; Ho, C. M.; Liu, Y.; Flood, A. H.; Bonvallet, P. A.; Tseng, H. R.; Stoddart, J. F.; Baller, M.; Magonov, S. A Nanomechanical Device Based on Linear Molecular Motors. *Appl. Phys. Lett.* **2004**, *85*, 5391−5393.
(430) Du, G. Y.; Moulin, E.; Jouault, N.; Buhler, E.; Giuseppone, N. Muscle-like Supramolecular Polymers: Integrated Motion from Thousands of Molecular Machines. *Angew. Chem., Int. Ed.* **2012**, *51*, 12504−12508.
(431) Berna, J.; Leigh, D. A.; Lubomska, M.; Mendoza, S. M.; Perez, E. M.; Rudolf, P.; Teobaldi, G.; Zerbetto, F. Macroscopic Transport by Synthetic Molecular Machines. *Nat. Mater.* **2005**, *4*, 704−710.
(432) Goujon, A.; Lang, T.; Mariani, G.; Moulin, E.; Fuks, G.; Raya, J.; Buhler, E.; Giuseppone, N. Bistable [c2] Daisy Chain Rotaxanes as Reversible Muscle-Like Actuators in Mechanicaly Active Gels. *J. Am. Chem. Soc.* **2017**, *139*, 14825−14828.
(433) Katsonis, N.; Lubomska, M.; Pollard, M. M.; Feringa, B. L.; Rudolf, P. Synthetic Light-Activated Molecular Switches and Motors on Surfaces. *Prog. Surf. Sci.* **2007**, *82*, 407−434.
(434) Silvi, S.; Venturi, M.; Credi, A. Artificial Molecular Shuttles: From Concepts to Devices. *J. Mater. Chem.* **2009**, *19*, 2279−2294.
(435) Pathem, B. K.; Claridge, S. A.; Zheng, Y. B.; Weiss, P. S. Molecular Switches and Motors on Surfaces. *Annu. Rev. Phys. Chem.* **2013**, *64*, 605−630.
(436) Bruns, C. J.; Stoddart, J. F. Rotaxane-Based Molecular Muscles. *Acc. Chem. Res.* **2014**, *47*, 2186−2199.
(437) Heinrich, T.; Traulsen, C. H. H.; Holzweber, M.; Richter, S.; Kunz, V.; Kastner, S. K.; Krabbenborg, S. O.; Huskens, J.; Unger, W. E. S.; Schalley, C. A. Coupled Molecular Switching Processes in Ordered Mono- and Multilayers of Stimulus-Responsive Rotaxanes on Gold Surfaces. *J. Am. Chem. Soc.* **2015**, *137*, 4382−4390.
(438) Deng, H.; Olson, M. A.; Stoddart, J. F.; Yaghi, O. M. Robust Dynamics. *Nat. Chem.* **2010**, *2*, 439−443.
(439) Fang, L.; Olson, M. A.; Benitez, D.; Tkatchouk, E.; Goddard, W. A., III; Stoddart, J. F. Mechanically Bonded Macromolecules. *Chem. Soc. Rev.* **2010**, *39*, 17−29.
(440) Vukotic, V. N.; Loeb, S. J. Coordination Polymers Containing Rotaxane Linkers. *Chem. Soc. Rev.* **2012**, *41*, 5896−5906.
(441) Yan, X.; Zheng, B.; Huang, F. Integrated Motion of Molecular Machines in Supramolecular Polymeric Scaffolds. *Polym. Chem.* **2013**, *4*, 2395−2399.
(442) Kobatake, S.; Takami, S.; Muto, H.; Ishikawa, T.; Irie, M. Rapid and Reversible Shape Changes of Molecular Crystals on Photo-irradiation. *Nature* **2007**, *446*, 778−781.
(443) Baroncini, M.; d'Agostino, S.; Bergamini, G.; Ceroni, P.; Comotti, A.; Sozzani, P.; Bassanetti, I.; Grepioni, F.; Hernandez, T. M.; Silvi, S.; et al. Photoinduced Reversible Switching of Porosity in Molecular Crystals Based on Star-Shaped Azobenzene Tetramers. *Nat. Chem.* **2015**, *7*, 634−640.
(444) Ohshima, S.; Morimoto, M.; Irie, M. Light-Driven Bending of Diarylethene Mixed Crystals. *Chem. Sci.* **2015**, *6*, 5746−5752.
(445) Recent example: Ryabchun, A.; Li, Q.; Lancia, F.; Aprahamian, I.; Katsonis, N. Shape-Persistent Actuators from Hydrazone Photoswitches. *J. Am. Chem. Soc.* **2019**, *141*, 1196−1200.
(446) Eelkema, R.; Pollard, M. M.; Vicario, J.; Katsonis, N.; Ramon, B. S.; Bastiaansen, C. W. M.; Broer, D. J.; Feringa, B. L. Molecular Machines: Nanomotor Rotates Microscale Objects. *Nature* **2006**, *440*, 163.
(447) Eelkema, R.; Pollard, M. M.; Katsonis, N.; Vicario, J.; Broer, D. J.; Feringa, B. L. Rotational Reorganization of Doped Cholesteric Liquid Crystalline Films. *J. Am. Chem. Soc.* **2006**, *128*, 14397−14407.
(448) Sun, J.; Lan, R.; Gao, Y.; Wang, M.; Zhang, W.; Wang, L.; Zhang, L.; Yang, Z.; Yang, H. Stimuli-Directed Dynamic Reconfiguration in Self-Organized Helical Superstructures Enabled by Chemical Kinetics of Chiral Molecular Motors. *Adv. Sci.* **2018**, *5*, 1700613.
(449) Sleczkowski, P.; Zhou, Y.; Iamsaard, S.; de Pablo, J. J.; Katsonis, N.; Lacaze, E. Light-Activated Helical Inversion in Cholesteric Liquid Crystal Microdroplets. *Proc. Natl. Acad. Sci. U. S. A.* **2018**, *115*, 4334−4339.
(450) Ryabchun, A.; Bobrovsky, A. Cholesteric Liquid Crystal Materials for Tunable Diffractive Optics. *Adv. Opt. Mater.* **2018**, *6*, 1800335.
(451) Recent account: Zeng, H.; Wasylczyk, P.; Wiersma, D. S.; Priimagi, A. Light Robots: Bridging the Gap Between Microrobotics and Photomechanics in Soft Materials. *Adv. Mater.* **2018**, *30*, 1703554.
(452) Orlova, T.; Lancia, F.; Loussert, C.; Iamsaard, S.; Katsonis, N.; Brasselet, E. Revolving Supramolecular Chiral Structures Powered by Light in Nanomotor-Doped Liquid Crystals. *Nat. Nanotechnol.* **2018**, *13*, 304−308.
(453) Chen, C.-T.; Chen, C.-H.; Ong, T.-G. Complementary Helicity Interchange of Optically Switchable Supramolecular-Enantiomeric Helicenes with (−)-Gel-Sol-(+)-Gel Transition Ternary Logic. *J. Am. Chem. Soc.* **2013**, *135*, 5294−5297.

DOI: 10.1021/acs.chemrev.9b00291
Chem. Rev. 2020, 120, 200−268

(454) Wezenberg, S. J.; Croisetu, C. M.; Stuart, M. C. A.; Feringa, B. L. Reversible Gel-Sol Photoswitching with an Overcrowded Alkene-Based Bis-Urea Supergelator. *Chem. Sci.* **2016**, *7*, 4341−4346.
(455) Yu, J.-J.; Cao, Z.-Q.; Zhang, Q.; Yang, S.; Qu, D.-H.; Tian, H. Photo-Powered Stretchable Nano-Containers Based on Well-Defined Vesicles Formed by an Overcrowded Alkene Switch. *Chem. Commun.* **2016**, *52*, 12056−12059.
(456) van Dijken, D. J.; Chen, J.; Stuart, M. C. A.; Hou, L.; Feringa, B. L. Amphiphilic Molecular Motors for Responsive Aggregation in Water. *J. Am. Chem. Soc.* **2016**, *138*, 660−669.
(457) Chen, J.; Leung, F. K.-C.; Stuart, M. C. A.; Kajitani, T.; Fukushima, T.; van der Giessen, E.; Feringa, B. L. Artificial Muscle-Like Function from Hierarchical Supramolecular Assembly of Photo-responsive Molecular Motors. *Nat. Chem.* **2018**, *10*, 132−138.
(458) Guidry, E. N.; Li, J.; Stoddart, J. F.; Grubbs, R. H. Bifunctional [c2]Daisy-Chains and Their Incorporation into Mechanically Interlocked Polymers. *J. Am. Chem. Soc.* **2007**, *129*, 8944−8945.
(459) Clark, P. G.; Day, M. W.; Grubbs, R. H. Switching and Extension of a [c2]Daisy-Chain Dimer Polymer. *J. Am. Chem. Soc.* **2009**, *131*, 13631−13633.
(460) Li, Q.; Fuks, G.; Moulin, E.; Maaloum, M.; Rawiso, M.; Kulic, I.; Foy, J. T.; Giuseppone, N. Macroscopic Contraction of a Gel Induced by the Integrated Motion of Light-Driven Molecular Motors. *Nat. Nanotechnol.* **2015**, *10*, 161−165.
(461) Colard-Itté, J.-R.; Li, Q.; Collin, D.; Mariani, G.; Fuks, G.; Moulin, E.; Buhler, E.; Giuseppone, N. Mechanical Behaviour of Contractile Gels Based on Light-Driven Molecular Motors. *Nanoscale* **2019**, *11*, 5197−5202.
(462) Foy, J. T.; Li, Q.; Goujon, A.; Colard-Itté, J.-R.; Fuks, G.; Moulin, E.; Schiffmann, O.; Dattler, D.; Funeriu, D. P.; Giuseppone, N. Dual-Light Control of Nanomachines that Integrate Motor and Modulator Subunits. *Nat. Nanotechnol.* **2017**, *12*, 540−545.

DOI: 10.1021/acs.chemrev.9b00291
Chem. Rev. 2020, 120, 200−268